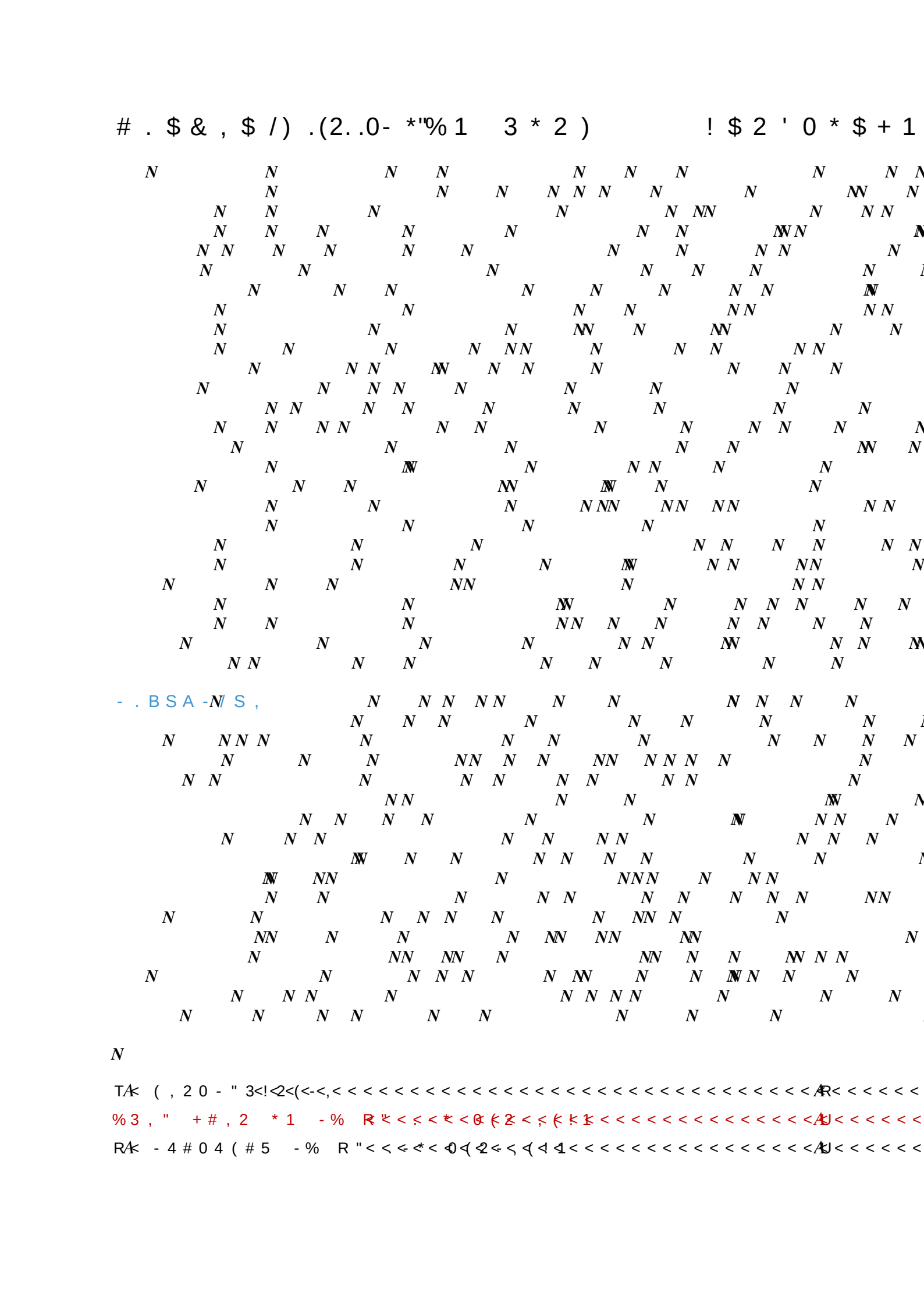


OA< &#,#0 2(-,: "#2#!2(-,: ," 120-,& !-3.*(,& -% "##.
.-* 0(2-,1 (, 4 ,"#0<5<<*1<<2#0<<*1<<<<<<<<<<A2<<<<<<

DA< %3," +#,2 *1 -% .* 1+-,1 <,<<25<12#"<R"<<<2T#A0<<*1<<

UA< R" .-* 0(2-,1 %-0 .0- (,& ,-,*-! * #%%#!21 ," !-*
TAU

CA< + 65#** ' +(*2-,(,<<(,<<R"<<<2#0(<<*1<<<<<<<T4F<<<<<<

!' 0 !2#0(8 2(<,<2#!<<,<3#1<<<<<<<<<<<<<<<<<<<<R40<<<<<<

A< R" + 2#0(*1 1##, 2'0-13#&1'1#2,'&##0*#,,1,<-%<<83(*,2&(0<<<<<<

2A< 2(1#.,' ,!#" , ,-1!-.11(#1*#%-0'-2–,((!!1 <(<,<R"<<<2&#0<(<<*1<

FA< #*#!20-, +(!0-1!-.7 ," 1.#!<20<<1<!<<.<7<%<0<RO"T<<<2#0<(<

#6!(2-,1 ," R" 1#<<(1<<,<3<2<01<<<<<<<<<<<<<<<<<<<<O40<<<<<<

TA< #6!(2-, .-* 0(2-,1<<(,<R"<<<2#0(<<*1<<<<<<<<C4D<<<<<<

TA< 23, *# #6!(2-,1 ," 20<(<-<,1<<(<,<<2<+<"<1<20<3<1<2303#0<#1<<<<

TA< 23,(,& -.2(! *#+(11(-, (, R" 1#+(!-„"'3!2*01(4&
DAT

TA< #,&(,##0#" !-,%(,#+#,2 -% #6!(2<,<1<(,<R"<D4U#<<(!<<,<"

,-,*(,# 0 ," 3*20 % 12<<<<2<(1<*<<<<#<,<<#<,<<<<<D4F<<<<<<

TA< 3*20 % 12 #6!(2-, "7, +(!1 (, 4<,<<"#0<5<D*F1<<#2#6

TA< /3 ,213+'#0#,2 !-3.1*((+,&,1(,-25*+ 2#0(*1 .0- #" 7
+3*2("(+#,1(-, *<1<#!20<1!<<,(<#1<<<<<<<<<<<<<<<<U40<<<<<<

TA< R" + 2#10(1#*"1 ,-,*(,#<0<<,<'<<2<<,(<!<1<<<<<<<<<<U*A<<<<<<

TA< ,-,*(,# 0 -.2(! * &#,#0 2(-, -% #,2 *,1&*#"C4R<3<,<2<3+

TA< ,-,*(,# 0 .-* 0(2-,(<1<(,<R"<<<2#0(<<*1<<<C4U<<<<<<

TA< ,-,*(,# 0 4 **#712 02((!1 .0" #*10%#4#0-1)#,127(+#207
R" + 2#0(<<*1<<<<<<<<<<<<<<<<<<<<<<<<<<<<<<<<C4F<<<<<<

RA< ,-,*(,# 0 1+.2(#2-(, R" + &,<#<2<(<!<<+<2<#0<(<<*1<<R<<<<<<

!'(0 *(27: 1(,&3* 0(2(#1: &#-+<#<2<0<(<!<<.<'<<1<#<1<:<<<U"<<+<-<(<0<

RA< /3 ,23+ &#-+#20(! .'-2-<,<(<!1<<(,<R"<<<2#0(<<*1<<<*U1<<<<<<

RA< 1(,&3* 0(2(#1 -% 0 ," -+ 5 4#1<<(<,<R"<<<2<#<0<(2<*<<.<*<<2

RA< R" 2-.-*-&(! *<<,<<*<<0<(2<<,<(<1<<<<<<<<<<<<<<<<<<<2<4U<<<<<<

RA< !'(0 *(2717(1,2#<<1(<0<$<<<<<<<<<<<<<<<<<<<<<<<<<<<<<<<2&0<<<<<<

RA< 25(12-.2(!1; !-,20-**(,& *(&'2 2 2<'<#<,<<,2<1<!<<*<#<5

RA< -.2(! *,(1-20-.7 -% R" <4<<,<<"<#0<5<<<*1<<<+<F2T#0<(<<*1<

+#2 130% !#1 ," #+<#<0&<(<,&<<<<2<#<0<(<<*1<<<<<<<<<<<<F4U<<<<<<

RA< .-* 0(2-,(! +#2 130% !#1 = !-3.*(,& R"<<<+<F2U#<0<(<<*1<

RA< 20 ,1(2(-, +#2 * "(!' *!-&#,("#1 %<<0<<.<<1<1F(24<#<<<,<"<

RA< 20 ,1"(+#,1(-, * + 2#0(*1 1 ,#5 .* 2<%<NO + %-0

ON< +6#,#1; #+#0&(,& .'<-<2<-<,<(<!<+<<2<#<0<(<<*<1<<<<<<T<N4<<<<<<

OA< '-2 #*#!20-, &#,#0 2(-, 7 (,#* 12(! 3402F5AN(2 2(-

OA< .* 1+-,(!112(+1*(%7#50 +#2 *1; -.2(! * !-,%(<,T#A0#<,2 ,

. . * (! 2 (- , 1 ; (, 2 # & 0 < 2 # ' < . < < 2 < ; (< 1 < < < < < < < < < < < < T < T A C < < < < < <

O 1 < (, 2 # & 0 . '2-#2"(5 1(2R' " + 2 # 0 < (< * < 1 < < < < < < < < < < < < < < < < < < < < < < < < T < T A C < < < < < <

O 1 < - . 2 - # * # ! 2 0 - , (! (, 2 # 0 ! - , , # ! 2 (- , <-%< .<-<*< <0<(<2<R4T<1< <(<,< <P

O 1 < # % % # ! 2 (4 # 0 # 1 . - , 1 # - % / 3 , 2 3 + + 2 # 0 (< * < 1 < T R 4 D 4 # ; < < 7

. . * (! 2 (- , 1 ; * (& ' 2 #<+<(<1<1<(<-<,< < <,<"< <"<#<2<#<!<2<(<-<,< < T R 4 < < < < < <

O 1 < 1 (, & * # 2 - , # + (< 2 < # 0 < 1 < < < < < < < < < < < < < < < < < < < < < < < < T < R 4 < < < < < <

O A < ,11"2 0 3 ! 2 3 0 # # , & (, #1# 0 ((2 & (%& 0 # * # (& 2 0 2 - , <2<3<,<,T<0<R<(<,<&< <"<#-

O 1 < . 0 - 1 . # ! 21(, %0 0 # 0 . ' - 2 - , (! " # 4 (! # 1 , "# 3 < , T < 4 U < 4 # < 2 (-

O P 1 < R " + 2 # 0 (* 1 *%(-,0" 1 3 -* *2 0 0 4 (- * # 2 < < .< '<-<2<-<,< <1<#<,<1<T(<4<2< < < < < <

D M 1 < * !) . ' - 1 . ' - 0 3 1 , " (2 1 <*<*<-<7< %<-<0< <(<,%<0< <0<B<A<T< <1<#<,<1<(

. . * (! 2 (- , 1 ; " (1 0 3 < 2 < 4 # < " < (0 # < 2 < (< ; 1 < < < < < < < < < < T < D 4 D < < < < < <

D 7 1 < R " + 2 # 0 (* 1 % - 0 . ' - 2 - , (! / 3 , <2<3<+< <(<,%<-<0<+<T<D4D<-<,< < .<0<-

D P 1 < R " + & , # 2 (! < . < ' < 2 < ; (< 1 < < < < < < < < < < < < < < < < < < < < < < < < T < D 4 2 < < < < < <

D 1 < ! - , ! * 3 < 1 < (< - <, < < < < < < < < < < < < < < < < < < < < < < < < < < < < < < < < < < T < U A T < < < < < <

N

$! 6 : I 1 ; 1 N 0 I 6 ; :

2 ! 6 J K í e n 3 J n 0 v ! 1 J : ! i e J , J k a D 2 k n D J , b 4 " ! # 8 ! 7 D N N e , k

$ O ; k O u P 3 1 E 1 D 1 0 8 ; E 8 P y E 8 3 I L 1 L P E m D 8 3 y % R P 1 R 8 1 p N S % 2 y) 8 1 1 L P) S ; G S P 3

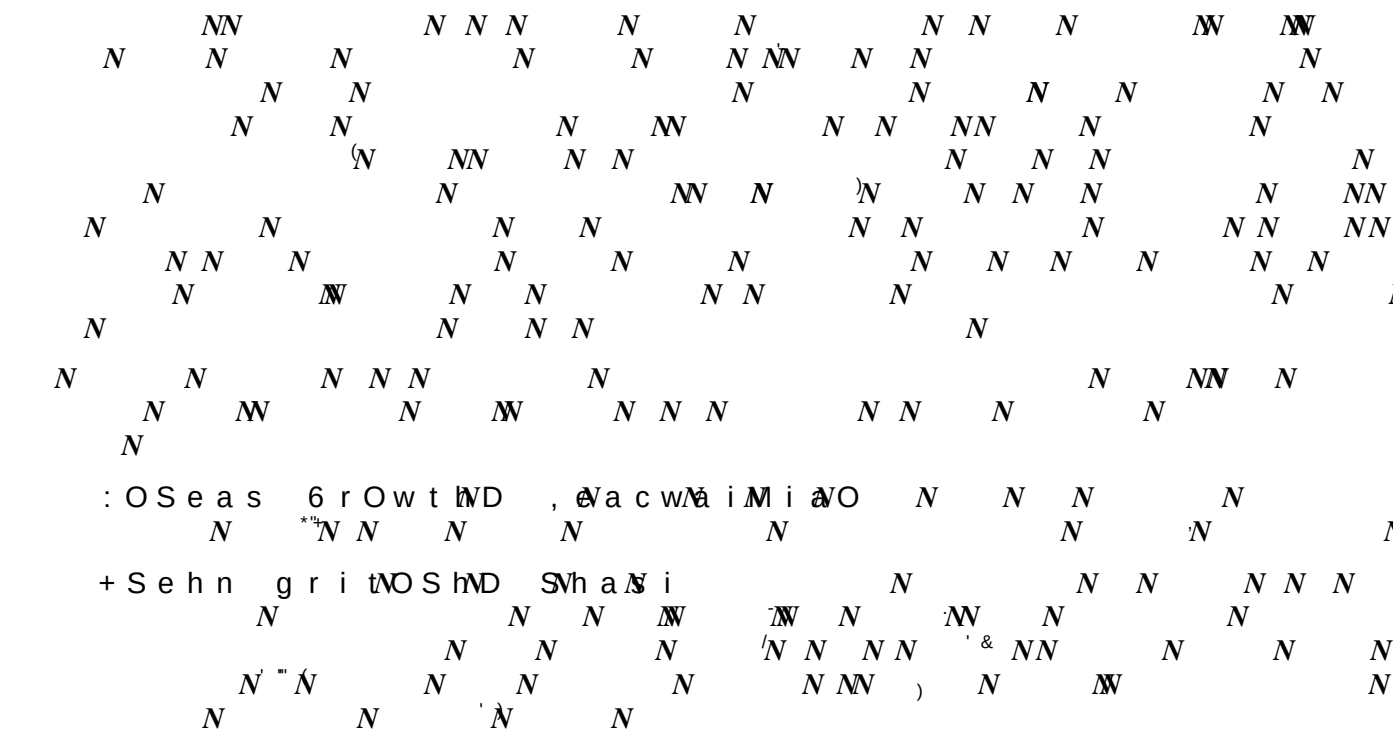
: S 2 y 8 v L P S % c í S E P

% O ; e & O P 3 1 / E , S 1 D 9 y E S P S 0 8 e 8 y S 8 1 2 3 y % S E S 3 = 3 8 1 L E ç p D E S P V D 8 b S + P , %) 1) *) : S

& < 8 í S 2 1 ç 8 P 1 L 6 R N 3 E y 3 % ; 0 L S v ç D ç 9 g h E 8 S P D q 8 P % E b i 8 8 2 U 3 E B 1 L N 2 % ó % * i . 8) U 9 B ç L 3

c 1 S 1 8 3

- 9 ; ; 2 < : 9 8 1 = 5 ç 8 S 3 E S 0 3 * E = 8 4 2 9 ' ; p ! S 2 y E S 0 8 S g S A L 8 P S P L í R L 1 L P E y 3 ' 8 3



: O S e a s 6 r O w t h D , e V a c w a i M i a O

+ S e h n g r i t O S h D S h a i

3 e a s 3 w c i O w M i

: O S e a s / w i D n . a h t i M i a O

: O S e a D e i t O S i e g a r w e t g i

1 w s : p g t i r O w o w D w O B O e . m O i a h D 7 i S O p o h O w e a

3 h S s i 5 e a D w a i h S 9 i g r e a g i

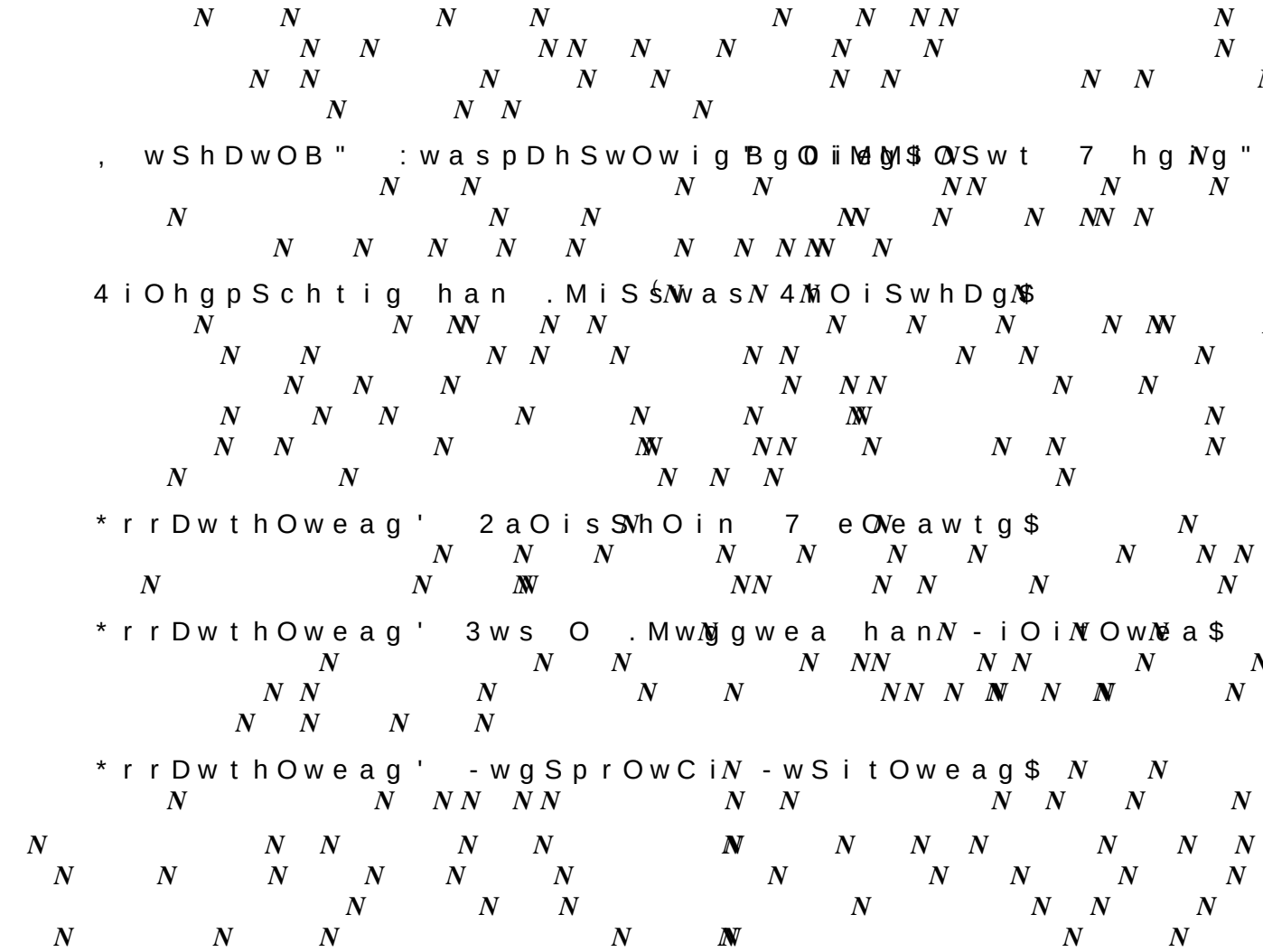
r e D h S w O e a g

/ p a n h M e a O & D g 7 e D h S w O e a g

, h S h t O i S w d h O w e a ; i t a w p i g

. m t w O e a g h a n & . i M w t e a n t O e S g

5 e a D w a i h S h a n < D O S h c h g O 6 r O w t h D 7 i a e M i a h



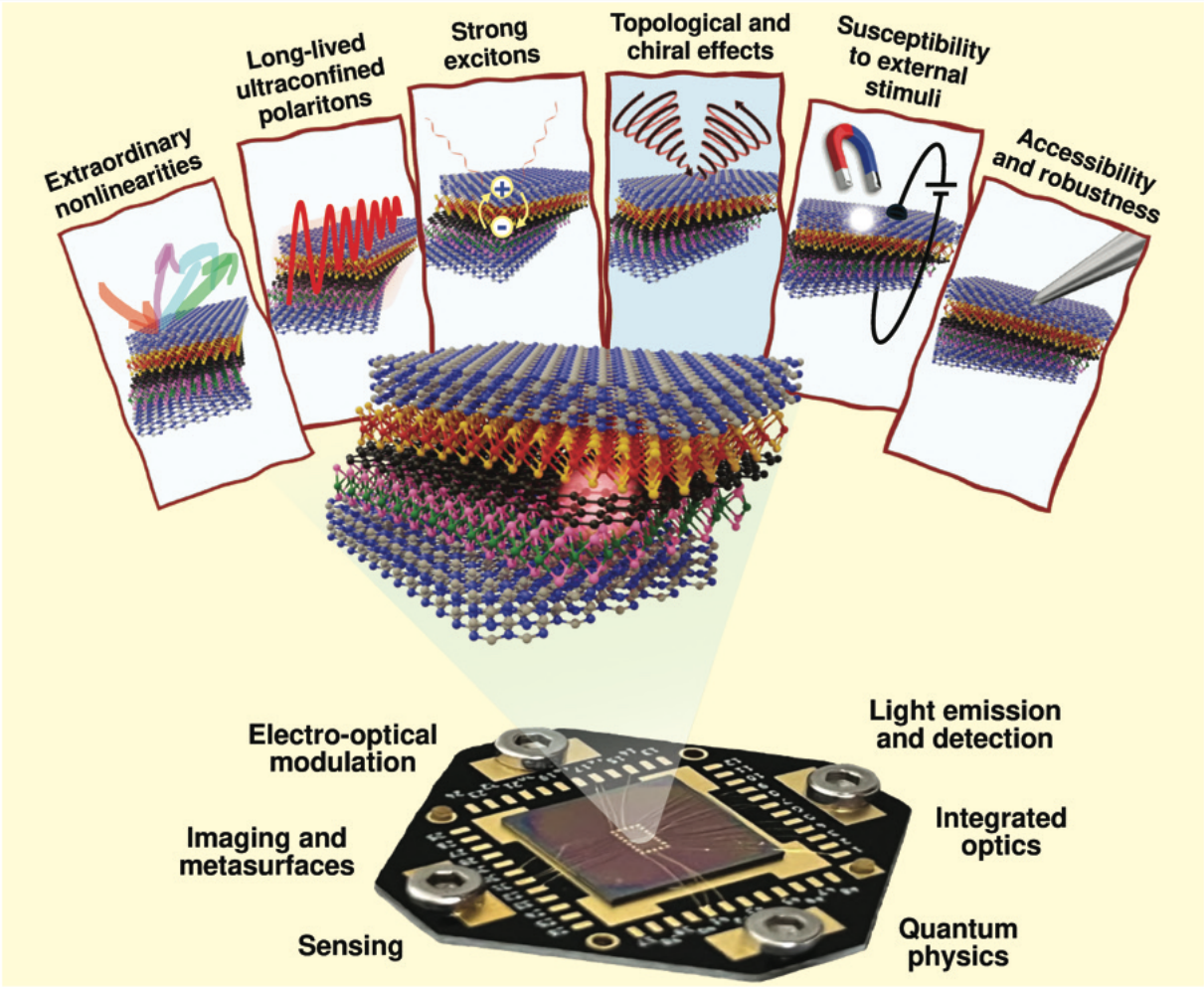


Figure 1. Chameleonic properties and uses of 2D materials. Driven by their exceptional properties and unique physical behavior (top), 2D materials are unlocking disruptive applications in photonics (bottom), as discussed in this Roadmap.

Fundamentals of 2D Polaritonics

This block describes the fundamentals of polaritons in 2D materials, which are understood here in a broad sense of material excitation modes that hybridize with light. This definition is in the spirit of Hopfield's pioneering work,[28] although the photonic component of 2D polaritons decreases with increasing in-plane wave vector, moving away from the light cone. In this sense, 2D polaritons permeate many other aspects of nanophotonics with 2D materials.

2. OVERVIEW OF 2D POLARITONICS

F. Javier García de Abajo[1,2,*]

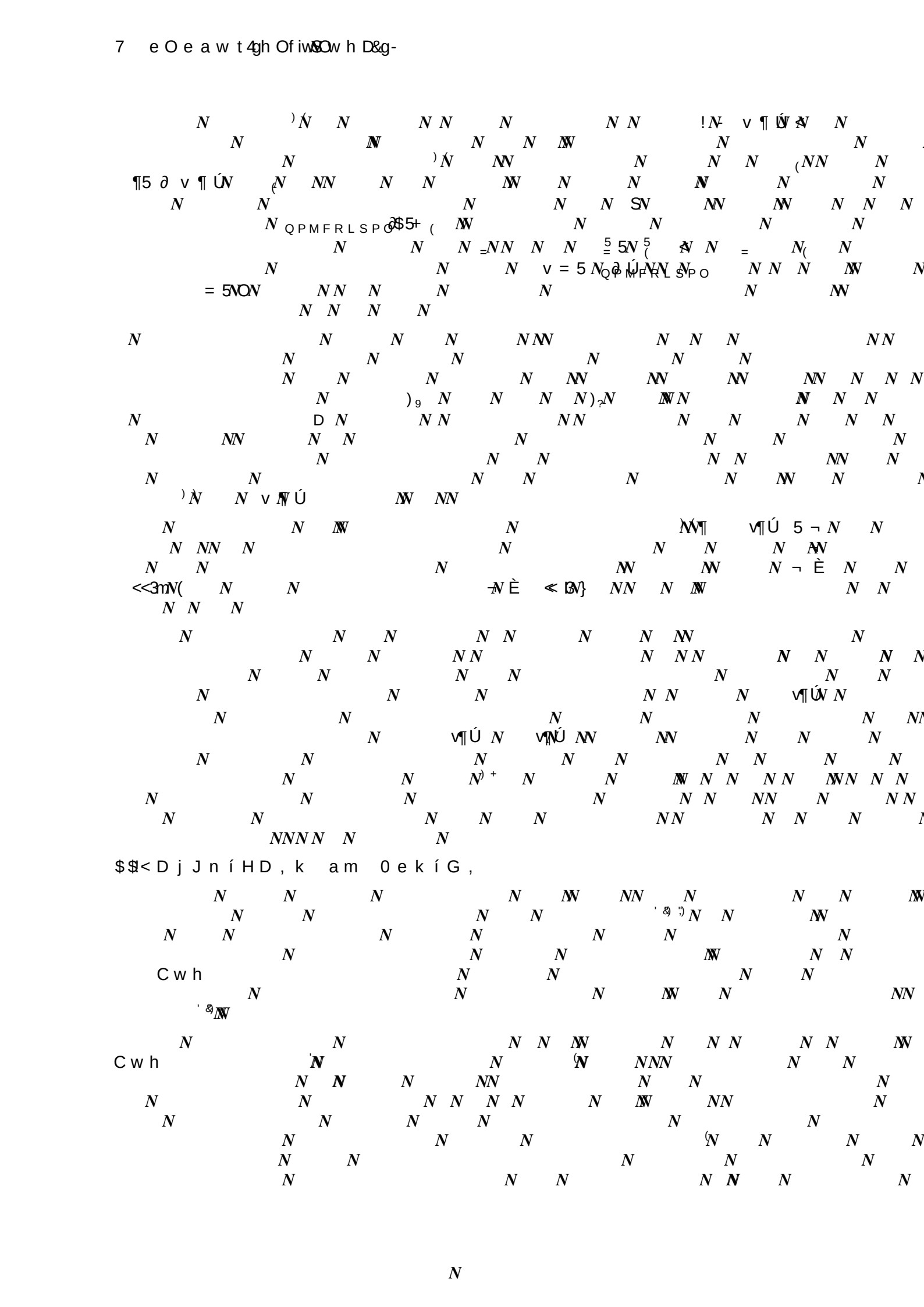
[1]ICFO-Institut de Ciencies Fotoniques, The Barcelona Institute of Science and Technology, 08860 Castelldefels, Barcelona, Spain

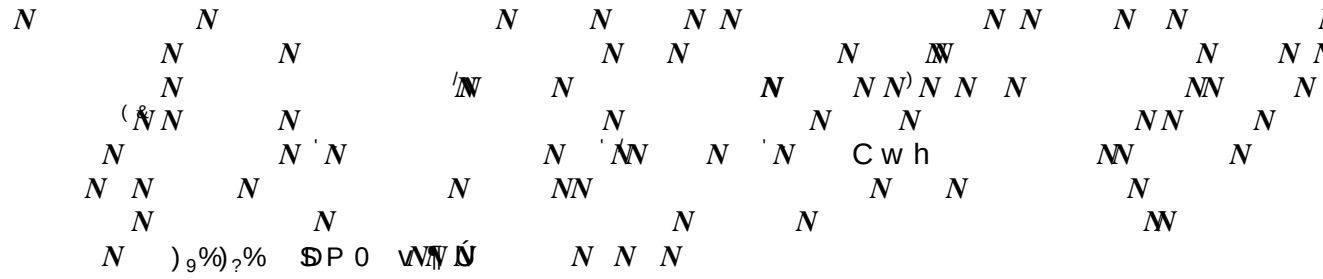
[2]ICREA-Institució Catalana de Recerca i Estudis Avançats, Passeig Lluís Companys 23, 08010 Barcelona, Spain

***Corresponding author.** Email: javier.garciadeabajo@nanophotonics.es

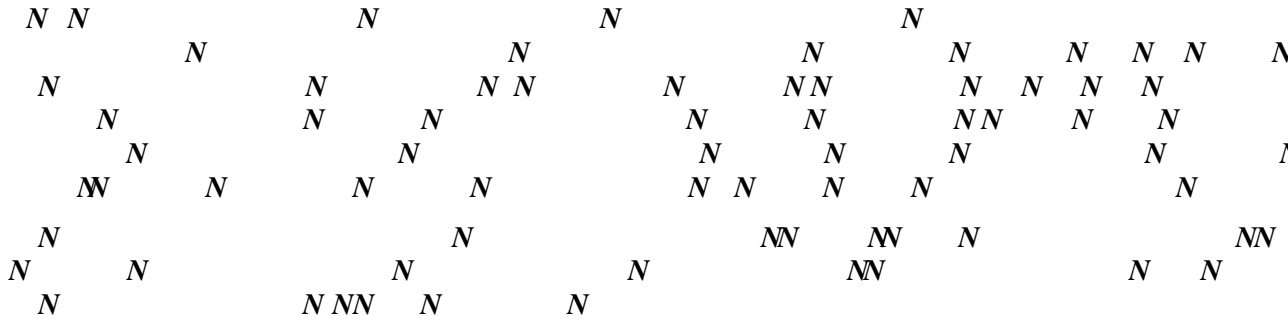
2.1 Local Description of 2D Polaritons

Polaritons are self-sustained charge oscillations mediated by electromagnetic interactions in different materials.[28] While nonlocality plays a substantial role in 2D plasmons when their wavelength is comparable to the Fermi wavelength (e.g., in extrinsically decorated[29] or laterally patterned[30] graphene, down to the molecular level[31]), the optical response of atomically thin 2D materials can be generally described through frequency-dependent surface conductivities $\sigma(\omega)$, ignoring nonlocal and out-of-

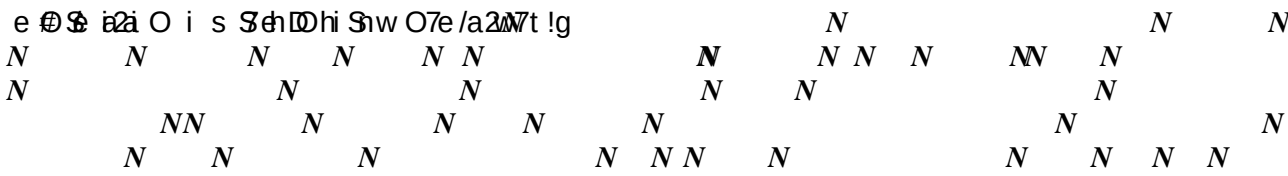




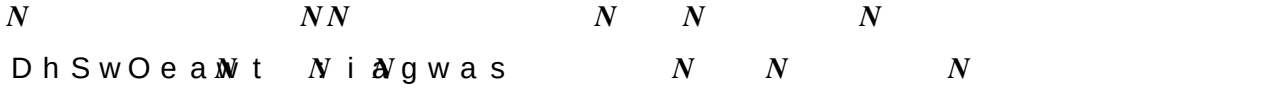
$%/ c J j j e , G e k J , i ; N N D n H L , í H í e k



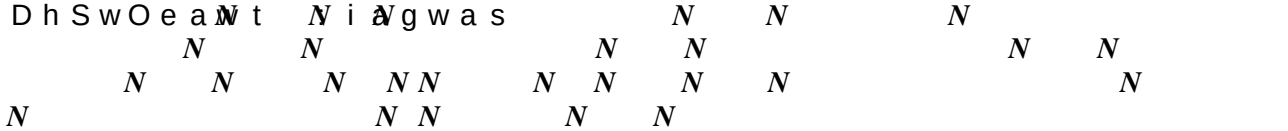
7 e eDSeiaaOisSzhDDhiSnwO7e/a2W7t!g



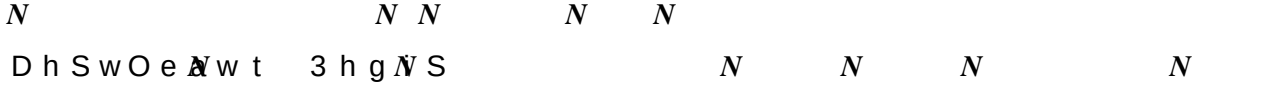
7eDhSwOeaWt NiaNgwas



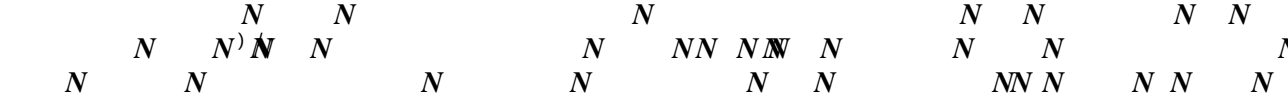
7eDhSwOeaWt 3hgNS



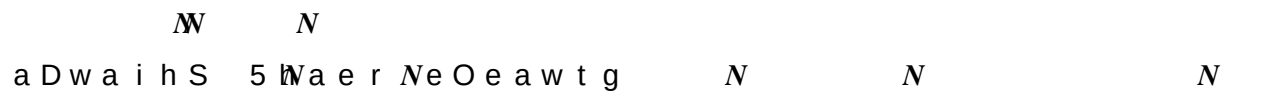
5eaDwaihS 5hNaerNeOeawtg



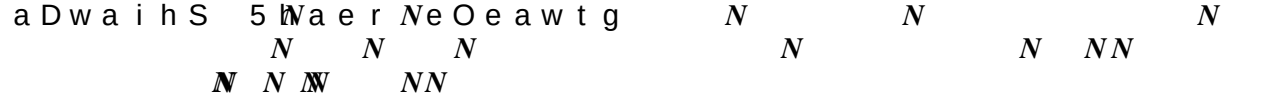
:wa#SDeiOea NMwOOiSg



2aOisShOin 8phaONpM 6NrOwtg%:iagwaNsN N



:Mh#DeDeOrSwaO 7NeOeniOiNOeSg



These items define an exciting research agenda with high potential for technological impact, stimulating the exploration of intriguing material properties and the discovery of novel phenomena associated with the two-dimensionality of these systems (see Sections 5 and 7).

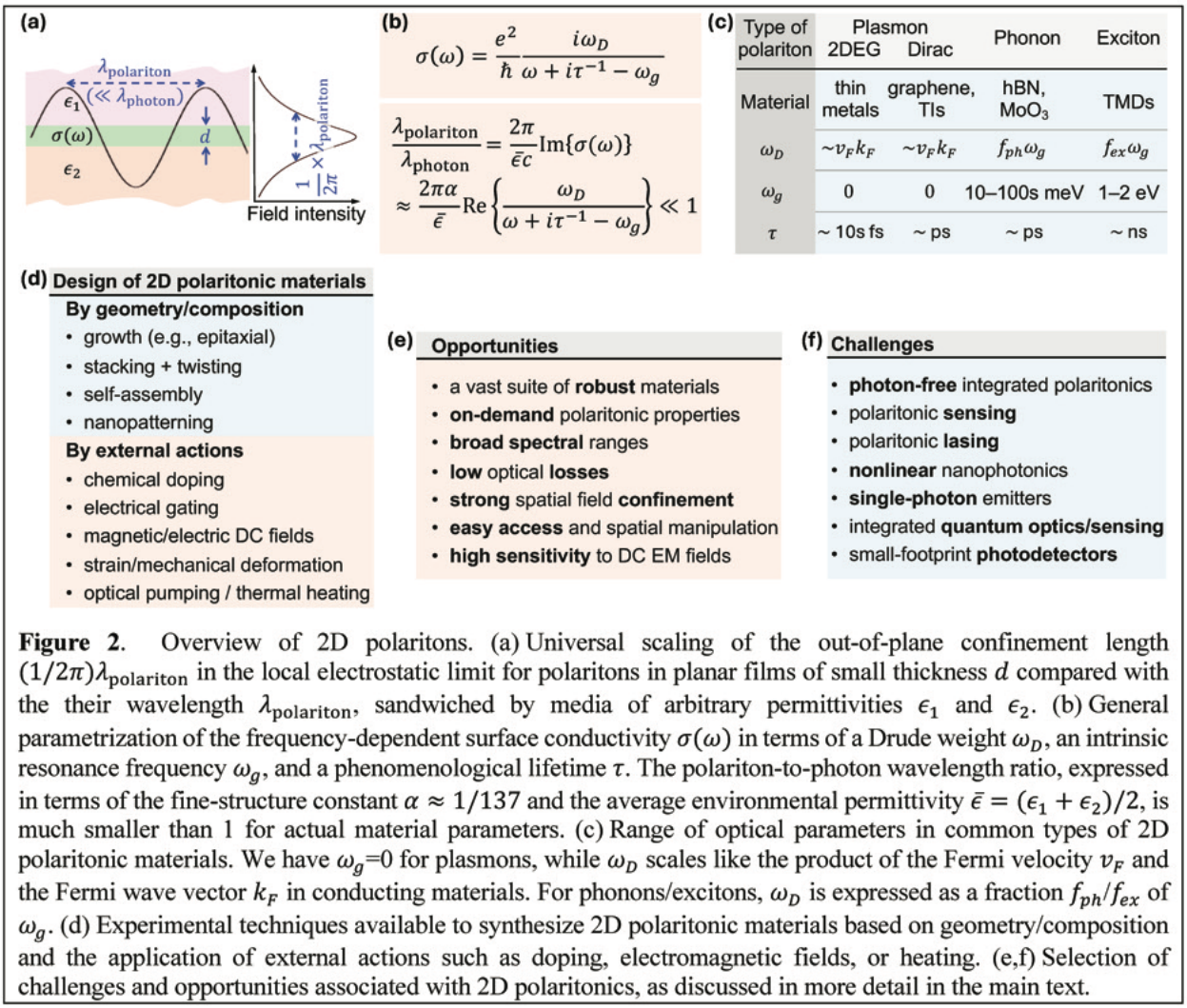


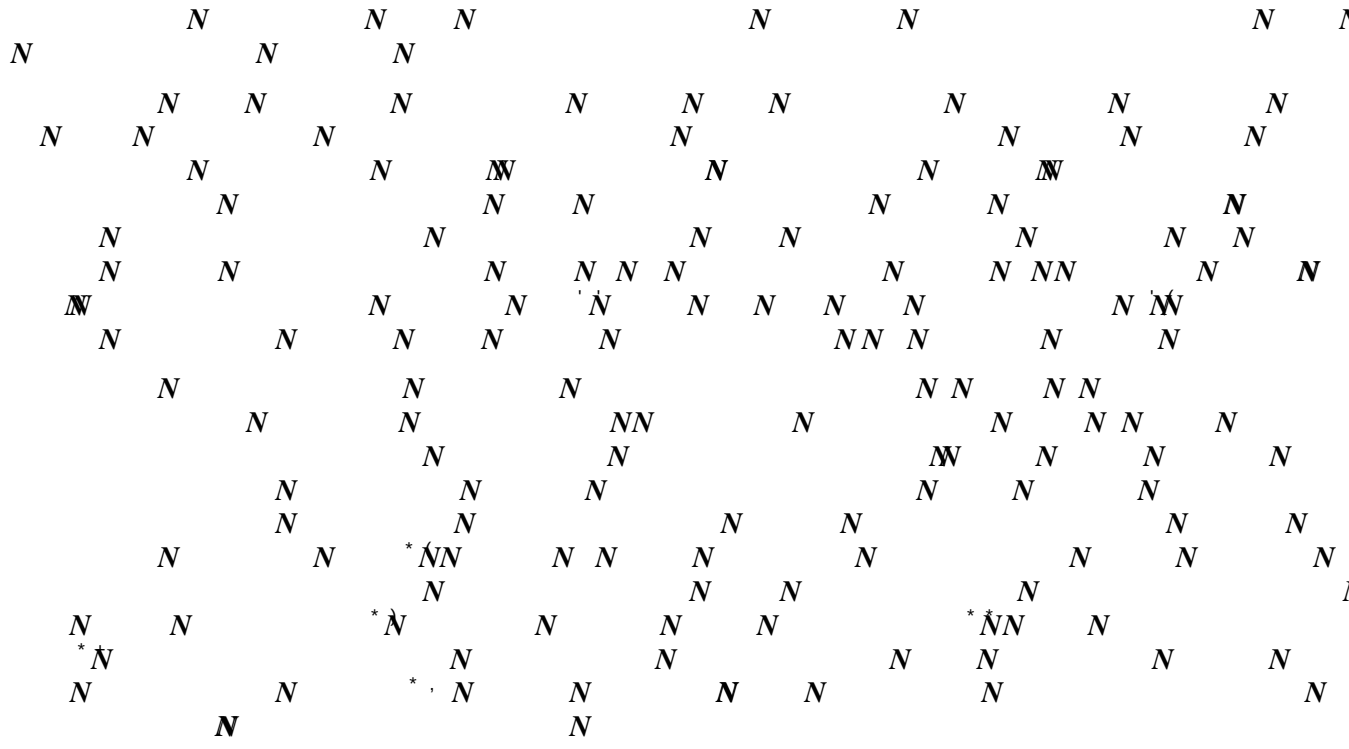
Figure 2. Overview of 2D polaritons. (a) Universal scaling of the out-of-plane confinement length $(1/2\pi)\lambda_{polariton}$ in the local electrostatic limit for polaritons in planar films of small thickness d compared with the their wavelength $\lambda_{polariton}$, sandwiched by media of arbitrary permittivities ϵ_1 and ϵ_2. (b) General parametrization of the frequency-dependent surface conductivity $\sigma(\omega)$ in terms of a Drude weight ω_D, an intrinsic resonance frequency ω_g, and a phenomenological lifetime τ. The polariton-to-photon wavelength ratio, expressed in terms of the fine-structure constant $\alpha \approx 1/137$ and the average environmental permittivity $\bar{\epsilon} = (\epsilon_1 + \epsilon_2)/2$, is much smaller than 1 for actual material parameters. (c) Range of optical parameters in common types of 2D polaritonic materials. We have ω_g=0 for plasmons, while ω_D scales like the product of the Fermi velocity v_F and the Fermi wave vector k_F in conducting materials. For phonons/excitons, ω_D is expressed as a fraction f_{ph}/f_{ex} of ω_g. (d) Experimental techniques available to synthesize 2D polaritonic materials based on geometry/composition and the application of external actions such as doping, electromagnetic fields, or heating. (e,f) Selection of challenges and opportunities associated with 2D polaritonics, as discussed in more detail in the main text.

3. GENERATION, DETECTION, AND STRONG COUPLING OF DEEP SUBWAVELENGTH HYPERBOLIC POLARITONS IN VAN DER WAALS MATERIALS

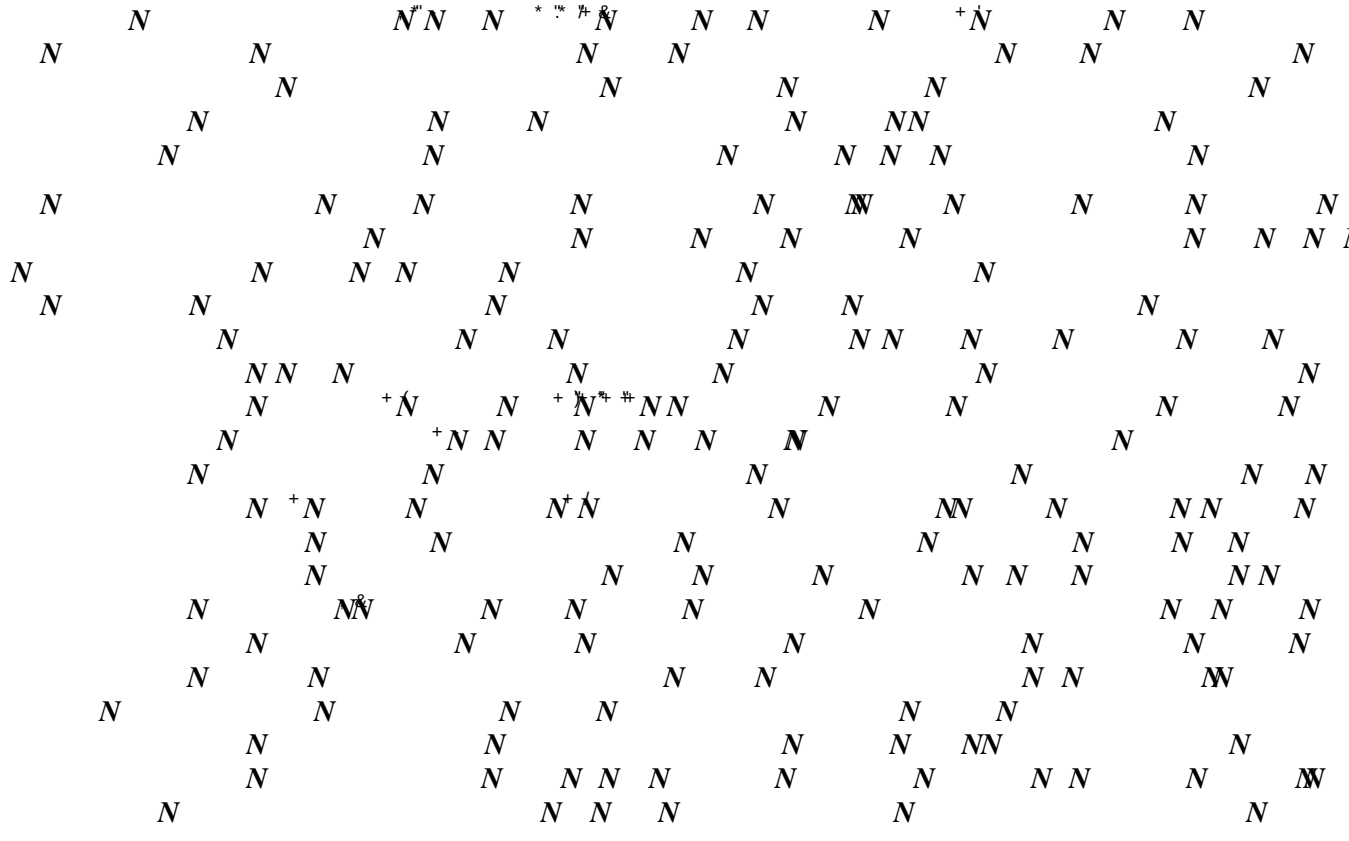
Lorenzo Orsini,[1] Matteo Ceccanti,[1] Sebastián Castilla,[1] and Frank L. H. Koppens[1,2,*]
[1]ICFO-Institut de Ciencies Fotoniques, The Barcelona Institute of Science and Technology, 08860 Castelldefels, Barcelona, Spain
[2]ICREA-Institució Catalana de Recerca i Estudis Avançats, Passeig Lluís Companys 23, 08010 Barcelona, Spain
***Corresponding author.** Email: frank.koppens@icfo.eu

3.1 Introduction

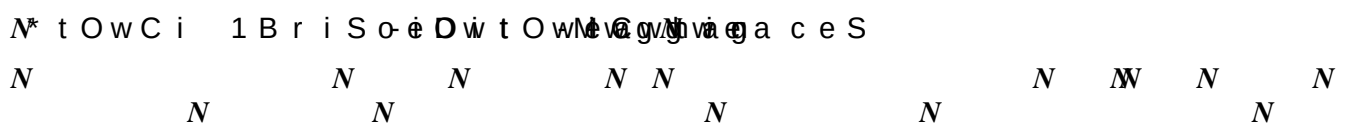
Hyperbolic materials are a special class of anisotropic media characterized by a dielectric permittivity tensor that has both positive and negative principal components within the same frequency range. Their discovery and exploration have been a significant breakthrough in nanophotonics for their ability to host hyperbolic polaritons, deep subwavelength electromagnetic waves with asymptotically large wave vectors, and extreme directional dependence. These features of hyperbolic polaritons can be readily visualized by comparing the isofrequency surfaces of an isotropic dielectric with those calculated for a hyperbolic material. Figure 3a shows the spherical isofrequency surface of an isotropic material, indicating that light can propagate with a finite wavelength in all directions. In contrast, as shown in Figure 3b, the isofrequency surface of a hyperbolic material takes on a more complex, open shape,

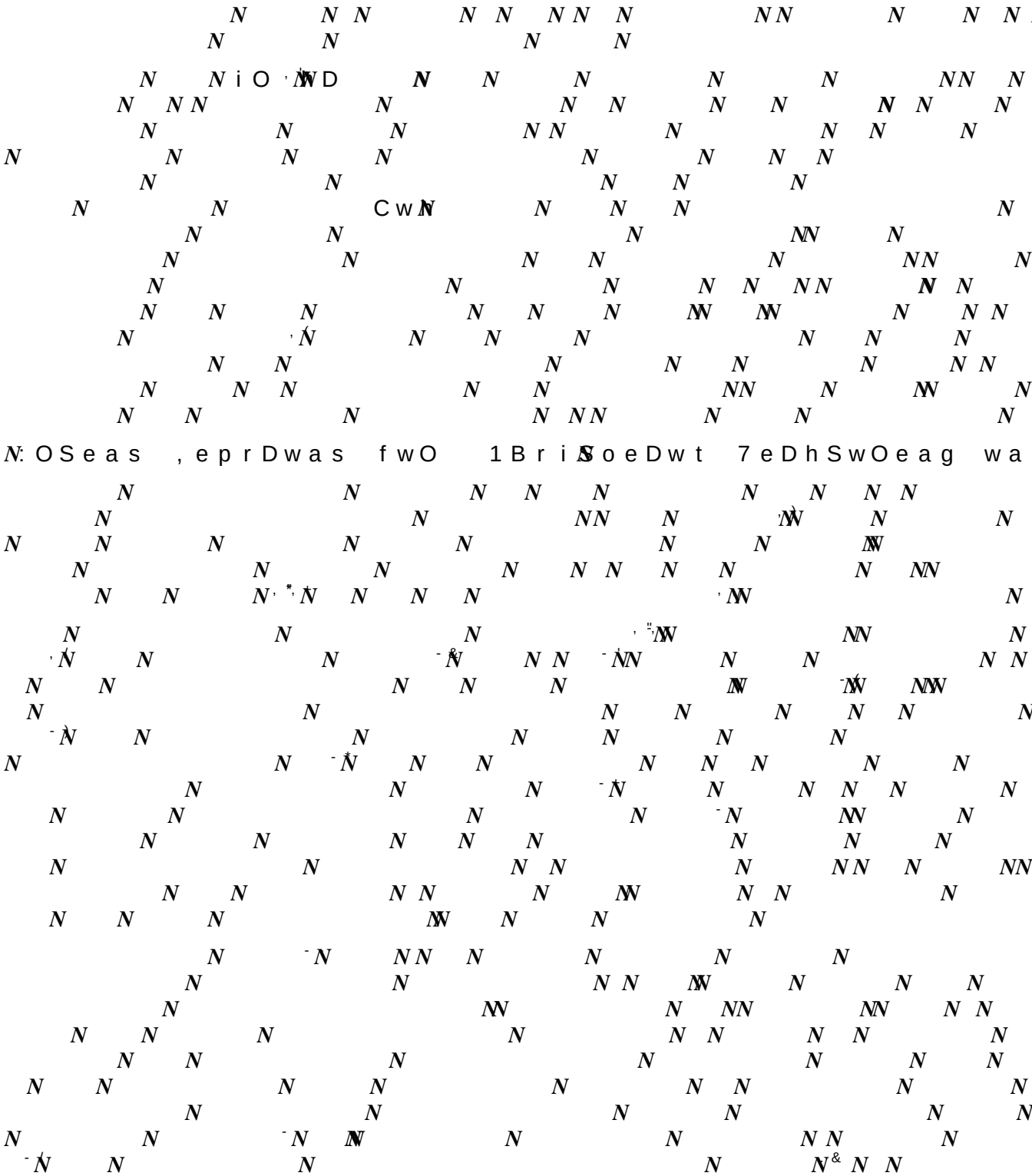


%! $mNenaDjív :J,DNcDHD,ívk



%!2%LHLne GDJjk





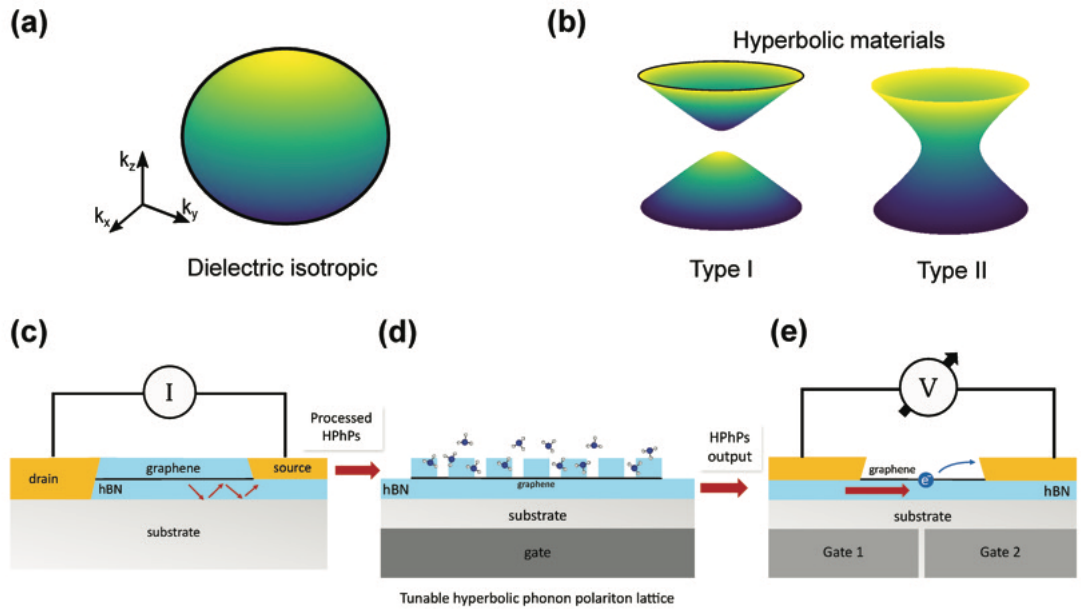


Figure 3. Illustration of isofrequency contours and the hyperbolic on-chip nanophotonic platform. (a) Isofrequency surface of a dielectric isotropic medium. (b) Isofrequency surface of a Type I hyperbolic material that is characterized by $\epsilon_{xx} = \epsilon_{yy} > 0$ and $\epsilon_z < 0$. Notably, for any pair of coordinates (k_x, k_y), it is always possible to find a point on the normal surface. (c) On-chip nanophotonic-platform generation: A high-bias current is driven through a graphene channel encapsulated with hBN, producing hyperbolic phonon polaritons (HPhPs) through electroluminescence. The schematic represents the cross section of a configuration in which HPhPs bypass the source contact and propagate for further processing. (d) On-chip nanophotonic-platform manipulation: A tunable polaritonic or topological crystal for molecule detection. The schematic illustrates the cross section of an hBN/graphene/hBN polaritonic lattice (hyperlattice) in which the polaritonic density of states can be electrically tuned by adjusting the gate voltage. This concept could enable molecular selectivity based on their interaction with the crystal lattice. (e) On-chip nanophotonic-platform detection: A graphene-based photo-thermoelectric detector. The schematic illustrates the processed HPhPs incoming from one side of the device being absorbed at the graphene PN junction defined by a split-gate structure. This absorption generates a photo-thermoelectric response, converting the polaritonic signal into an electrical output.

4. FUNDAMENTALS OF PLASMONS IN TWISTED 2D MATERIALS

Lorenzo Cavicchi[1,2] and Marco Polini[2,3,*]

[1]Scuola Normale Superiore, Piazza dei Cavalieri 7, I-56126 Pisa, Italy

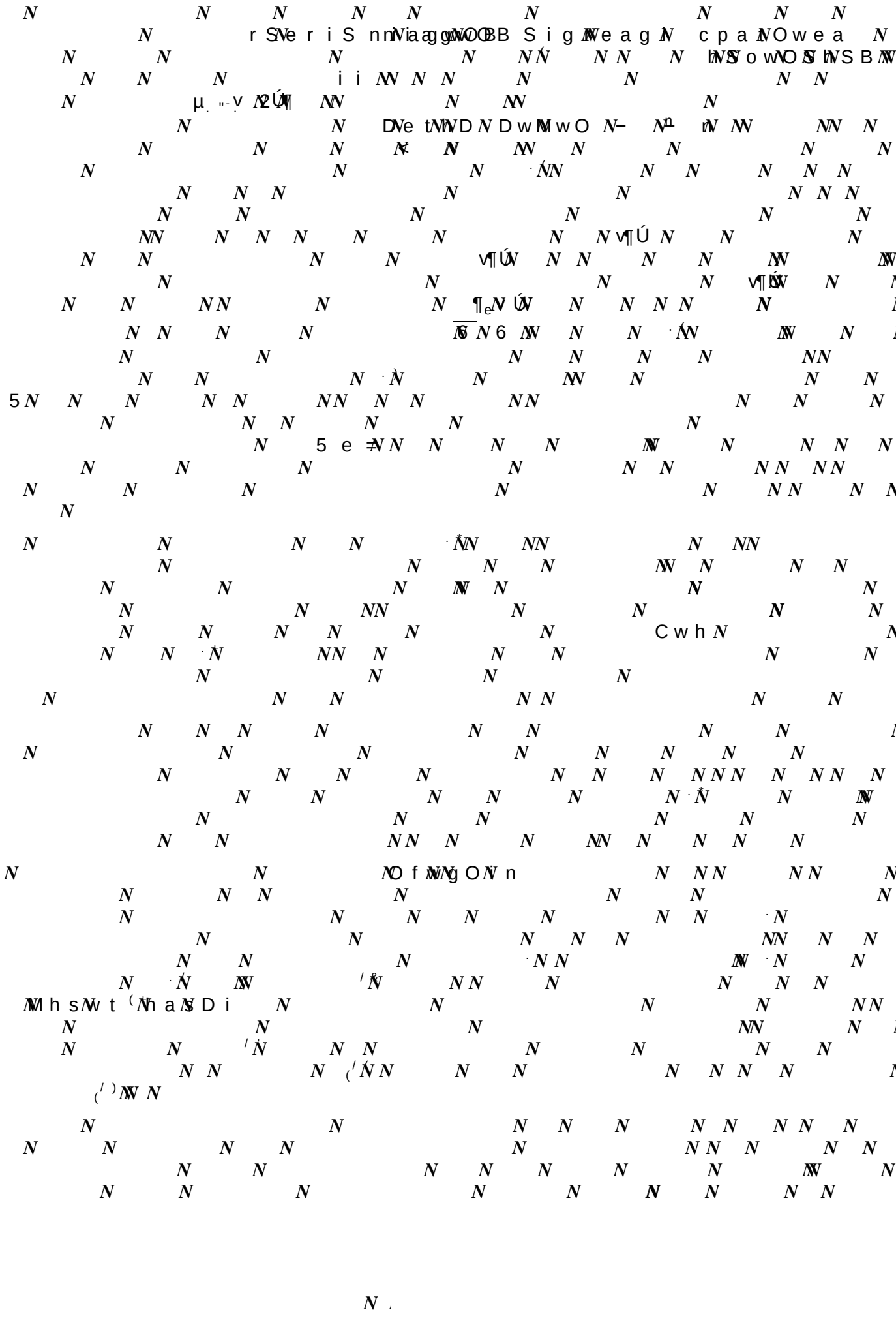
[2]Dipartimento di Fisica dell'Università di Pisa, Largo Bruno Pontecorvo 3, I-56127 Pisa, Italy

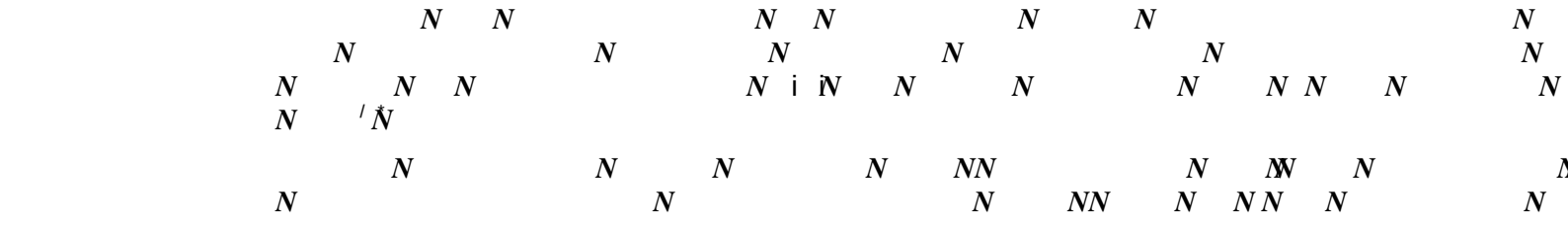
[3]ICFO-Institut de Ciencies Fotoniques, The Barcelona Institute of Science and Technology, 08860 Castelldefels, Barcelona, Spain

***Corresponding author.** Email: marco.polini@icloud.com

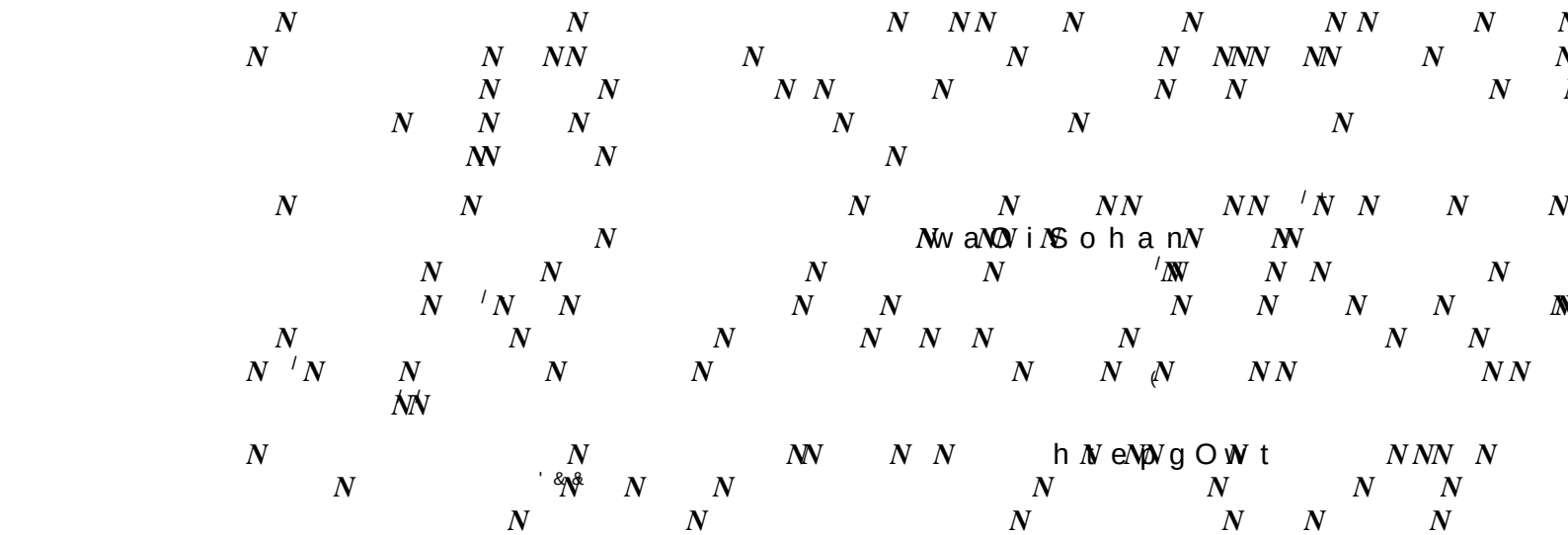
Plasmonics is a branch of optoelectronics that revolves around the excitation and manipulation of collective modes, known as *plasmons*, which arise from the interaction between electromagnetic fields and free electrons, typically at metallic or conductive interfaces. At the beginning of the 21st century, plasmons were seriously considered as potential candidates for revolutionizing technology, promising a new generation of superfast computer chips and ultrasensitive molecular detectors.[81]

But what is a plasmon? At a fundamental level, a plasmon is a pole of the density–density response function[82] $\chi_{\mathbf{G},\mathbf{G}'}(\mathbf{q},\omega)$, which is a causal (i.e., retarded) linear response function. Such a singularity, physically denoting a self-sustained oscillation of the electron density, emerges for certain values of the momentum $\hbar\mathbf{q}$ and energy $\hbar\omega$ transfer. The position of the pole in the $\mathbf{q}$ and ω plane, $\hbar\omega_p(\mathbf{q})$, is called the plasmon dispersion. In a crystal, the density–density response function also depends on two reciprocal lattice vectors, $\mathbf{G}$ and $\mathbf{G}'$.[82] This matrix form in reciprocal lattice space is crucial to capture crystalline local field effects (LFEs).

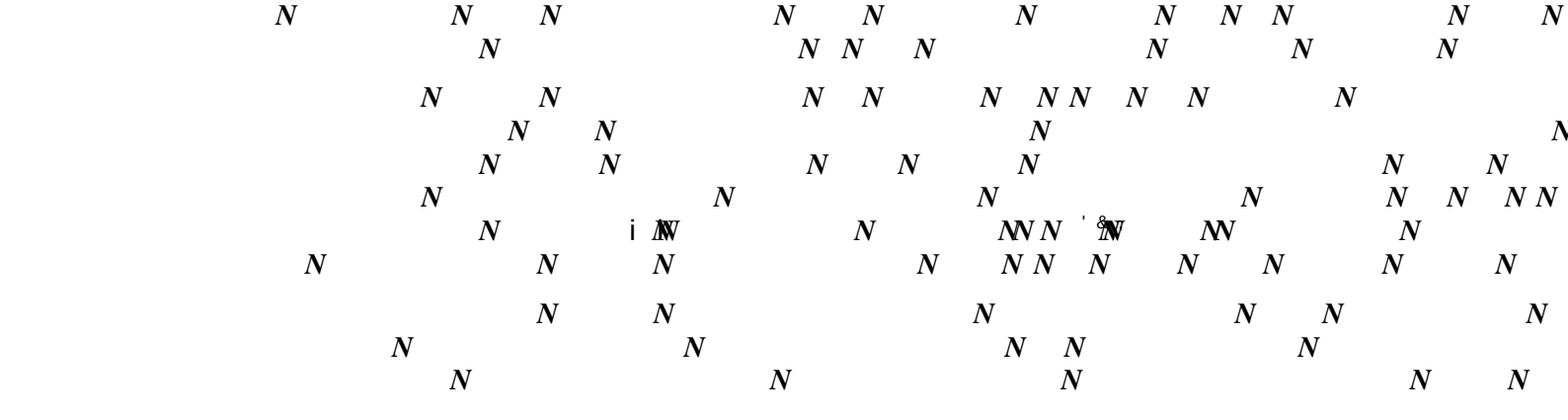


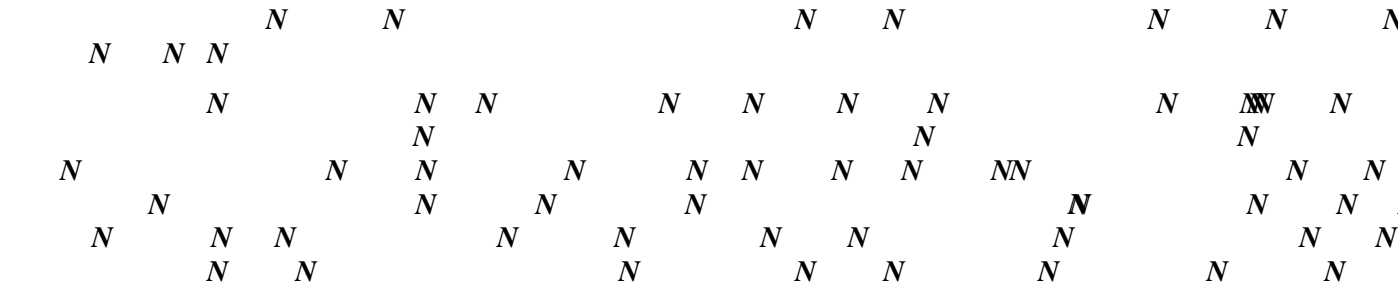


&! # / LB HnJ H ke t e H

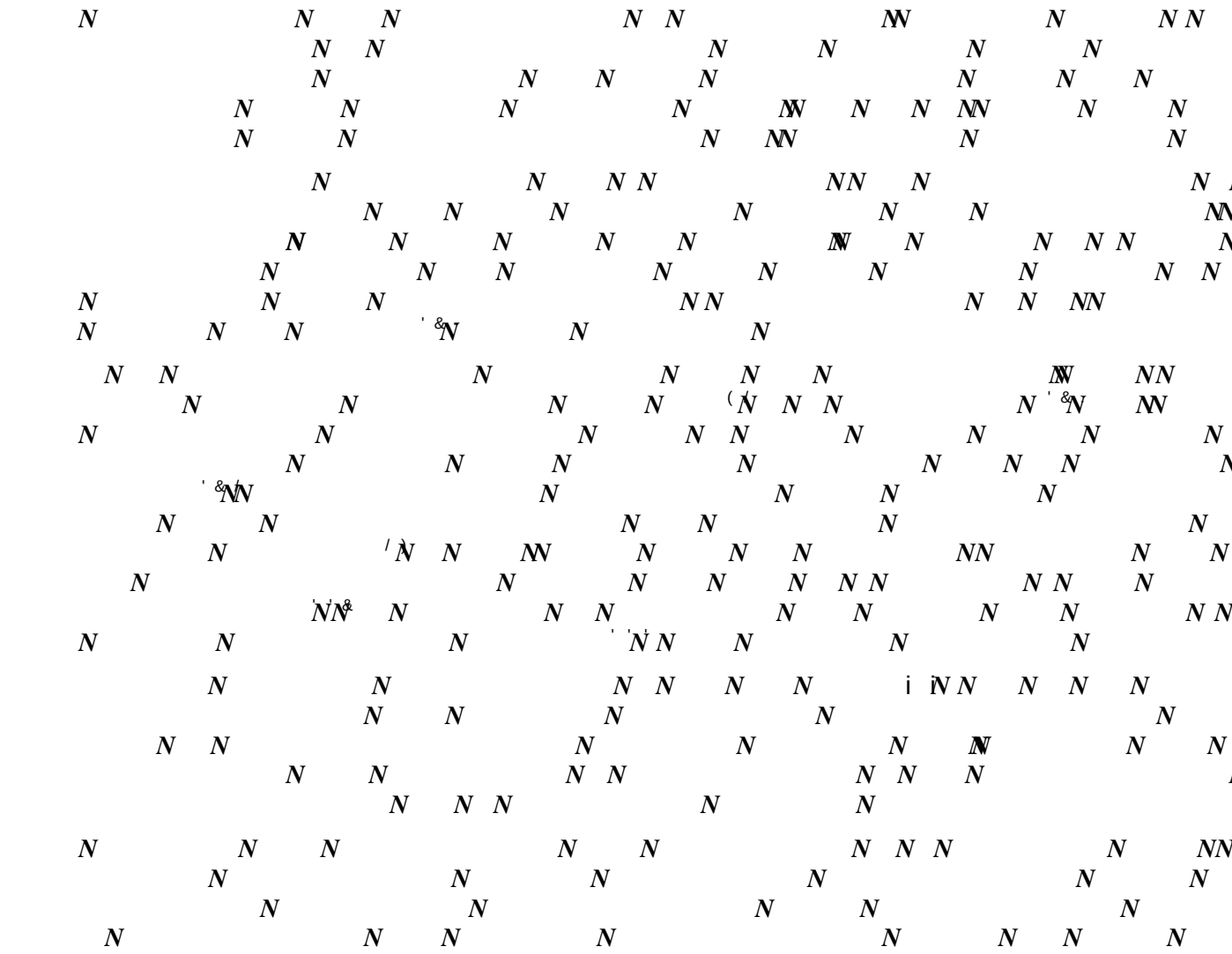


&! $ / c J j j 2e L, H Gle k a jJ i





&! % B L GOGíenkeHveHíÝ Ð e,3HD JHjDk



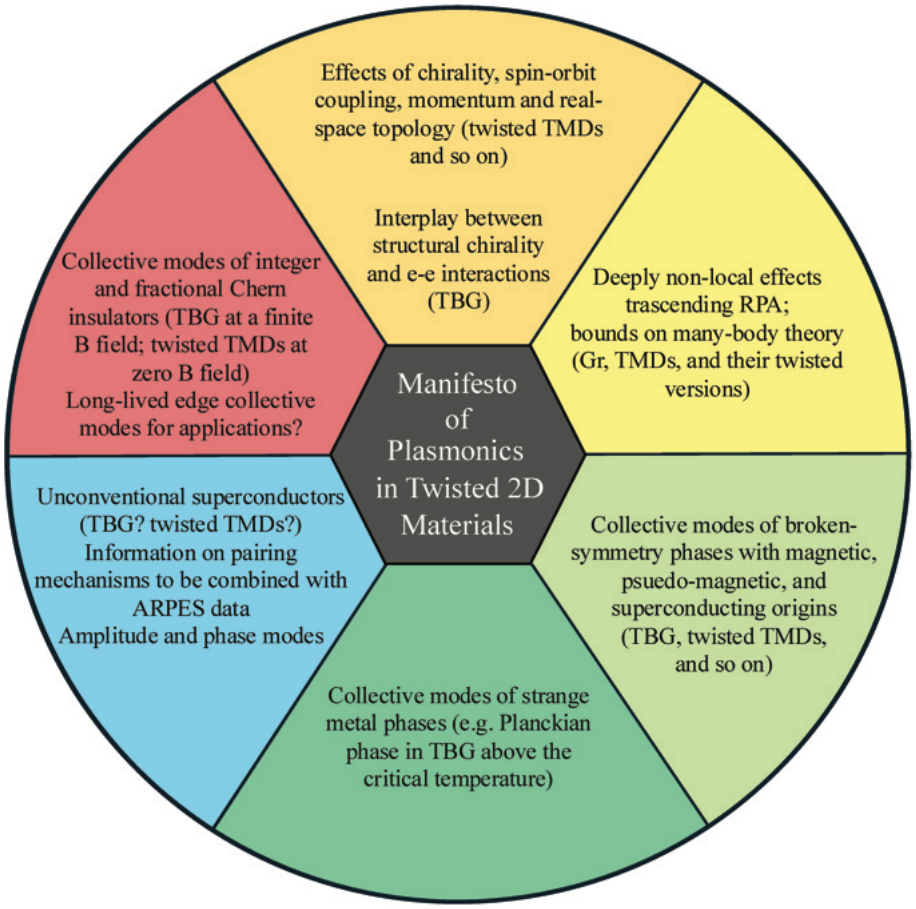


Figure 4. Manifesto of plasmonics in twisted 2D materials. We list future challenges and potential outcomes of plasmonics applied to twisted 2D materials.

5. 2D POLARITONS FOR PROBING NONLOCAL EFFECTS AND COLLECTIVE MODES IN CONDENSED MATTER

P. A. D. Gonçalves,[1,*] A. T. Costa,[2] N. M. R. Peres,[3,4] and N. Asger Mortensen[4,5]

[1]ICFO-Institut de Ciencies Fotoniques, The Barcelona Institute of Science and Technology, Castelldefels (Barcelona) 08860, Spain

[2]International Iberian Nanotechnology Laboratory (INL), Av Mestre José Veiga, 4715-330 Braga, Portugal

[3]Centro de Física (CF-UM-UP) and Departamento de Física, Universidade do Minho, P-4710-057 Braga, Portugal

[4]POLIMA—Center for Polariton-driven Light–Matter Interactions, University of Southern Denmark, Campusvej 55, DK-5230 Odense M, Denmark

[5]Danish Institute for Advanced Study, University of Southern Denmark, Campusvej 55, DK-5230 Odense M, Denmark

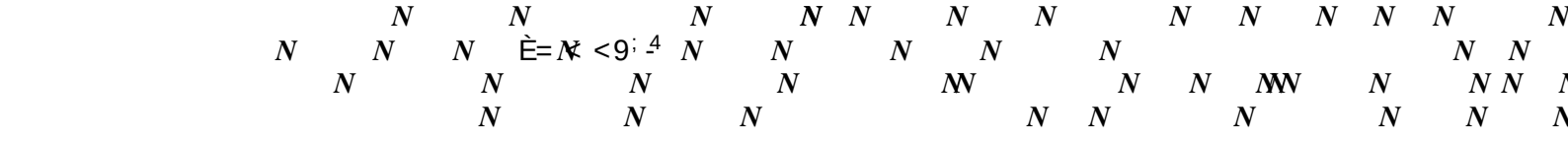
***Corresponding author.** Email: padgo@mci.sdu.dk

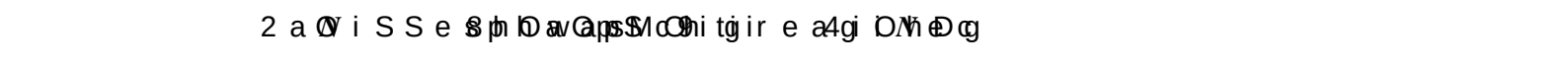
5.1 Current State of the Art

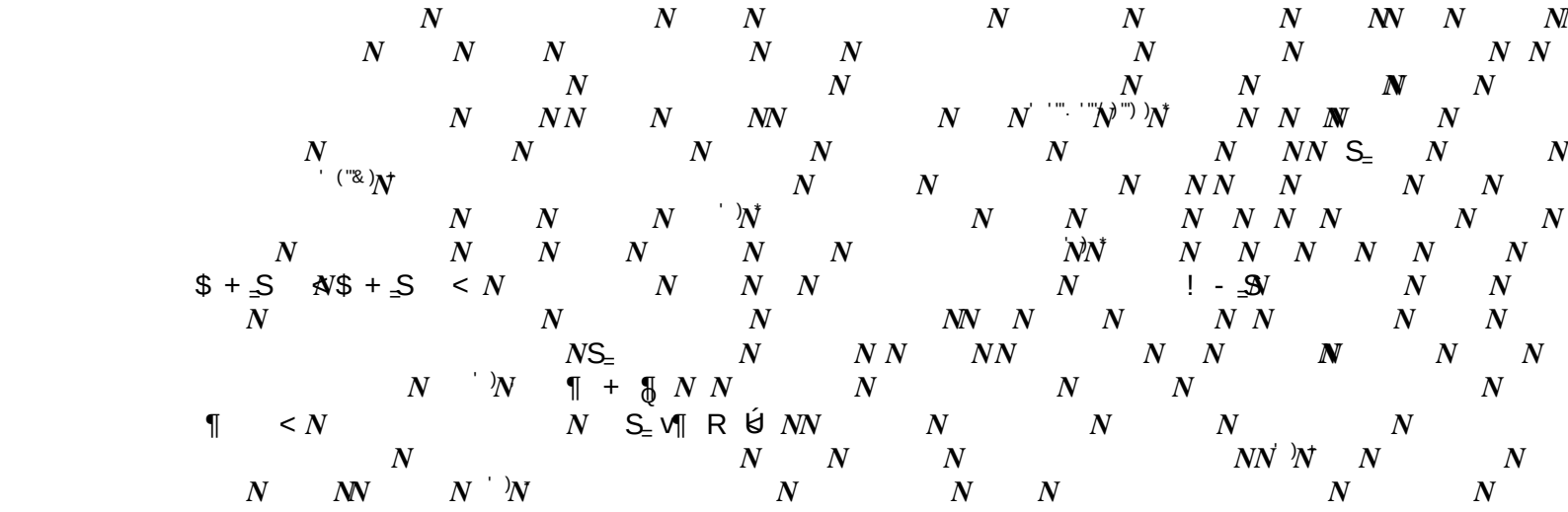
The interaction between electromagnetic radiation and charged particles is a central and recurring problem in condensed-matter physics and nanophotonics. Notably, this interaction can be significantly enhanced by exploiting polaritons, formed through the hybridization of photons with collective oscillations of polarization charges in materials[112] (e.g., plasmons, optical phonons, excitons). Polaritons enable the confinement of electromagnetic fields below the diffraction limit, leading to enhanced light–matter interactions.[113] Over the past few decades, this property has been exploited for various purposes, including the realization of subwavelength nanophotonic circuitry and the control of emitter dynamics. More recently, the advent of 2D materials—such as graphene, hBN, and TMDs—and related vdW heterostructures[63,114] (vdWH) has significantly expanded the range of possibilities for polariton-

8 ph a epaM Dec t h D t0S g r w a i a i

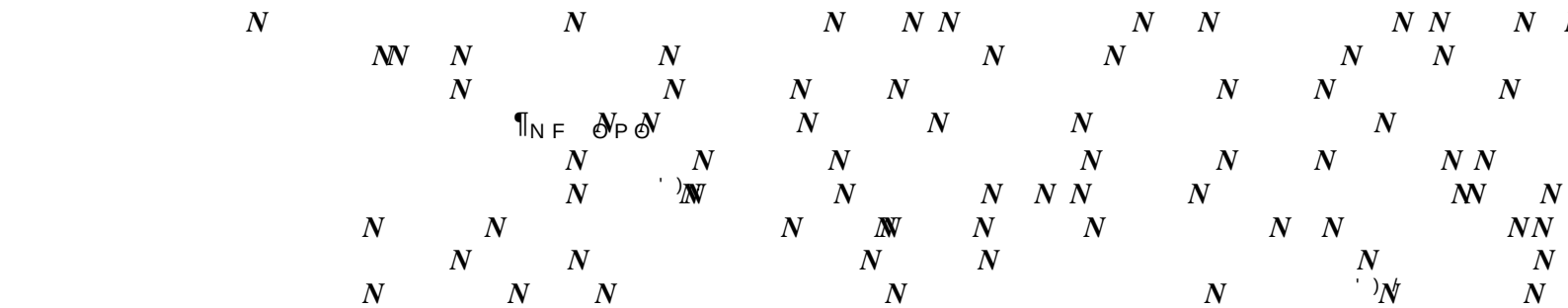
7 S e o,ve a D i 4teOnwiCgip rwiaS t e a n p t O e S g



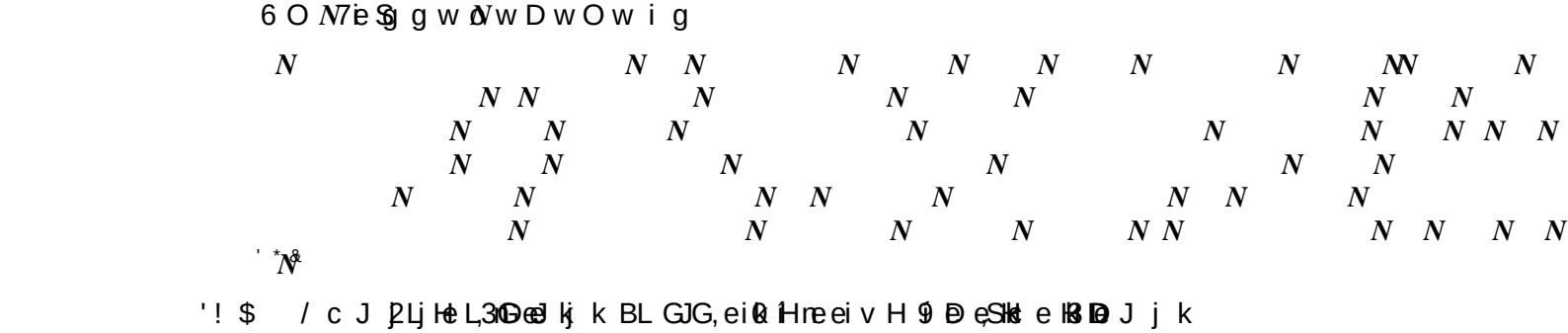


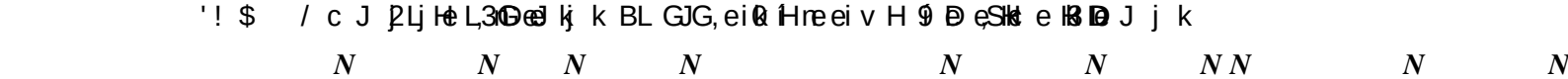




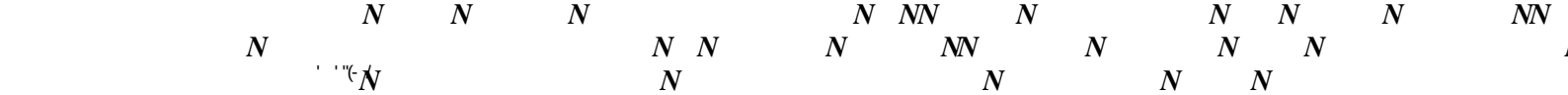






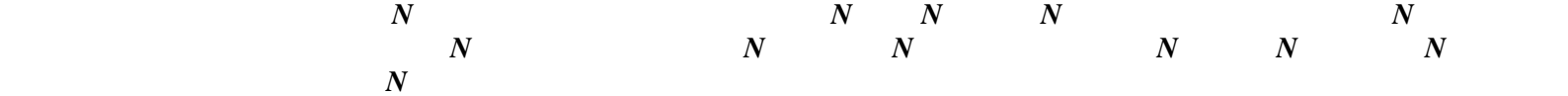




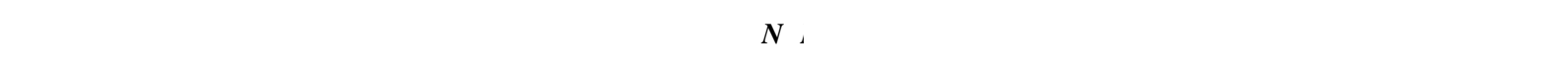


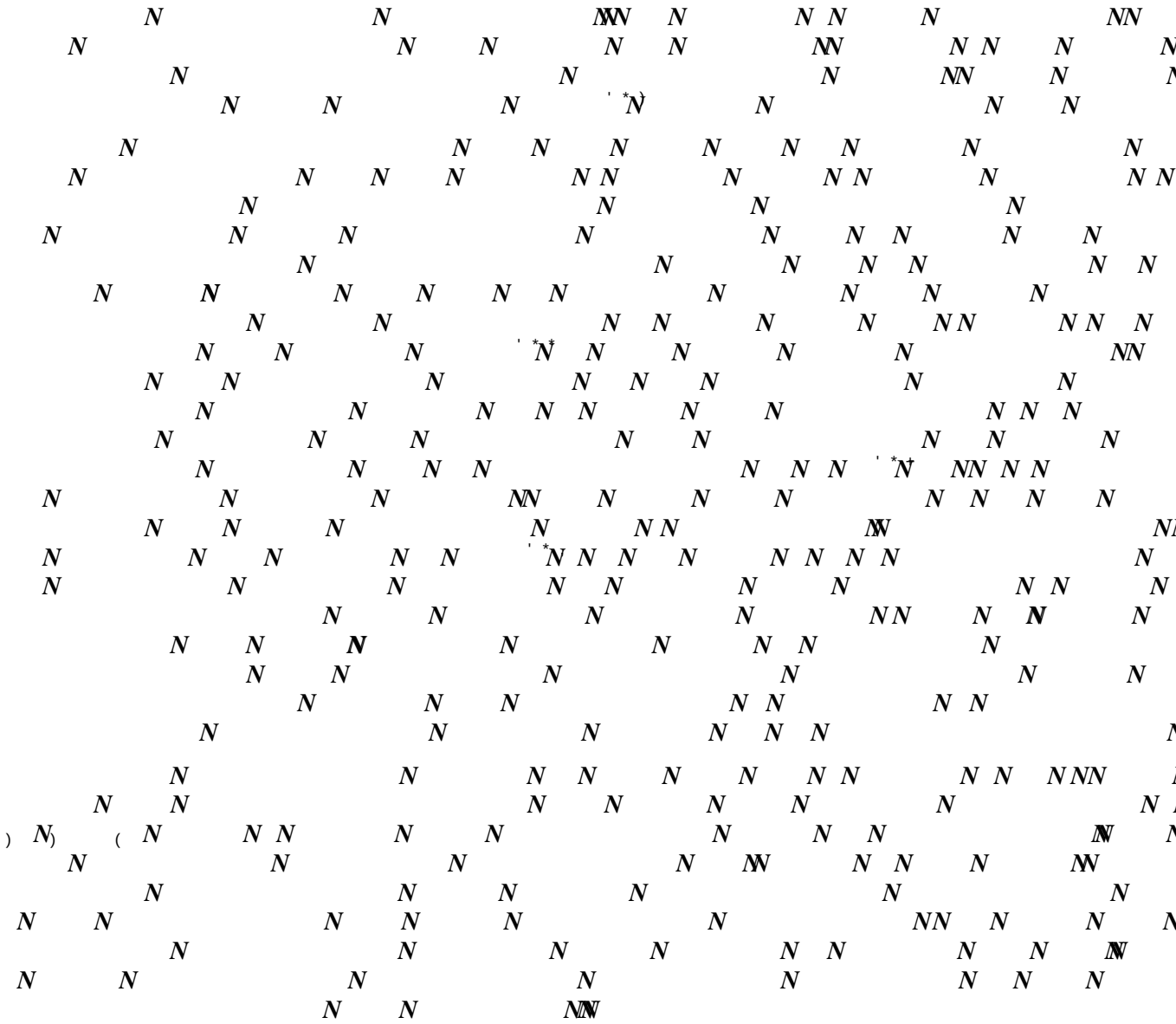












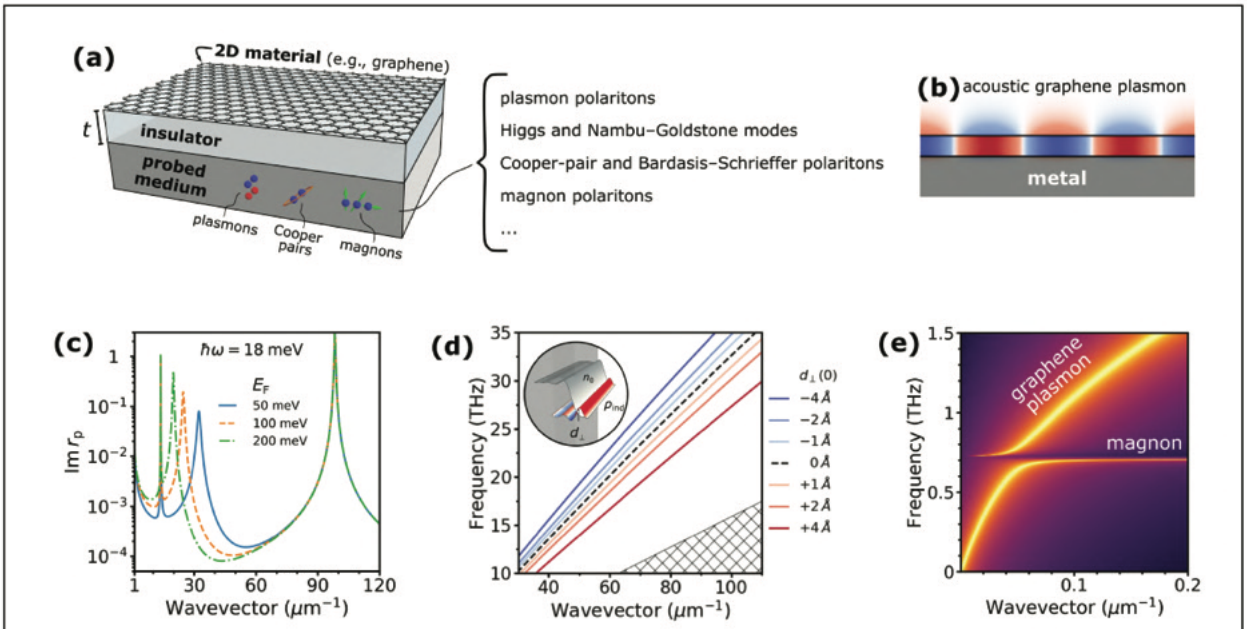


Figure 5. Harnessing ultraconfined graphene plasmons to probe collective excitations and strongly correlated phenomena in condensed-matter systems. (a) Schematic of a 2D material (here represented by graphene) in the vicinity of a probing material, separated by a thin insulating slab. The field provided by the 2D polaritons can couple to quasiparticles in the nearby medium, thereby probing the response and collective excitations of the material. (b) Illustration of the out-of-plane component of the electric field associated with acoustic graphene plasmons (AGPs) in a graphene–dielectric–metal (GDM) configuration. (c) Collective modes, emerging as features in Im r_p, of a 2DSC–G–2DSC heterostructure. The 2D superconductors (2DSC) is FeSe, with a superconducting gap of 23 meV at zero temperature and supporting a Bardasis–Schrieffer mode at 18.2 meV. See ref 124 for details. (d) Dispersion relation of AGPs in a GDM configuration. The metallic quantum surface response (encoded through the Feibelman $d_\perp$-parameter; see inset) leads to sizable spectral shifts, underscoring the potential of AGPs to infer quantum nonlocal effects in nanoplasmonics. Adapted with permission from ref 134 (Copyright 2021 Springer Nature). (e) Dispersion relation exhibiting the hybridization between graphene plasmons and the uniform ($q = 0$) magnon mode of monolayer CrI_3 in a heterostructure composed of three single layers: graphene–hBN–CrI_3. Adapted with permission from ref 126 (Copyright 2023 American Chemical Society).

6. MAXWELL HAMILTONIAN IN 2D MATERIALS

Sathwik Bharadwaj[1] and Zubin Jacob[2,*]

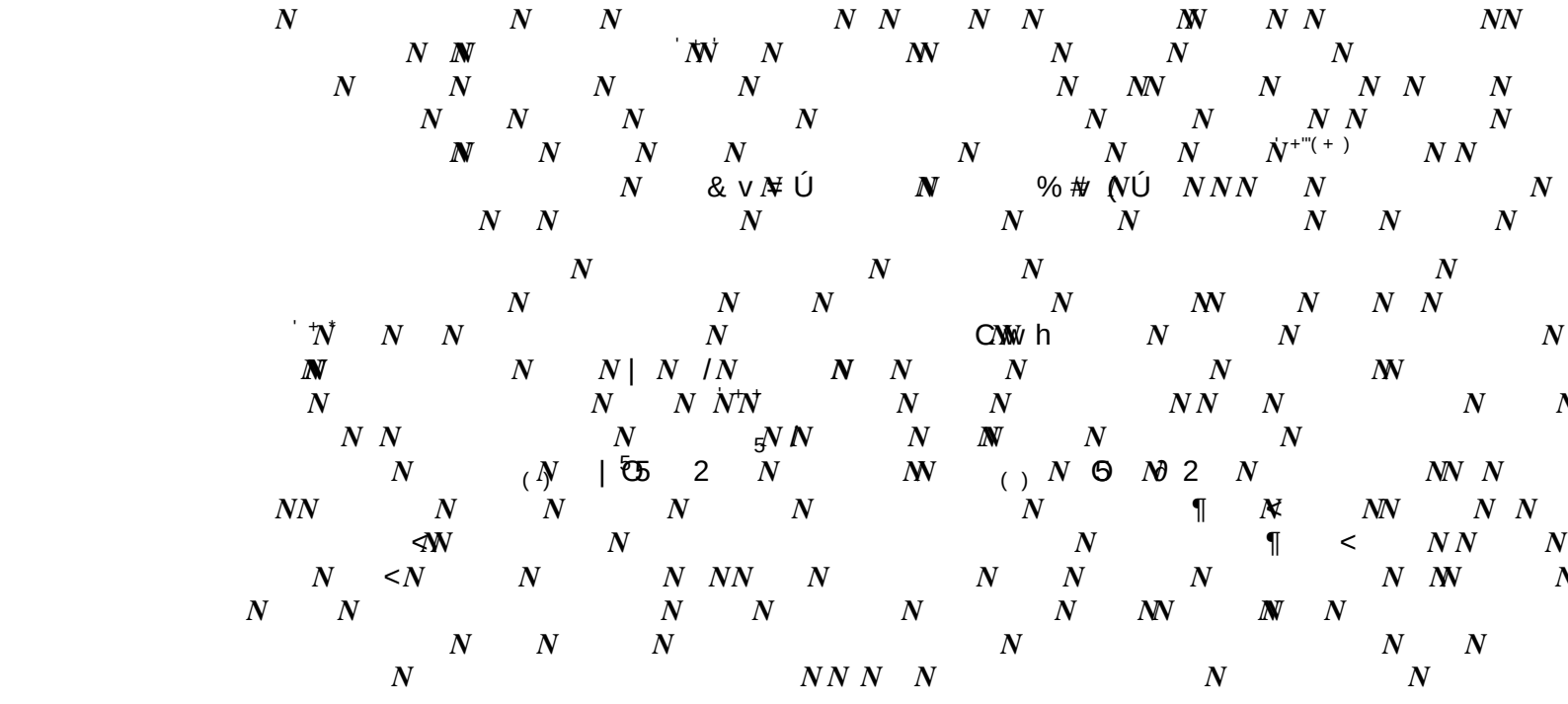
[1]Elmore Family School of Electrical and Computer Engineering, Birck Nanotechnology Center and Purdue Quantum Science and Engineering Institute, Purdue University, West Lafayette, Indiana 47907, United States

[2]Elmore Family School of Electrical and Computer Engineering, Birck Nanotechnology Center and Purdue Quantum Science and Engineering Institute, Purdue University, West Lafayette, Indiana 47907, United States

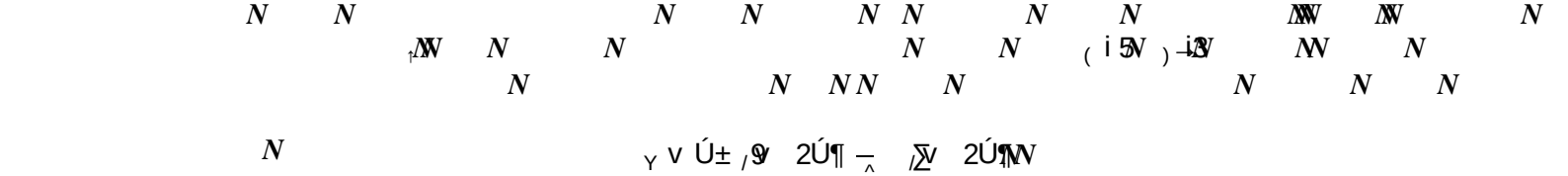
***Corresponding author.** Email: zjacob@purdue.edu

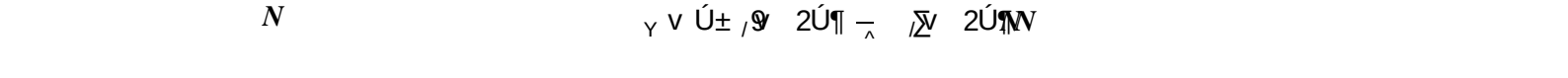
6.1 Introduction

Nanophotonics—the study of light–matter interaction at length scales smaller than the wavelength of radiation—has widespread applications ranging from plasmonic waveguiding[147] and topological photonic crystals[148] to super-lensing.[149] Nanophotonic structures are artificial materials made up of two or more dielectric constituents. The wave dynamics governing these structures can be effectively described by the classical Maxwell equations in continuous media. In contrast, it has been a long-standing problem for more than 40 years to understand the dynamics of optical waves within a crystalline material at the lattice level.[150] For the past century, manifestations of the Schrödinger, Dirac, and Frohlich Hamiltonians have pushed the frontier in the discovery of numerous electronic and phononic phases of 2D materials. It is pertinent to ask what role crystal symmetries play in light–matter interactions and whether a description shift emerges at the sub-nanometer regime in crystalline materials. To address this, we have introduced a Maxwell-Hamiltonian theory of matter combined with a quantum theory of deep microscopic optical polarization.

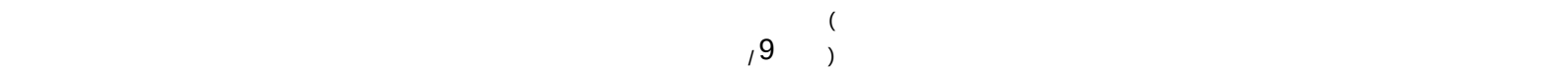




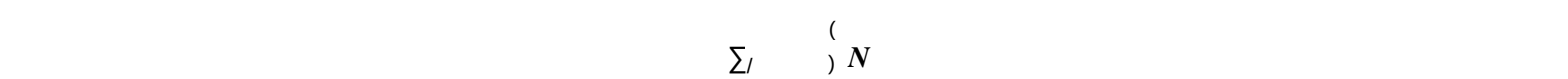




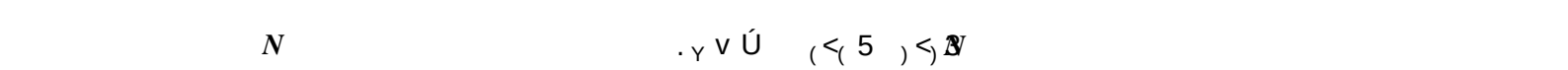


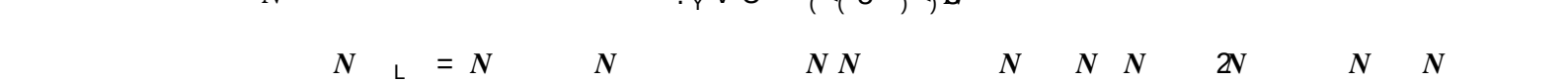


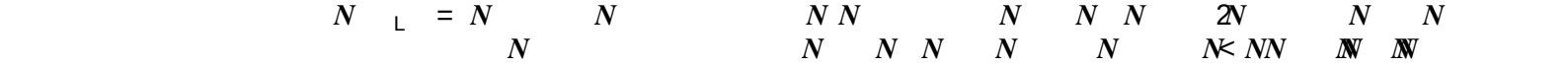




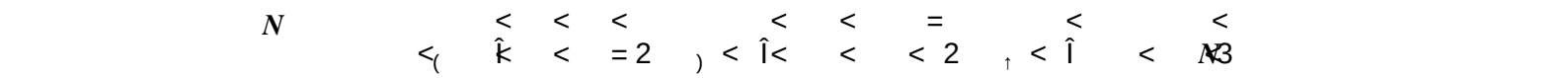


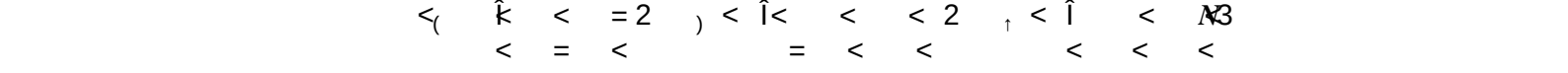




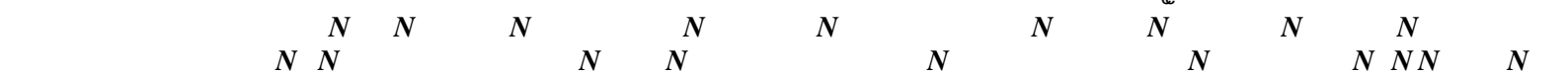




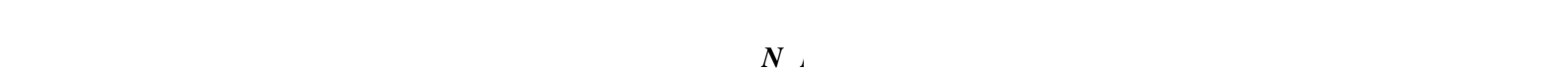


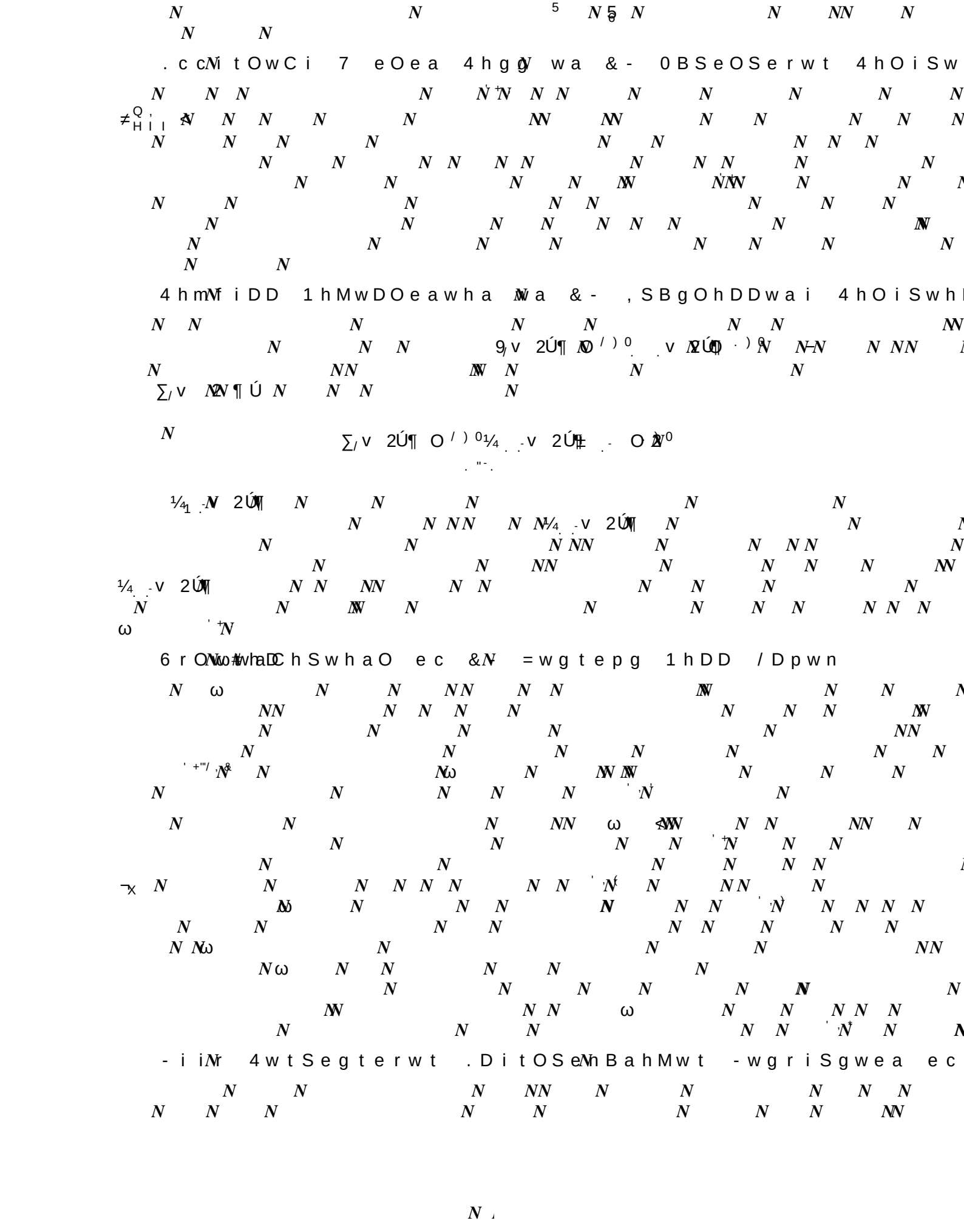


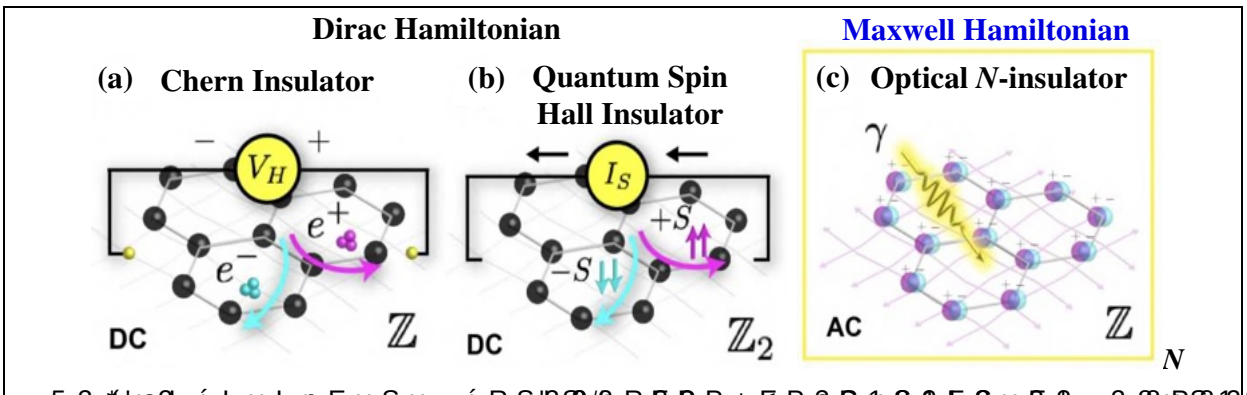






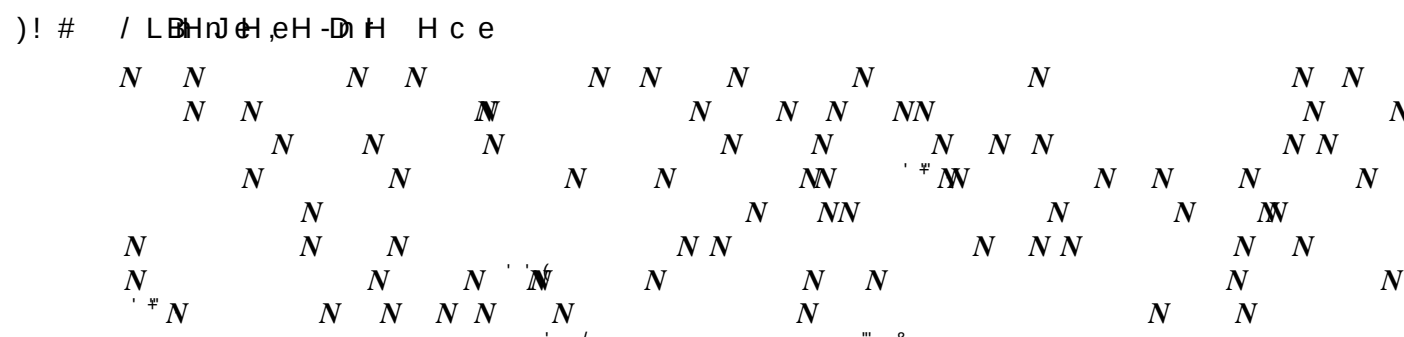


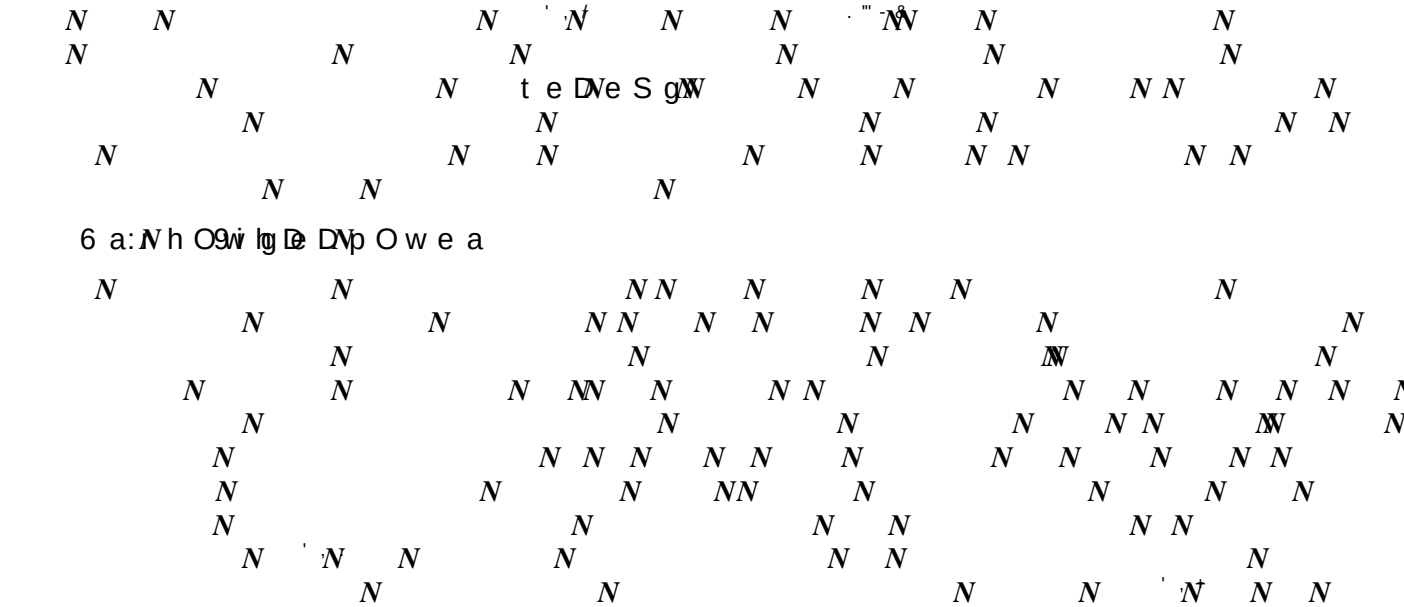


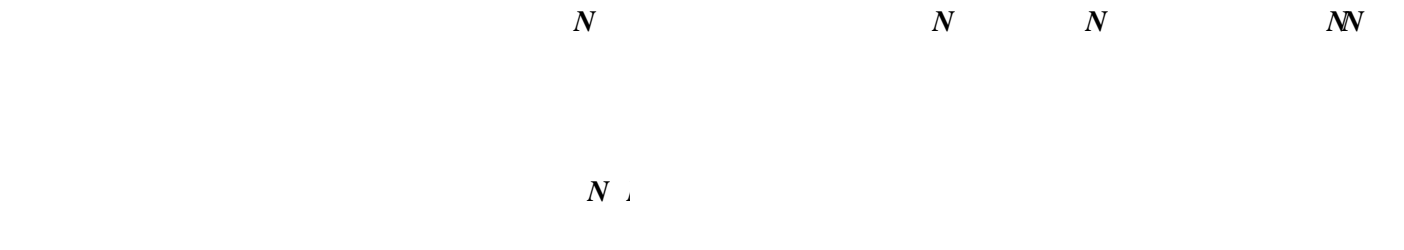

Dirac Hamiltonian
Maxwell Hamiltonian
(a) Chern Insulator
(b) Quantum Spin Hall Insulator
(c) Optical N-insulator
DC
DC
AC

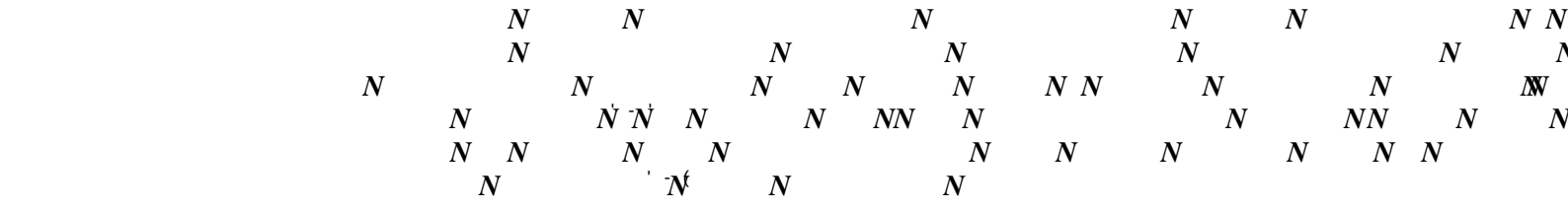
/ c J n J v H e S e í t J H í D e k



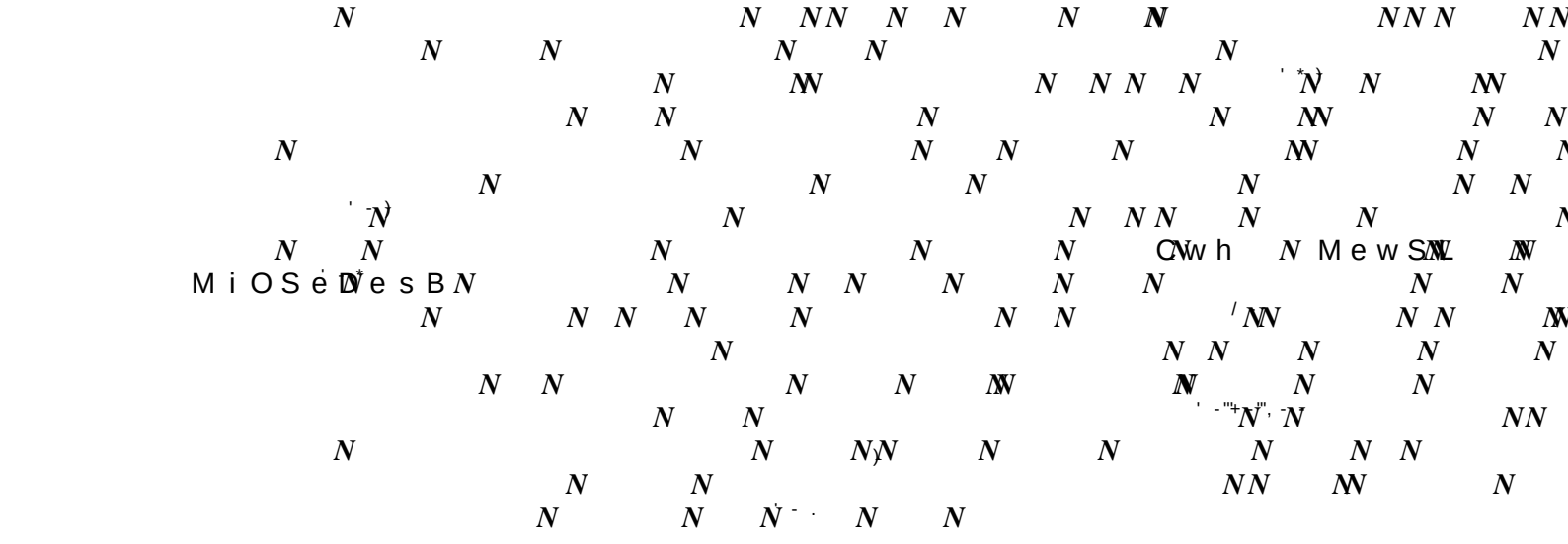




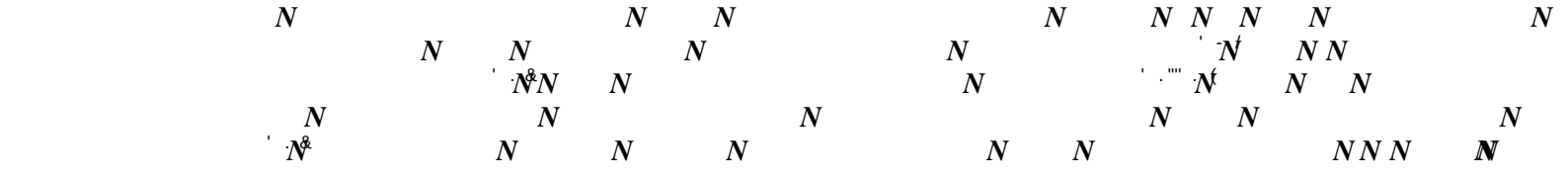




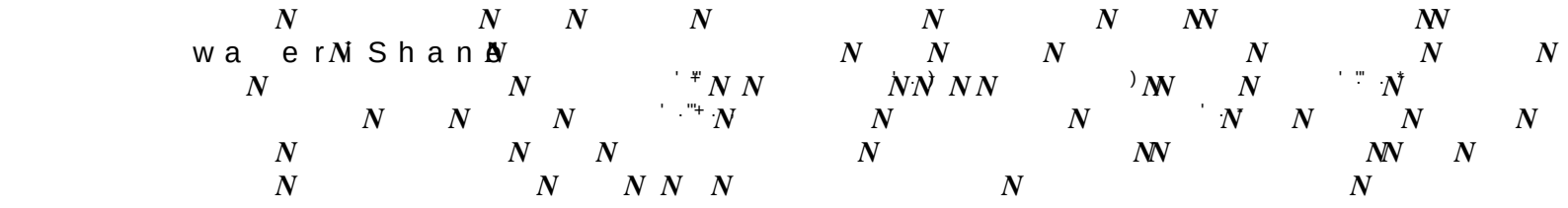
6 a4 w SiLt e a g O Sp t O w e a g



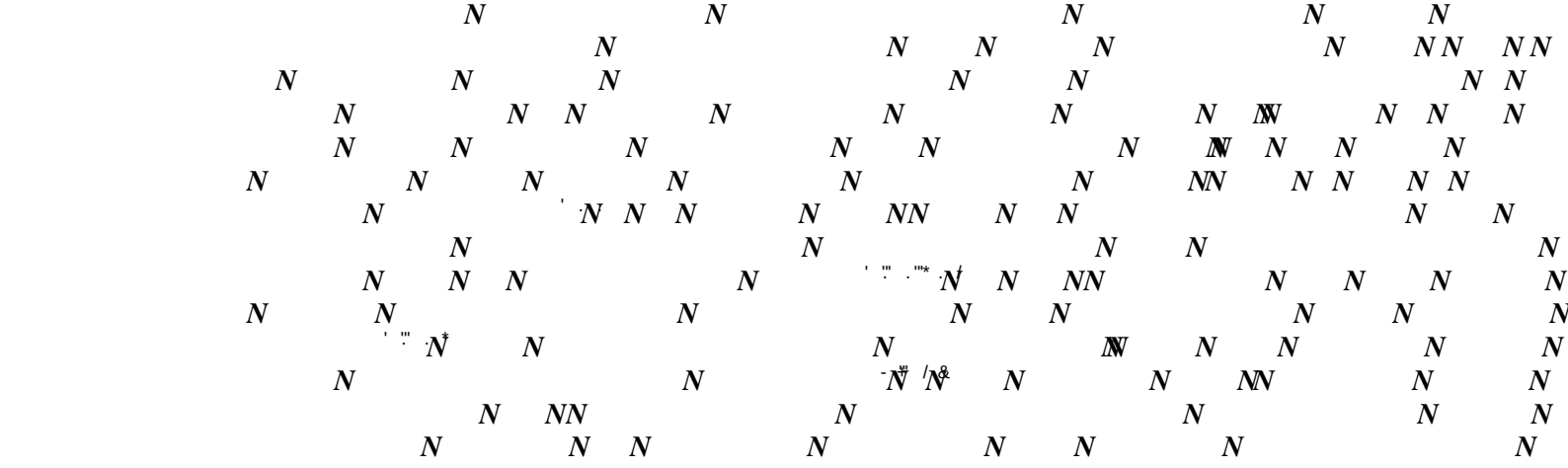
5 h a 6 O w 2 h D w a: sM v e t c e a n p4th O w iaS w h &D-g

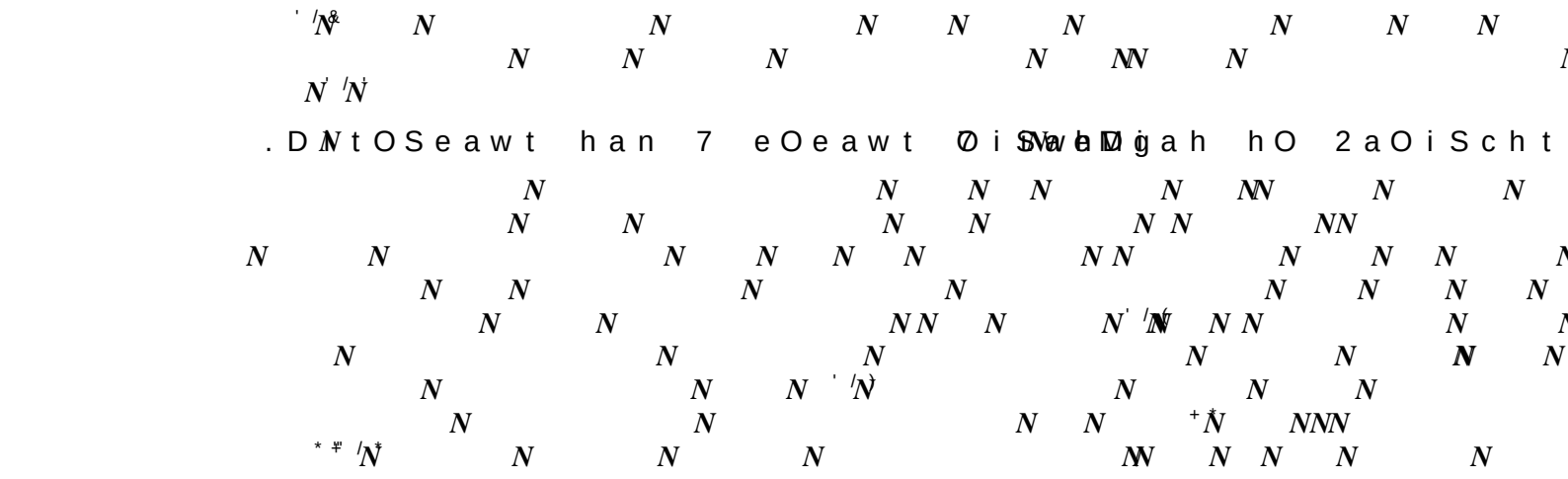


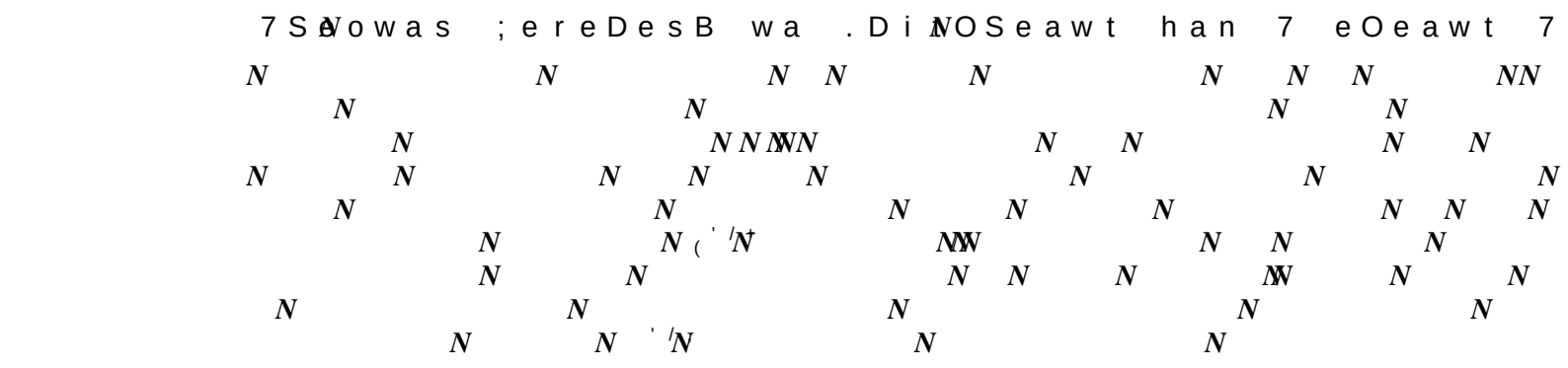
2 a 6 r i S h M h s w a 5 h a r n i t 5 h a e g t e r B

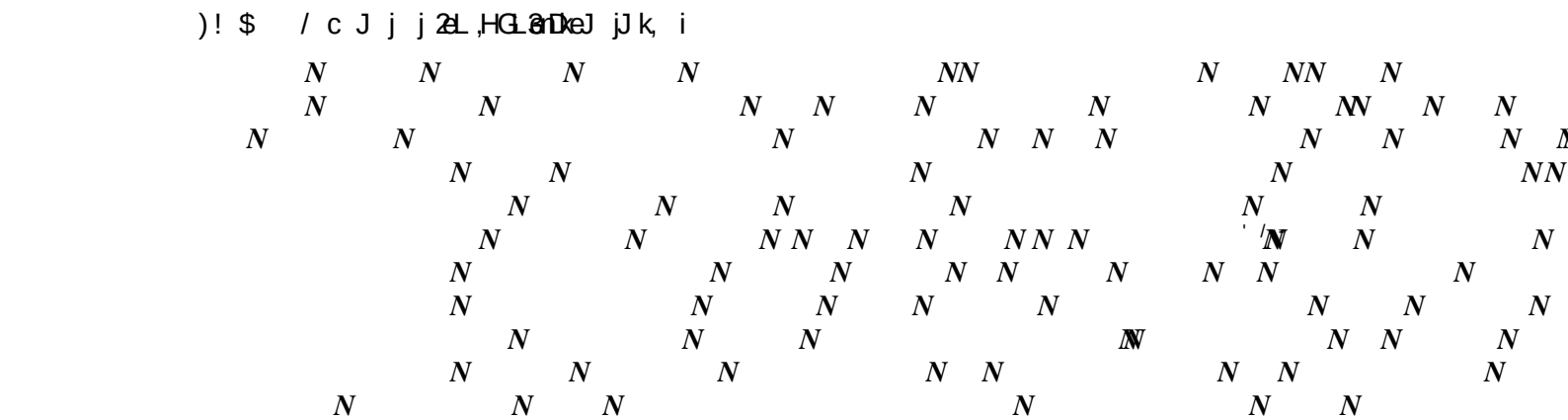


6 a : r h O w e O i r e S h D 2 M h s w a s

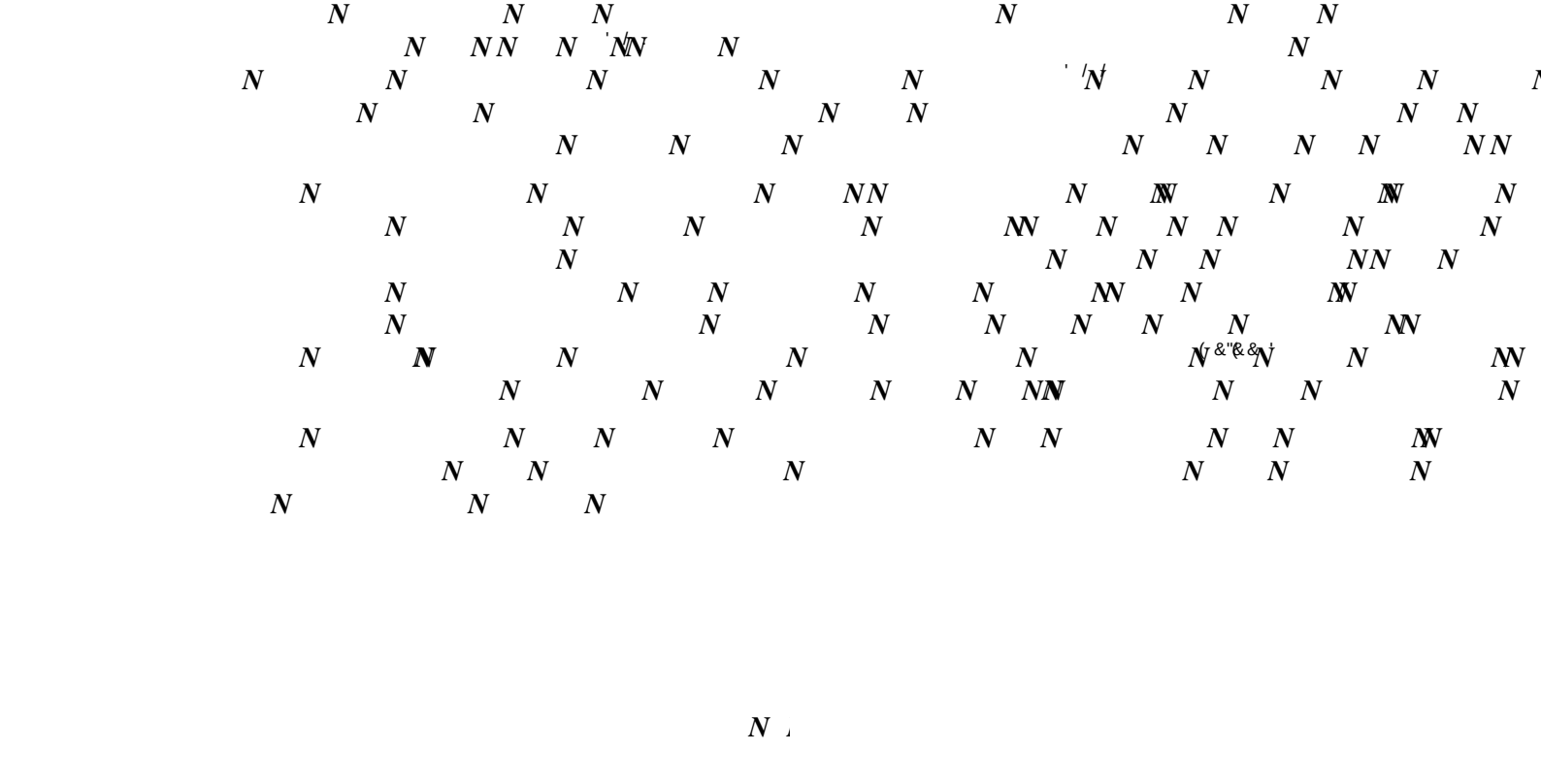








)! $ /cJjj2eL,HGLaDeJjJk,i



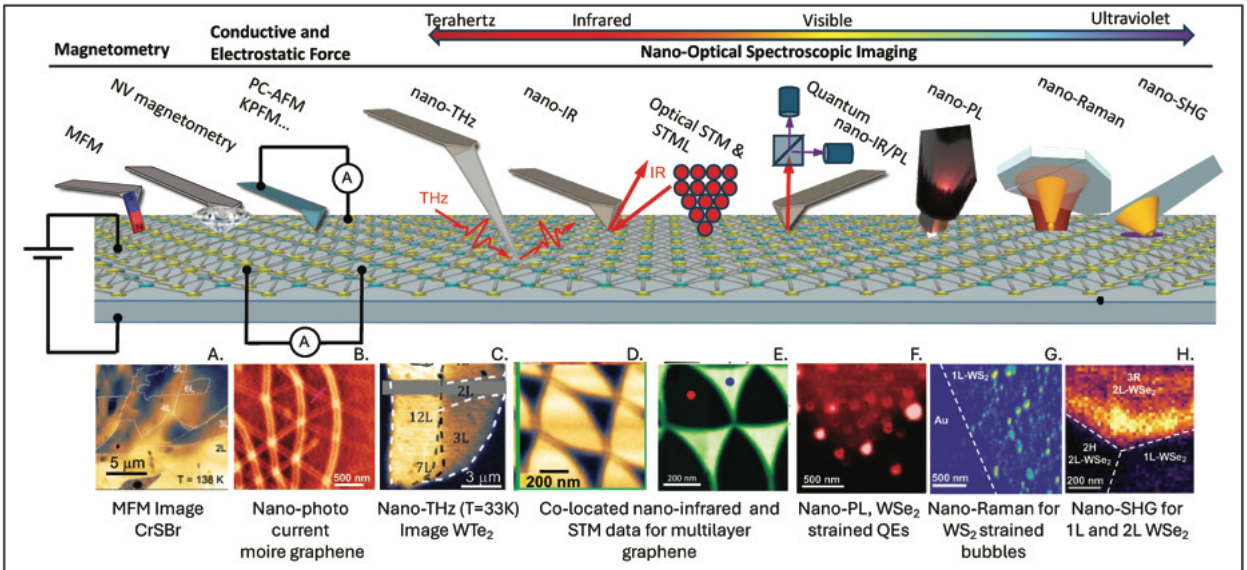


Figure 7. Multi-messenger scanning probe nanoimaging is based on AFM and STM platforms. Top panel: Schematic representation of scanning probe imaging modalities commonly applied to the exploration of 2D materials and their heterostructures. Bottom panel: Examples of images of different classes of 2D materials reported by co-authors. From left to right: A) MFM imaging of atomically layered magnetism in semiconducting CrSBr;[202] B) Nano-photocurrent in minimally twisted graphene;[203] C) Nano-THz response of a few layer WTe_2 microcrystals;[204] D and E) Co-located nano-IR and STM studies of nonlocal relaxation dynamics in twisted trilayer graphene moiré superlattices;[205] F) Nano-PL image of a strained nanobubbles in a WSe_2 monolayer on Au substrate;[206] G) Nano-Raman image of WS_2 monolayer bubbles on a Au substrate;[207] H) Nano-SHG characterization of layer stacking in WSe_2.[182]

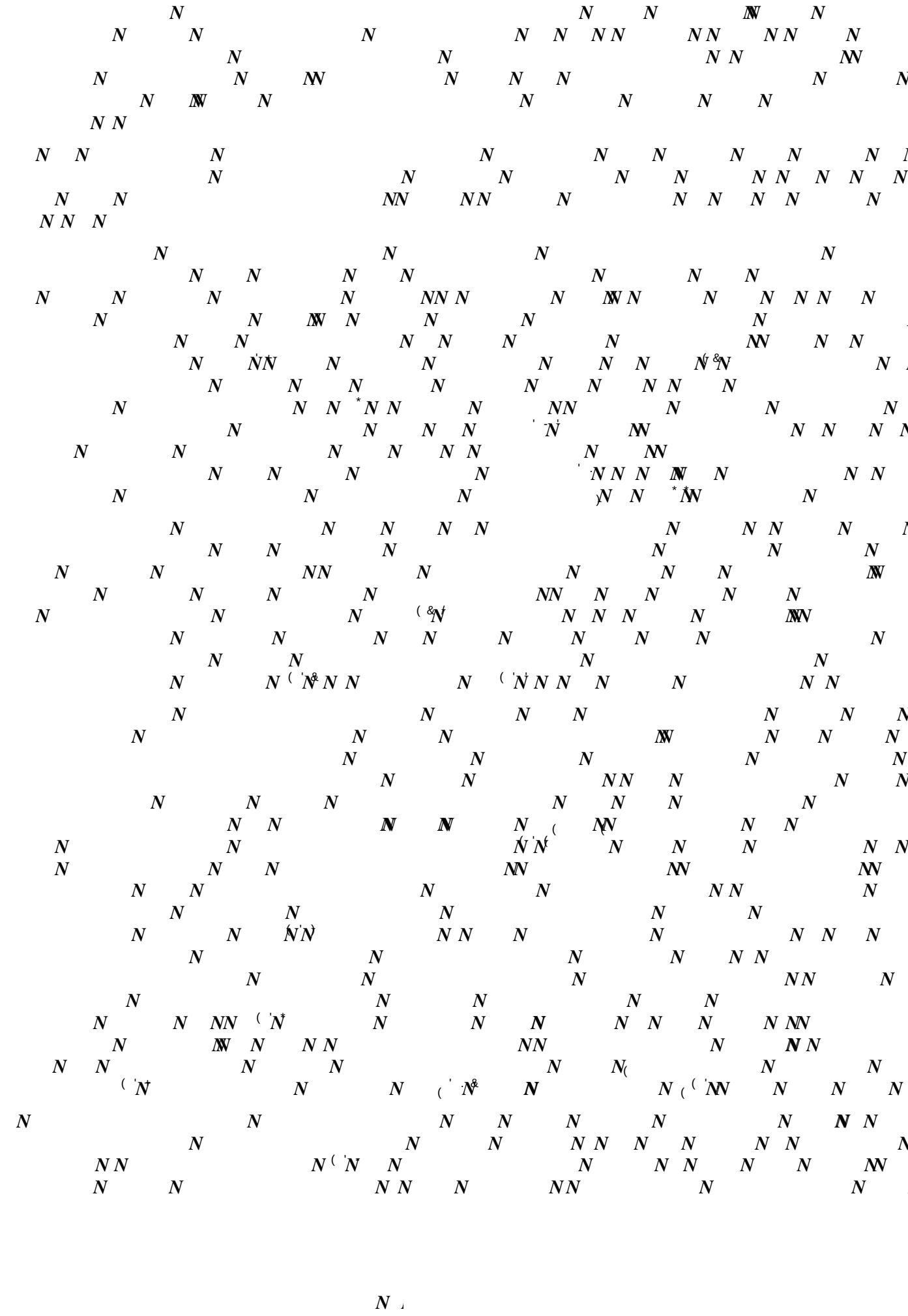
8. TIP-ENHANCED NANOSCOPIES FOR ATOMIC-SCALE PHOTONICS IN 2D MATERIALS

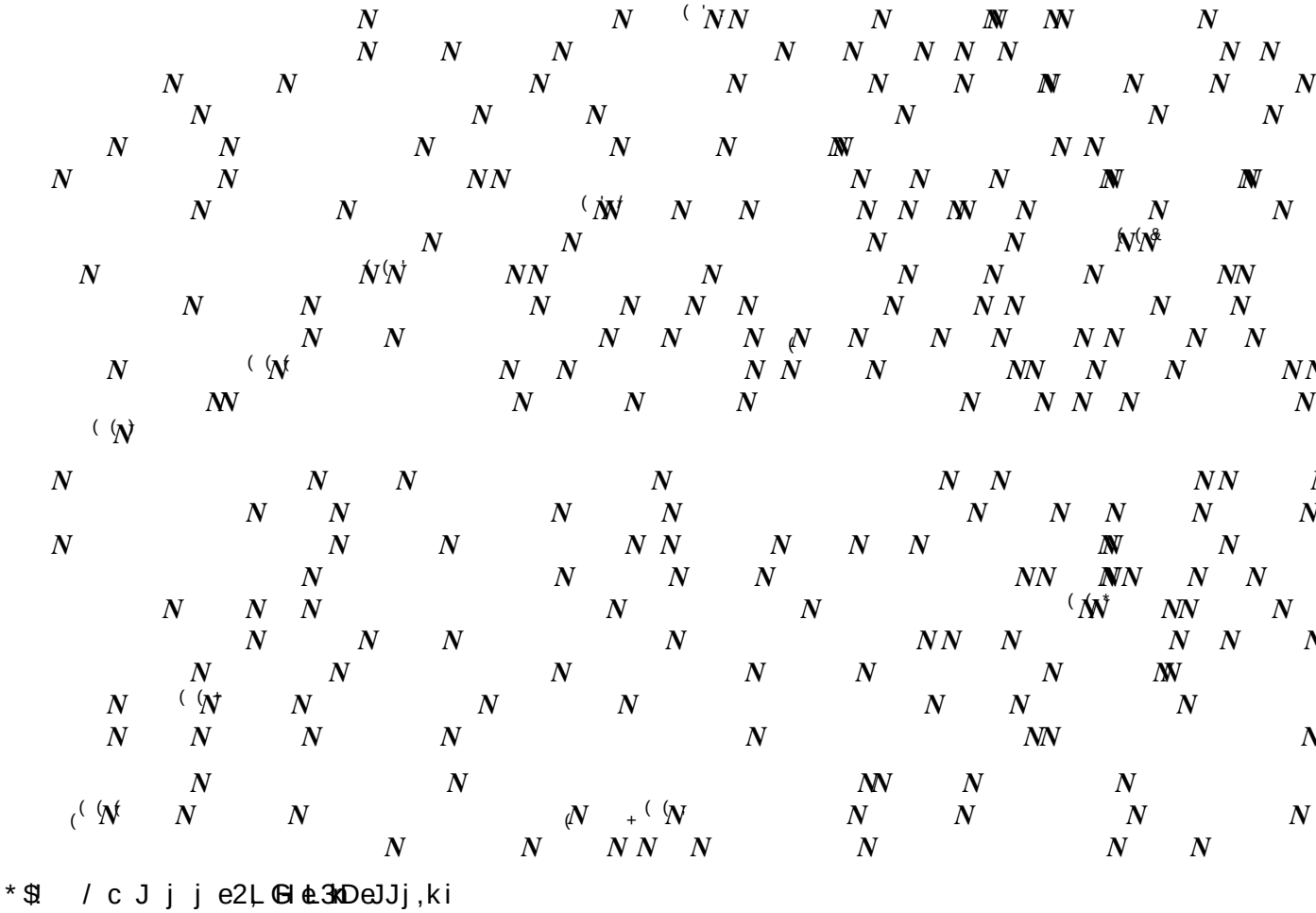
Aitor Mugarza,[1,2,*] Pablo Merino,[3] Marc G. Cuxart,[1] Emigdio Chávez-Angel,[1] and Martin Svec[4,5]
[1]Catalan Institute of Nanoscience and Nanotechnology (ICN2), CSIC and BIST, Bellaterra, 08193 Barcelona, Spain
[2]ICREA—Institució Catalana de Recerca i Estudis Avançats, 08010 Barcelona, Spain
[3]Material Science Institute of Madrid (ICMM-CSIC), 28049, Madrid, Spain
[4]Institute of Physics, Czech Academy of Sciences, Praha 6 CZ16200, Czech Republic
[5]Institute of Organic Chemistry and Biochemistry, Czech Academy of Sciences, Praha 6 CZ16000, Czech Republic
***Corresponding author.** Email: aitor.mugarza@icn2.cat

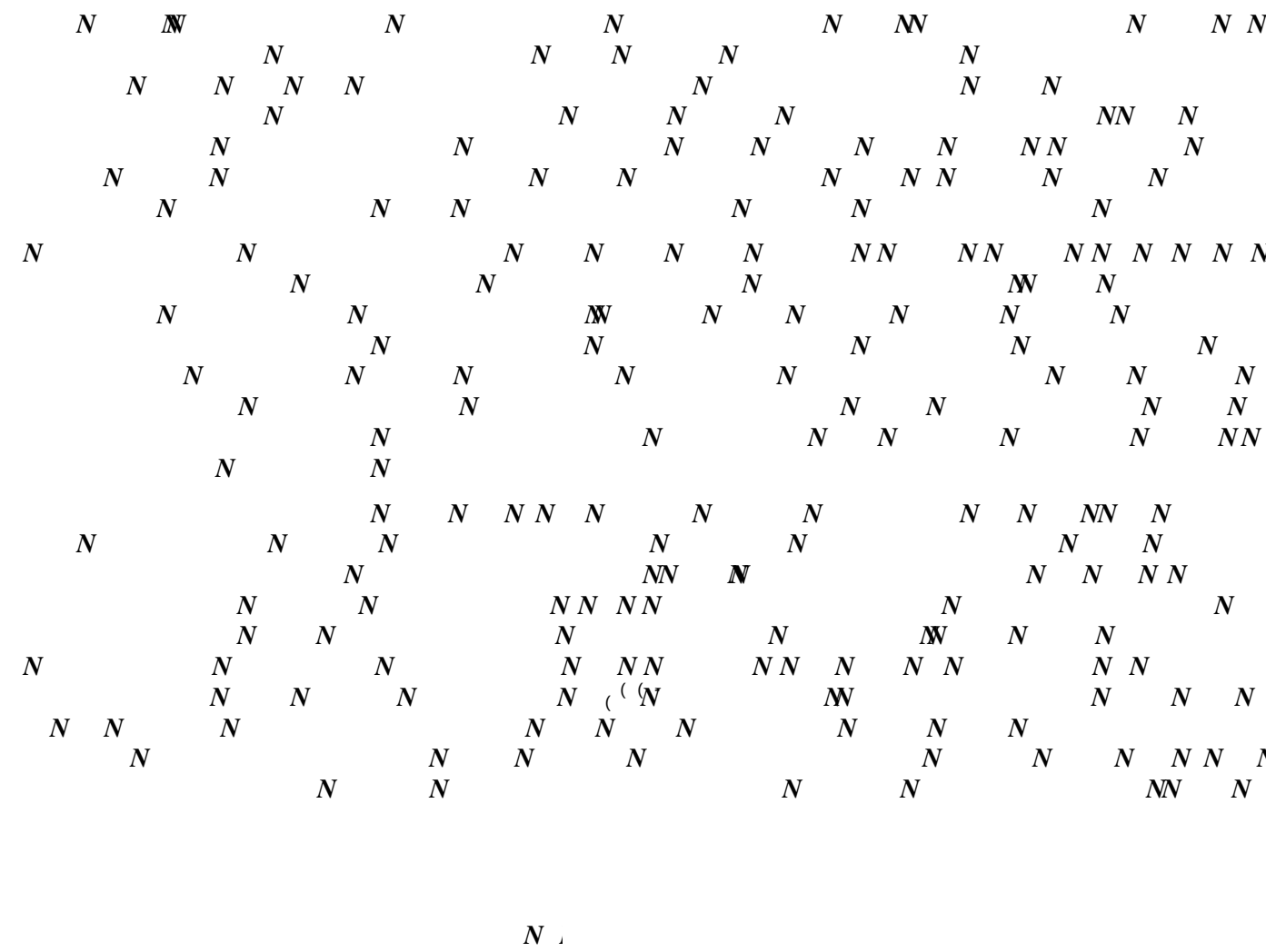
8.1 State of the Art

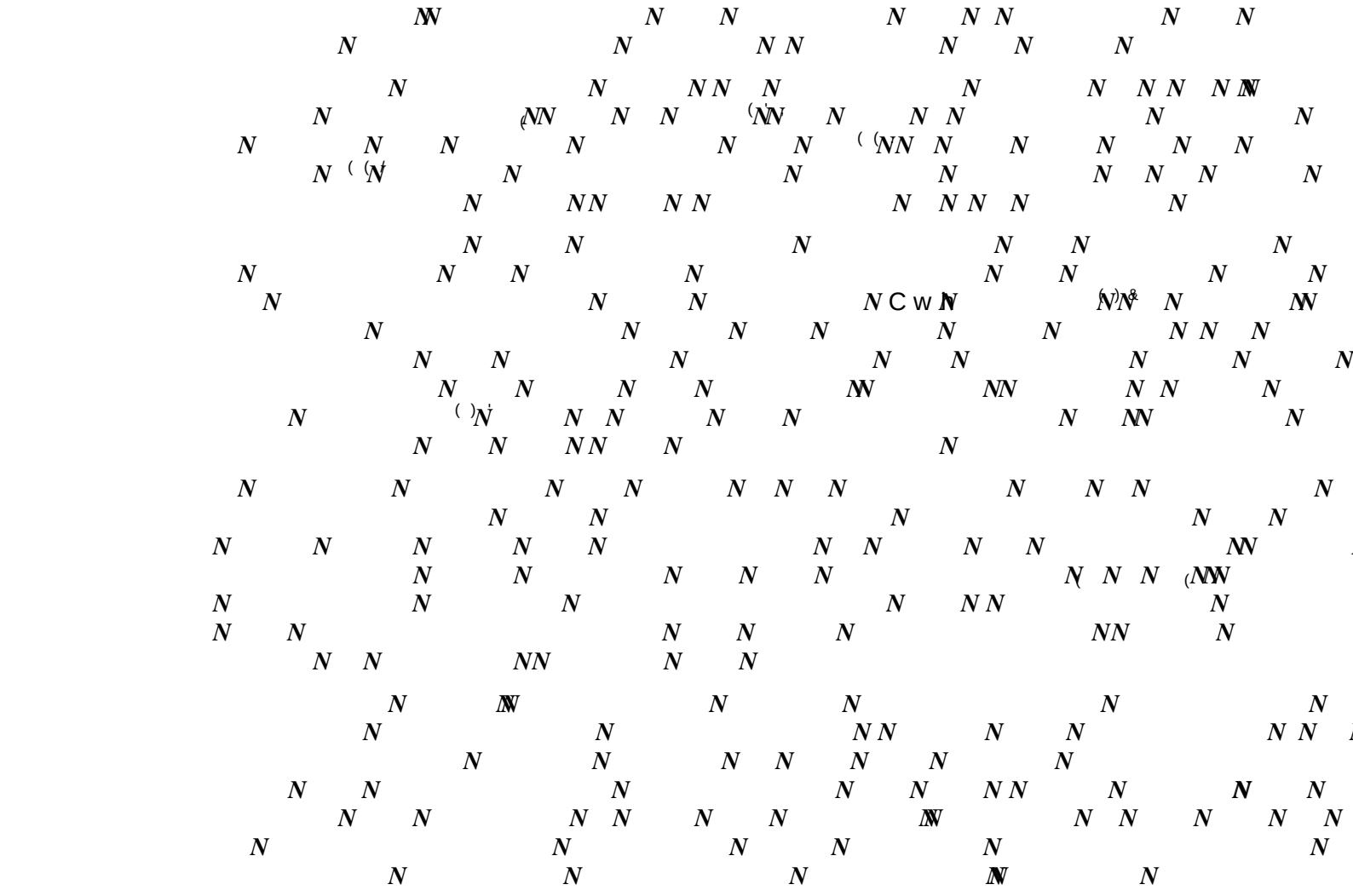
Recent advancements in the field of tip-enhanced nanoscopies have opened new avenues for studying light–matter interactions and manipulating quasiparticles down to the atomic scale. These techniques typically involve positioning a sharp metallic tip at nanometer-scale distances from the surface of the material under investigation, while illuminating it with highly focused light. This configuration creates a nanocavity that can significantly enhance and localize electromagnetic fields to volumes well below the diffraction limit. It also facilitates the exchange of photons between the near and far-field, allowing for the coupling of external light sources to the nanocavity or guiding light generated beneath the tip to optical detectors.

Depending on the specific systems and processes being examined, a variety of excitation light sources can be used, spanning from THz to UV wavelengths (1 meV-10 eV). Many of these techniques employ conventional methodologies for photonic absorption, emission, and scattering, with some of the most common being scattering-type scanning near-field optical microscopy (s-SNOM), tip-enhanced Raman spectroscopy (TERS), and tip-enhanced photoluminescence (TEPL). The incorporation of a conducting tip further expands the methodological toolkit, enabling techniques that rely on electronic excitation or detection. For instance, tunneling electrons induced by static or pulsed bias voltages can generate

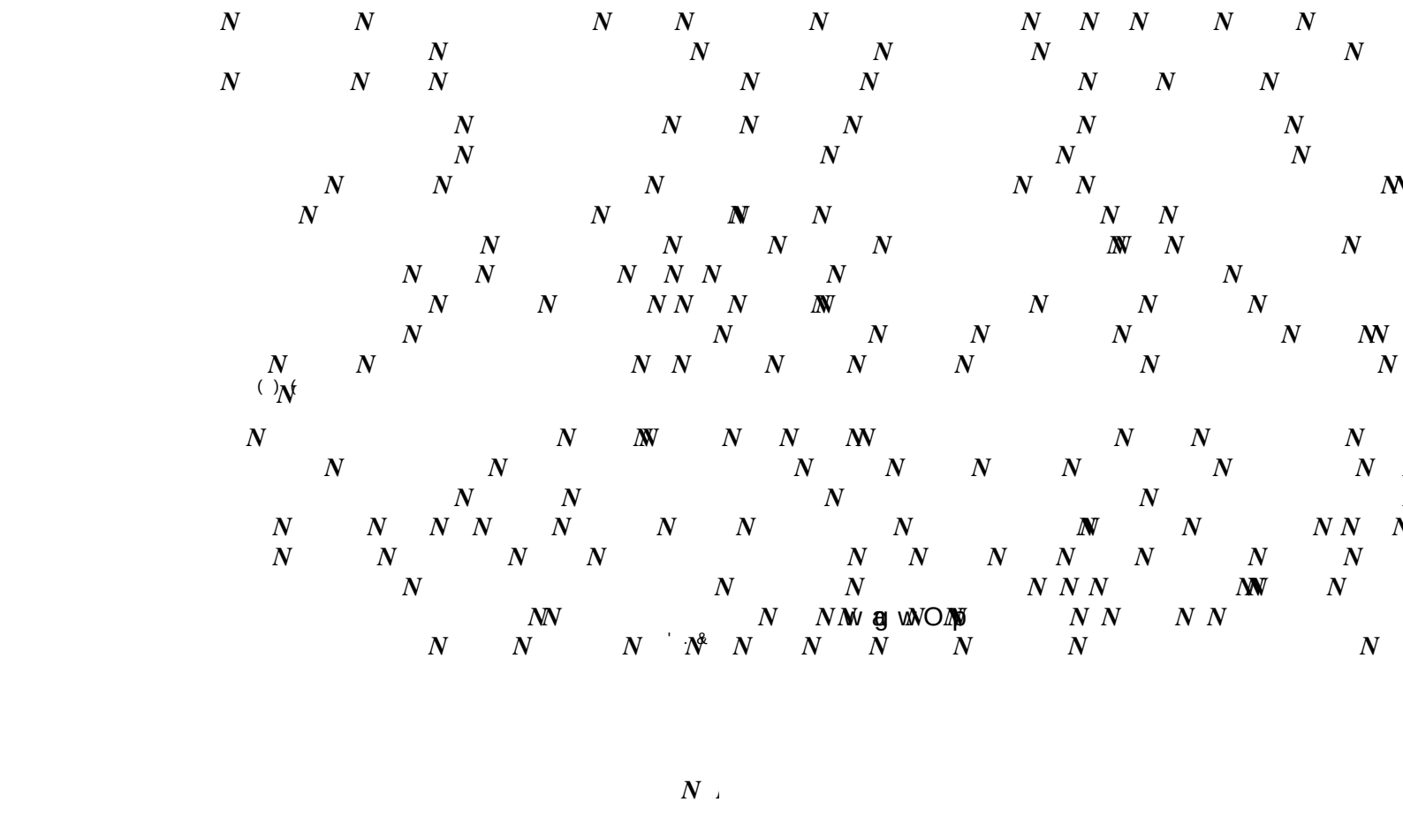


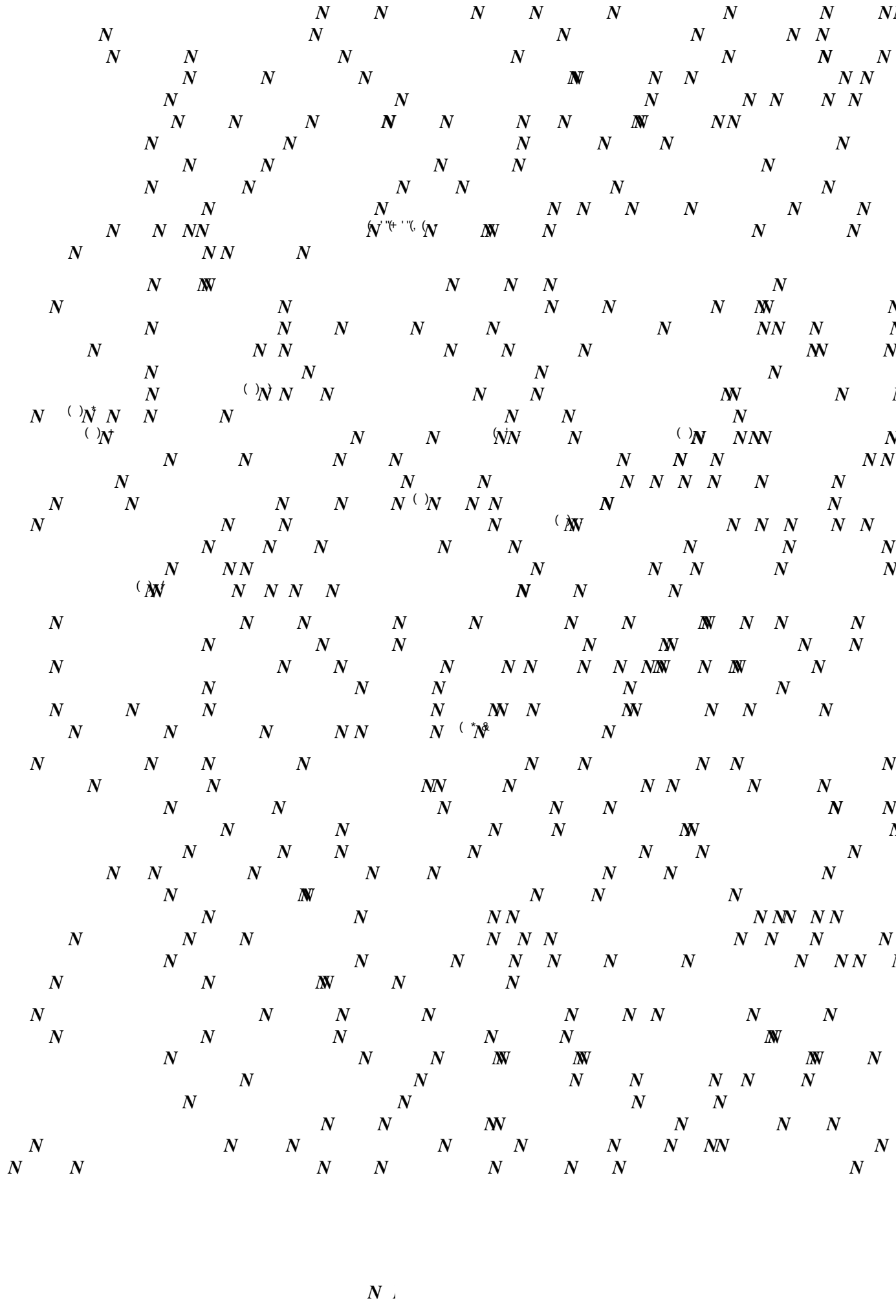






*! % B L G0Gíenke-HveHi í D , k H D 9 e e H S c e k e 3 D J j k





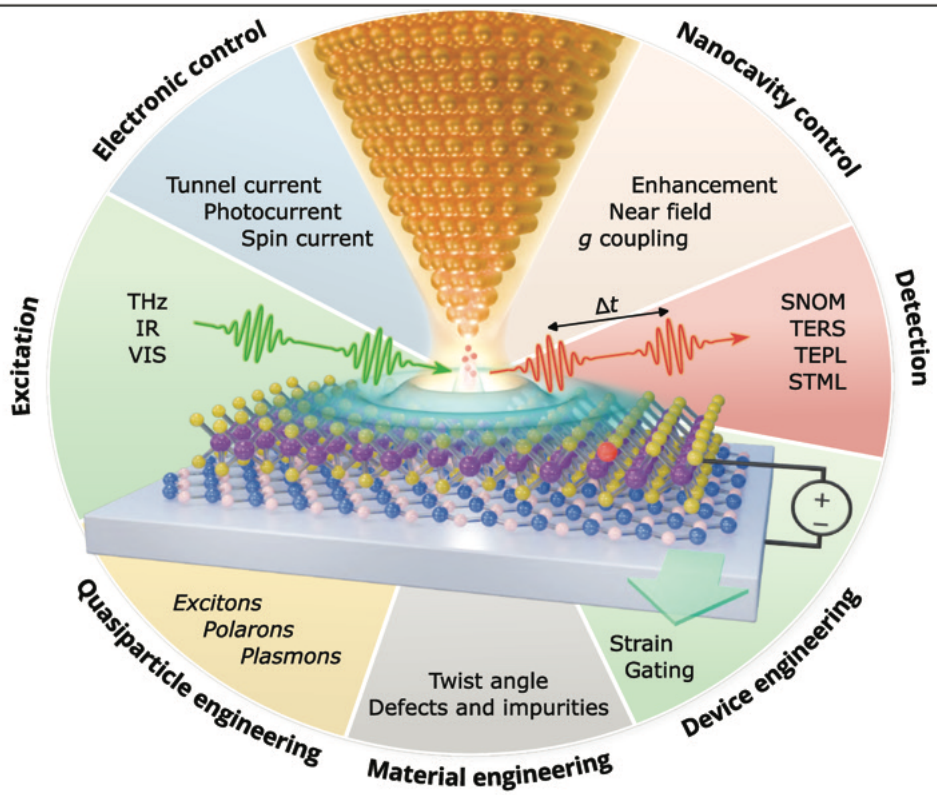


Figure 8. Schematic illustration of tip-enhanced nanoscopies applied to the study of photonics in 2D materials. The tip–sample nanocavity can confine electromagnetic fields and couple near- to far-field photons, and vice versa, enabling local probing of optical and electronic excitations with atomic-scale spatial resolution. This can be done by using photons or tunneling electrons for excitation and detection. The intrinsic surface sensitivity and sub-nanometer spatial resolution of tip-enhanced techniques make them especially suited for studying and controlling light–matter interaction phenomena in 2D systems. The spatial resolution is particularly useful for the study of systems exhibiting nanometer-scale lateral modulations or inhomogeneities such as moiré superlattices, nanostructures, lateral heterostructures, or defects. The application of external stimuli such as strain, electrical gating, and magnetic fields can be incorporated for the manipulation of the local properties and correlating it with mesoscopic properties *via in operando* studies. Incorporating fast detection or pump-probe schemes adds time resolution to study quasiparticle dynamics with the same spatial resolution. All these elements converge in a toolbox of techniques that enable deterministic characterization and manipulation of photonic phenomena at the ultimate spatiotemporal limits of picometers and attoseconds.

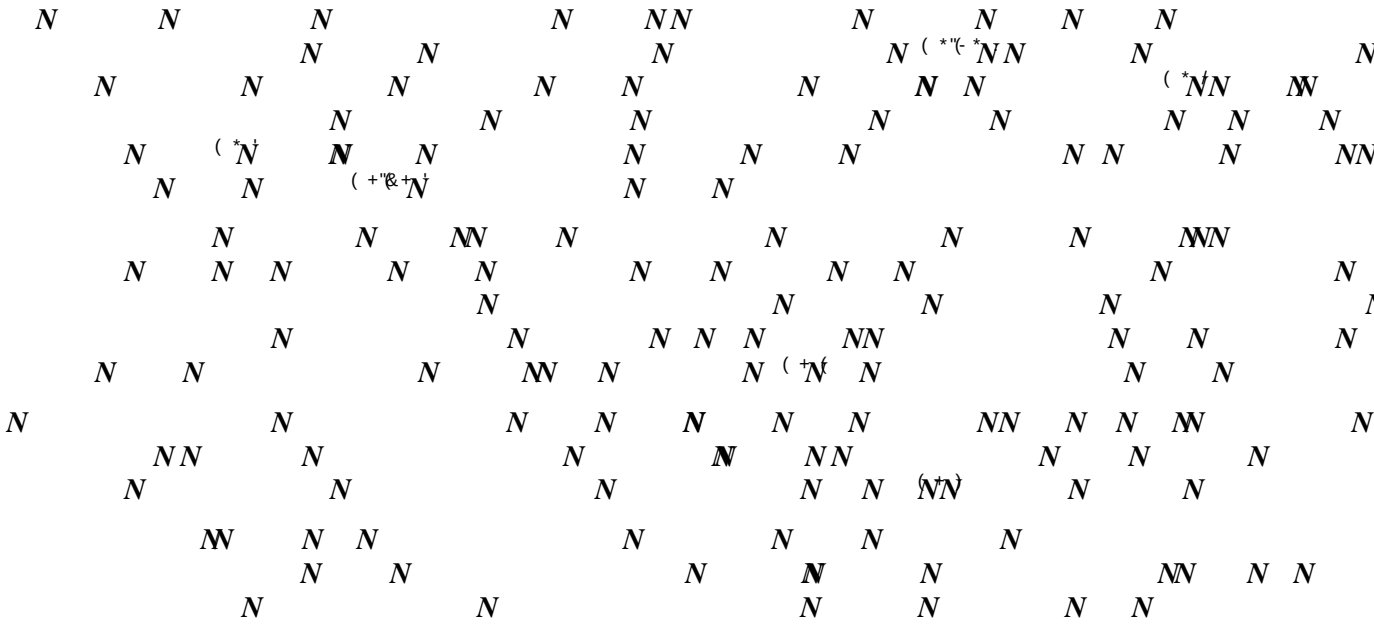
9. ELECTRON MICROSCOPY AND SPECTROSCOPY FOR 2D MATERIALS

Luiz H. G. Tizei[1,*]
[1]Université Paris-Saclay, CNRS, Laboratoire de Physique des Solides, 91405 Orsay, France
***Corresponding author.** Email: luiz.galvao-tizei@universite-paris-saclay.fr

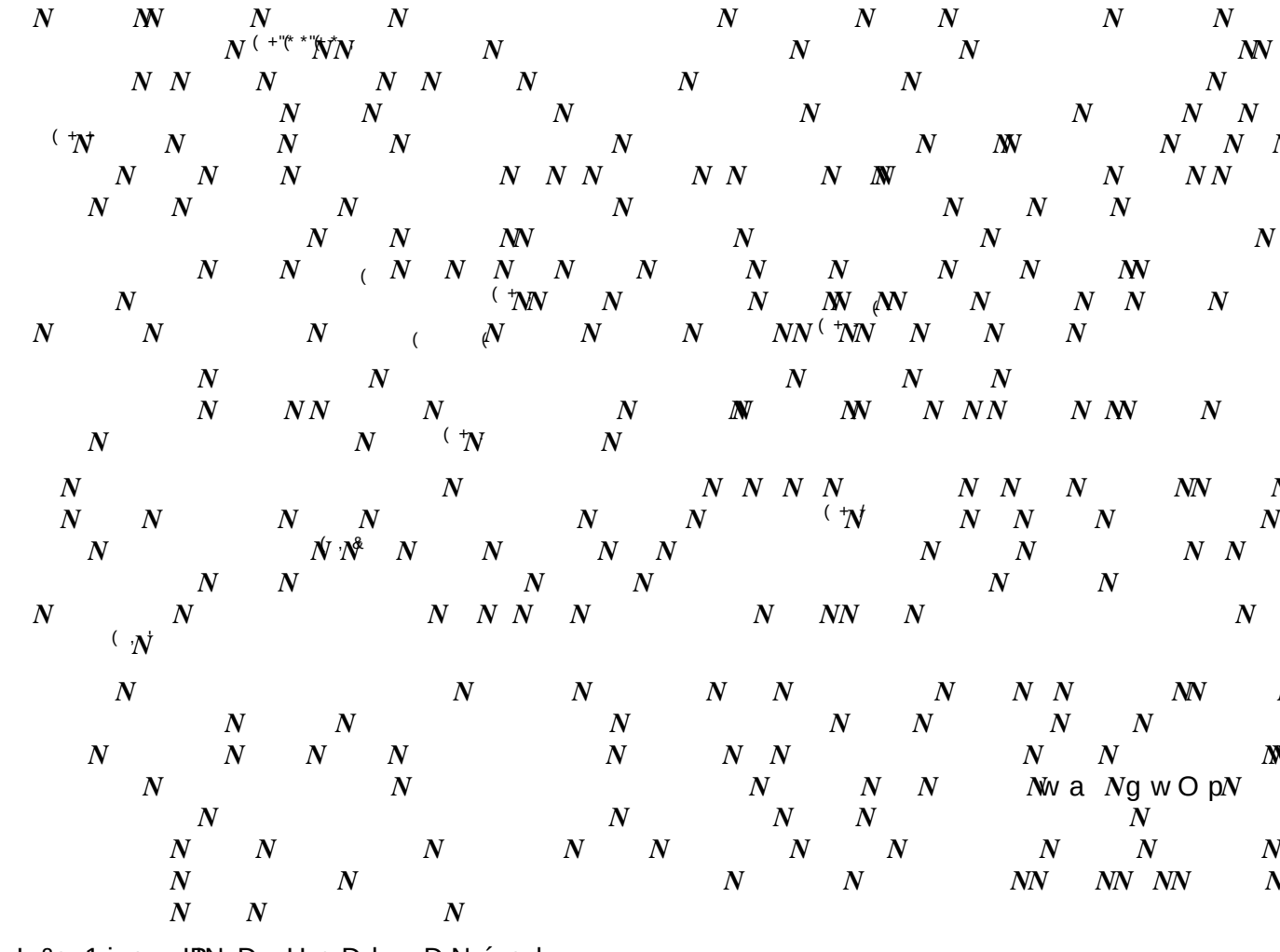
9.1 Introduction

Electron microscopy has become an indispensable tool for investigating the properties of 2D materials at the atomic scale. The structure, morphology, chemistry, vibrational response, and optics of these materials have been extensively studied down to the atomic level using electron microscopy (EM) and spectroscopy. Since the initial production of 2D materials, EM contributed to different aspects of their understanding. Imaging and diffraction can map deformation in 2D monolayers;[241] electron energy-loss spectroscopy[242] (EELS) (Figure 9a) and energy-dispersive X-ray (EDS) spectroscopy[243] allow for the chemical identification of individual atoms in 2D layers. Vibrational EELS can map the vibrational response of a single Si atom on a graphene monolayer.[244] EELS and cathodoluminescence (CL) have been shown to measure spectra similar to those of optical absorption and photoluminescence in hBN-encapsulated WS_2[245,246] (Figure 9b). The objective of this section is not to be an extensive review of electron microscopy and spectroscopy for 2D materials, but to give a perspective of which technical developments could help solve standing questions for these materials.

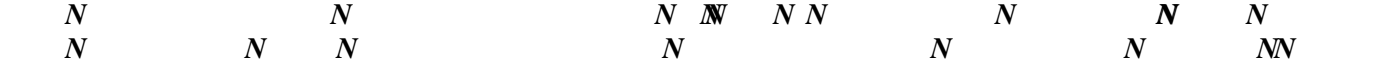
+! $ B H n/Lcvelo Lírkde-H,1jme v H B-Dn,LívvH L n e

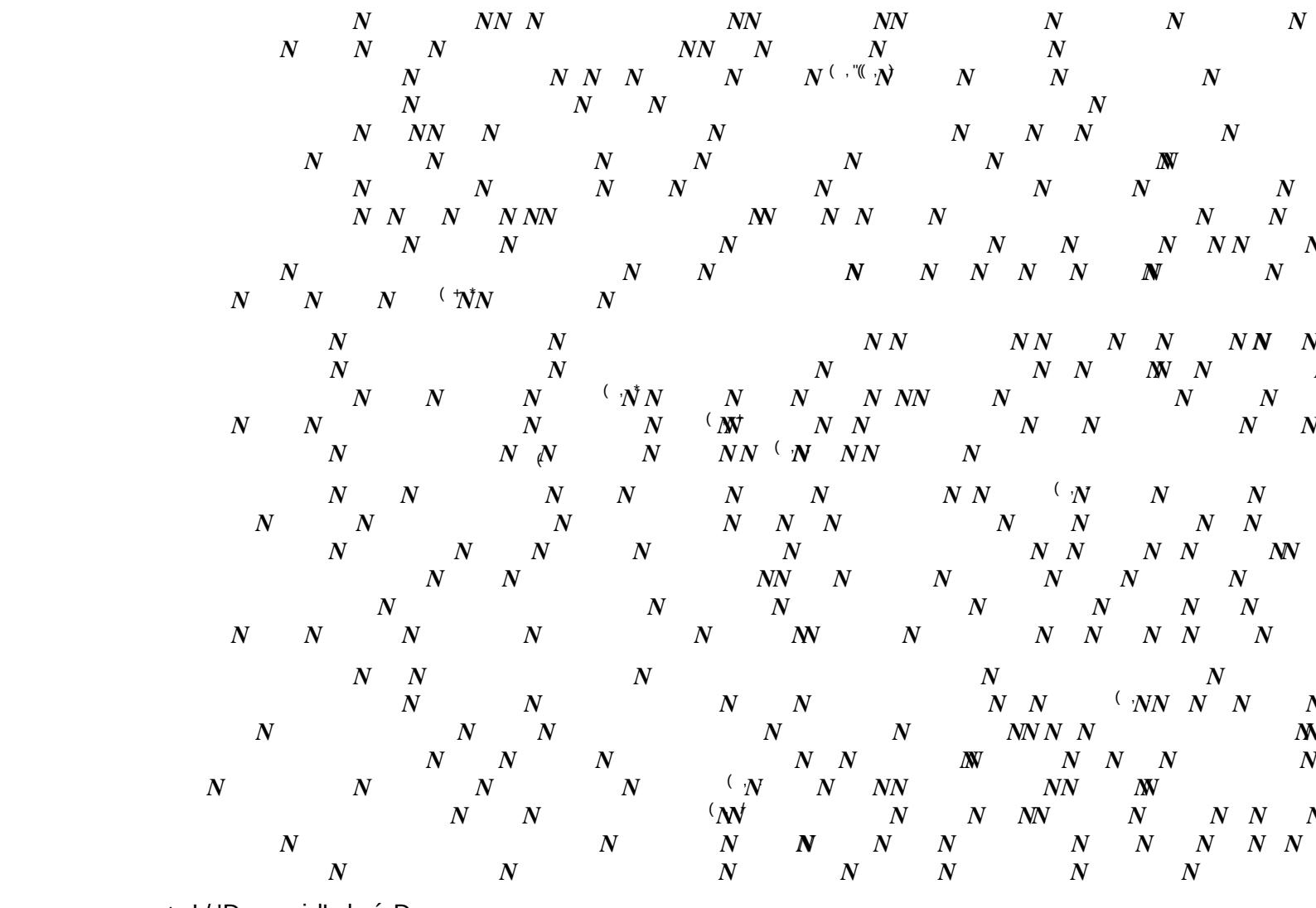


+ !:%J , D,N H í v k

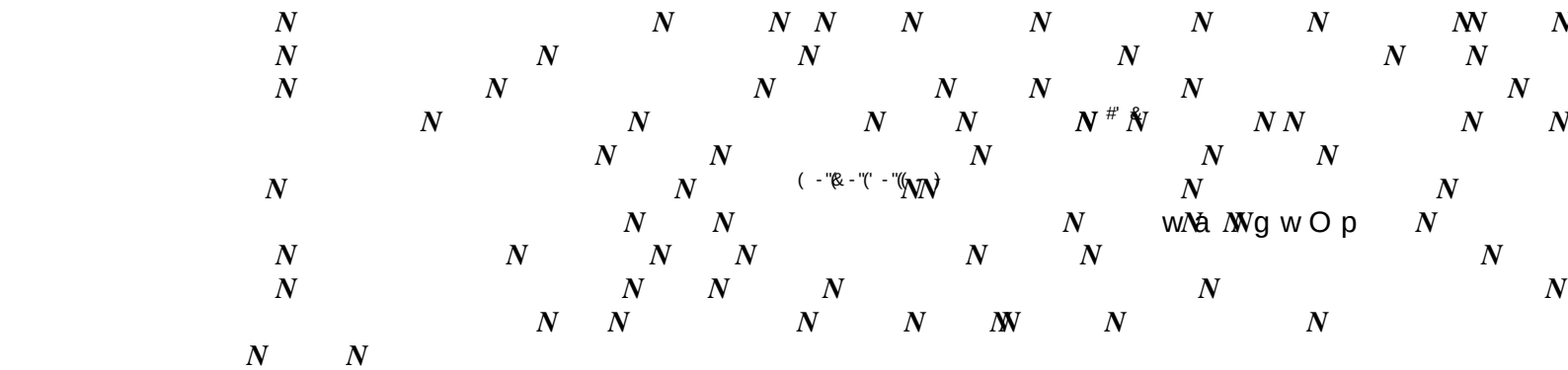


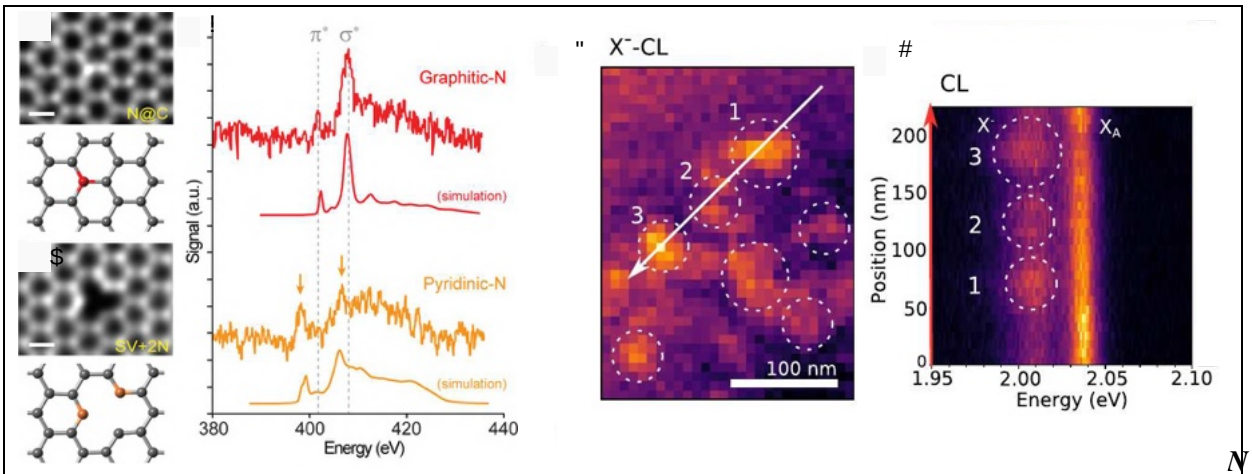
+ !:&e p1j e v HBNeDv,H n D k v D N í e k





+ !/'D , v jkL k í D ,





N

. 5 3 *+ ;! 2 R 8 ç E 3 1 2 N % 8 v % S P 1 0 2 LL P í E 1 y E y 3 1 2 L D 6 y 1 + D < 2 8 ç S 1 8 2 E S v ' 3 & S U E 1 R 6
g # v 8 y & ç 1 E 2 y L 2 P L E y ç S p í N 3 S P 0 ç L 0 8 v 6 L 2 P E 1 2 L p 8 P L B 6 1 E p D 2 S E 1 P E L p P 2 3
" y = # v 8 y 1 2 L & P L 3 3 P 8 3 2 í p 8 N + y = 1 s 2 y L L 3 2 y 8 L 3 í 3 N 3 ' í 8 y 1 2 S S P 0 3 E ç D l v S 1 E ç 1 P 6 L 2
E P 1 R 8 p 2 S í R E 1 E y S P 0 % í 1 N 2 2 E E L 0 Y E S P ' E R y L 0 y L L V P D 6 ç E # D E 2 3 6 y 1 E R L P 8 & " ç ' S D # ' T
E P 1 8 P 3 E 1 N 3 í L 1 3 S 2 8 P D ç g 8 2 8 y 0 L ç S í P S 0 2 8 ç 0 8 2 & ú E 8 1 0 R 1 g ' N 8 v # 0 ' S 2 ' R 8 8 E v y 8 E
S 2 2 L U # % E P 3 R " L U E P p & 1 & P 8 U D 1 2 P S & v 3 2 5 E y E E 1 L P ; s 8 ç E 3 3 E S L P P 8 & y 8 3 b L S v 8 b 8 8 3 L
S 0 S í 1 8 0 U E 1 R í + 8 - 2 " * ç ; E L 3 í 3 N E 2 L E P p ç 6 & 2 2 L E g y S 2 2 8 6 9 3 3 L y E S 1 E L P 6 L # 4 1 R 8 9
S P 8 & 8 3 # S 0 2 8 í 1 8 0 U E 1 R í 8 + 2 - ç ; E ; 3 L 3 í E N L 2 P E p 9 R ç 1 & 2 ç + E) y 2 8 8 P 6 9 3 3 L y E S 1 E L P
9 0 b S P y 8 ç 8 P 1 ' L 6 c y E 8 P y 8

1 u v í H D $, 0 k B e , o í v D , i L v H D n k

$ # 2 O 0 6 I ; : < ; 8 . 1 6 I ; : . 6 : % 1 9 . I 2 1 6 . 8 .

2 j D n í J , 0 " 4 h í a # e G ń k H í J , $ J B , v i c , R e í í , i D e ń n 9 e , D ,

$ o q t c y R L L v L 6 i S 1 D 2 S v o y 8 E y 8 R P y E 8 y 3 S % v q R P N E 3 b E B y 2 3 E < 1 8 N í S 1 2 6 1 ç 8 D P 1 E % y F
C 8 2 ç S P N

% R N 3 E y 3 < 8 í S 2 1 ç 8 P 1 % q P E b 8 2 3 E 1 N L 6 y R 1 E y 8 1 E p S 1 P %) 2 %) q ç 8 R D 2

& O P 3 1 E 1 D 1 6 J 2 % R N 3 2 E v ó % L P S ó u D 3 8 1 E @ 8 1 w ó N q P E D 1 2 8 0 2 % 3 E C 1 B @ 2 1 ç S u P W 0 8 P g D

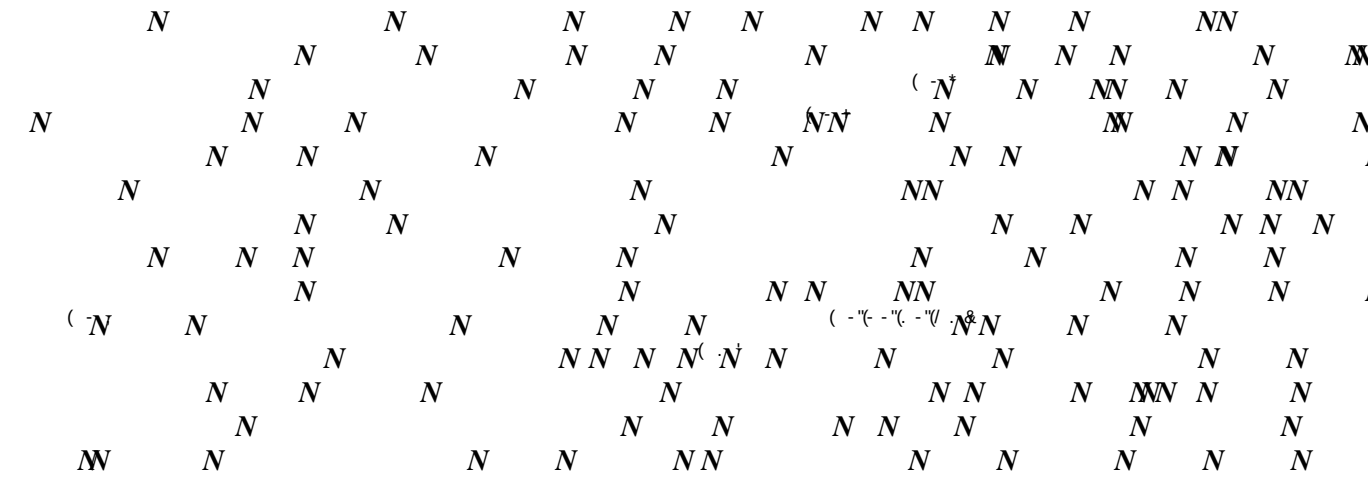
' < 8 í S 2 1 ç 8 P % L ; 6 1 N R N 1 E y 8 p 8 L 6 i 8 U B L 2 ó % * /) ; L P b 8 P 1 9 b 8

(< 8 í S 2 1 ç 8 P 1 L 6 R N 3 E y 3 % o E R 1 8 N C L 2 6 S 0 i D 8 S U 1 8 B L ; 2 8 ó P %) d 8 i 2 8 % U ; B E L 1 2 N ó % q P i E

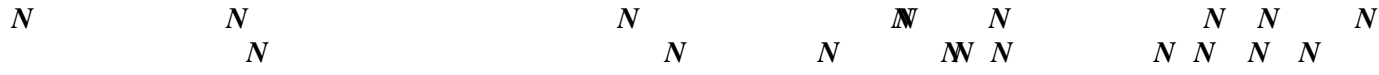
- 9 ; ; 2 < : 9 8 1 = 5 ç 8 S 3 E ç v 0 3 * P = L 4 P 9 8 ; y ! y P N ' y D P N ' 8 0 D

! # / L B H n J e H , e H - D n H H c e

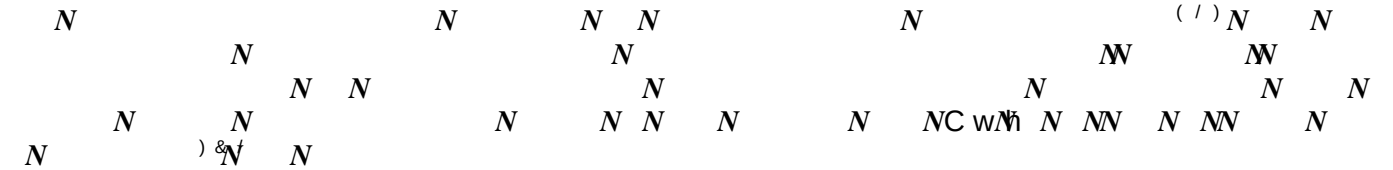
2 a O S e n p t O w e a



4 h O i S w h D g

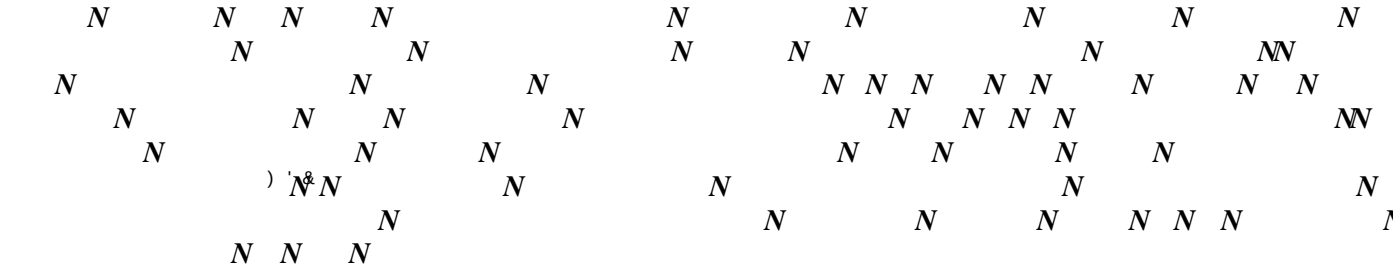


7 i a e M i a h

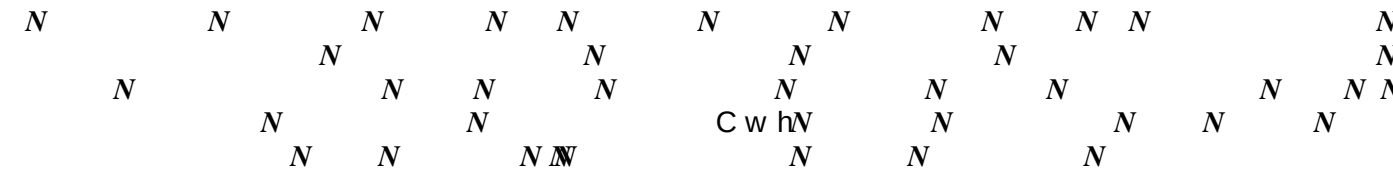


'$! / c J j j e2L GHle3kDeJJj,ki

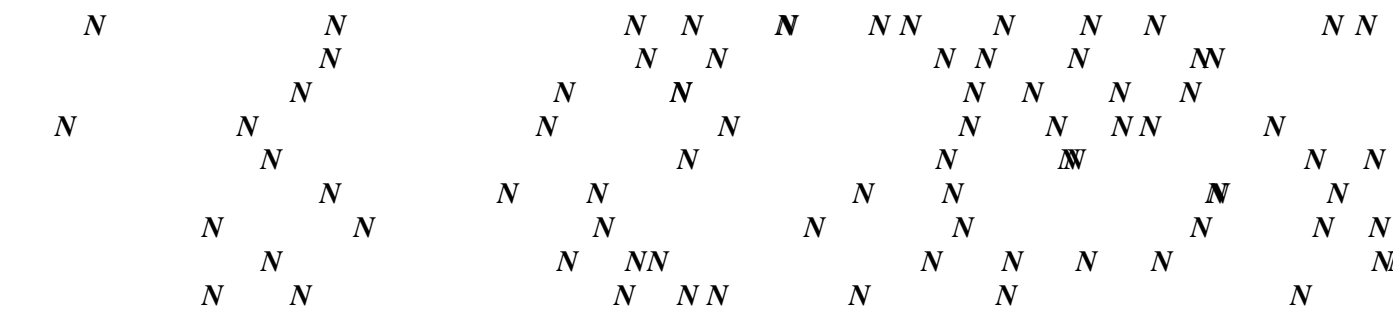
, S B gwOdhiD



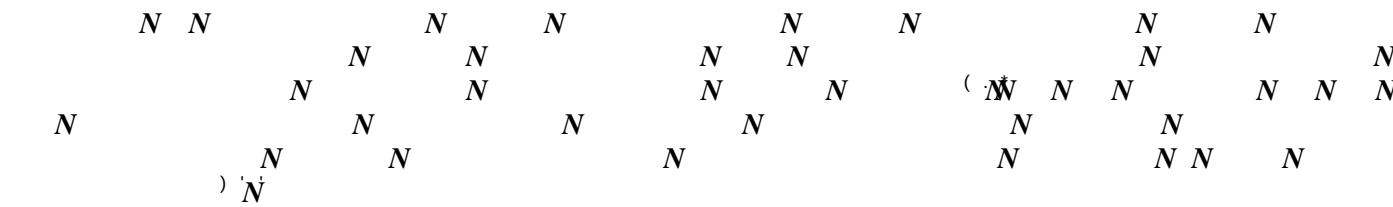
5 e a D w a i h S w O B



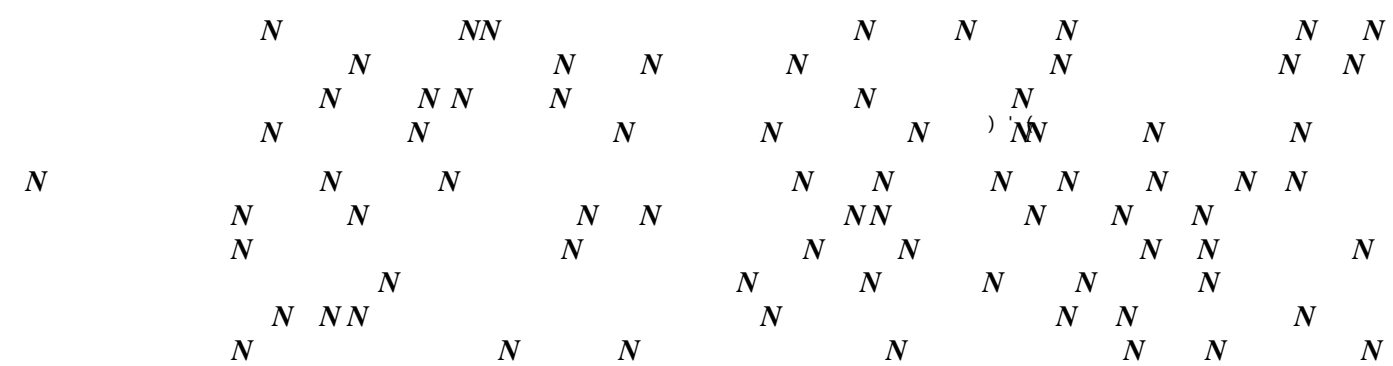
, e p r-Di isnS i /Sgi ience M



, e p r DDwiatsO S7 eeaO;Sa a g r e S O



%! B L G Gé k kle e H 9 Ð e Sk e k J j k



substantially from exploring new materials and quasiparticle interactions. From the cavity engineering point of view, a promising direction currently pursued is using chiral cavities for breaking symmetries and allowing new functionalities of optical devices.

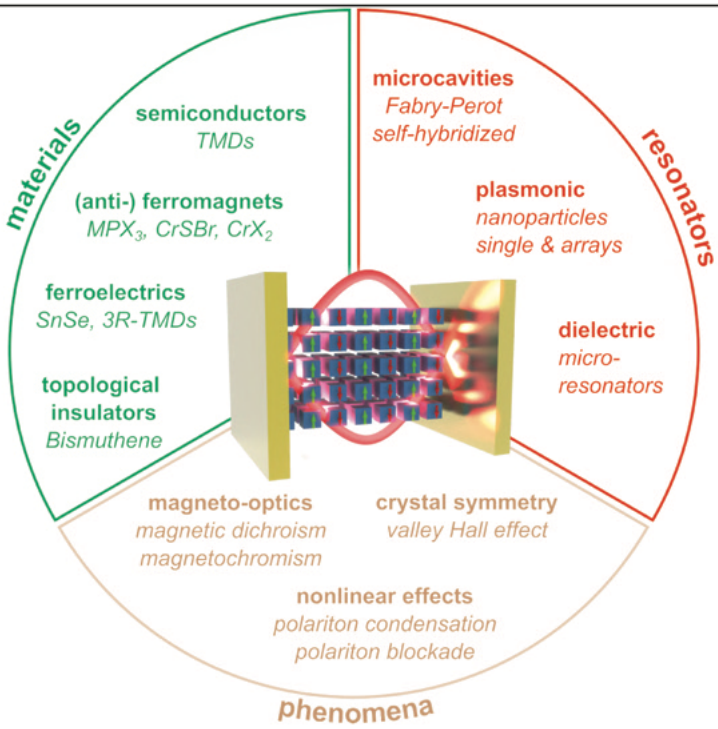


Figure 10. Study of strong exciton–photon coupling in 2D vdW crystals combines different classes of materials with optical resonators to investigate intriguing phenomena related to optics and photonics.

11. TUNABLE EXCITONS AND TRIONS IN TMD STRUCTURES

Thorsten Deilmann,[1,*] Alexey Chernikov,[2] and Kristian S. Thygesen[3]

[1]Institut für Festkörpertheorie, Universität Münster, 48149 Münster, Germany

[2]Institute of Applied Physics and Würzburg-Dresden Cluster of Excellence ct.qmat, TUD Dresden University of Technology, 01062 Dresden, Germany

[3]Computational Atomic-Scale Materials Design (CAMD), Department of Physics, Technical University of Denmark, 2800 Lyngby, Denmark

***Corresponding author.** Email: thorsten.deilmann@uni-muenster.de

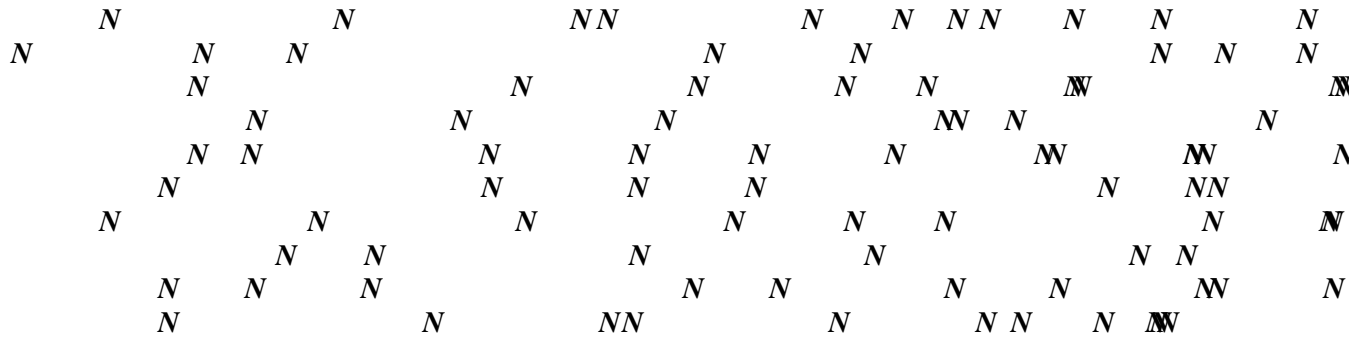
11.1. Current State of the Art

Mono- and few-layer structures of semiconducting TMDs host strongly bound excitons with binding energies of several hundred meV.[313] These binding energies are much larger than those of their bulk counterparts due to quantum confinement and reduced dielectric screening leading to strong electron–hole Coulomb attraction. In the presence of free charge carriers the neutral excitons may capture a free electron or hole and form charged excitons called trions (see Figure 11a).[314,315] An alternative description increasingly used at higher doping densities is that of the Fermi polaron corresponding to the exciton being dressed by the excitations of the Fermi sea.[283,316] Typical binding energies of the extra charge carrier to the exciton in monolayer TMDs are a few tens meV making them observable even at room temperature for sufficiently high doping. Experimentally, excitons, trions, and Fermi polarons can be probed by optical absorption and emission-type measurements as well as a variety of nonlinear and time-resolved techniques.[313] Theoretical calculations of excitons can be based on *ab initio* many-body methods like GW and Bethe-Salpeter equation (BSE),[317] analytical effective Hamiltonian approaches,[315] or employing the Bloch equations methods.[318] Altogether, the stability of the excitonic complexes combined with design flexibility of TMD structures and their tunability renders them excellent platforms for exploration and manipulation of fundamental exciton physics as well as for optoelectronic and excitonic devices operating up to room temperature.

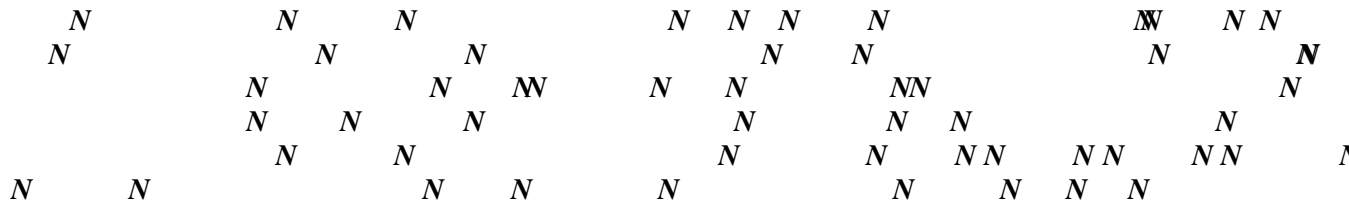
C w h

$! / c J j j e , G eJk, B L2GLGHeLkrHee i3VD0Jínke v H í D , k

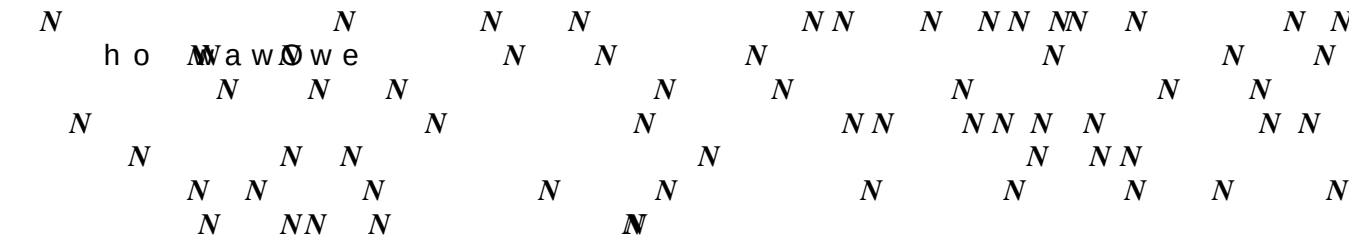
, e W r D i m : O S p t O p S i g



1 w s W i a g w O B 9 i s w M i



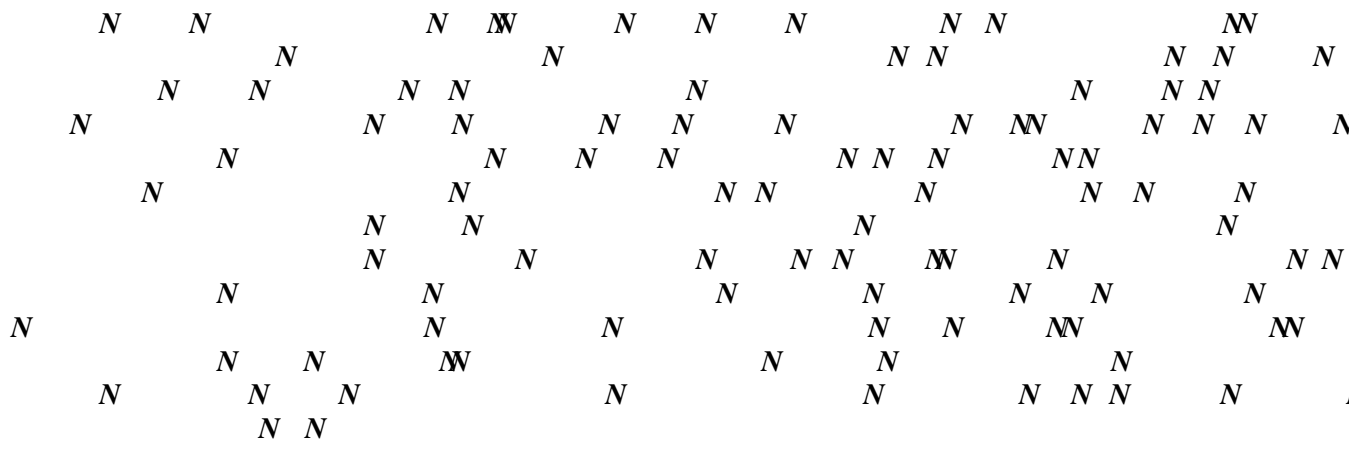
. m N w O e a N - B a h M w t g



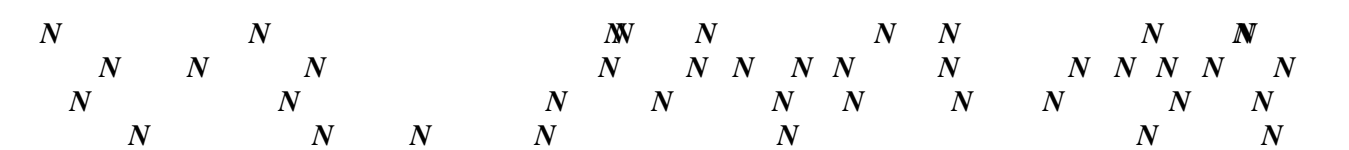
h o W a w O w e

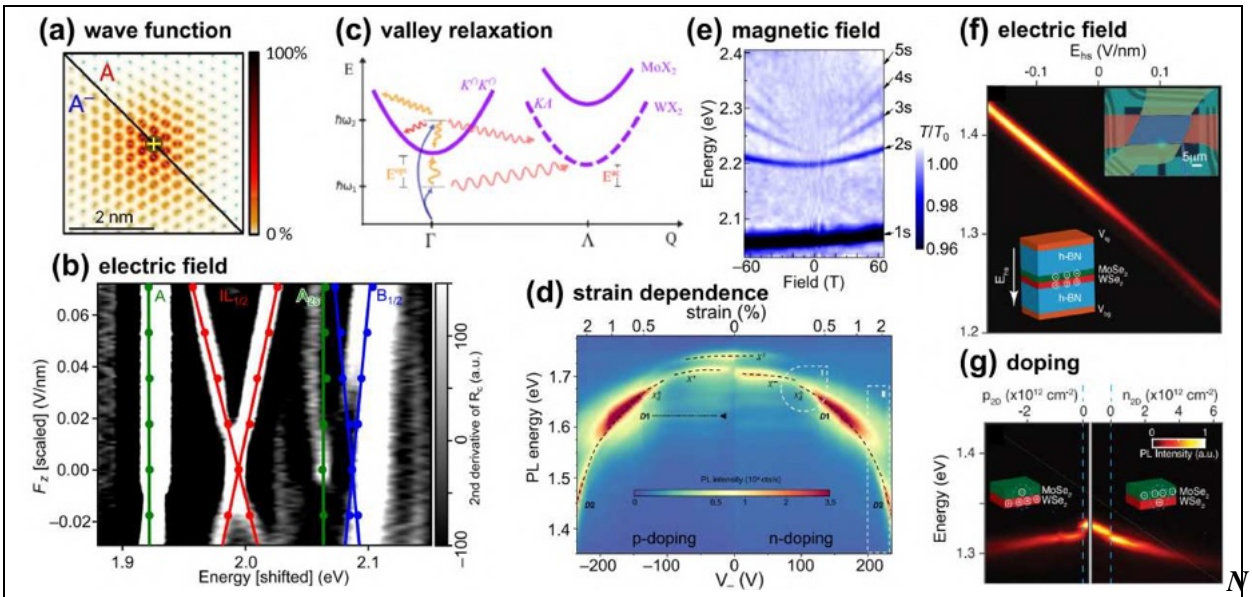
g O S p t O p S h i D c D W a i f N i D g D h M r D i g

; w W i i g e D C i n 2 M h s w a s e a 5 h a e M i O i S : t h D i



- B a h M w t g e c . D i t O S e a w t , g S S i D h O w e a g c S e M . m t w




(a) wave function
A
A⁻
2 nm
100%
0%
(c) valley relaxation
E
MoX2
WX2
Γ
Λ
Q
(e) magnetic field
Energy (eV)
Field (T)
5s
4s
3s
2s
1s
T/T0
1.00
0.98
0.96
(f) electric field
Ehs (V/nm)
5μm
h-BN
MoSe2
WSe2
(b) electric field
A
IL1/2
A2s
B1/2
Fz [scaled] (V/nm)
Energy [shifted] (eV)
2nd derivative of Rc (a.u.)
(d) strain dependence
strain (%)
PL energy (eV)
p-doping
n-doping
V− (V)
(g) doping
p2D (x10¹² cm⁻²)
n2D (x10¹² cm⁻²)
PL intensity (a.u.)
Energy (eV)

E P 1 8 2 v S N 8 2 8 5 (yT E 1 8 L 8 P 1 3 8 2 E L P g E S v S N 8 2 8 U E p 1 R 2 8 8 v 3 í y L 1 P 2 0 E E y P p 6 E E B R v A 0 8 y 1
y R S 2 p 8 3 0 8 M S L P 8 1 N 2 S 3 1 E E P p 1 8 2 8 8 N 8 8 2 8 1 8 6 p E 3 1 8 0 U E 1 R, , +8 2 ç E 3 3
" ; L í N+2)E*p2R 19 ç 8 2 E y S P 9 3 3 L y E S 1 E L P 6 L 2 1 R 8 9 0 b S P y 8 ç 8 P 1 L 6

$ % ! N : 6 : 4 ; < I 6 0 . 8 2 9 6 . . 6 ; : 6 : % 1 . 2 9 6 0 ; : 1 N 0 I ;
6 : I 2 1 0 . 8 . I 6 ; : . : 1 . 8 8 ; D 6 : 4

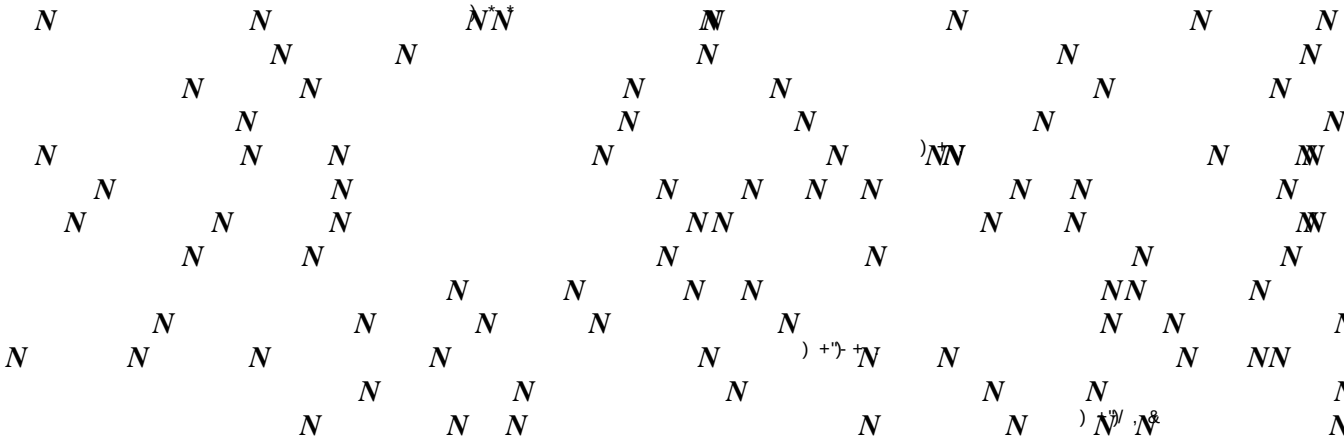
F D c J , , e k " 9 - J a L J n H e v í D # R S é n D D , e k $ J B J i, G 9 p J J n b 9 ! % & 4 e n k J o
$ < 8 í S 2 1 ç 8 P 1 L 6 R N 3 E y 3 S P p 0 E S 9 % 3 1 9 2 1 L R P 8 L P ç 3 N % % C q 8 P L E 2 b p 8 E 2 S 3 E , 1) N /) L + 6 % C
% < 8 í S 2 1 ç 8 P 1 L 6 R N 3 E y 3 % E d 1 R N 8 % q 8 P H E P b 3 N 2 v 3 b E S 1 P N E S S c 2 1 6 S % 1 8 9 q P * E / b 1 8) 2
& < 8 í S 2 1 ç 8 P 1 L 6 t S 1 8 2 E S v 3 R U 8 y 3 E 1 8 P 2 y P 8 q S P H E 0 b 8 = 2 P 3 p E E 1 P N 8 % 8 2 = E b P S p P % 3 1 L L P 2
c 1 S 1 8 3
' < 8 í S 2 1 ç 8 P 1 L 6 ; R 8 ç E 3 1 2 N % L P i % 2 C 1 v R v U E B P 3 L 1 E B 3 2 P /) q + P) E 1 b % 8 2 q P H E E 1 N 8 % 0 = b
(< 8 í S 2 1 ç 8 P 1 L 6 = v 8 y 1 2 E y S 1 v R U S 8 P 3 1 8 , 1 P ç í D P 1 E B 2 8 2 = 8 P b H E P N % 8 2 = E b P S p P % 3 1 L L P 2
c 1 S 1 8 3
- 9 ; ; 2 < : 9 8 1 N 5 L 8 P 3 S P 0 P * 8 = 3 4 ' 9 S ; g , S 1 8 8 D p S ' 8 0 D

$ # ! / L n n e , H B H J H e D r H c e - n H

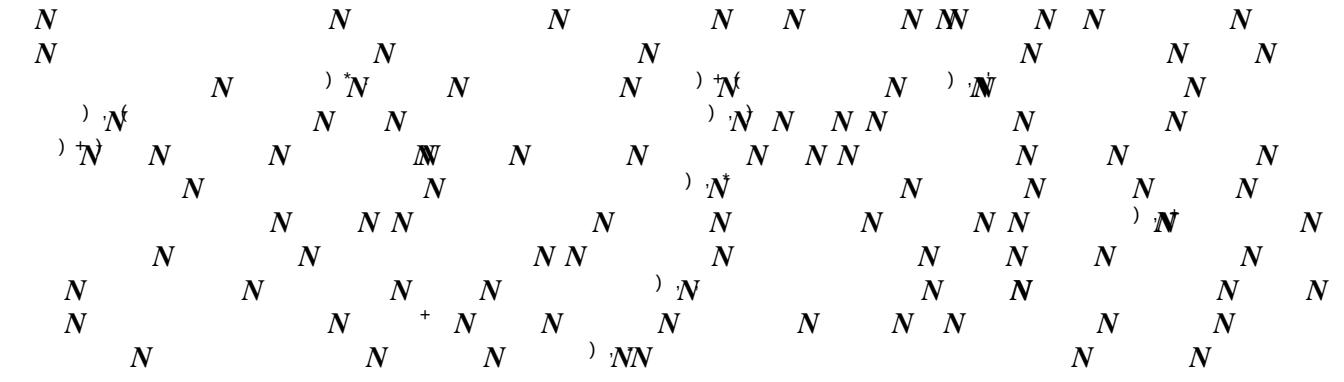
2 a O S e M i p t O w e a

: B a O N i g w g

, h S h t O i S w d h O w e a

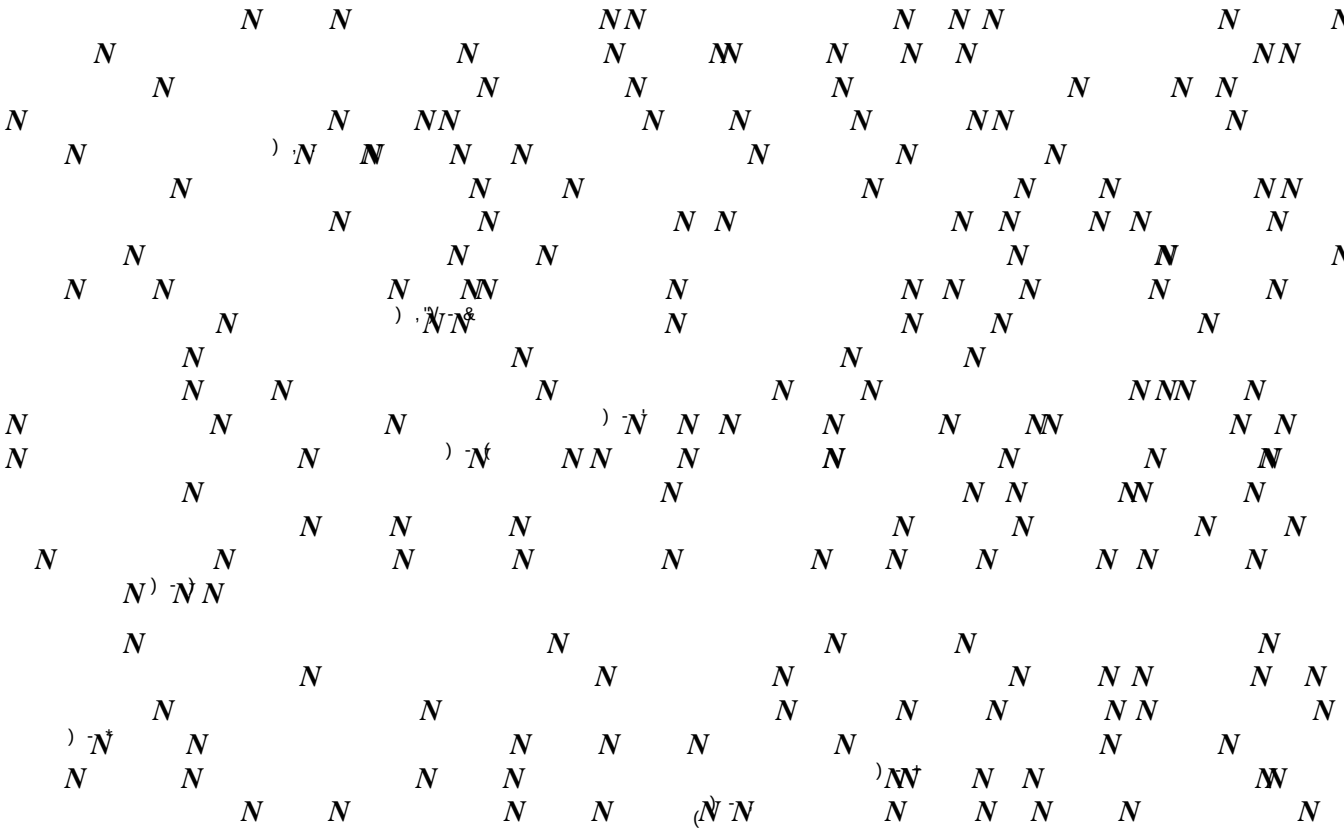


* r r D w t h O w e a g



$ $! / c J j j e , G e k J , i ; N N D n H L , í H í e k

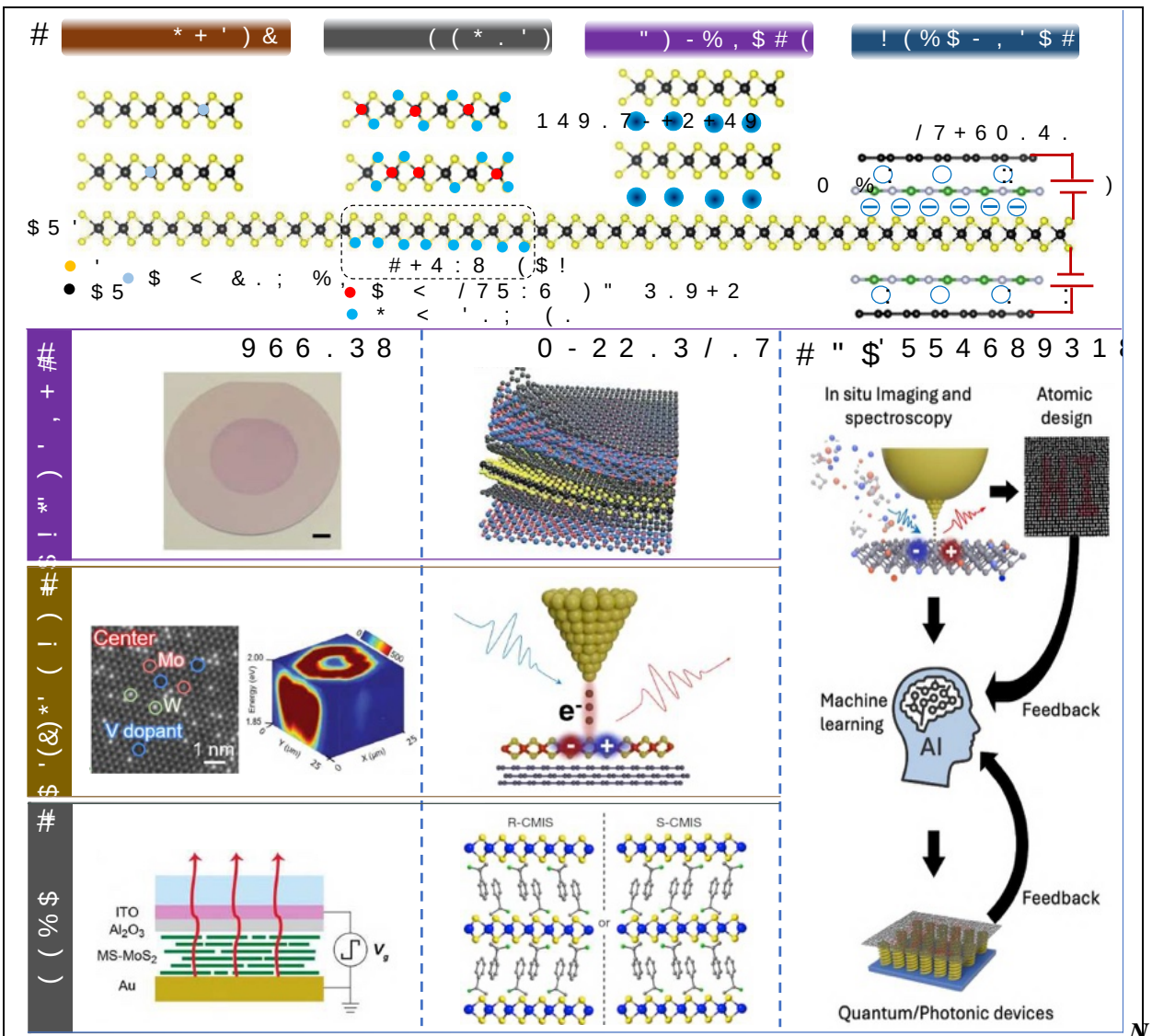
: B a O i g w g

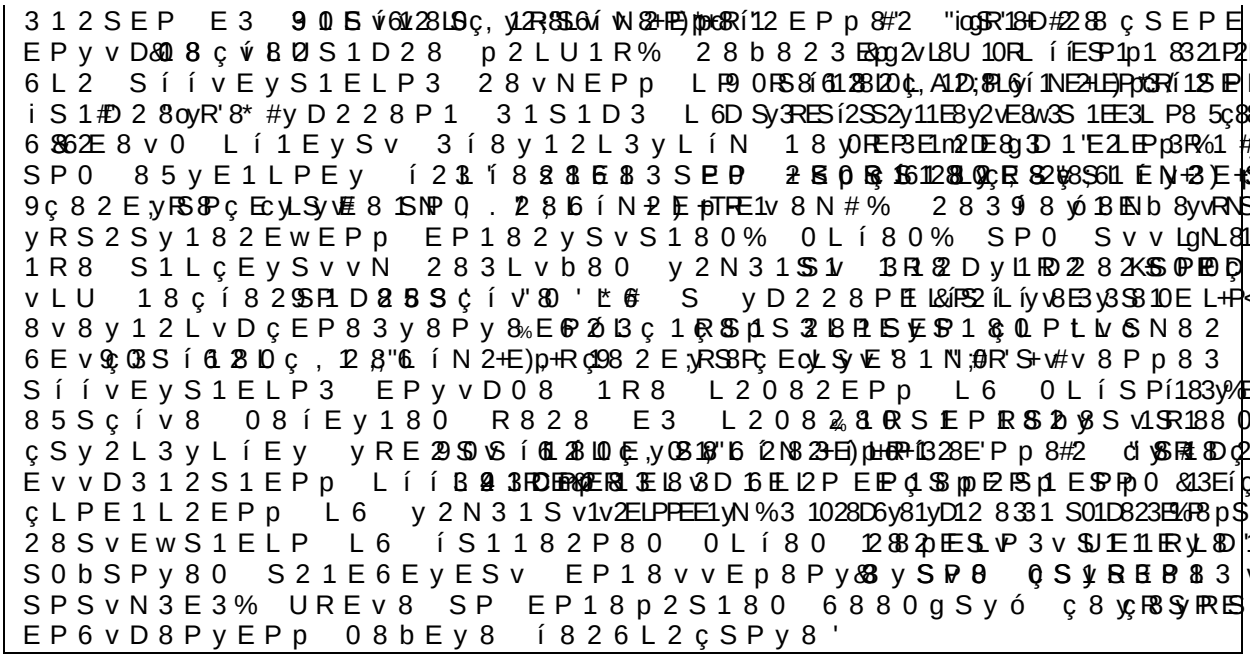


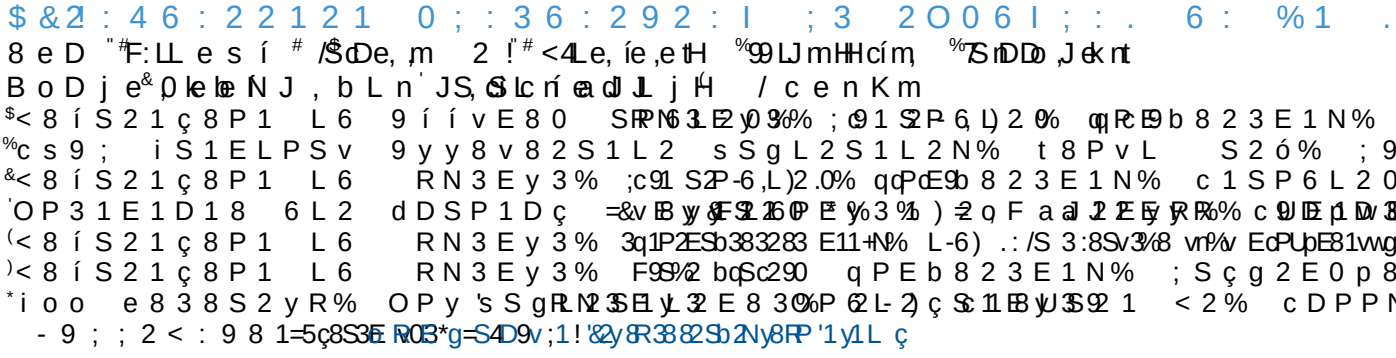
, h S h t O i S w d h O w e a

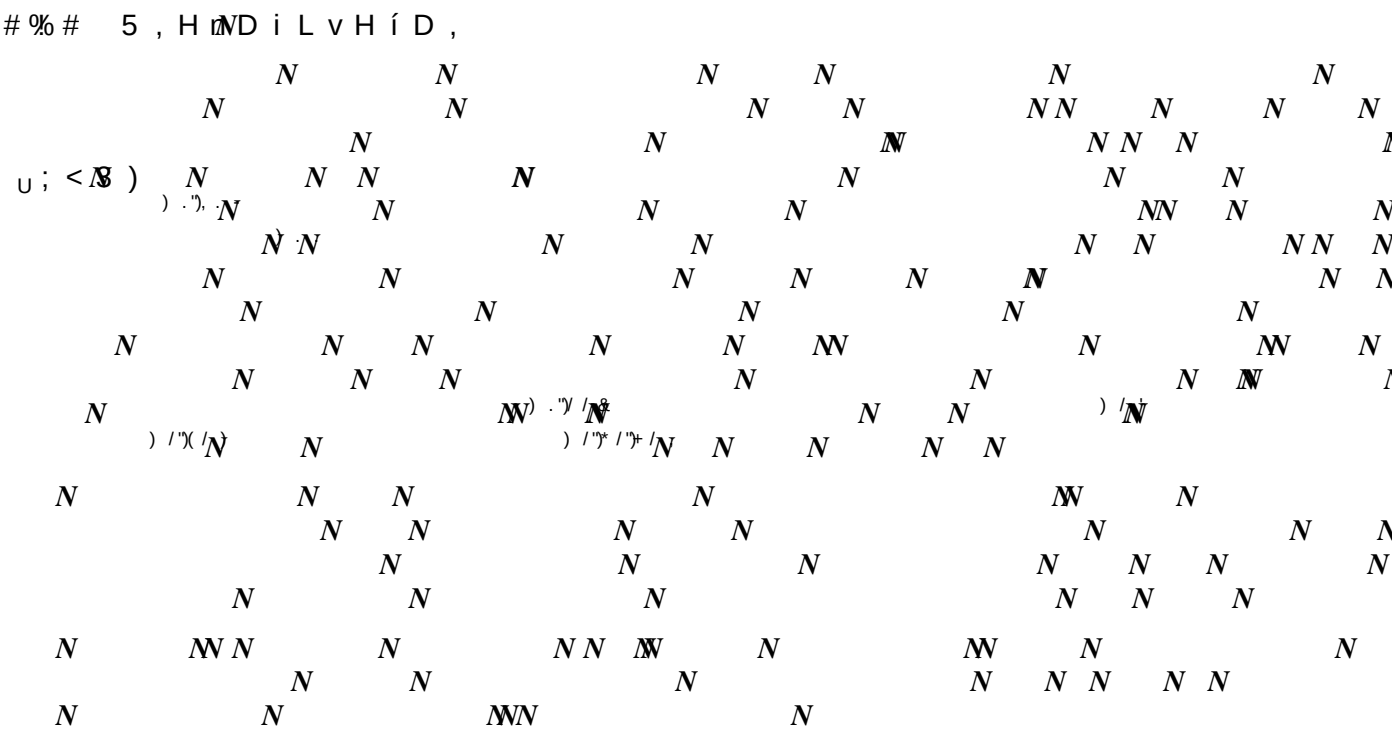
2 ag wO p w g wO p

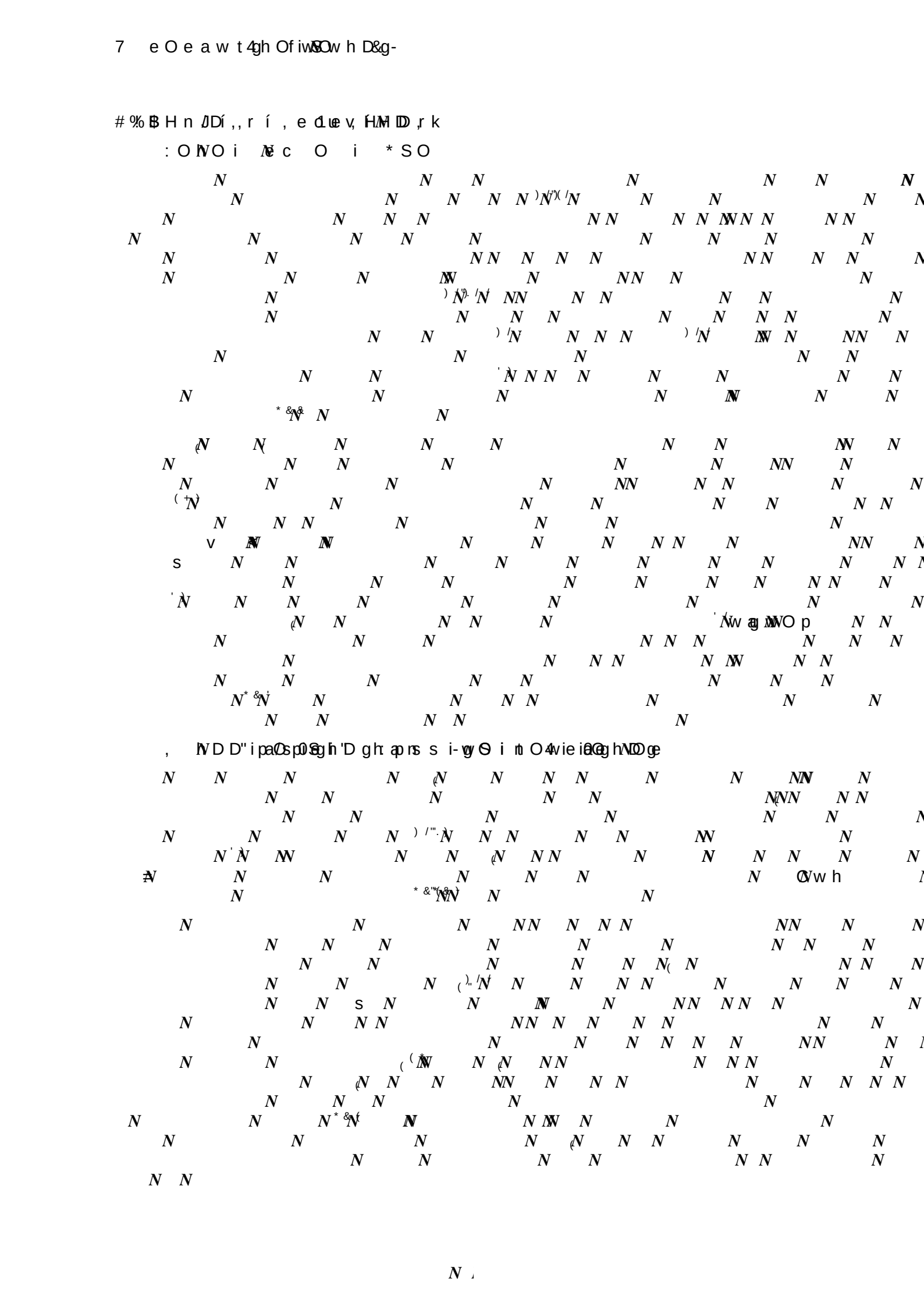
* r r D w t h O w e a g

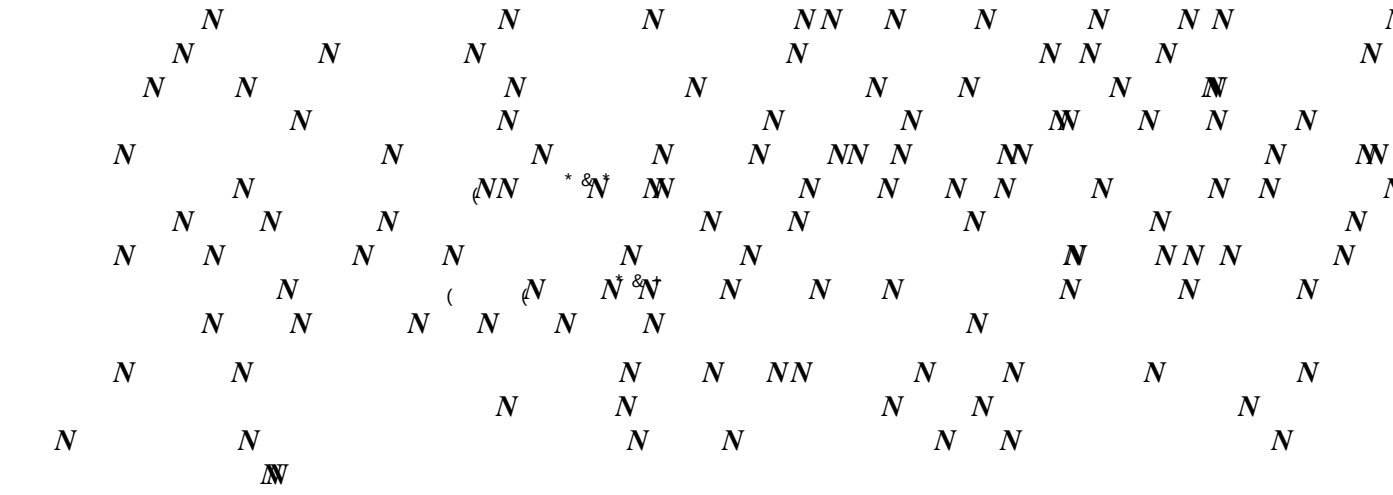

Center
Mo
W
V dopant
1 nm
ITO
Al_2O_3
MS-MoS_2
Au
V_g
R-CMIS
S-CMIS
or
e-
In situ Imaging and spectroscopy
Atomic design
Machine learning
AI
Feedback
Feedback
Quantum/Photonic devices

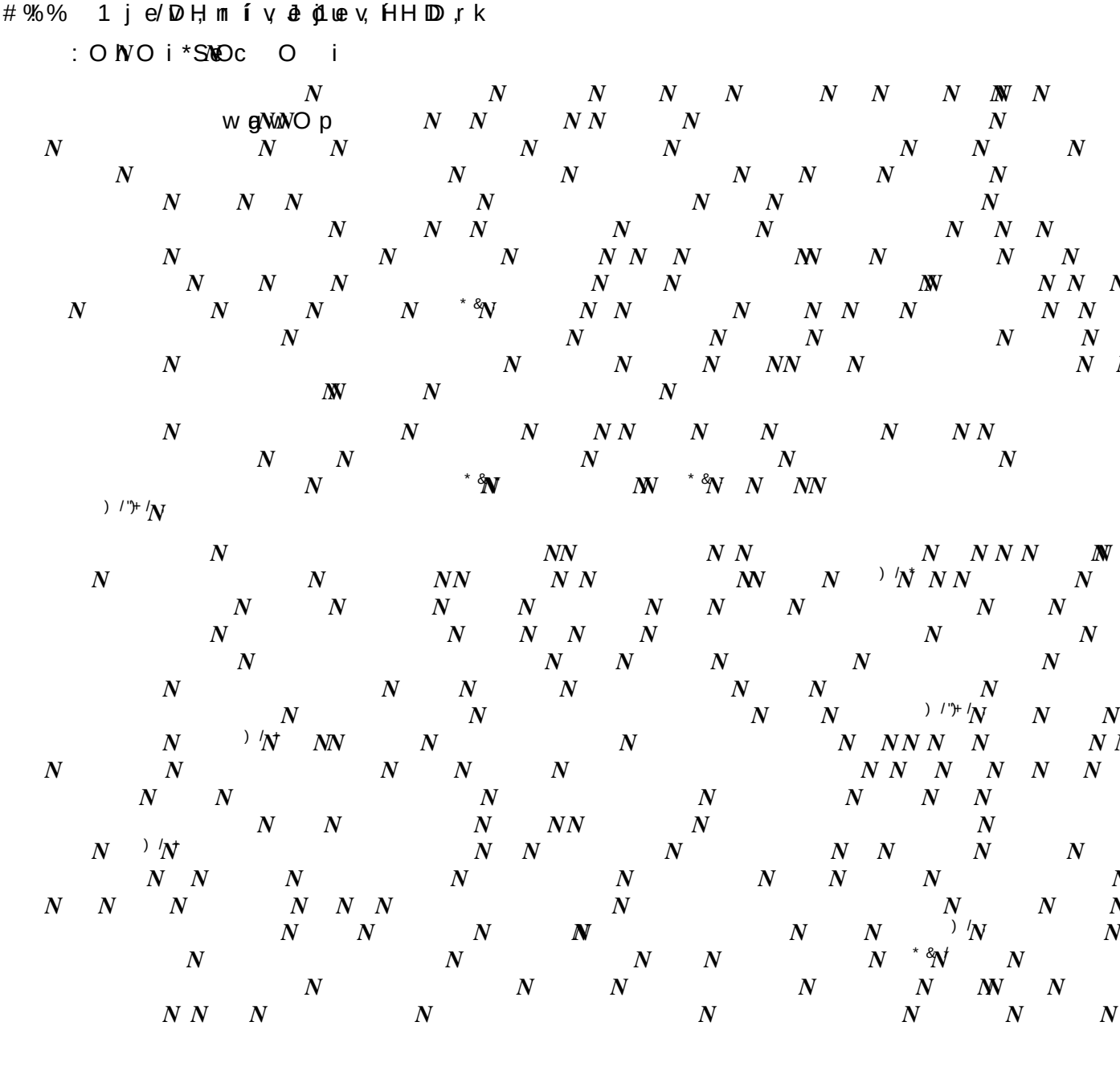


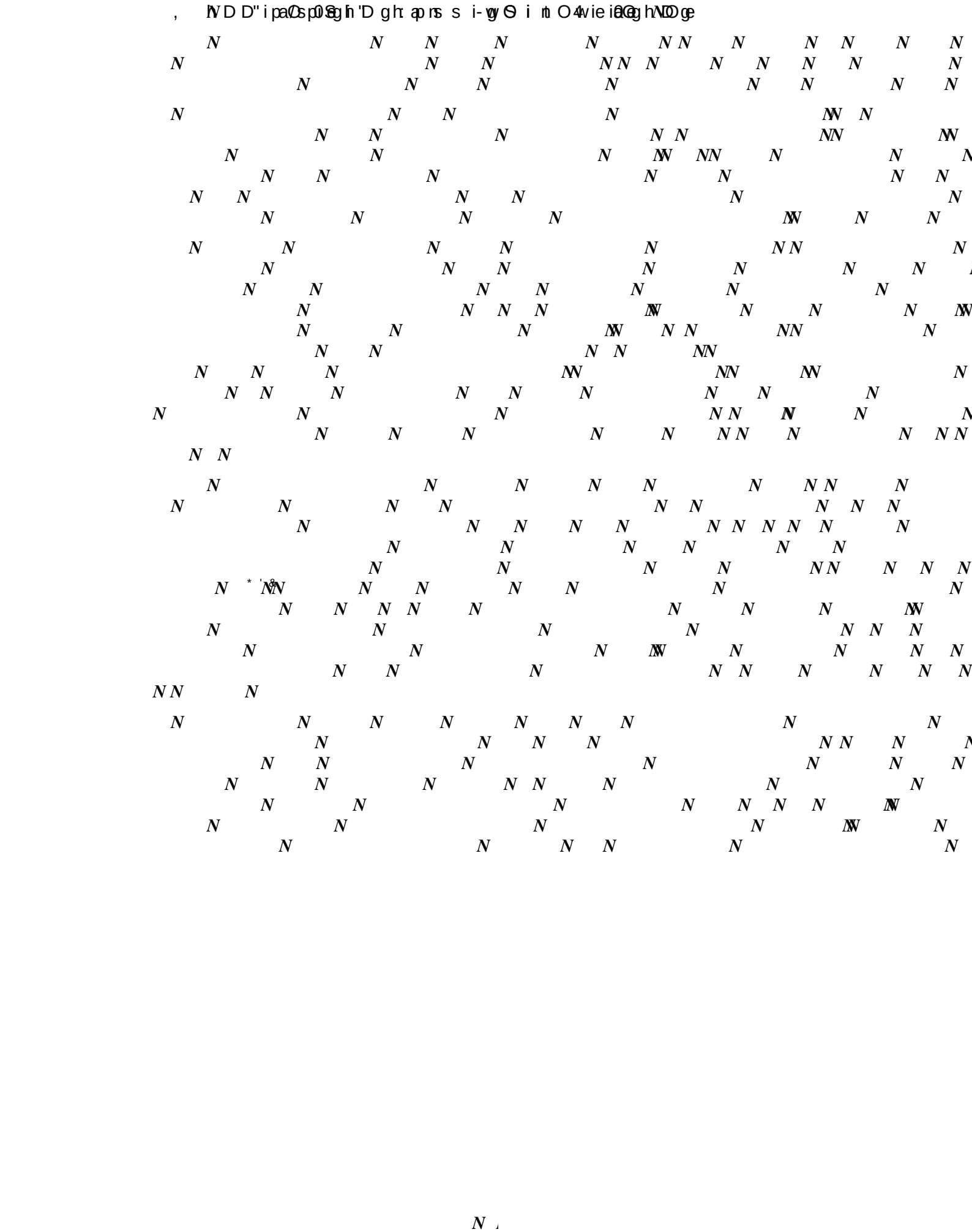












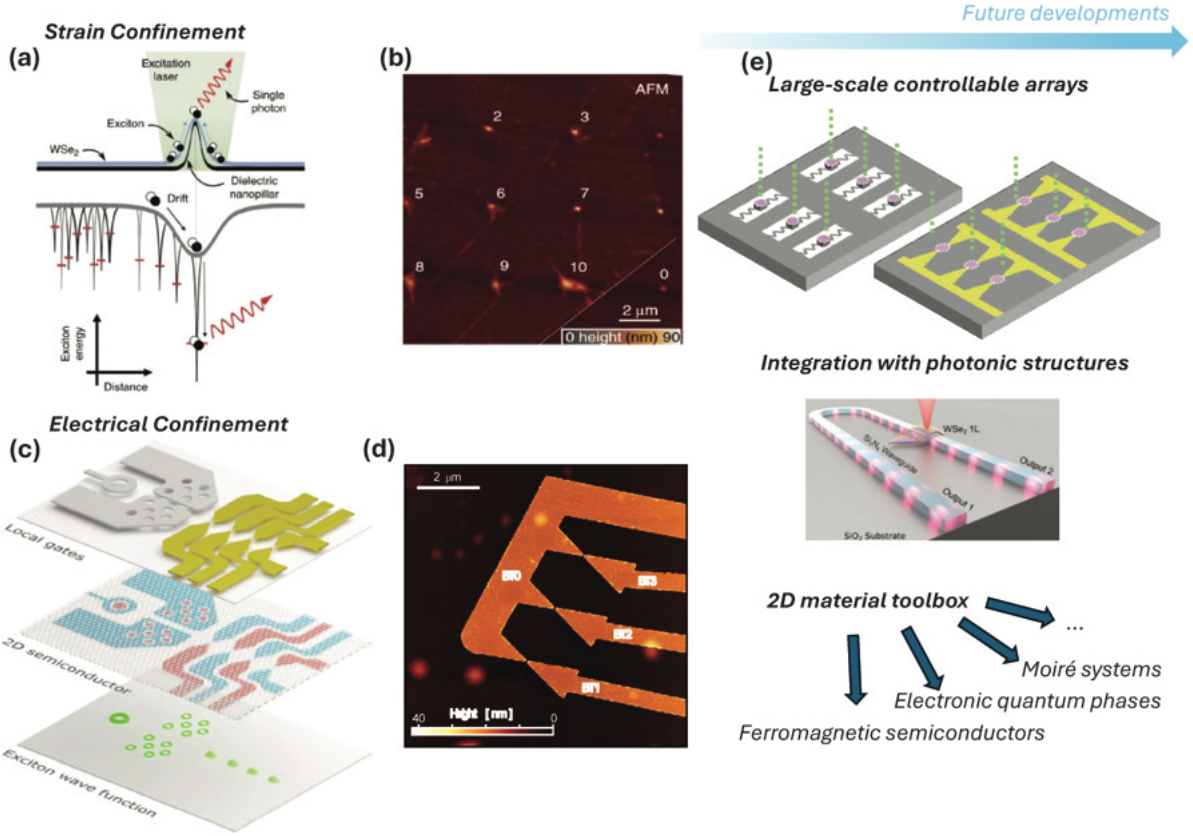


Figure 13. Strain and electrostatic engineering for monolayer exciton confinement. (a,b) The principle of strain-induced quantum confinement (a) and representative site-controlled quantum emitters (b). Reproduced with permission from ref 397 (Copyright 2017 Springer Nature). (c,d) Structures for 0D electrostatic quantum confinement of intra-layer excitons with position and energy tunability. Reproduced with permission from ref 395 (Copyright 2024 The American Association for the Advancement of Science). (e) Some future possibilities for scaled-up arrays of controlled QEs, interfacing with photonic integrated circuits, and new interfaces with 2D material platforms. Adapted with permission from ref 411 (Copyright 2021 American Chemical Society).

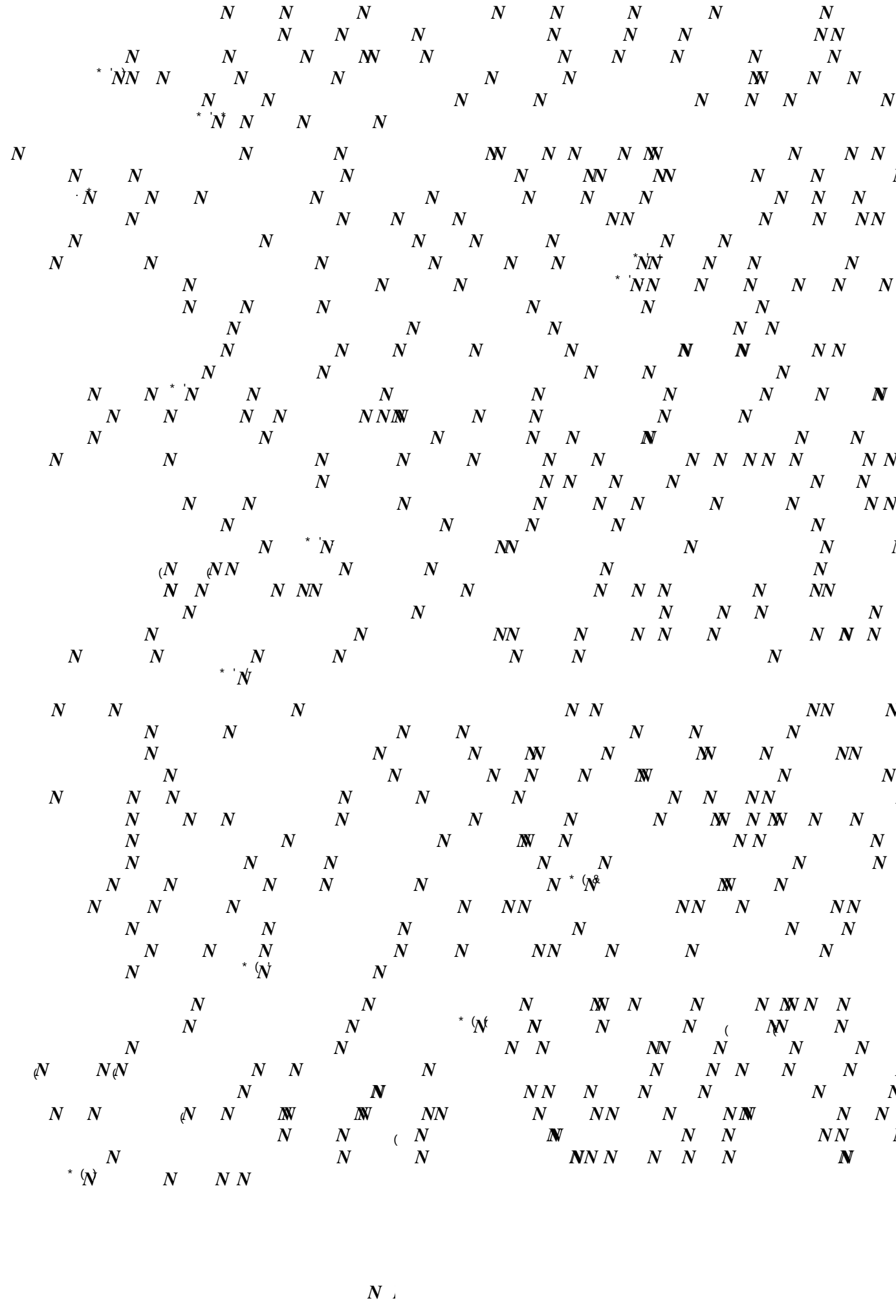
Nonlinear and Ultrafast Optical Phenomena

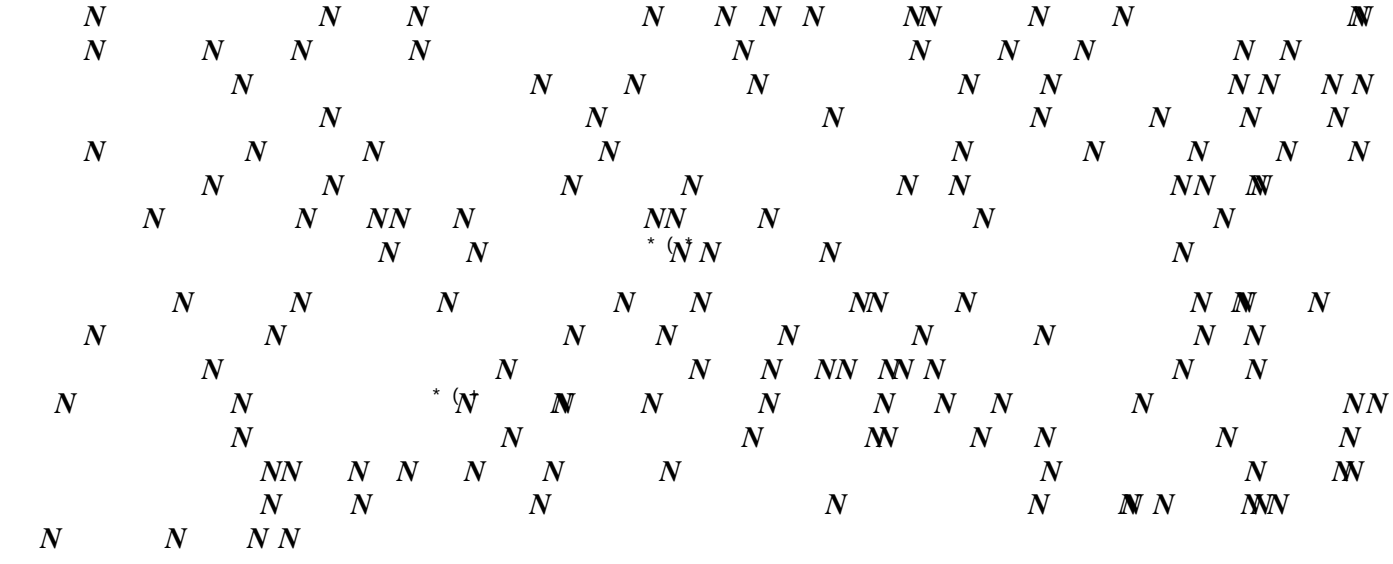
14. ULTRAFAST EXCITON DYNAMICS IN VAN DER WAALS HETEROSTRUCTURES

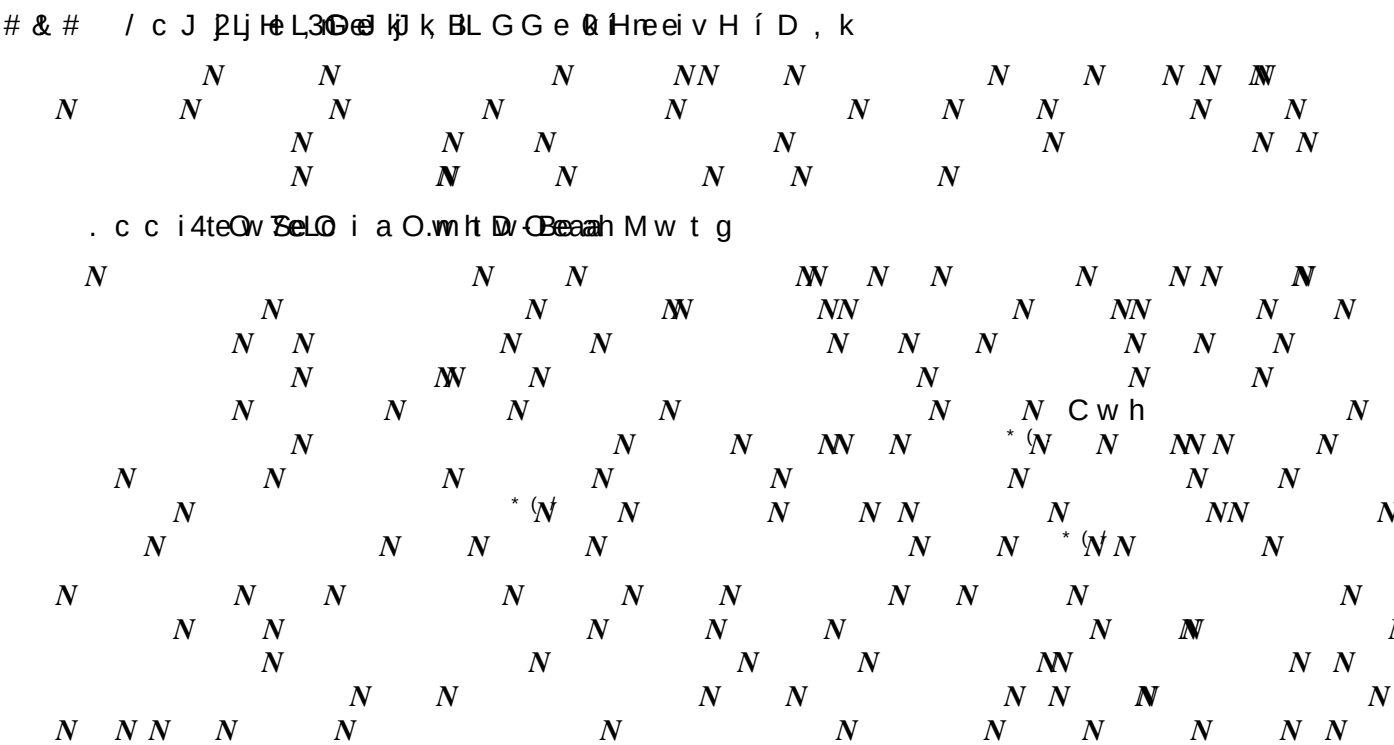
Armando Genco,[1] Chiara Trovatello,[1,2] Giulio Cerullo,[1] and Stefano Dal Conte[1,*]
[1]Politecnico di Milano, Dipartimento di Fisica, Piazza Leonardo da Vinci 32, Milano (MI), Italy
[2]Department of Mechanical Engineering, Columbia University, New York, NY 10027, USA
***Corresponding author.** Email: stefano.dalconte@polimi.it

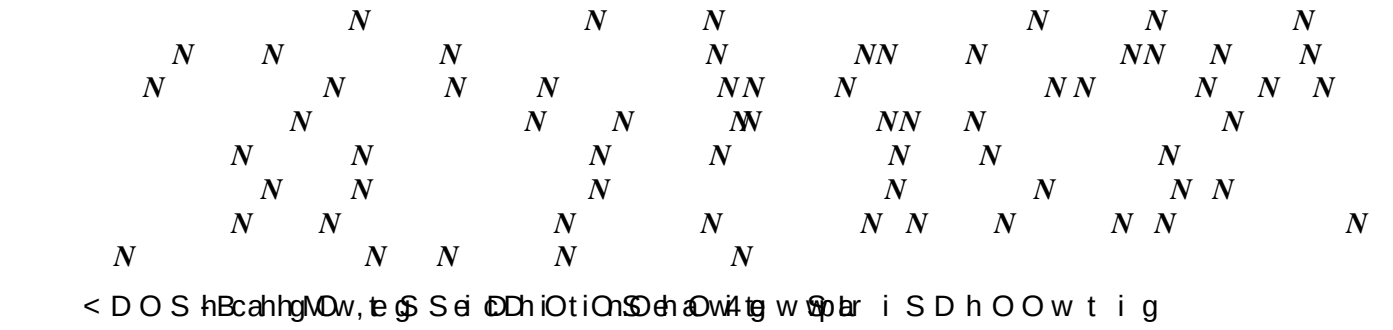
Two-dimensional TMDs have been at the forefront of research on condensed matter physics due to their unique optoelectronic properties enabled by strong light–matter interaction. Quantum confinement and reduced Coulomb screening make TMDs an ideal playground to study excitons and their many-body complexes (i.e., trions, biexcitons, and other multiparticle states) and to investigate their tunability with external parameters like electric/magnetic fields and the lattice strain. Moreover, the possibility to optically address and manipulate the spin/valley degree of freedom further increased interest in these materials.[412]

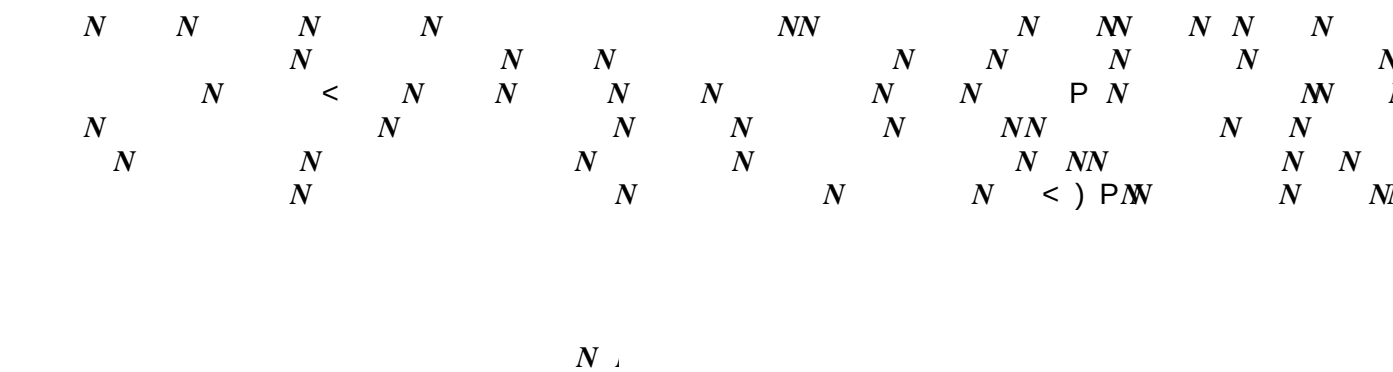
Since the advent of 2D materials, out-of-equilibrium spectroscopies have been extensively used to study the mechanisms of formation, relaxation, and recombination of excitons occurring on different timescales, ranging from tens of femtoseconds to nanoseconds. Exciton line-shape analysis performed at different delay times has shown that the transient optical response as measured by pump-probe optical

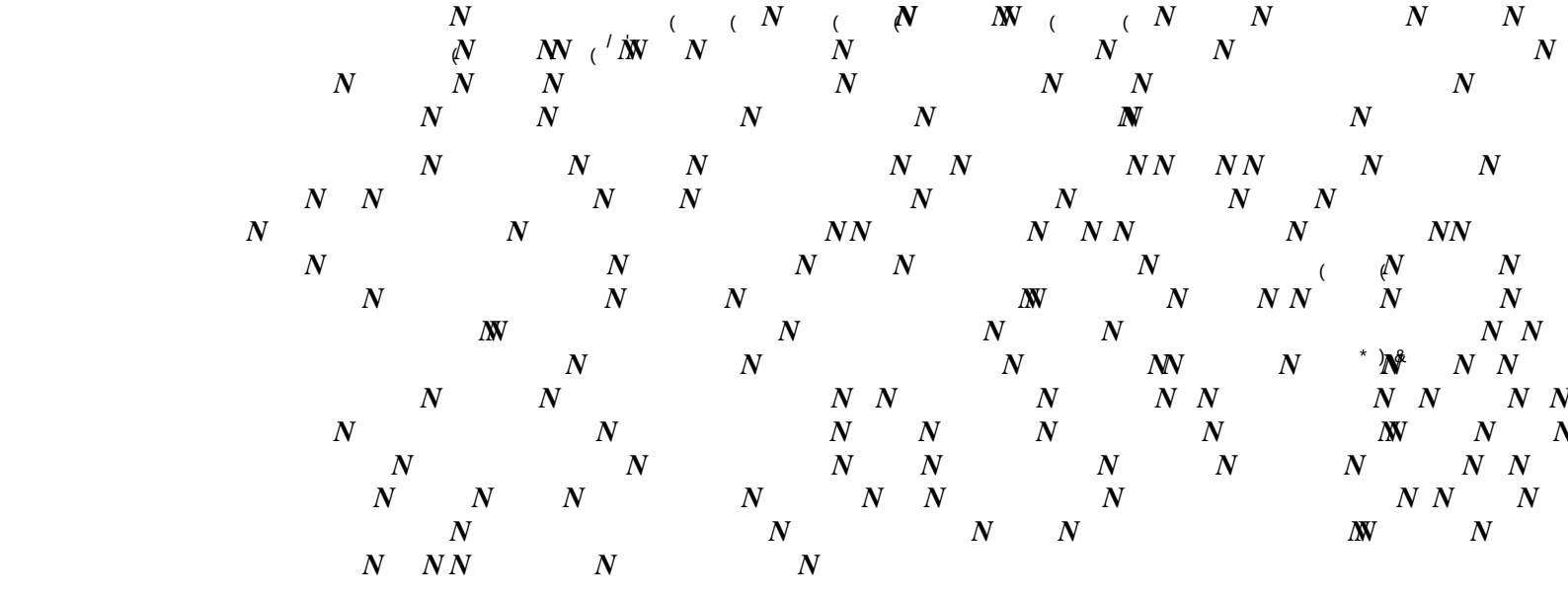




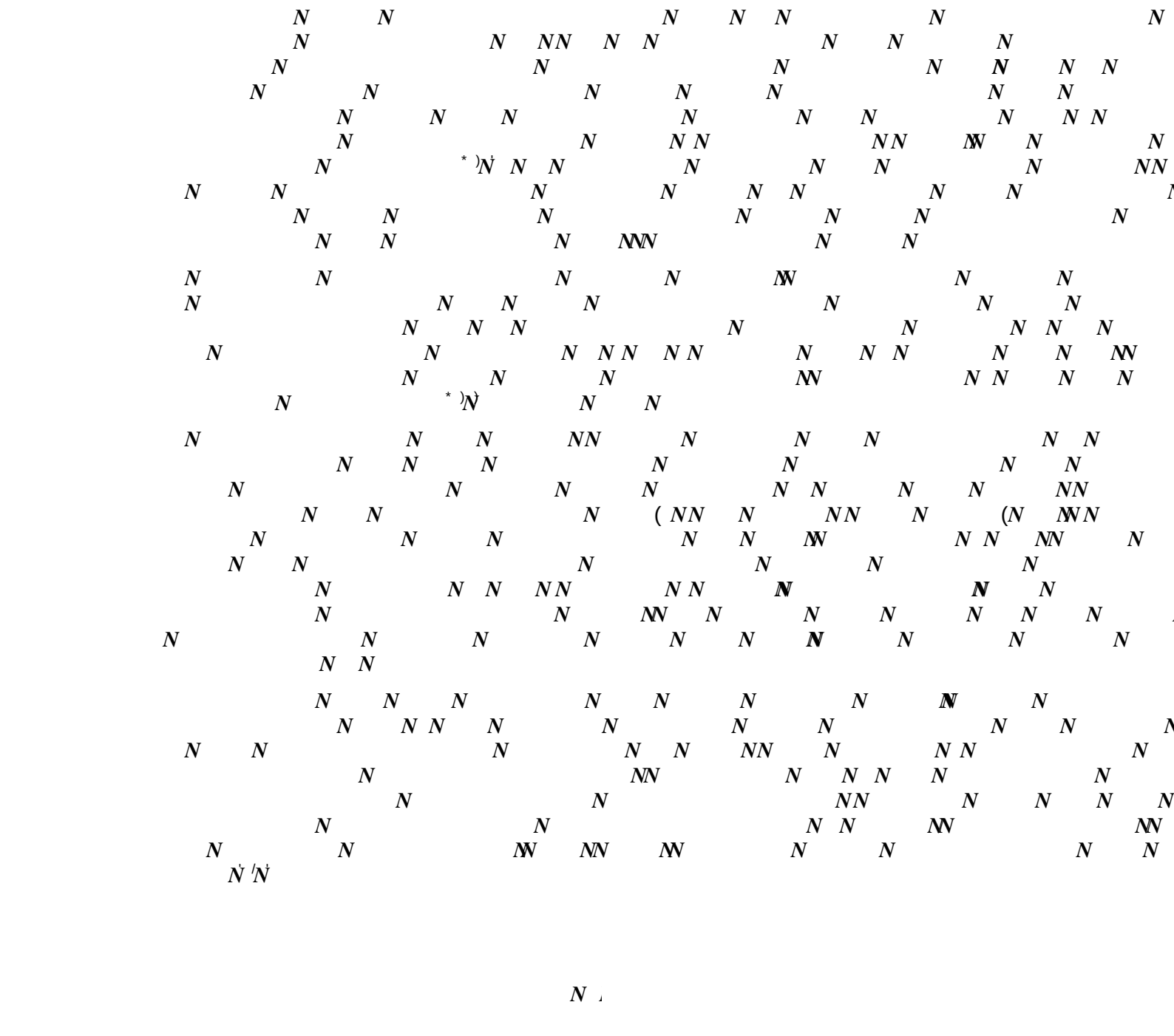








* n C h a t-D G S lwraihtgOOS e igtt earwBl p i g



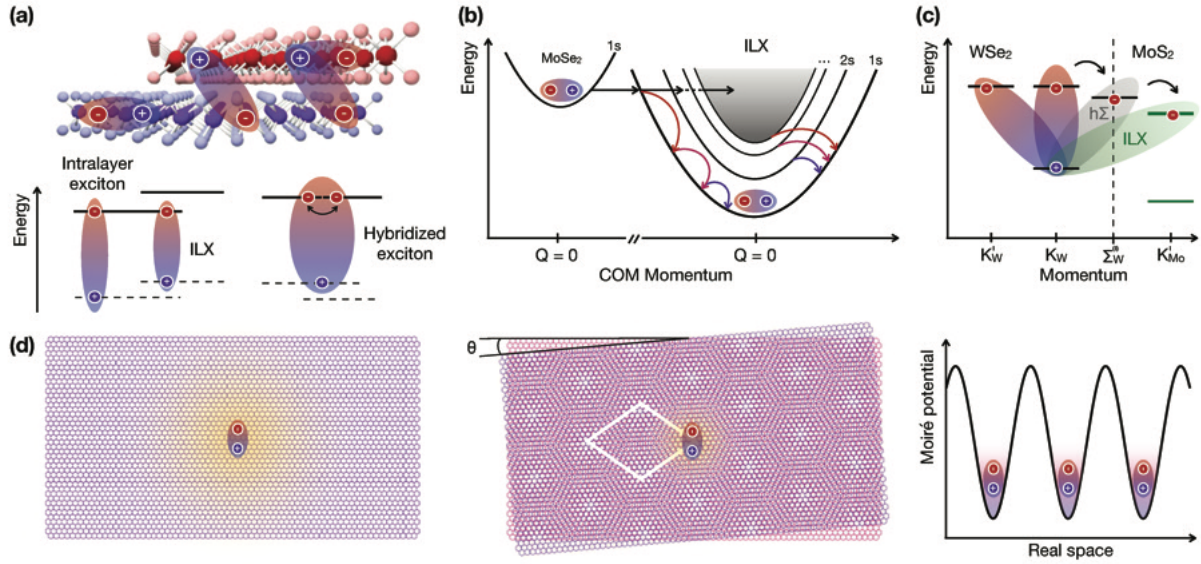


Figure 14. Ultrafast optical processes in vdW heterostructures. (a) Sketch of a TMD heterostructure illustrating intralayer, interlayer, and hybrid excitons, along with the simplified representation of the heterostructure band structure with the different band alignments hosting different excitonic species. Hybrid exciton results from resonant interlayer electron tunneling. Adapted with permission from ref 434 (Copyright 2021, American Chemical Society). (b) Graphical representation of the interlayer-exciton (ILX) formation process in a $MoSe_2/WSe_2$ heterostructure upon resonant photoexcitation of the bright exciton in $MoSe_2$. Hole transfer results in the formation of a hot ILX population with finite momentum Q. Hot ILXs quickly relax to the optically bright ILX ground state by exchanging energy and momentum with phonons. Adapted from ref 419 (Creative Commons CC BY). (c) Sketch of the single-particle valleys of MoS_2/WSe_2 heterostructures at some high-symmetry points (i.e., K and Σ). After resonant photoexcitation of the intralayer exciton in MoS_2, an ILX at the K valleys forms *via* intermediate phonon-mediated scattering with hybrid exciton (hΣ). Adapted with permission from ref 423 (Copyright 2023 IOP Publishing). (d) Exciton diffusion in TMD heterostructures with and without moiré superlattice (left and center panels). θ is the twist angle between the two monolayers. The moiré potential (sketched in the right panel) tends to localize ILXs and to hinder their diffusion.

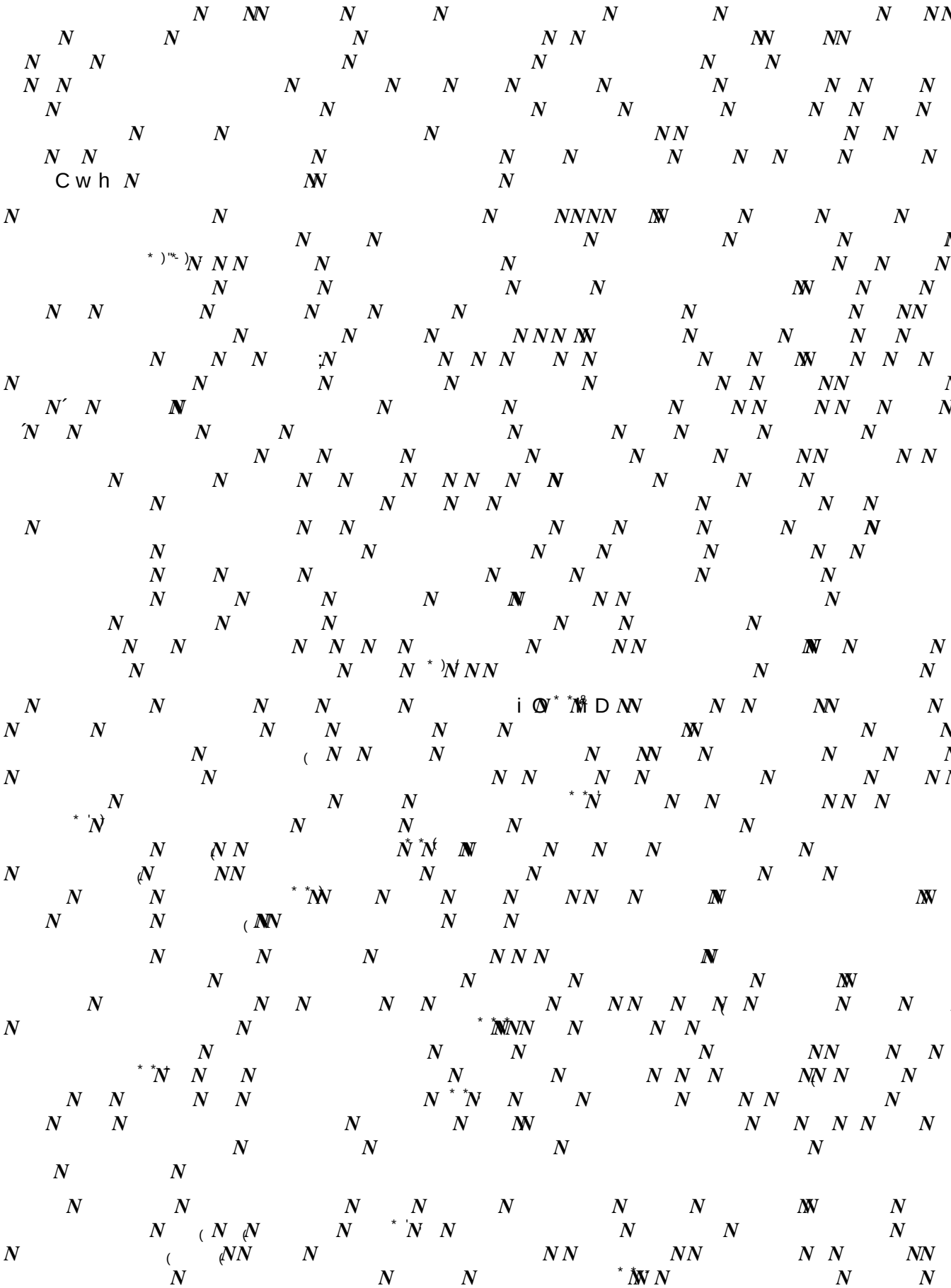
15. QUANTUM-COHERENT COUPLING IN TWO-DIMENSIONAL MATERIALS PROBED BY ULTRAFAST MULTIDIMENSIONAL SPECTROSCOPIES

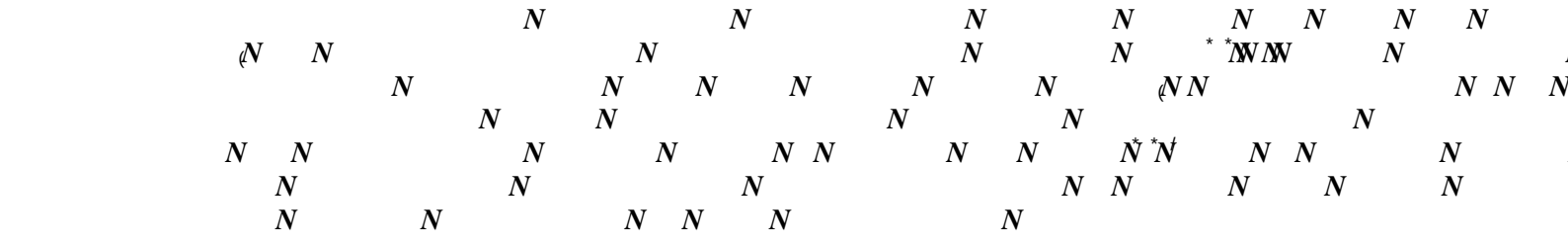
Daniel Timmer,[1] Antonietta De Sio,[1,2] and Christoph Lienau[1,2,*]
[1]Institut für Physik, Carl von Ossietzky Universität, 26129 Oldenburg, Germany
[2]Center for Nanoscale Dynamics (CeNaD), Carl von Ossietzky Universität, 26129 Oldenburg, Germany
***Corresponding author.** Email: christoph.lienau@uni-oldenburg.de

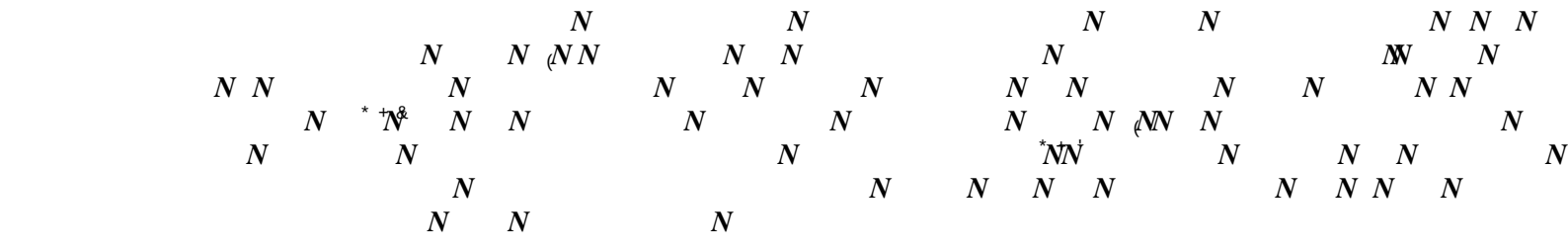
15.1. Current State of the Art

Transition metal dichalcogenide monolayers present a fascinating nanoscale laboratory for probing coherent couplings and many-body interactions (MBI). Already their linear optical properties are governed by strong Coulomb correlations, forming excitons with binding energies of up to several hundred meV, stable even at room temperature.[313,435] Their unusual band structure and broken inversion symmetry couples spin and valley degrees of freedom. This makes the optical absorption spectra of different valleys sensitive to the circular polarization of the incident light, opening up the field of valleytronics. Weak dielectric screening enhances the formation of charged quasiparticles with properties that can be controlled by chemical doping and/or electrostatic gating. This weak screening also makes excitons in TMD monolayers particularly sensitive to strain-induced variations in the potential landscape, resulting in exciton localization and the creation of single photon sources[436] with direct applications in quantum communication, metrology, and computing.

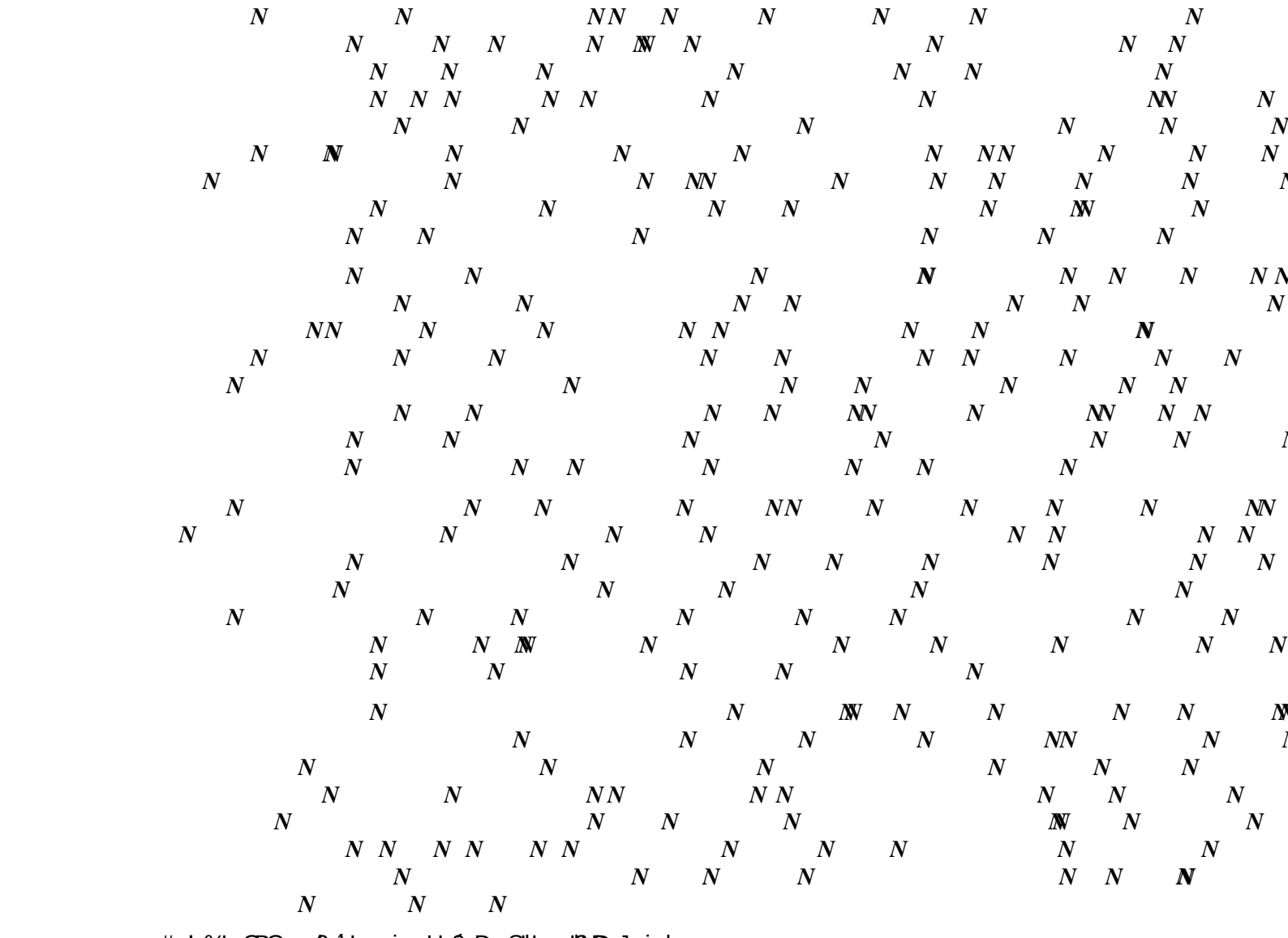
Coherent couplings and MBI govern not only the linear but also the nonlinear optical properties of TMDs. Their optical nonlinearities largely arise from MBIs such as excitation-induced dephasing (EID) and resonance energy shifts (EIS).[437] For sufficiently low temperatures, biexcitons and charged exciton complexes appear as new resonances in the nonlinear spectra. Importantly, coherent couplings among



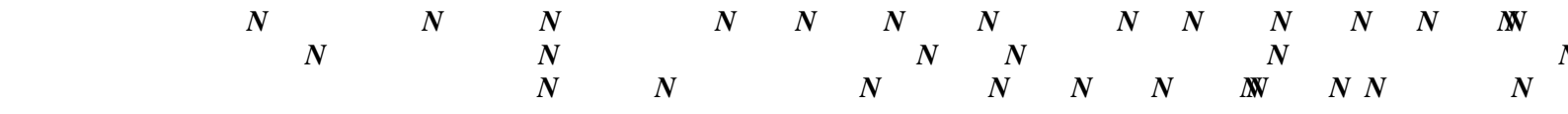




! $ / c J j j 2eL,HGLeDkeJjR,i



! %L GBGe0iHneeiv H9 Ð eSkkeHRDJ j k



covering the full visible range[452] and extending into the UV range. Current 2DES experiments have resolved coherent coupling with energies of up to ~ 400 meV corresponding to oscillation periods in the 10-fs range, which represents the upper limit of what can be reached in current 2DES setups. Improved time resolution will be essential to achieve broader spectral coverage. Combinations of supercontinuum white light generation with light field synthesis[453] and/or pulse shaping have the potential for designing pulses with durations of <3 fs. Yet such pulses have not been applied in 2DES experiments so far.

Equally important are efforts to enhance sensitivity and reduce the acquisition time of 2DES experiments. Here, the implementation of recent developments in ultrafast dual- and multi-comb spectroscopy for ultrafast 2DES seems promising, as they enable rapid optical delay scans without moveable parts and noise suppression.[454,455,456]

Not only the recording but also the interpretation of experimental 2DES data needs further development. This includes, for example, the use of rapidly developing artificial intelligence methods for spectral analysis as well as of automated schemes to compare experiments and simulations based on model Hamiltonians. We emphasize that high-quality 2DES measurements provide an important benchmark for theoretical descriptions of nonequilibrium quantum dynamics in TMDs, using, for example, semiconductor Bloch equation calculations. Improving the merger between theory and experiment will therefore be crucial for future advancements. This is especially true for the development of *ab initio* descriptions which still are in a very early stage.[457]

So far, all the discussed experiments have used all-optical 2DES detection schemes. Time- and angle-resolved photoelectron spectroscopy has provided crucial insight into momentum-resolved incoherent exciton dynamics[458] and interlayer exciton formation.[422] Integrating such momentum-resolved photoelectron detection schemes with ultrafast 2DES may give intriguing new insight into the coherent quantum dynamics in TMDs and their heterostructures. Equally promising are combinations of 2DES with high-resolution microscopy techniques. This includes both further improvements of far-field 2DES microscopy[447] and in particular also the development of entirely new detection schemes providing nanometer-scale spatial resolution and few femtosecond temporal resolution. A promising step in this direction is the coherent 2D optical nanoscopy technique reported in ref 459. More generally, combining 2DES with action-based detection schemes, such as, for example, photocurrent or photoelectron emission microscopy, or with the all-optical readout of the optical field emitted from the junction of a scanning probe tip, may bring 2DES microscopy of TMD materials to the nanometer scale. These advancements will enable deeper and more detailed exploration of spatio-temporal light-driven quantum transport in 2D materials and heterostructures.

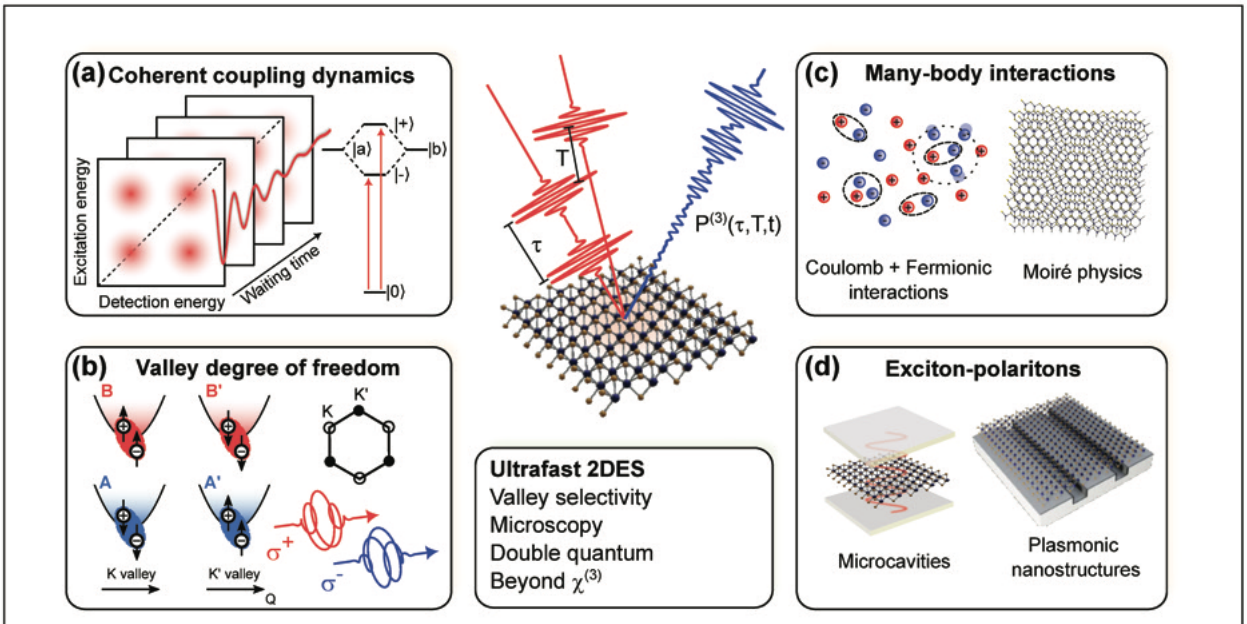
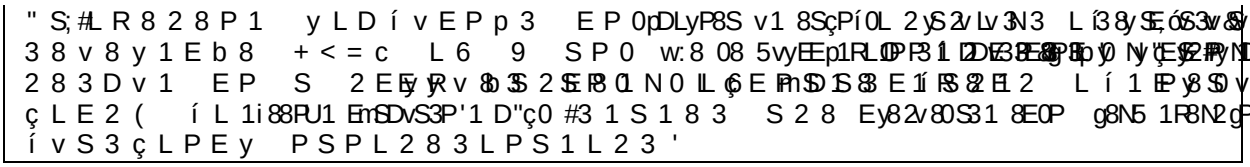
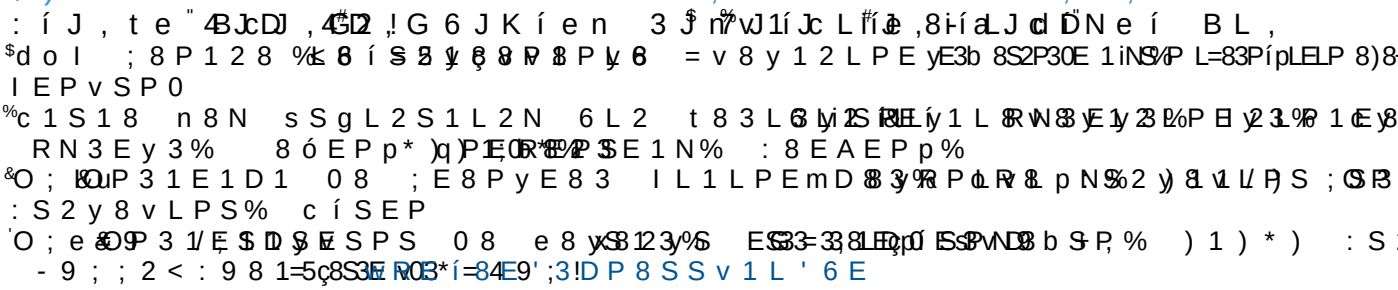


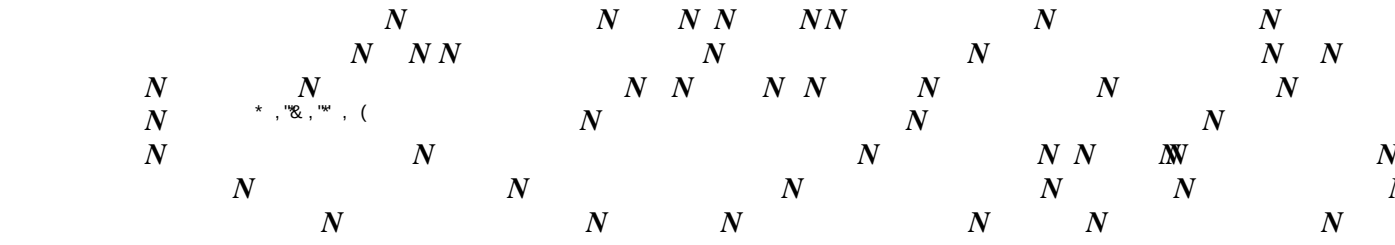
Figure 15. Ultrafast 2D electronic spectroscopy of 2D materials. The sample is resonantly excited with a phase-locked pulse pair with delay τ. A probe pulse at waiting time T induces a nonlinear polarization in the material.



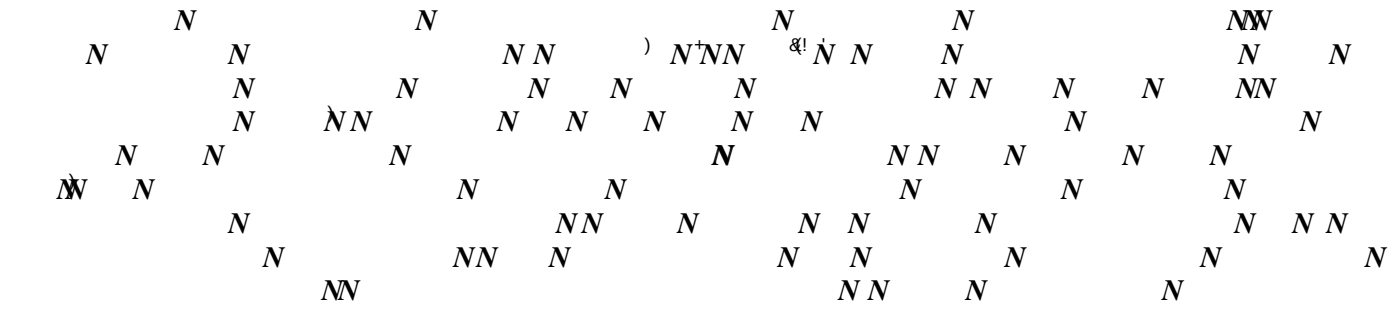
$)%1 9 . I 2 1 6 . 8 . / . . 2 1 : ; : 8 6 : 2 . 1 < 5 ; I ; : 6 0 .



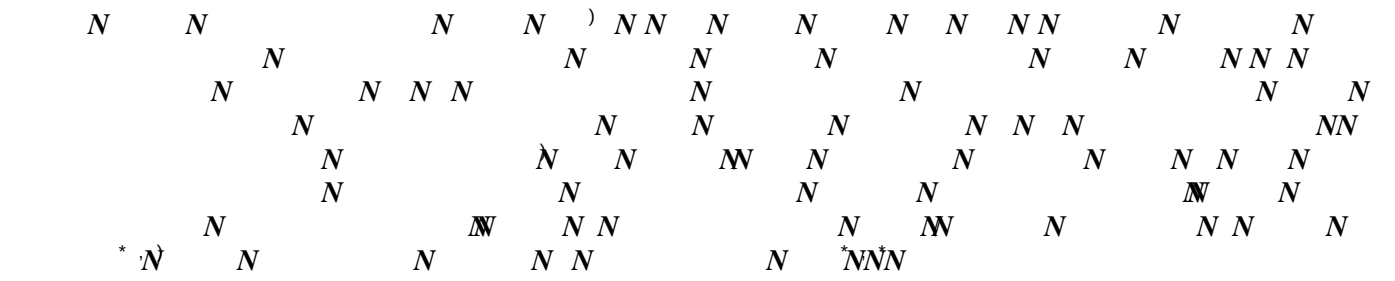
(5 , H n D i L v H í D ,



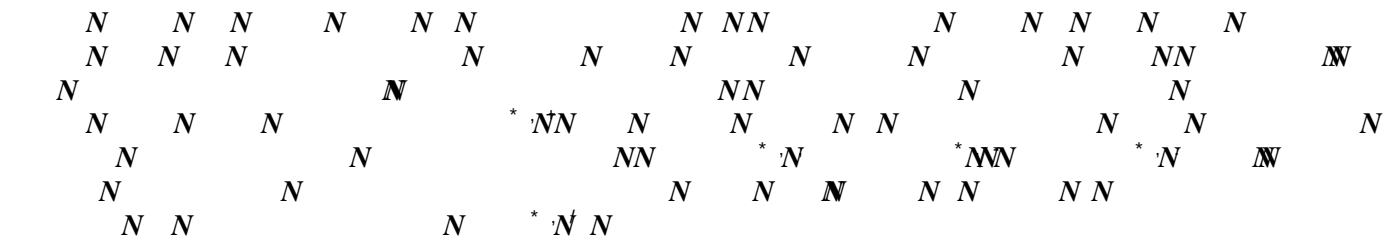
($! L n n B H , J H H e - D m H H c e



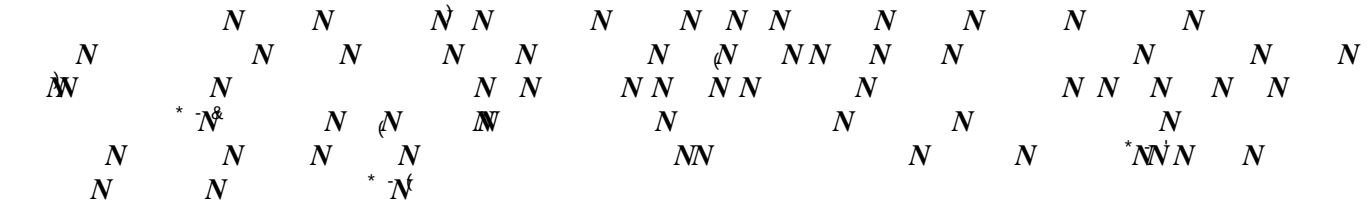
; W S h n S M e O a i w a t i S N h O w e a



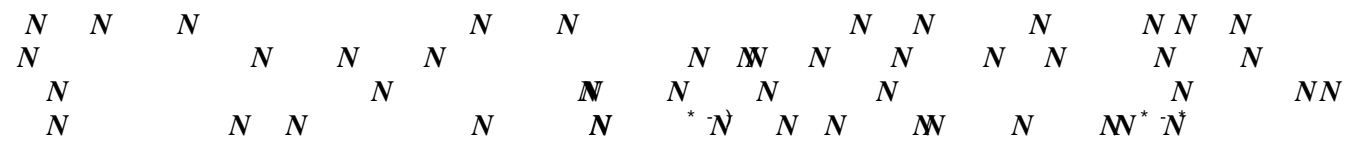
/ e p V B h C 4 i w m N w a s



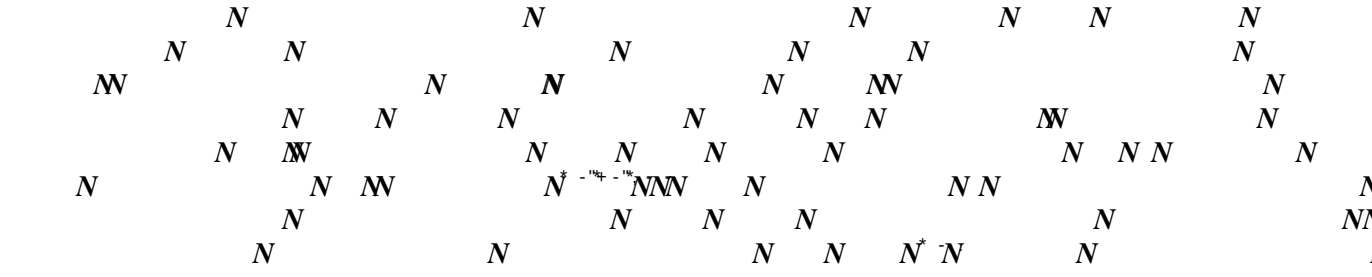
; f#7 e O*e g e S r O w e a ; 7 * !



: h O p Sdhgp DSi r O*e a

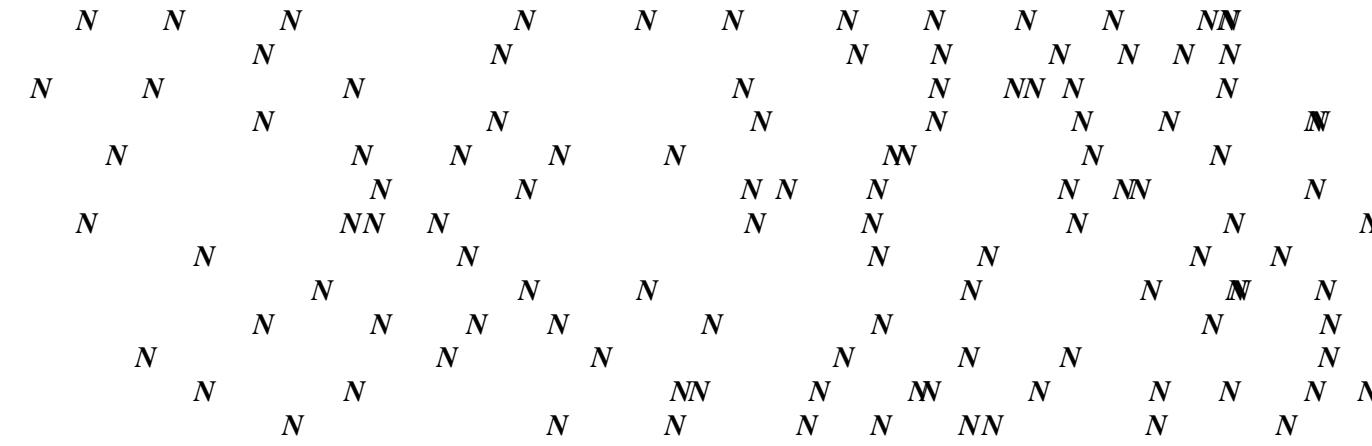


1 w h S Me0aiwati S h O w e a 1 1 0 !

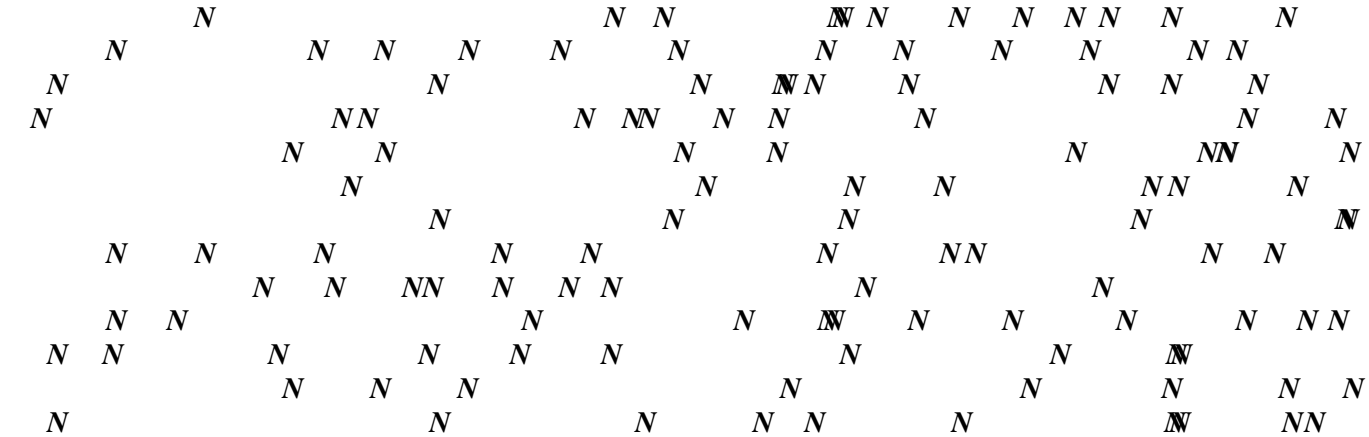


%! c J j j e , 2LeHkLAmeJk,eicJ0ní vn e v-Hí D , k

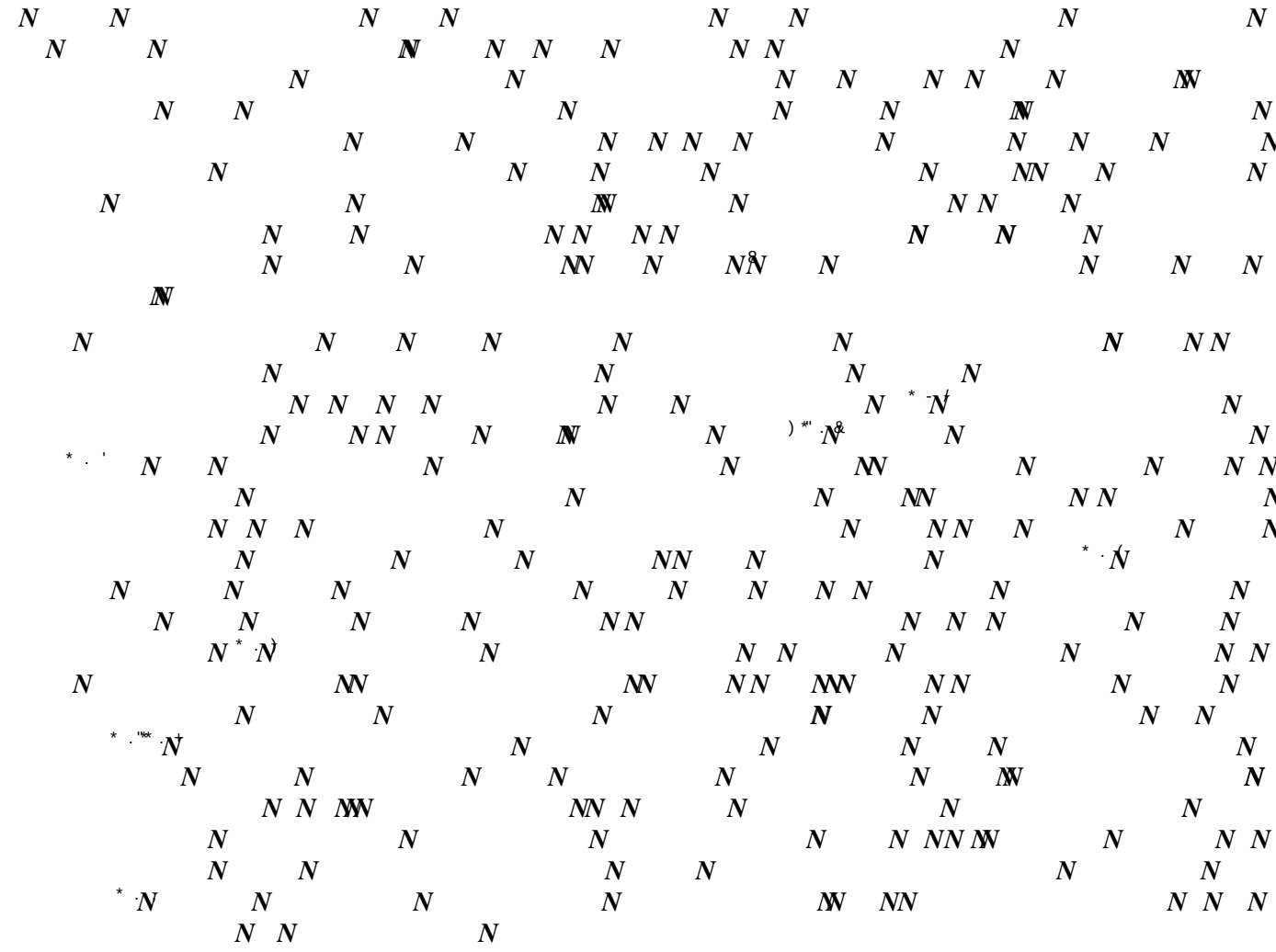
; e S ,i OhwDtDhiDa s i g



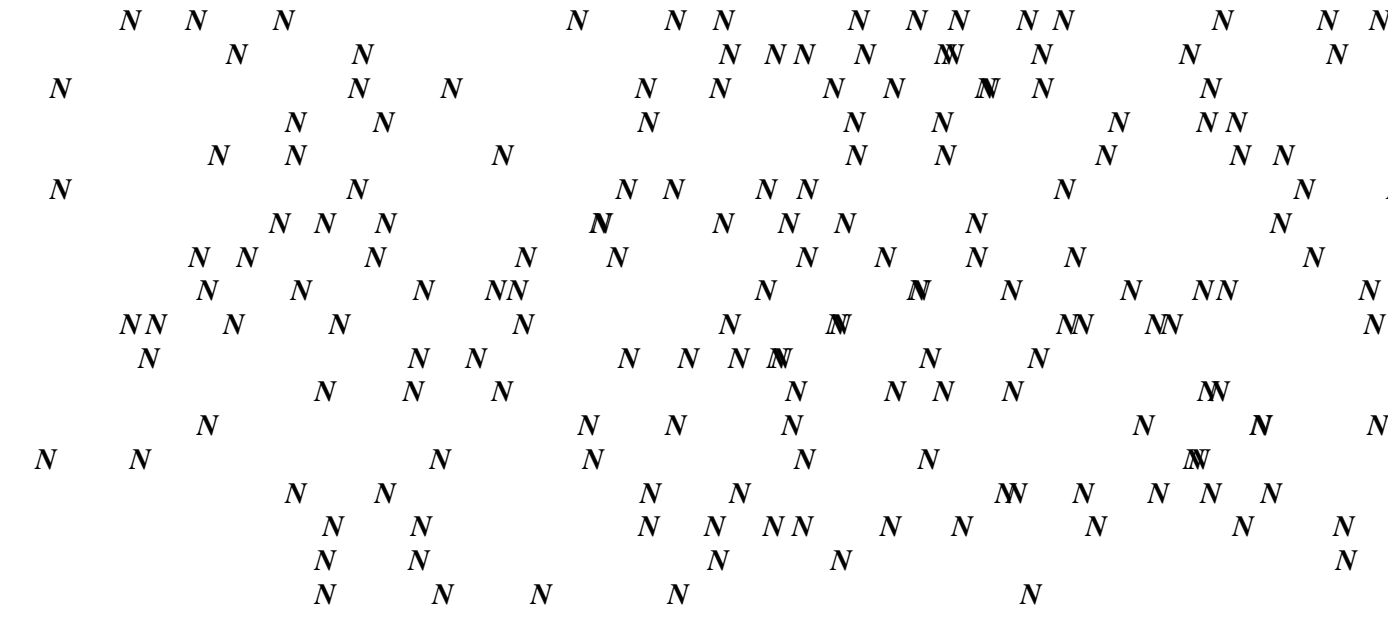
- i g wa&s-4 h O i S w h 1D g 5e D wa Oi Bh S



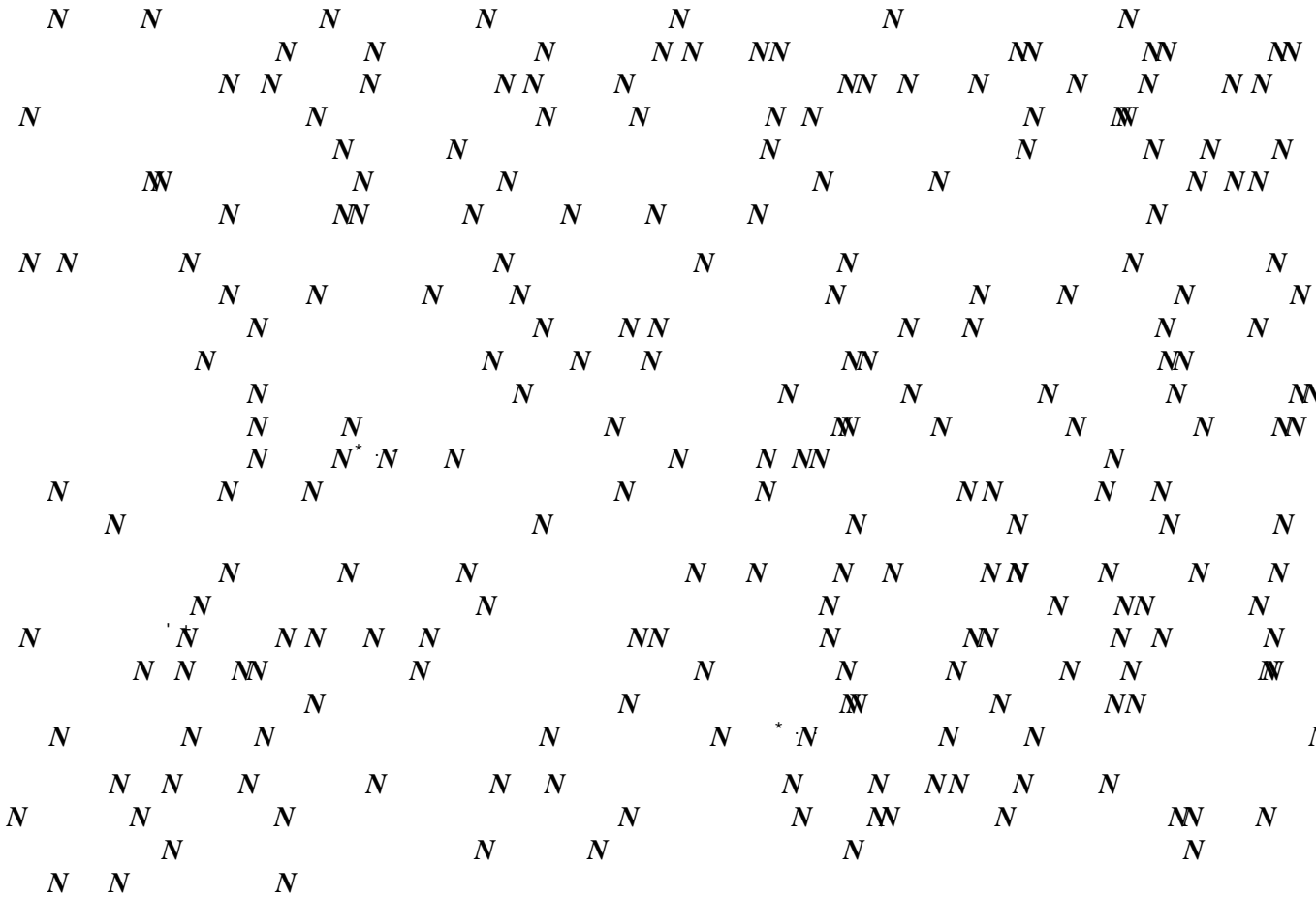
3 w s4 hOO 2aiOSi S h.aOwea i M i a O



2 aONi s,S hODwDgiaa s i



* r N D w 7 ihSOgwreiat O w C i g



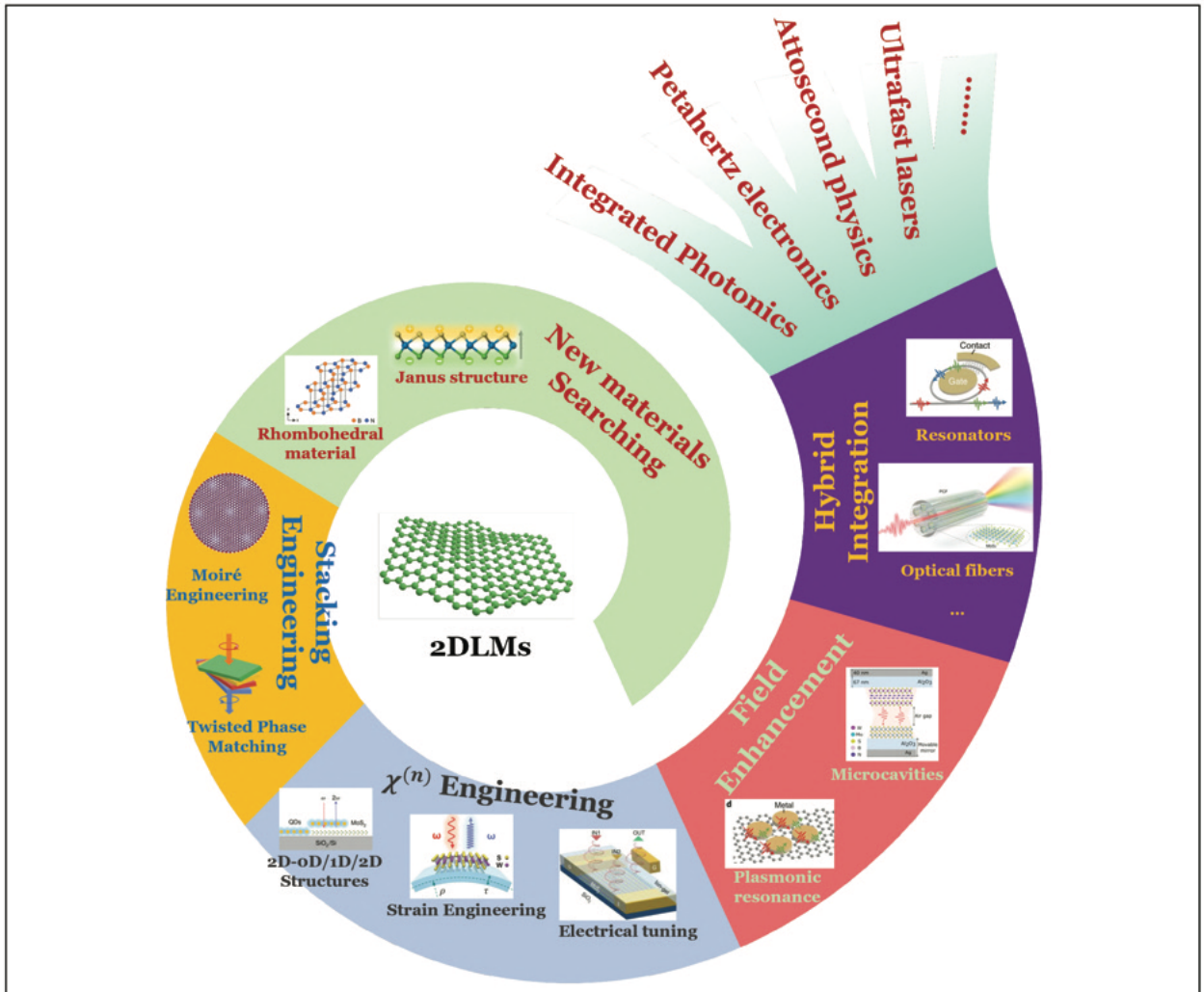
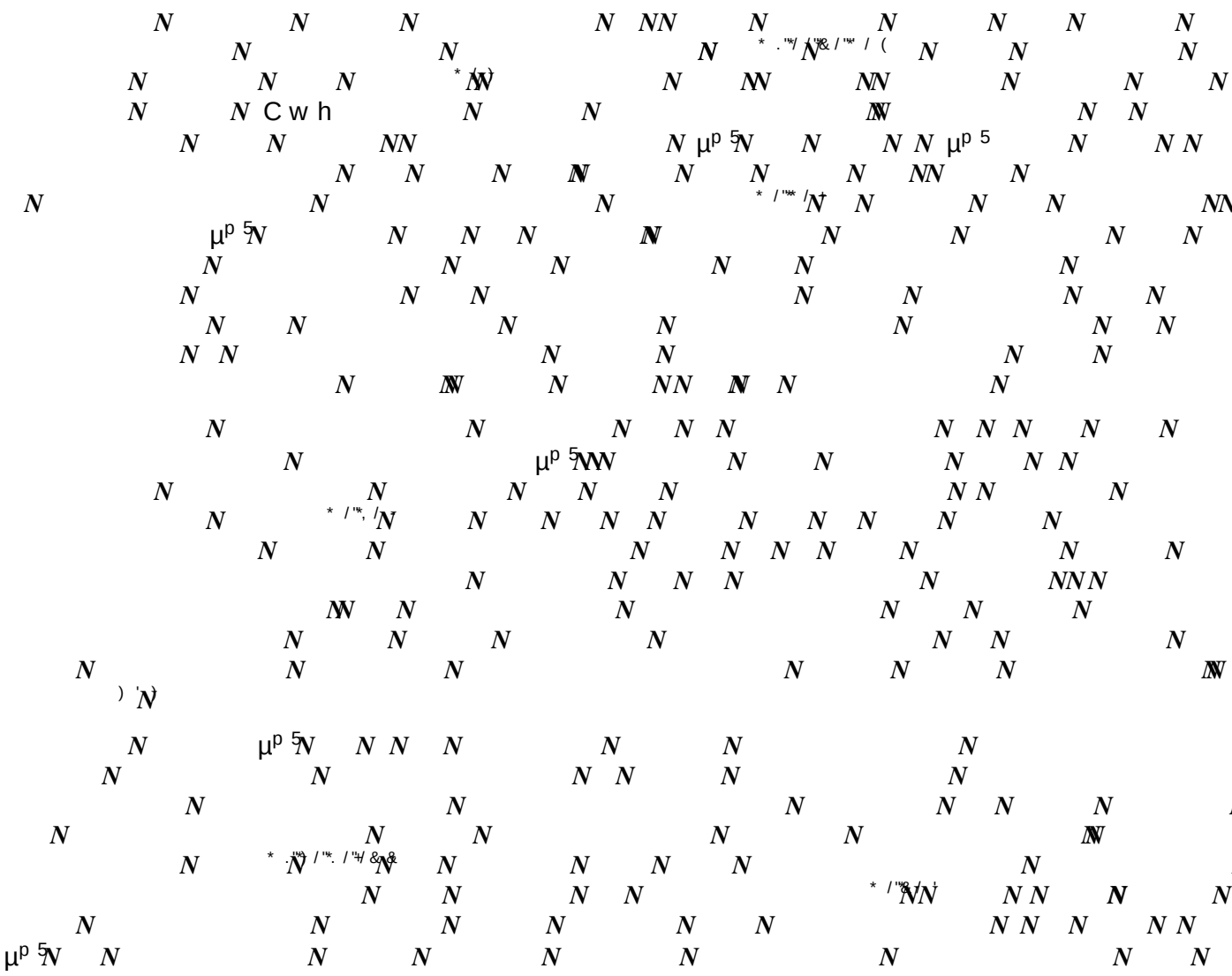


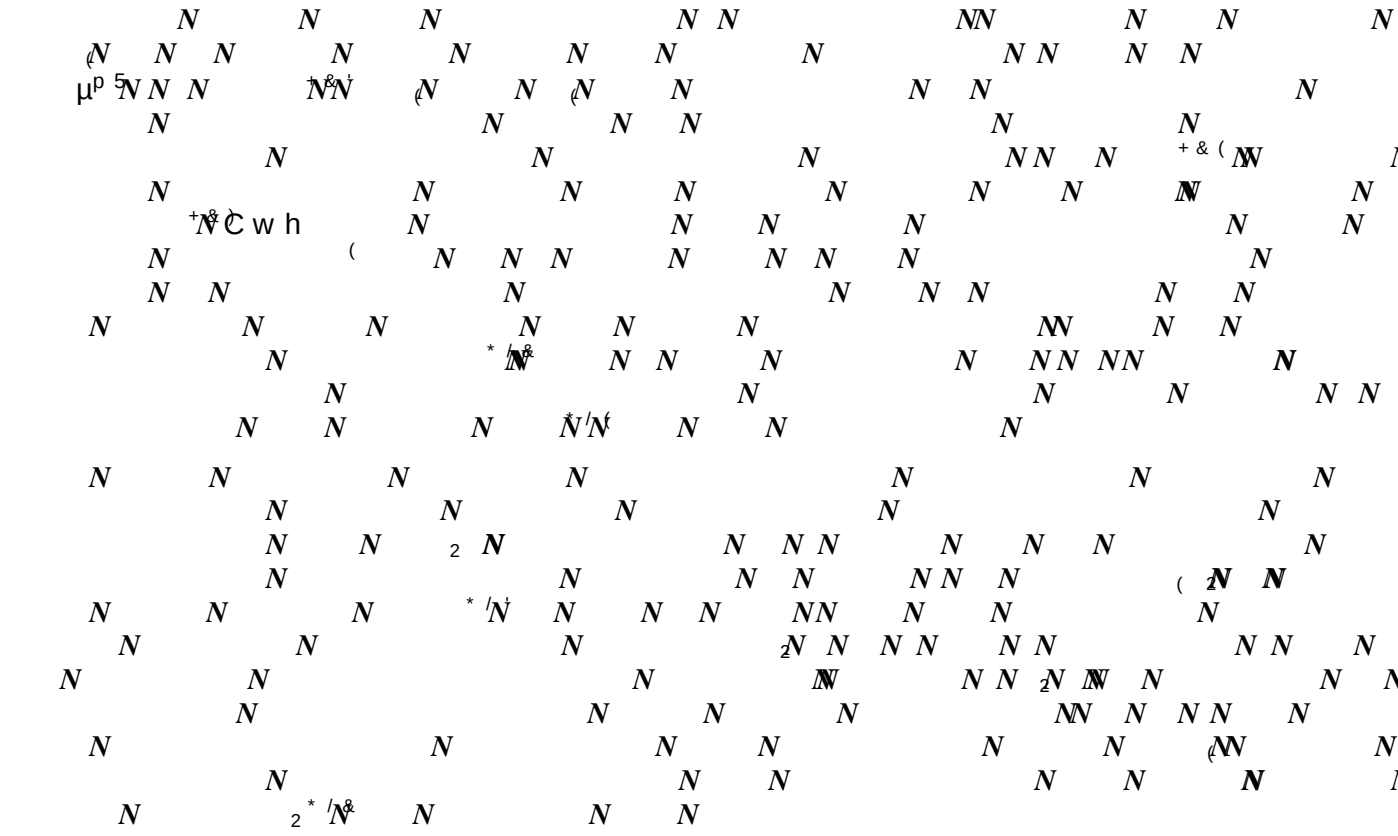
Figure 16. The representative path toward next-generation photonics based on high-order nonlinearities in 2D layered materials (2DLMs). Stacking engineering, $\chi^{(n)}$ engineering, field enhancement, and hybrid integration methods can be used for the overall enhancement of the nonlinear conversion efficiency of 2D materials. With new emergent 2D materials exhibiting better nonlinear performance, disruptive advances and revolutionary findings can be foreseen in integrated photonics, attosecond and strong-field physics, petahertz electronics, and ultrafast lasers.

$ * :! ; : 8 6 : 2 . 1 ; < I 6 0 . 8 4 2 : 2 1 . I 6 ; : ; 3 2 : I . : 4 8 2 1
6 : %1 9 . I 2 1 6 . 8 .

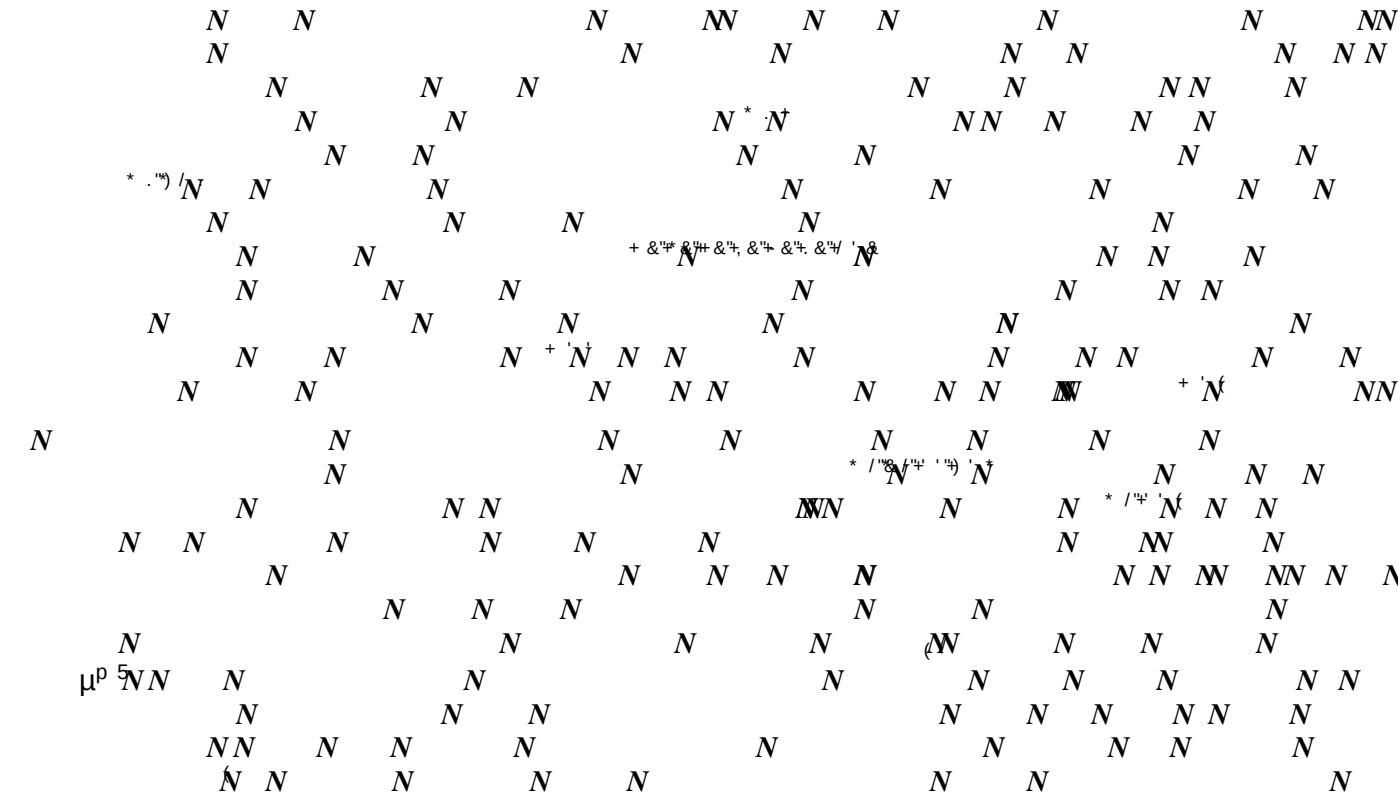
< ! 6 J o e k /BcvícJLnvJb S n H K l H é D f B e e L j J D A< D tíejóí JN %C J j H c e n
- , i n e J - , ijn e J 9 Jínvíc,eíj e 9 D H J h L r A e $ D e j =0L!e í:n!D t . J k D K
: F ! . c L
$< 8 í S 2 1 ç 8 P 1 L 6 t 8 y R S P E y S vE 1=NP%p E iP 88U8 2EELP2p0%% ; iL8vUD çBgLE2Só q*P)E)b+8
%< E í S 2 1 E ç 8 P 1 L 0 E I E 3 E y S % +) t y E % 8 Q P S y N 0 E t E v S P L % t E v S P
&q P E b 8 2 3 E 1 N L 6 , E 8 P P S % I S6yLD2v 1dND SLP61 D çR Nc3yEEy83P%y 8, ES8PP0P So 8;y8RP
e 8 3 8 S 2 y R i 8 1 U L 2 ó d D S P 1 D ç 9 3 í 8 E 8 P P S % 0 D S 1 2 E 6 E ç 8 " o q e O
'q P E b 8 2 3 E 1 N L 6 , E 8 P P S % I S6yLD2v 1dND SLP61 D çR Nc3yEEy83P%y 8, ES8PP0P So 8;y8RP
e 8 3 8 S 2 y R i 8 1 U L 2 ó d D S P 1 D ç 9 3 í 8 E 8 P P S % 0 D S 1 2 E 6 4 ç 8 R 2 E 6 4 E
s S g L 2 S 1 L 2 N 6 L 2 R L 1 I LSPyEDw 1dND SLP61 D çR N;3 LEçy í3D%1 8q2P%E b 8 2 3 E 1 N L 6
(R L 1 L PEy 3 O P E 1 E S 1 E b 8 % 9 0 b S P y 8 1 0 N dLy6E 8iP8yU8 BeL8 2 3 6 8%S 2iy8RU ;B8LP2 1c
B L 2 ó *)) , * % q P E 1 8 0 c 1 S 1 8 3 1 4 8 2 R L N 6 3 E 1 y R 3 8 ;2EL 1pN2 SqçP%E bC8 2 2 S 3 0 E D 1 S N 1 8 L 6
i 8 U B L 2 ó *)) * / % q P E 1 8 0 c 1 S 1 8 3
)< E í S 2 1 E ç 8 P 1 L 0 E c y E 8 P w 8 0 8 I p E v 3 E E y c R 1 8 D 0 8 E ;0 R 8 E v ç v E X y 9 R m 8 D % E v q S P % E b s 8 X 2 9 3 m E
*o R 8 O P 3 1 E 1 D 1 8 L 6 u í 1 E y 8 3 3 % 1 8 q 2 P % E b i 8 8 2 U 3 E B 1 L N 2 ó L 6 * -e /L+y 0 R % 8 3 q 1 L P 8 E 2 1 % 8 0 e L
+< 8 í S 2 1 ç 8 P 1 L 6 ; R 8 ç E 3 1 2 N % ; L B v L D 2 ç ó g E * S)) q + P 0 E % b 8 q 2 P 3 E E 1 1 8 N 0 % c i 1 8 S U 1 8 E 3 L
'< 8 í S 2 1 ç 8 P 1 L 6 R N 3 E y 3 % ;0 L S v ç D ç 9 g h E 8 S P D q 8 P % E b i 8 8 2 U 3 E B 1 L N 2 % ó % * * i . 8) U 9 B ç L 3
c 1 S 1 8 3
- 9 ; ; 2 < : 9 8 1=5ç8S3E v0 8* '=34y9R;D!y ó 8 y L v D ç g E S ' 8 0 D

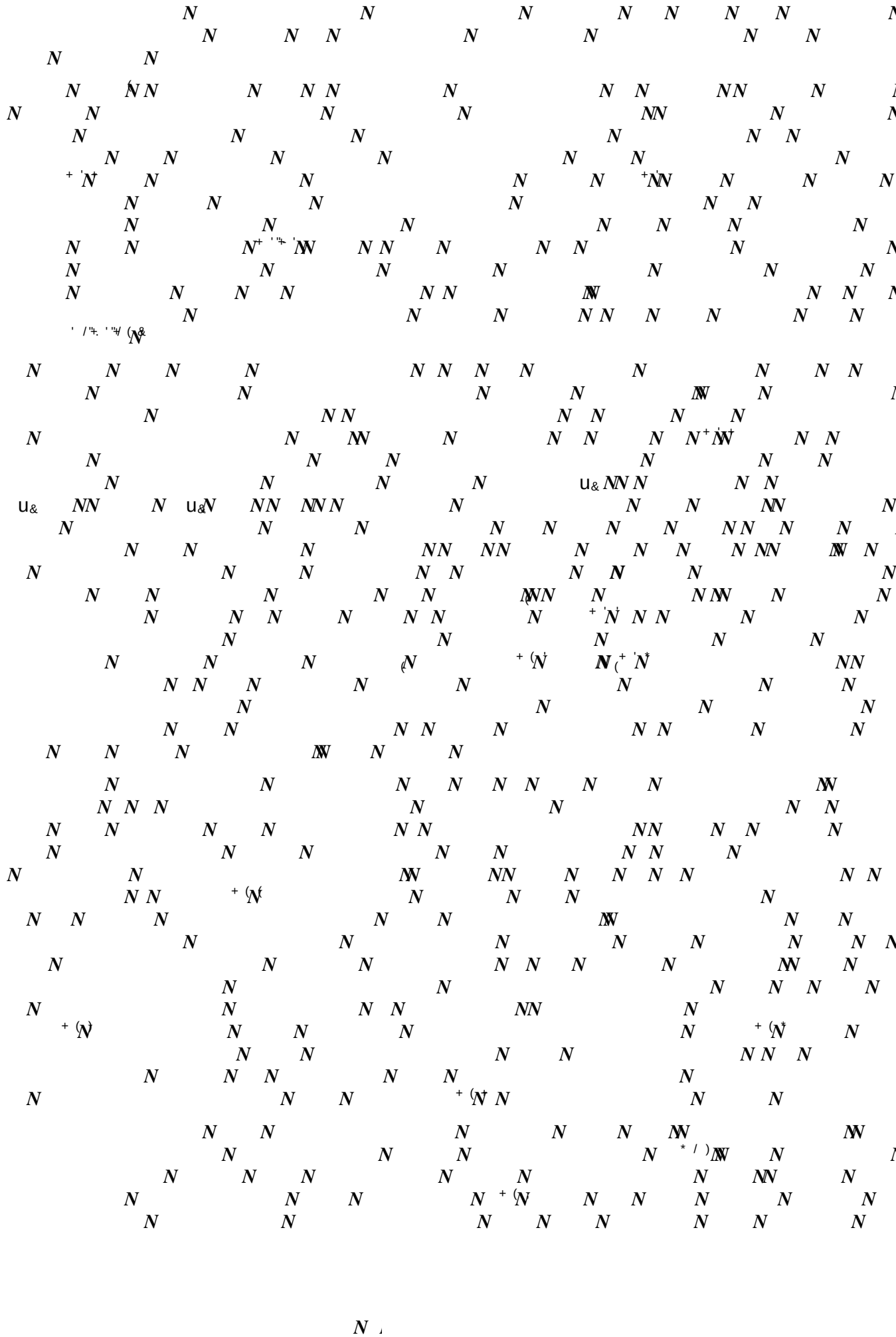
) ! L # n n / e , H B H J H e D r H c e - n H

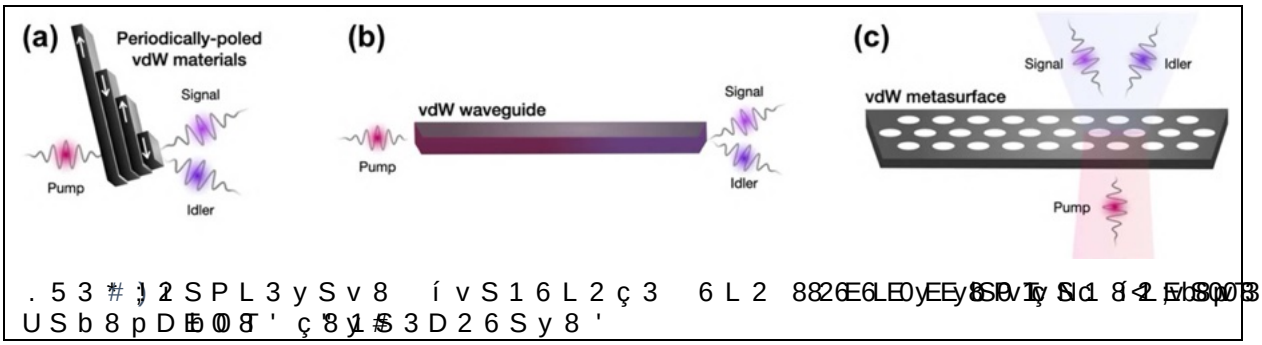




) ! c$J j/ j e , G e k 2 L H L n e 3 D J j k J , i B L G G e k H e i 0 í n e v H





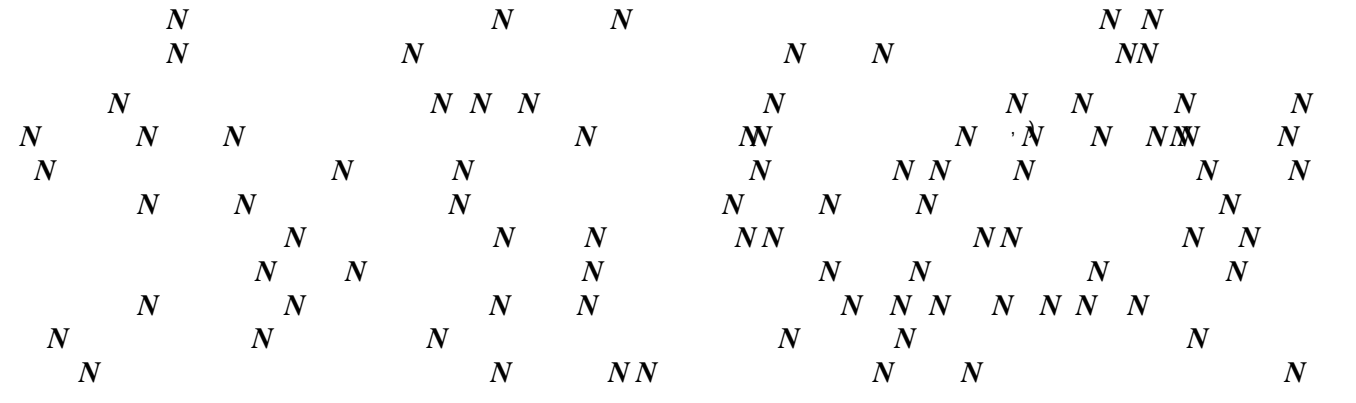


. 5 3 #) 2 S P L 3 y S v 8 í v S 1 6 L 2 ç 3 6 L 2 8826E6LEDyEEy8SPv1ç v Nd 1 8 <2 Lsb8Q03P 8 2'Sg1#E
U S b 8 p D E 0 8 ' ç 8 y 1 S 3 D 2 6 S y 8 '

$ + :! ; : 8 6 : 2 . 1 < ; 8 . 1 6 l ; : 6 0 . 6 : %1 9 . l 2 1 6 . 8 .

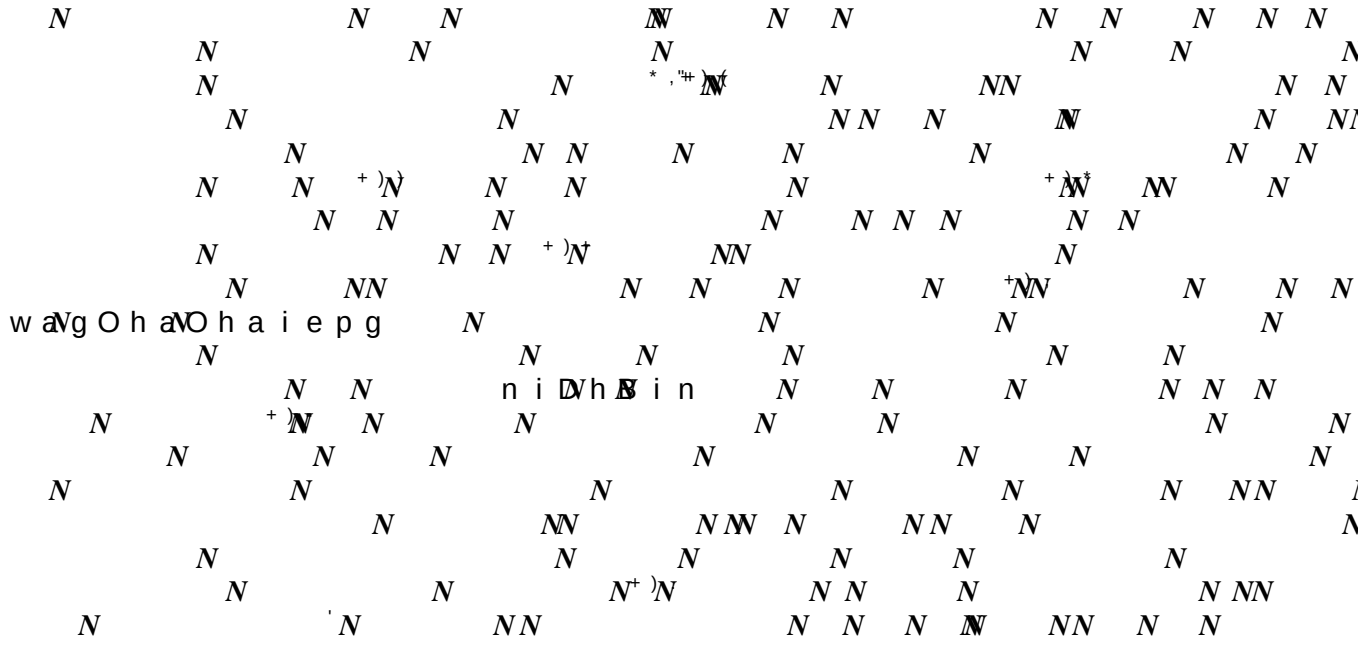
6 D e j Ö !# 1 i/ LD J u n i D 6 O j K J n D í A R i n 1 $ C L i e f j 1 % m J b i é J H
9 J n & J, í i 2 ! 6 J K í e n % ' 3 J n v 1 J i e - a J d D
$ u s O ; t 9 8 P 1 8 2 6 8 0 2 2 E b L 8 V R S 3 1 E 1 p 8 R P 1 O P 1 8 2 S y 1 E L P 3 % q P ; E S b ç 8 í 2 D 3 3 E b 1 8 N A L
. . % & < n) u 0 8 P 3 8 t % < 8 P ç S 2 ó
% < S P E 3 R O P 3 1 E 1 D 1 8 6 L 2 9 0 1 R S 1 2 y P 8 0 < 8 e P 1 ç D S 0 2 N 0 % & q + S E ç) í 8 u 2 0 3 8 E P A 3 N 8 . L t @ % e
< 8 P ç S 2 ó
& t S & L & O P 3 1 E 1 D 1 % * + - 1 2 : 8 2 v E P % C 8 2 ç S P N
' O ; K u P 3 1 E 1 D 1 0 8 ; E 8 P y E 8 3 I L 1 L P E m D 8 3 y % R P 0 L R 8 p N % 2 y) 8 1 1 L P) S ; G S P 3
: S 2 y 8 v L P S % c í S E P
(< E í S 2 1 E ç 8 P 1 L 0 E c y E 8 P w 8 0 8 I p E v 3 E E y c R 1 8 D 0 8 E ; 0 R 8 E v ç v E X y 9 R m 8 D % E v q S P % E b s 8 X 2 9 3 m E
) O ; e & O 9 P 3 1 / E ; S 1 D 9 & E S P S 0 8 e 8 y S 8 1 2 3 y % S E S 3 = 3 ; 8 1 L E ç p Ú E s s P v N D 8 b S + P ; %) 1) *) : S
- 9 ; ; 2 < : 9 8 1 = 5 ç 8 S 3 E v 0 3 * 8 = ç 4 y 9 E ; ' ! 3 0 D ' 0 ó

! # 5 , H n D i L v H í D ,

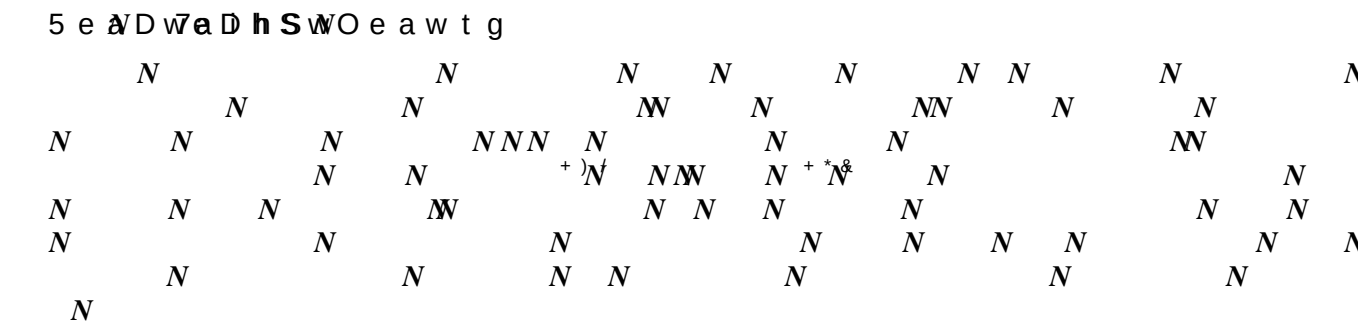


! $ L n n H , J H H c e H

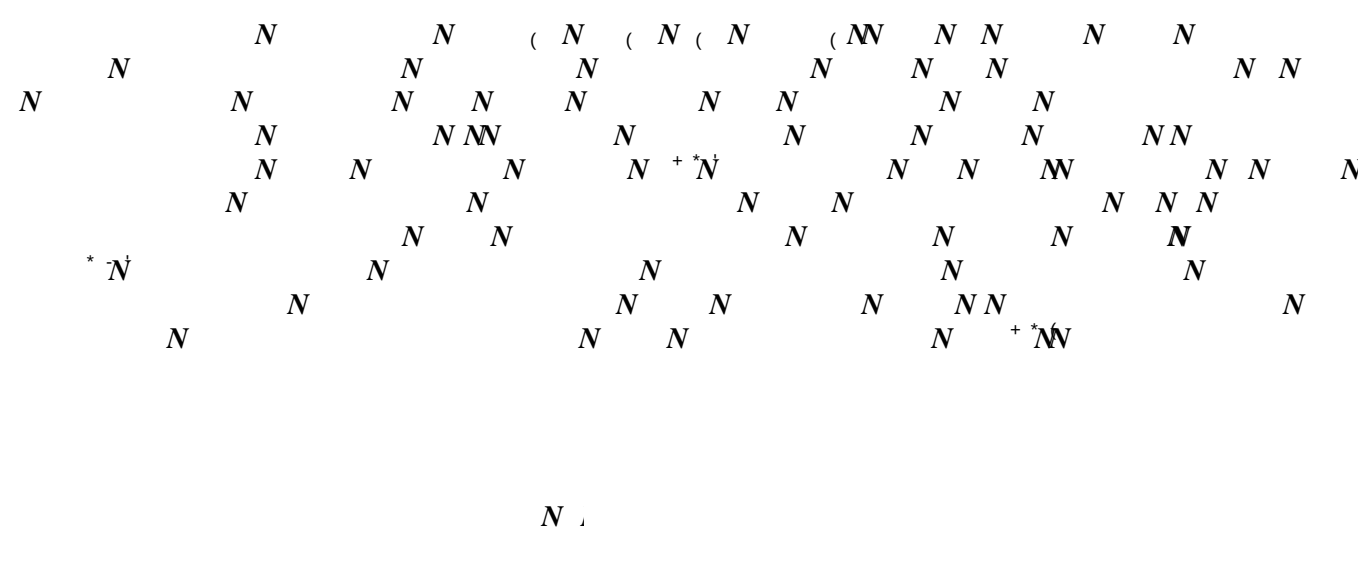
5 e a D w 0 S h n S 7 D a g M e a w t g



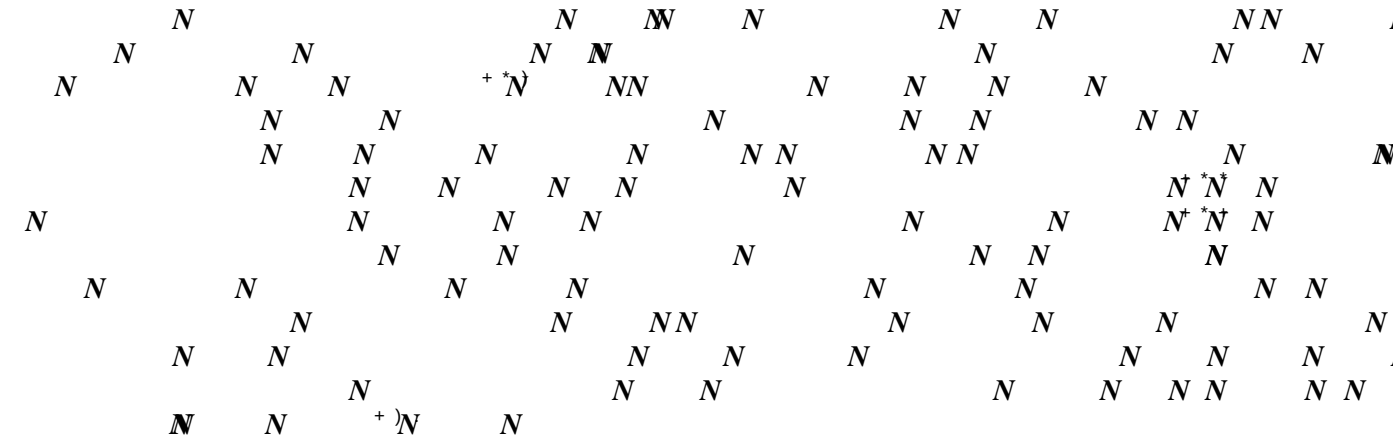
w a g O h a O h a i e p g



5 e a D w 7 a D h S w O e a w t g

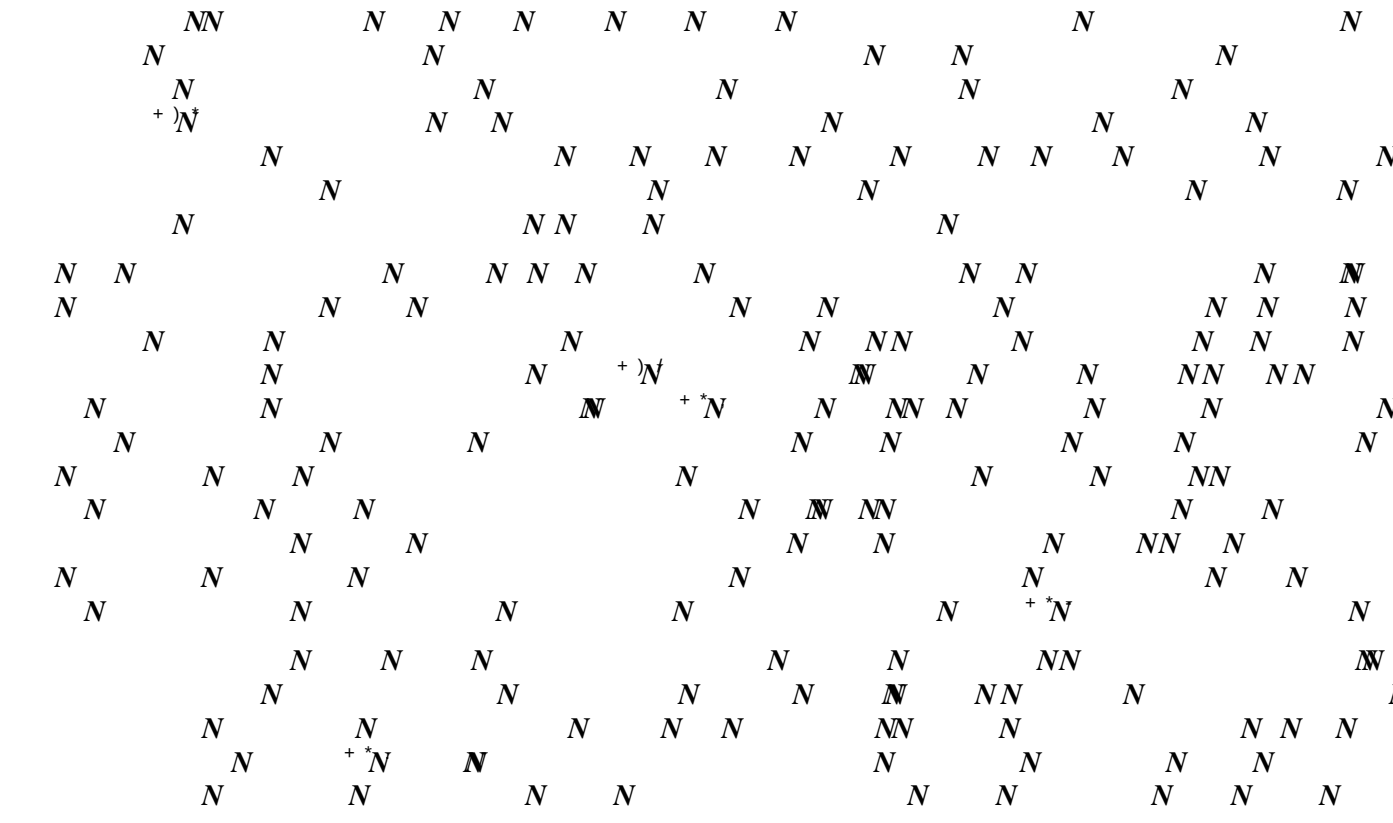


5 e a D w 5 a i e S e O 3 e a # w t M g i a w g a S e B a g M O D h D g

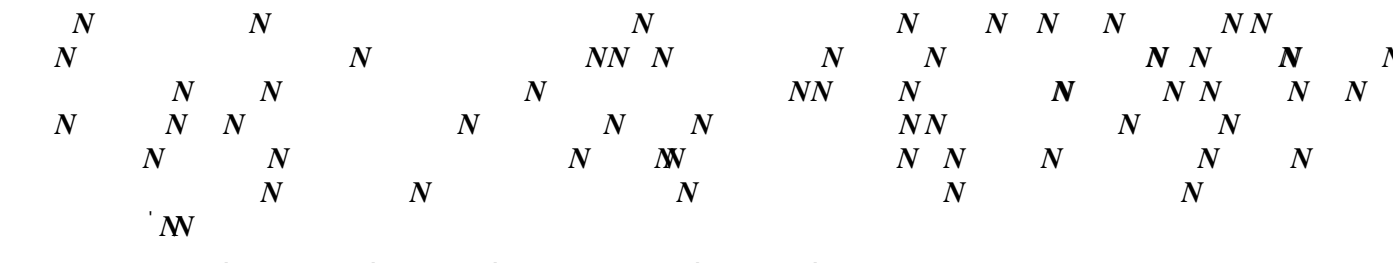


! % c J j j e , 2 L e H k L 3 D e J , j i k

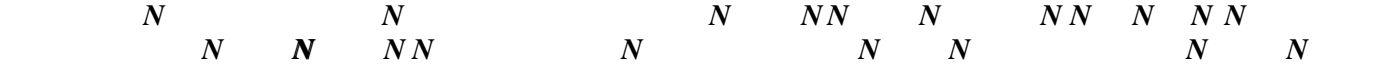
, e i S e 7 i D a h O S # v s O v e 5 a i a D w 6 a r i O h w 3 t h i D a e M i a h



7 e O e O 5 e i a S D M w h a D i h 2 a w t O e w i 7 g S i i h a a O M i a h



! & L G G e 0 k í H h e i v H í : D „ k j í r , D < D j n J S 0 H D , í v k



holds intriguing possibilities to harness quantum finite size effects in the nonlinear plasmonic response of structures with lateral sizes below the Fermi wavelength ~10 nm.[534] For instance, the large photothermal response of relatively few electrons in small graphene nanoislands is predicted to enable unity-order modulations in plasmon resonances triggered by single-photon absorption (see Figure 18g),[534] while narrow graphene nanoribbons could be optically pumped to support near-IR thermoplasmons that can drive a coherent nonlinear plasmonic response.[549]

In phonon polaritonics, the vibrational origin of the nonlinear optical response allows for larger applied light intensities without boosting optical losses associated with electronic degrees of freedom. Additionally, introducing strong in-plane DC fields can actively modify the nonlinear response, further enhancing the control over the system. Indeed, as shown in Figure 15f, by introducing in-plane DC fields through, for example, lateral gating, significant shifts are predicted to occur in the frequency of phonon polaritons in monolayer hBN, exceeding the spectral widths of the modes.[539]

The design of atomically thin heterostructures comprised of materials with complementary optoelectronic properties can open new paths to enhance nonlinear light–matter interactions at the nanoscale. Polaritons in 2D materials interfacing with noble metal films (behaving as perfect conductors) can hybridize with their mirror images to form so-called image polaritons,[550] reaching extreme light-focusing regimes for nonlinear optics. This concept has been demonstrated for graphene–dielectric–metal heterostructures,[22] and should similarly produce large polariton-driven optical nonlinearity in other 2D systems. In a related approach, the strong coupling of excitons in TMDs with optical cavity modes can be leveraged for nonlinear light–matter interactions such as saturable and multiphoton absorption.[546,551] Turning to the intrinsic nonlinear optical response of 2D materials, moiré electronic-structure engineering offers an appealing route to tailor anharmonic electron motion,[481] with polaritons supported by twisted 2D materials or nearby metal–dielectric interfaces enhancing nonlinear light–matter interactions.

In quantum nonlinear optics, recent theory proposals to generate entangled photon pairs directly in the guided modes of optical waveguides show promise for emerging quantum photonic technologies. These strategies can be mapped directly to waveguided 2D polaritons in nanophotonic architectures (e.g., the optical generation of plasmon-polariton pairs in graphene nanoribbons *via* spontaneous parametric down-conversion[552]). In an alternative scheme, free electrons that impinge normally to a 2D waveguide can excite guided polaritons that are entangled in energy and momentum, and heralded by measuring the energy loss of undeflected electrons.[553]

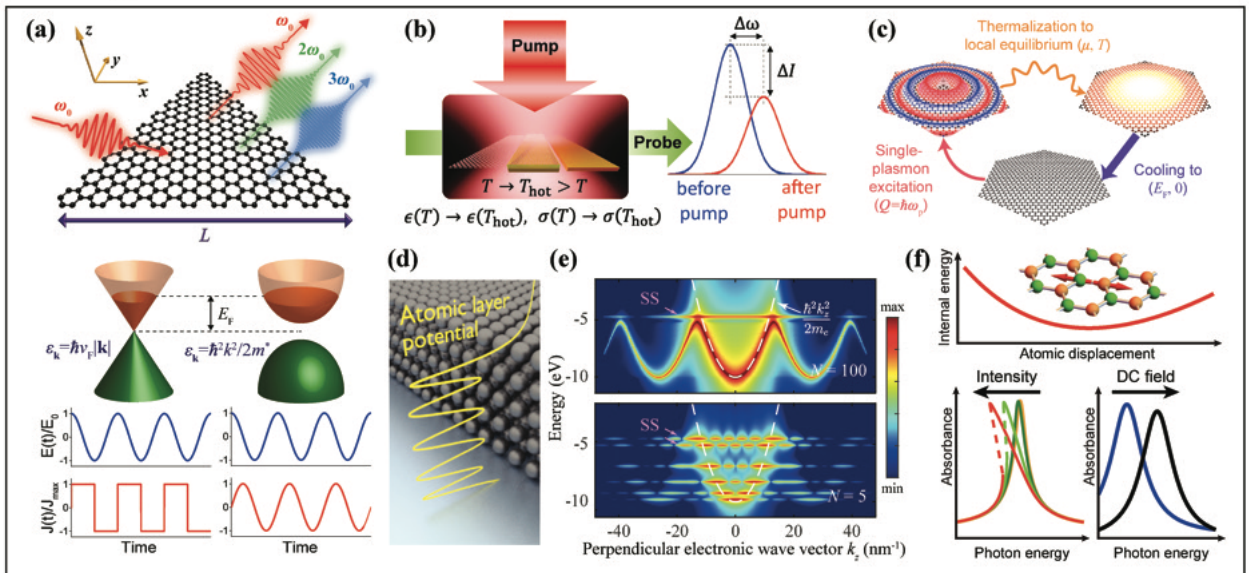
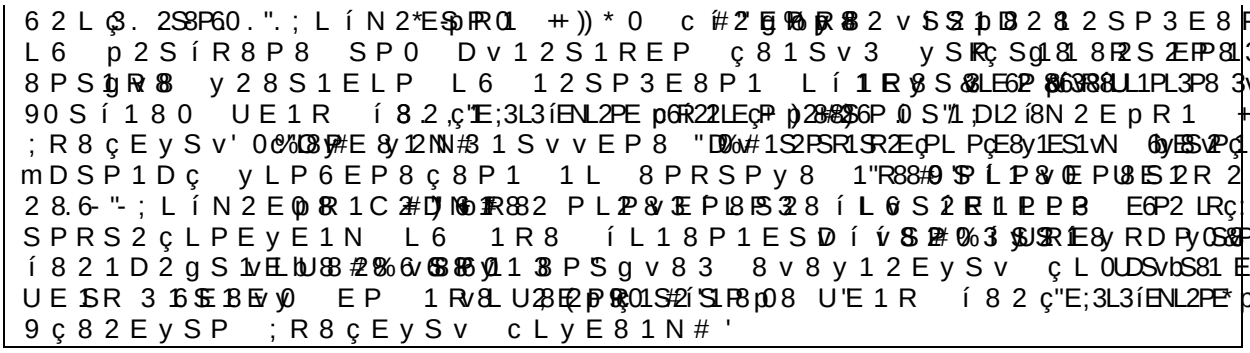
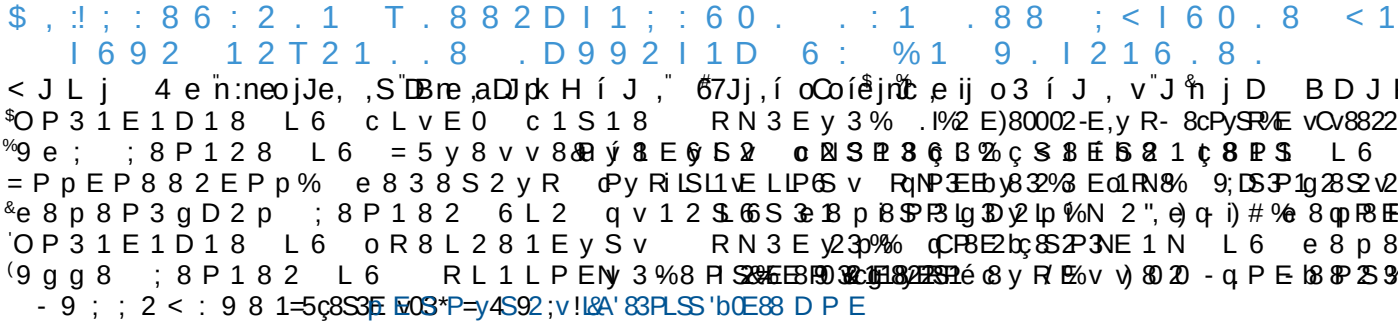


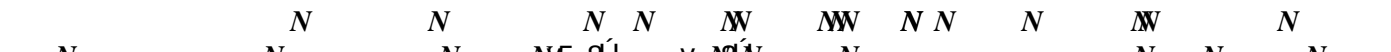
Figure 18. Nonlinear polaritonics in 2D materials. Nonlinear polaritonics in 2D materials. (a) Intense high-harmonic generation from graphene nanostructures (upper part) is predicted to arise from the combination of plasmonic field enhancement and anharmonic electron motion associated with the conical band structure of graphene (left-lower part), the latter attribute leading to an intrinsically nonlinear optical response that contrasts the harmonic response exhibited by a parabolic electron dispersion (right-lower part). Adapted with permission

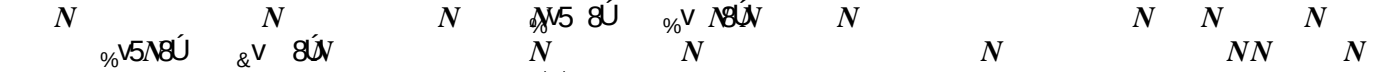


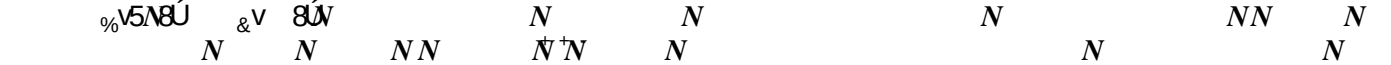




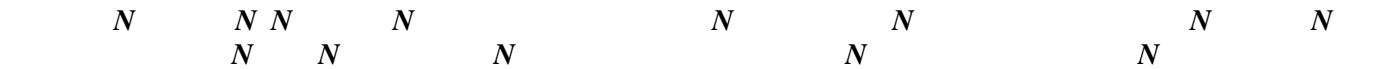


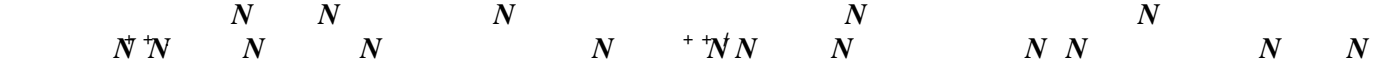


























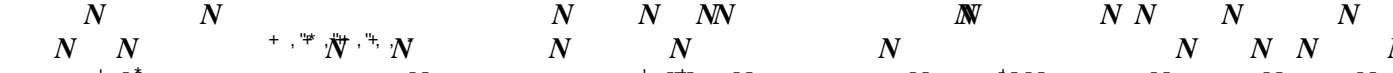


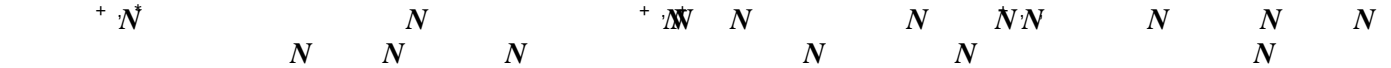








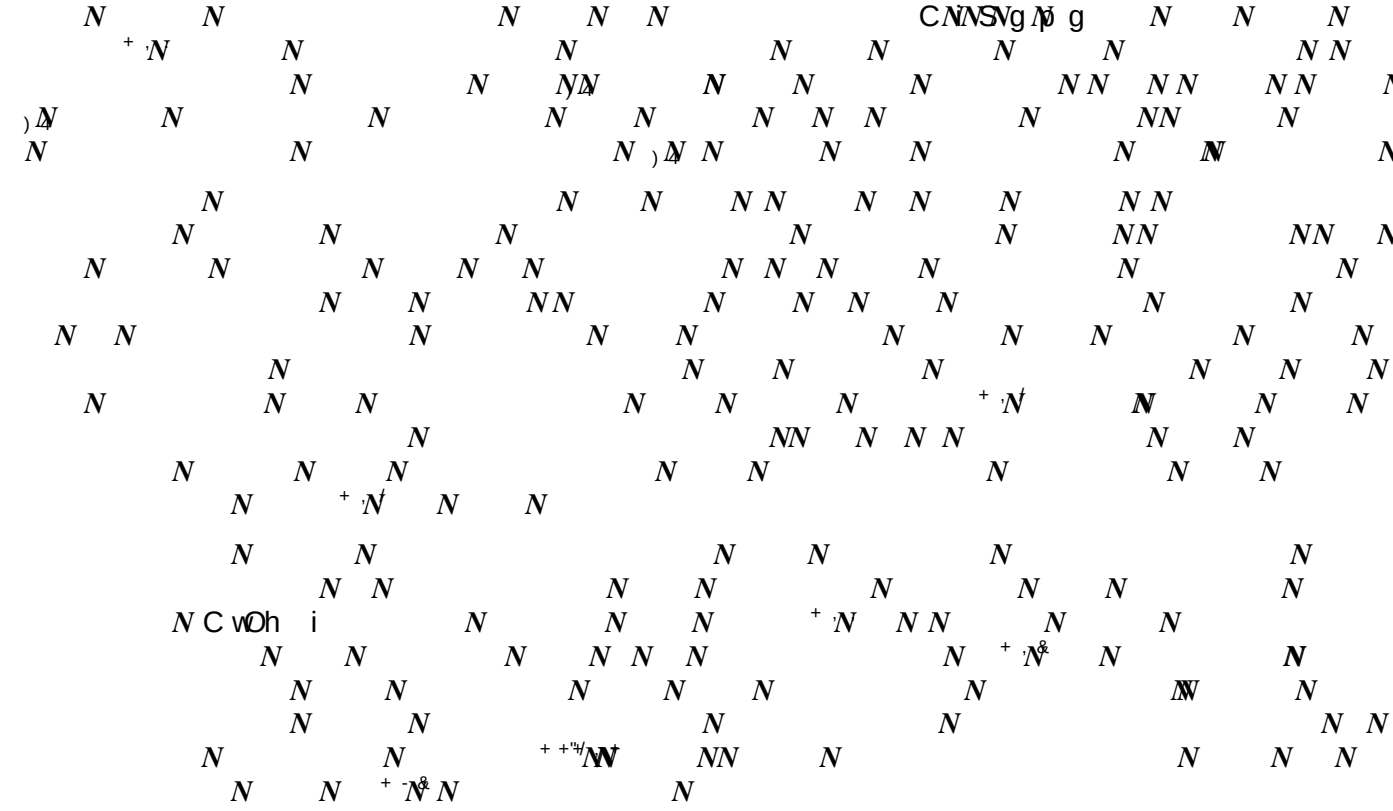


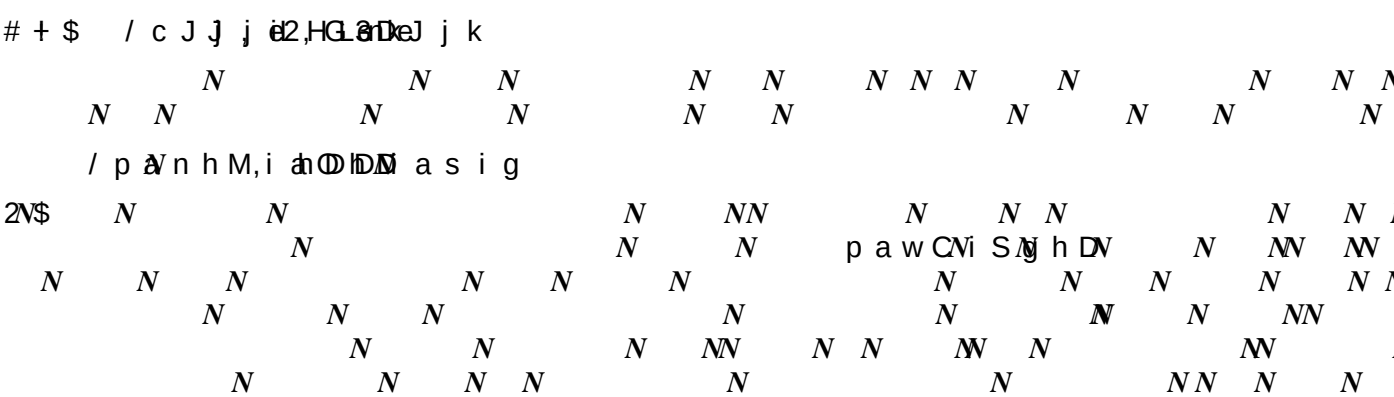


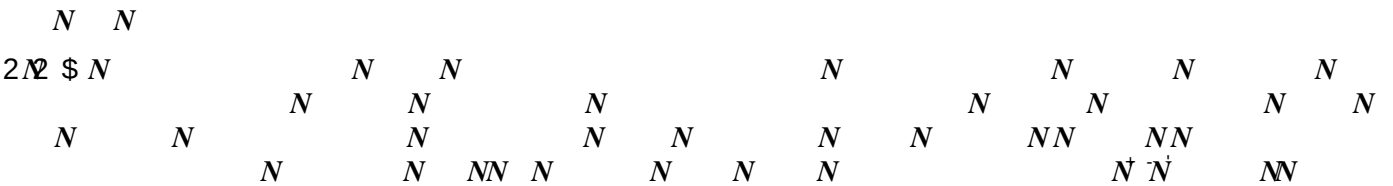


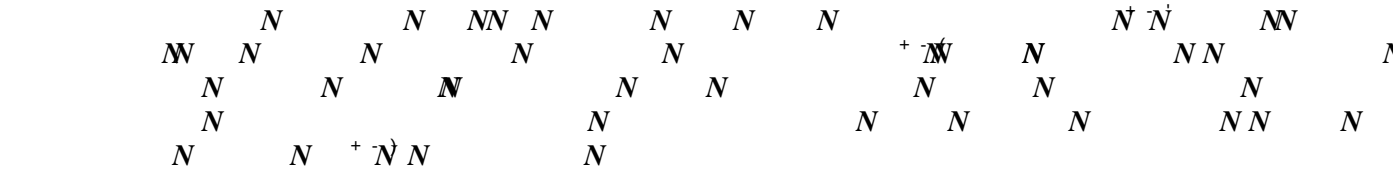


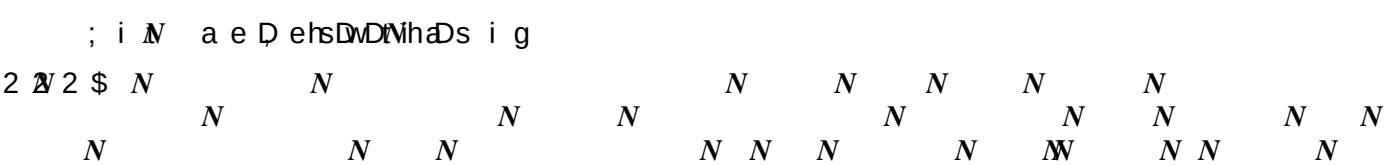


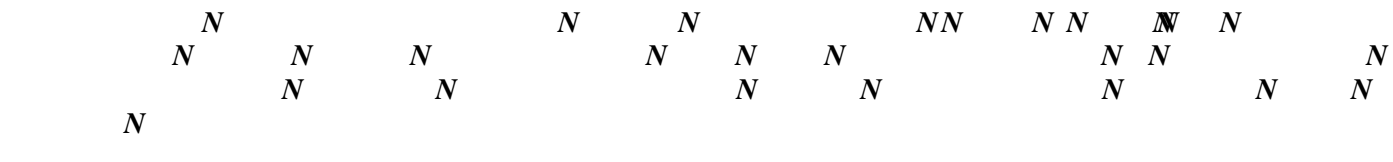


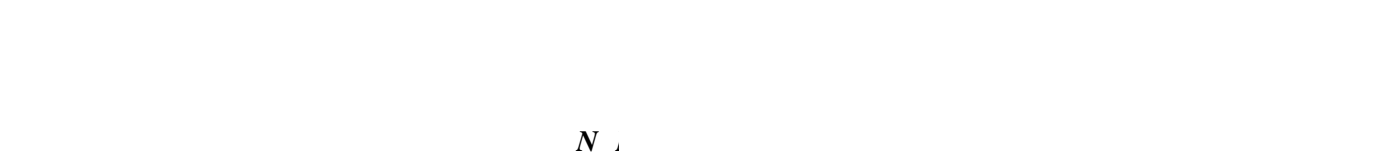


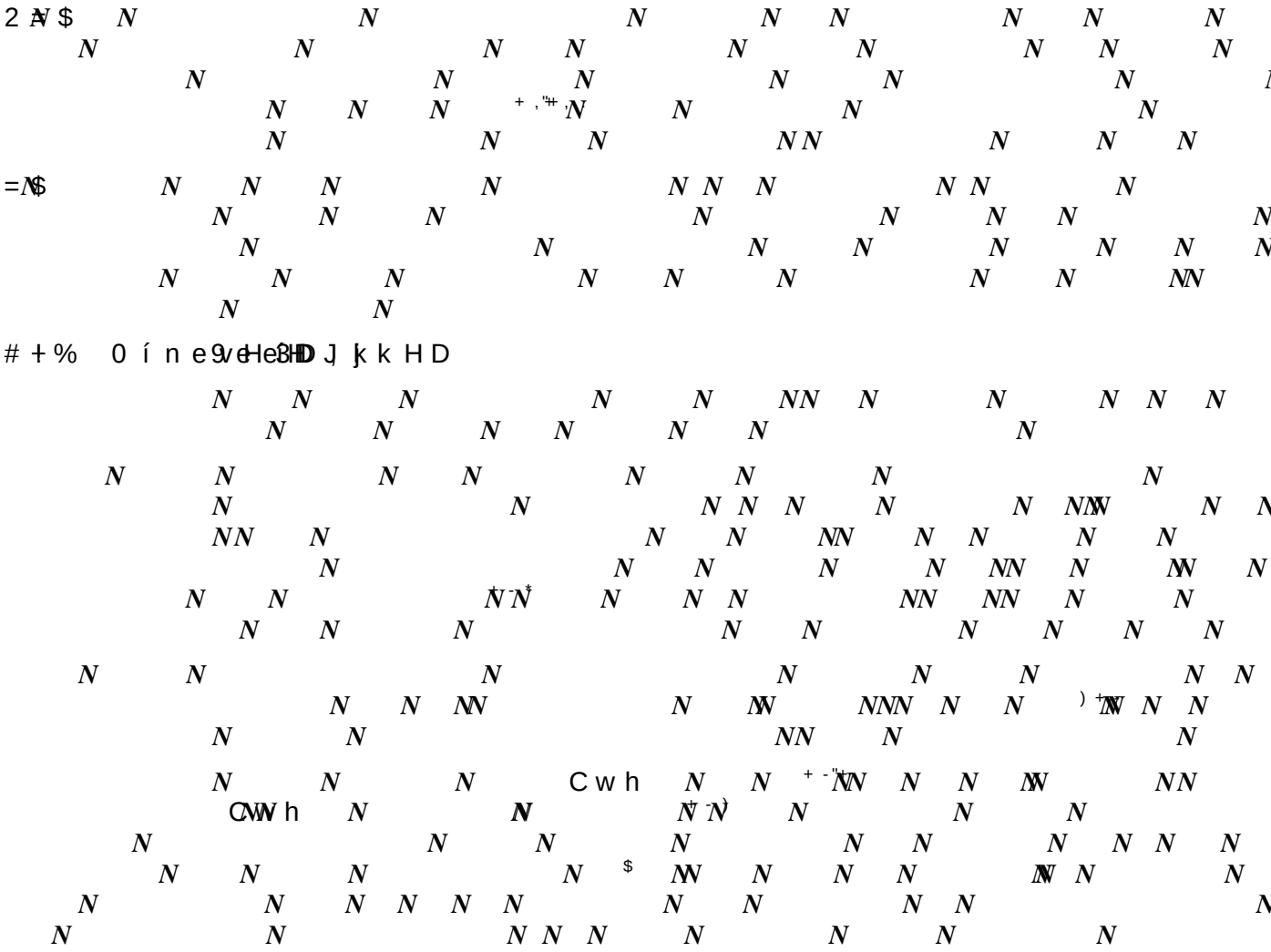












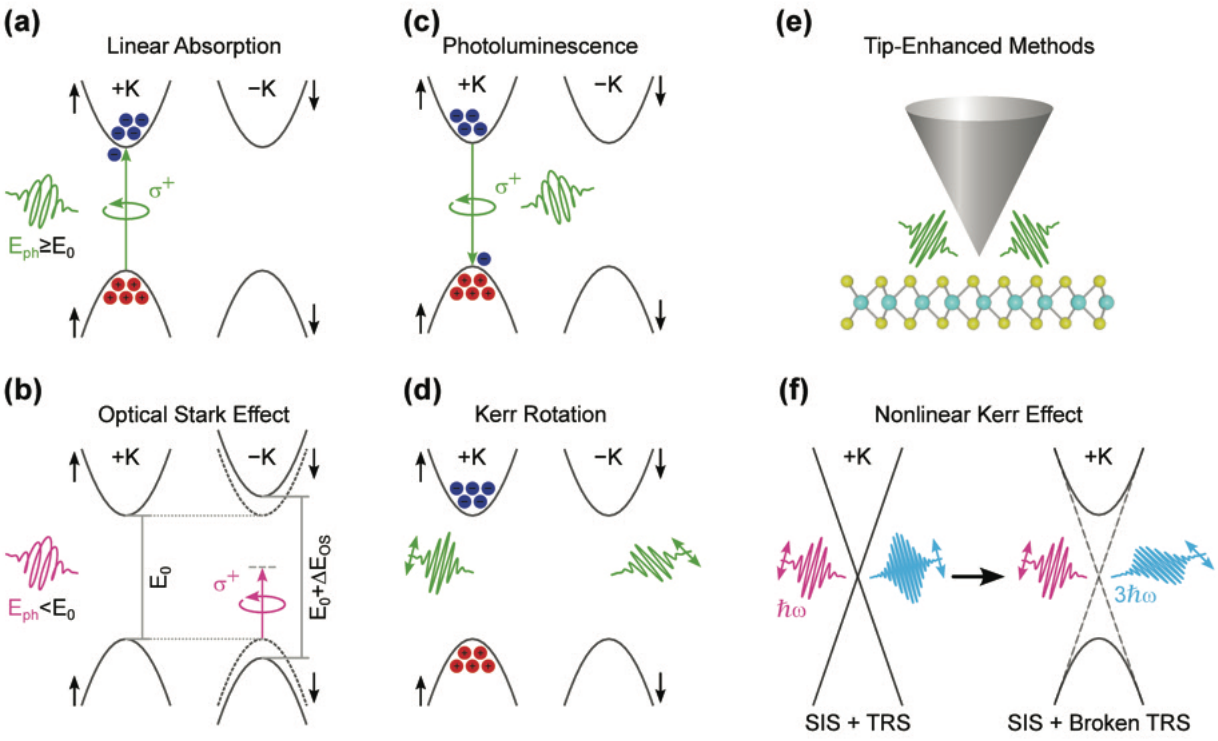


Figure 19. Schematic of all-optical valleytronic operations and time-reversal symmetry (TRS) modulation/detection. A valley imbalance can be generated by resonant one-photon absorption of circularly polarized light (a) or the coherent valley-selective optical Stark effect (b). The valley imbalance is typically measured *via* helicity-resolved PL (c) or ultrafast resonant Kerr rotation (both linear and nonlinear) (d). Future valleytronic devices could use local field enhancement *via* metallic tips (e) and potentially probe broken TRS even in centrosymmetric crystals by nonlinear third-harmonic Kerr rotation.

20. NONLINEAR MAGNETO-OPTICS IN 2D MAGNETIC MATERIALS

Zeyuan Sun[1] and Shiwei Wu[1,2,*]

[1]State Key Laboratory of Surface Physics, Key Laboratory of Micro and Nano Photonic Structures (MOE), and Department of Physics, Fudan University, Shanghai 200433, China

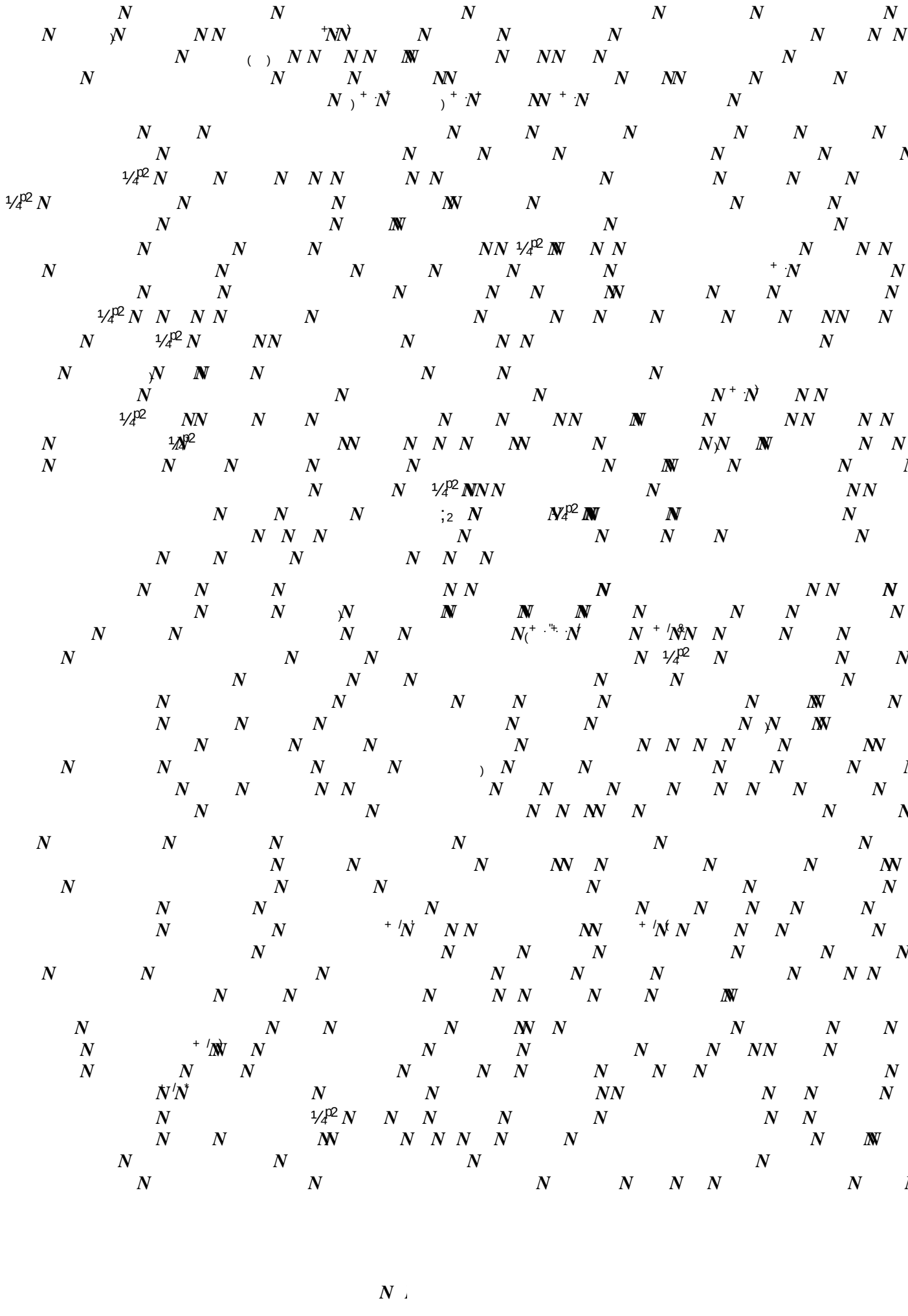
[2]Institute for Nanoelectronic Devices and Quantum Computing, and Zhangjiang Fudan International Innovation Center, Fudan University, Shanghai 200433, China

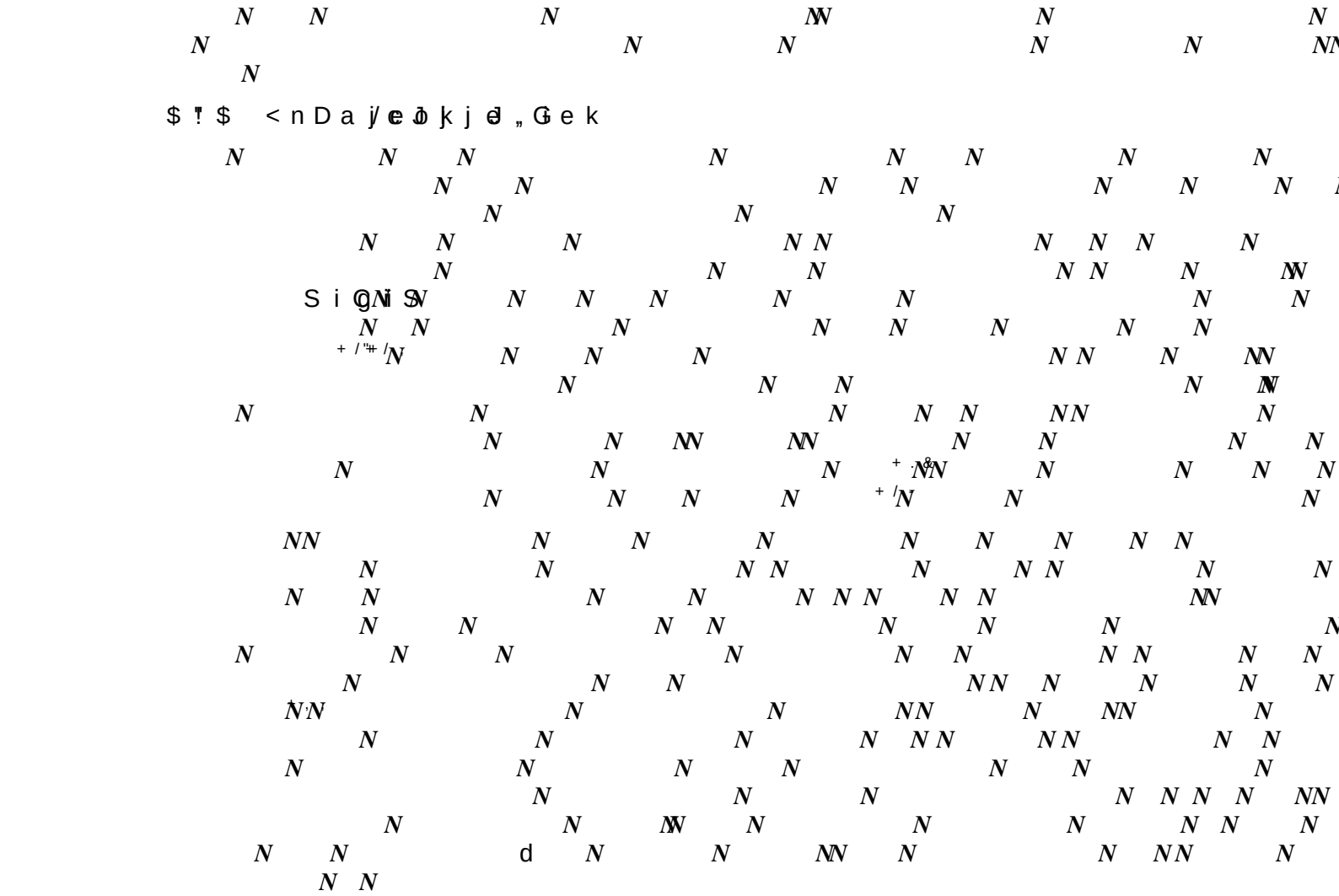
***Corresponding author.** Email: swwu@fudan.edu.cn

20.1 Current State of the Art

The discovery of 2D magnetic materials such as CrI_3 and $Cr_2Ge_2Te_6$ has greatly benefited from linear magneto-optical effects including Kerr rotation and reflective magneto-circular dichroism (RMCD).[576,577] These linear magneto-optical effects are sensitive to nonzero total magnetization of the materials and, thus, effective in detecting ferromagnetic states or materials. In contrast, the nonlinear magneto-optical effects such as magnetic second-harmonic generation (SHG) are sensitive to the breaking of spatial inversion symmetry in spin lattices under study.[578,579] This spatial inversion symmetry breaking often occurs in antiferromagnetic materials or at the surface of ferromagnetic materials.

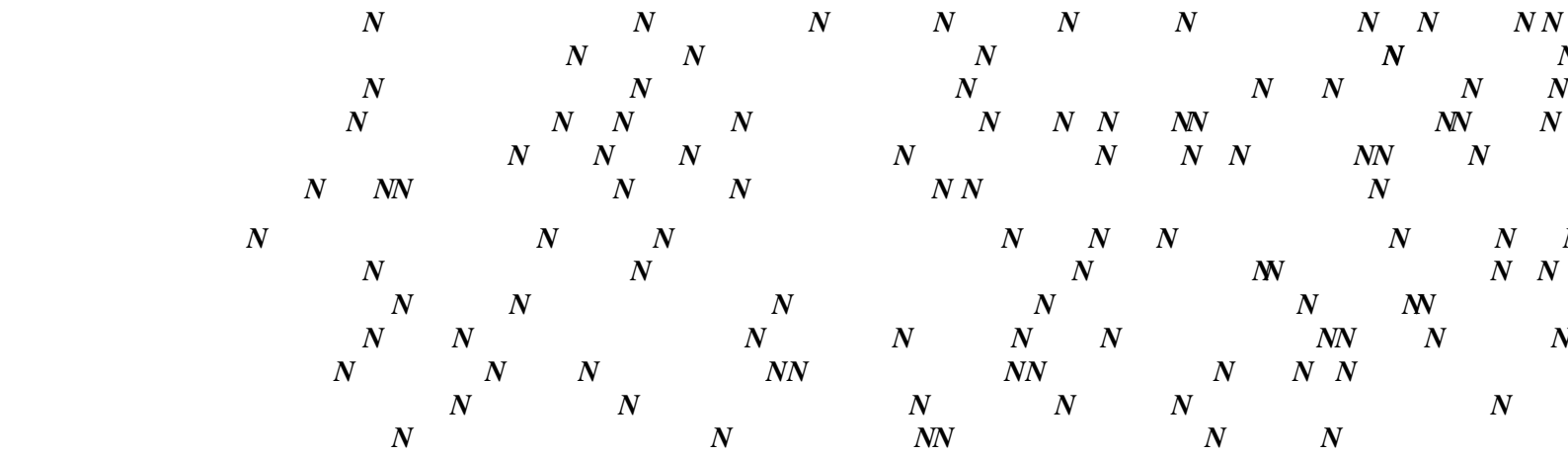
Indeed, the very first observation of magnetic SHG was done on a Fe(110) surface under ultrahigh vacuum conditions by Reif *et al.* in 1991.[580] Consistent with the theoretical prediction by Pan *et al.* in 1989,[581] the intensity of observed SHG changed with the reversal of the magnetization. Later, magnetic SHG was detected in the antiferromagnetic bulk crystal Cr_2O_3 by Fiebig *et al.* in 1994.[582] Since then, magnetic SHG has become a powerful tool to study multiferroic orders in functional oxide materials.[578] However, the second-order nonlinear optical susceptibility arising from magnetic orders in these bulk materials is typically weak, in comparison to that contributed by the crystallographic structures with





$! $ < n D a j/ e J k j e „ G e k

$! # 2 L O H L e e H í 3 D , J k j k J , i



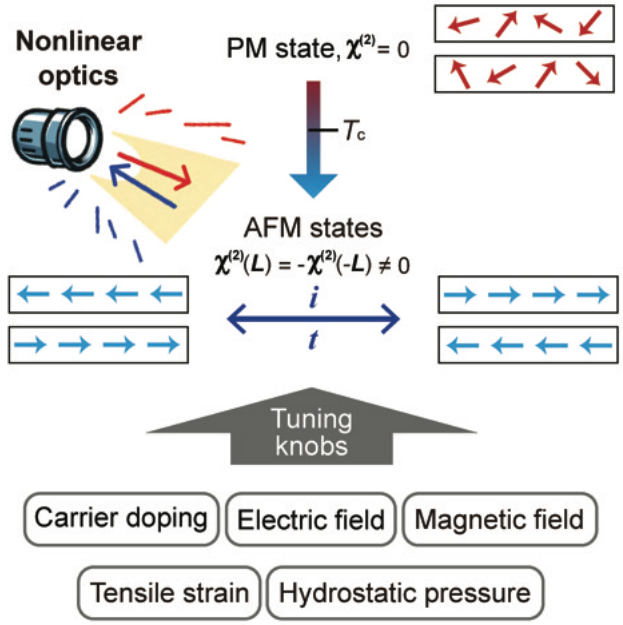


Figure 20. Symmetry-sensitive nonlinear optics as a powerful tool for probing 2D magnets under external stimuli. PM and AFM represent paramagnetic and antiferromagnetic, respectively. T_c denotes the Néel temperature of the magnetic phase transition. The symbols ***i*** and ***t*** indicate spatial inversion and time reversal operations, respectively.

Chirality, Singularities, Geometric Phases, and Moiré Systems

21. QUANTUM GEOMETRIC PHOTONICS IN 2D MATERIALS

Ying Xiong,[1,2] Oles Matsyshyn,[1] Roshan Krishna Kumar,[3,4] and Justin C. W. Song[1,*]

[1]Division of Physics and Applied Physics, School of Physical and Mathematical Sciences, Nanyang Technological University, Singapore 637371

[2]Science, Mathematics and Technology (SMT), Singapore University of Technology and Design, 8 Somapah Road, 487372 Singapore

[3]Catalan Institute of Nanoscience and Nanotechnology (ICN2), CSIC and BIST, Campus UAB, Bellaterra 08193, Barcelona, Spain

[4]ICFO - Institut de Ciencies Fotoniques, The Barcelona Institute of Science and Technology, 08860 Castelldefels (Barcelona), Spain.

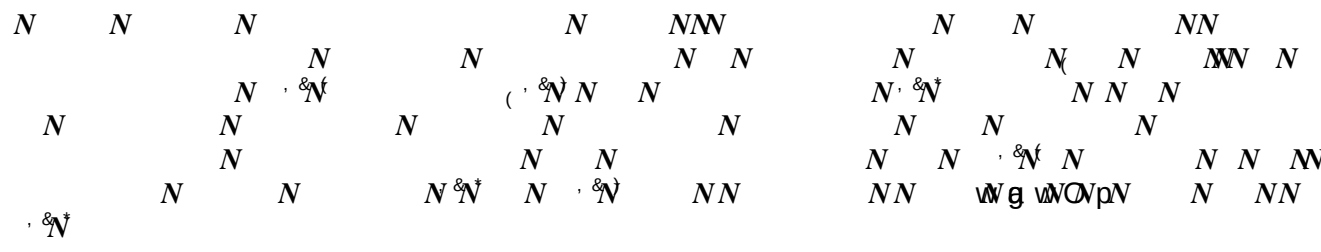
***Corresponding author.** Email: justinsong@ntu.edu.sg

21.1 Introduction

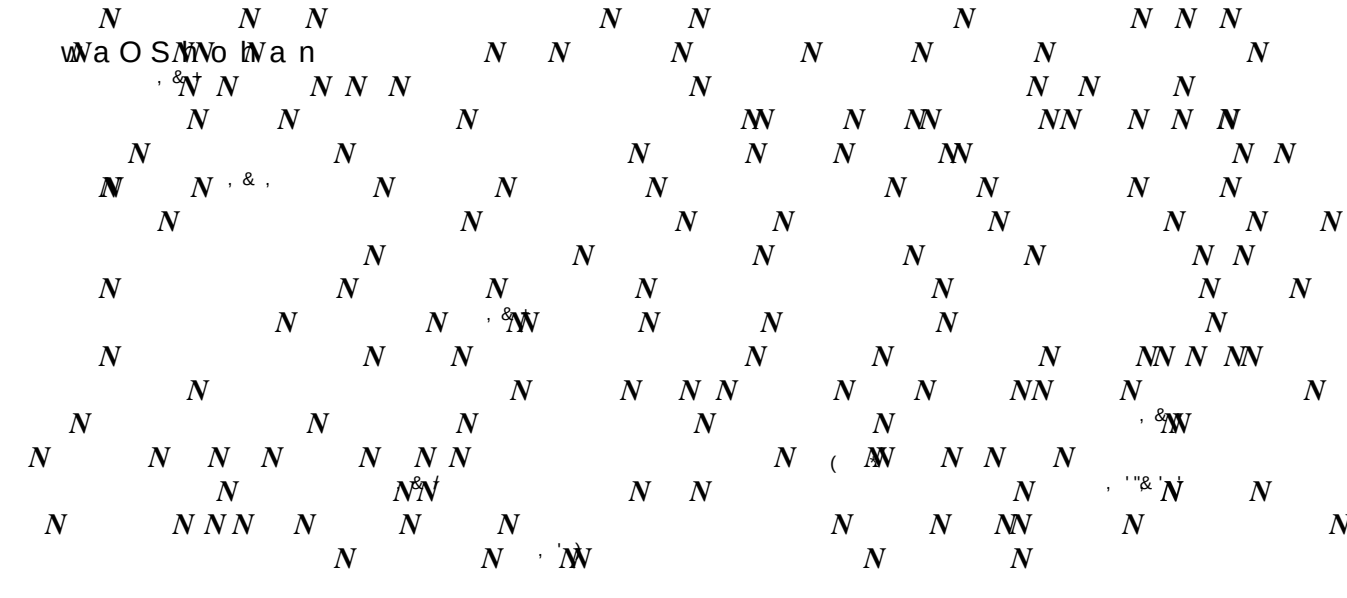
Unlike conventional optoelectronics that are dominated by free-particle-like dynamics and scattering, a new range of optoelectronic responses are emerging that directly rely on the winding of the Bloch wave functions in quantum materials—termed quantum geometry. Such quantum geometric optoelectronic responses have now recently exploded in 2D material. For instance, valley circular dichroism and a light-induced Hall effect can be controlled by the Bloch band Berry curvature;[598] nonreciprocal propagation of collective modes (such as plasmons) can be controlled by the quantum metric dipole.[599]

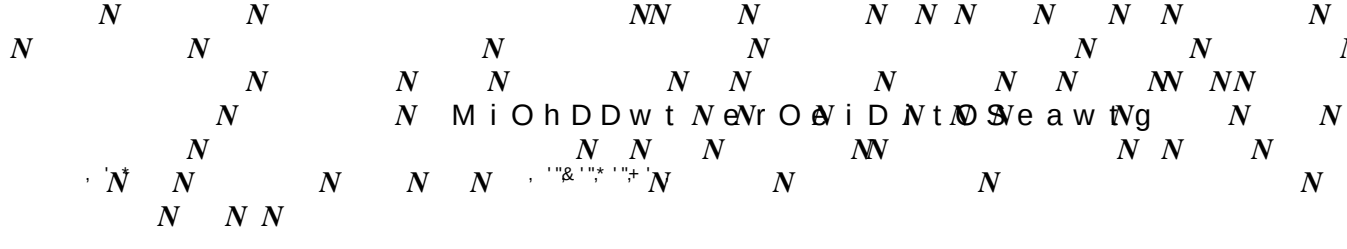
Recent attention, however, has focused on bulk quantum geometric photocurrents induced even in the absence of a p–n junction. In these, photocurrents flow in a direction determined by a material's intrinsically broken centrosymmetry. Unlike built-in fields that control the conventional photovoltaic effect, or temperature gradients and the Seebeck coefficient for the photothermoelectric effect, bulk photocurrents are now understood to strongly depend on the intrinsic properties of Bloch wave functions[573] (see Figure 21). For instance, when electrons are photoexcited in non-centrosymmetric materials, light-induced coherences during the interband transition from a valence-to-conduction band change a material's electric polarization. Such a continuous rate of change of electric polarization produces a shift photocurrent. Shift photocurrents have been related to a range of quantum geometric properties, including a Pacharatnam–Berry phase[600] and a Hermitian connection,[601] and contribute to a bulk photocurrent response for linearly polarized irradiation in non-magnetic materials. Similarly, under

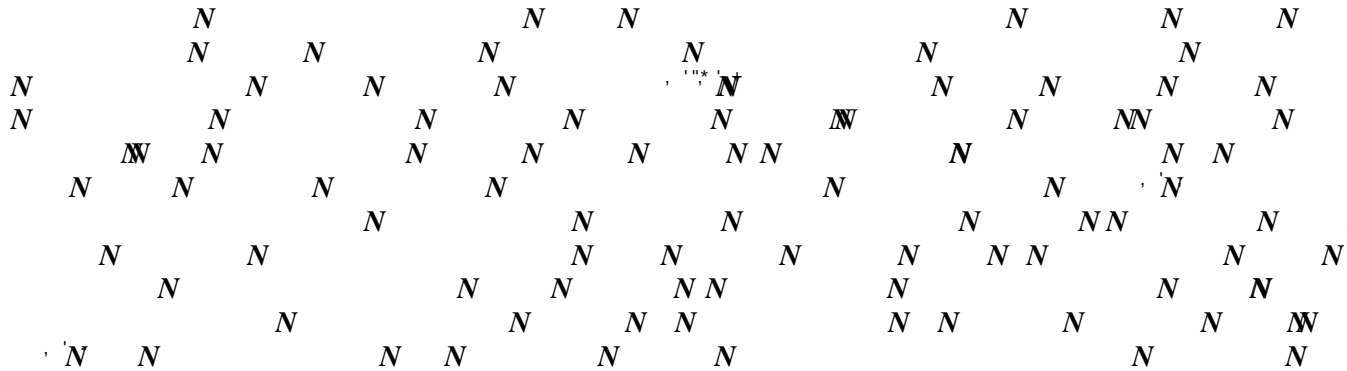
$ # ! $ BHJHe Dr Hce 2íejí

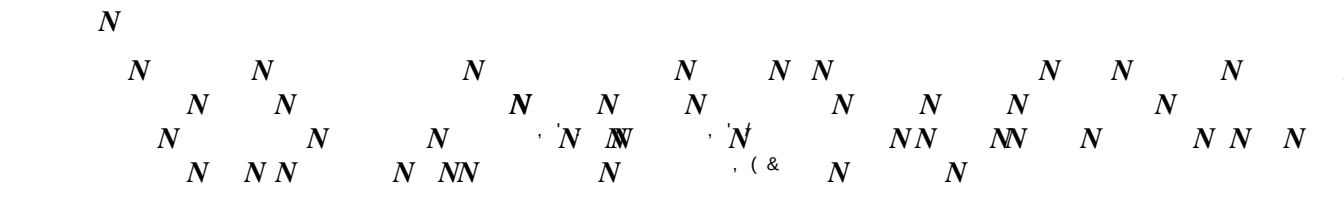


4 i O h D w a t O p k M i O r S w e t i D i t O S e a w t g



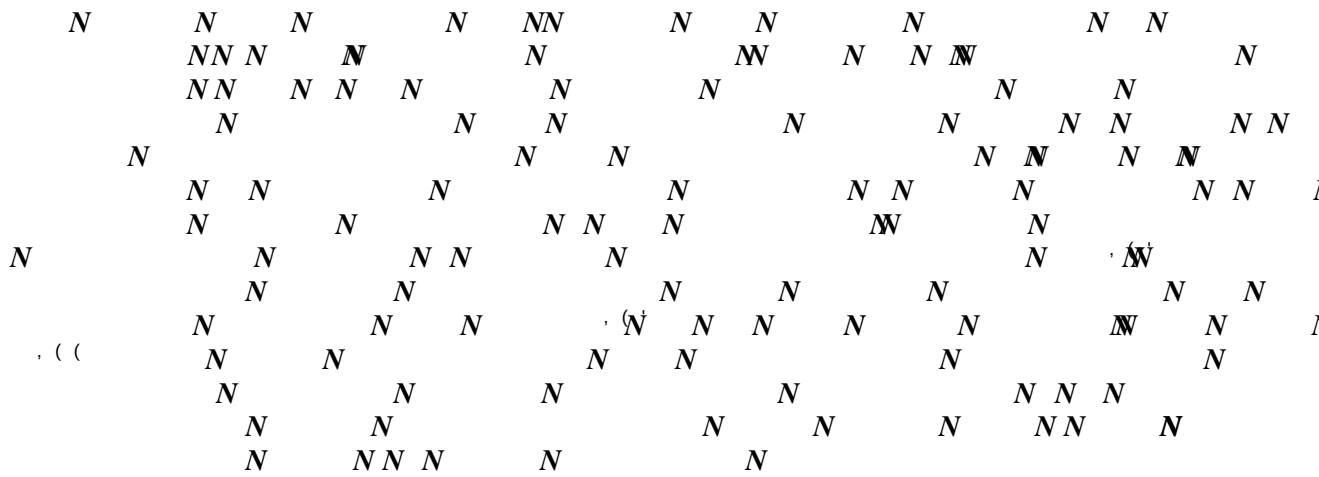




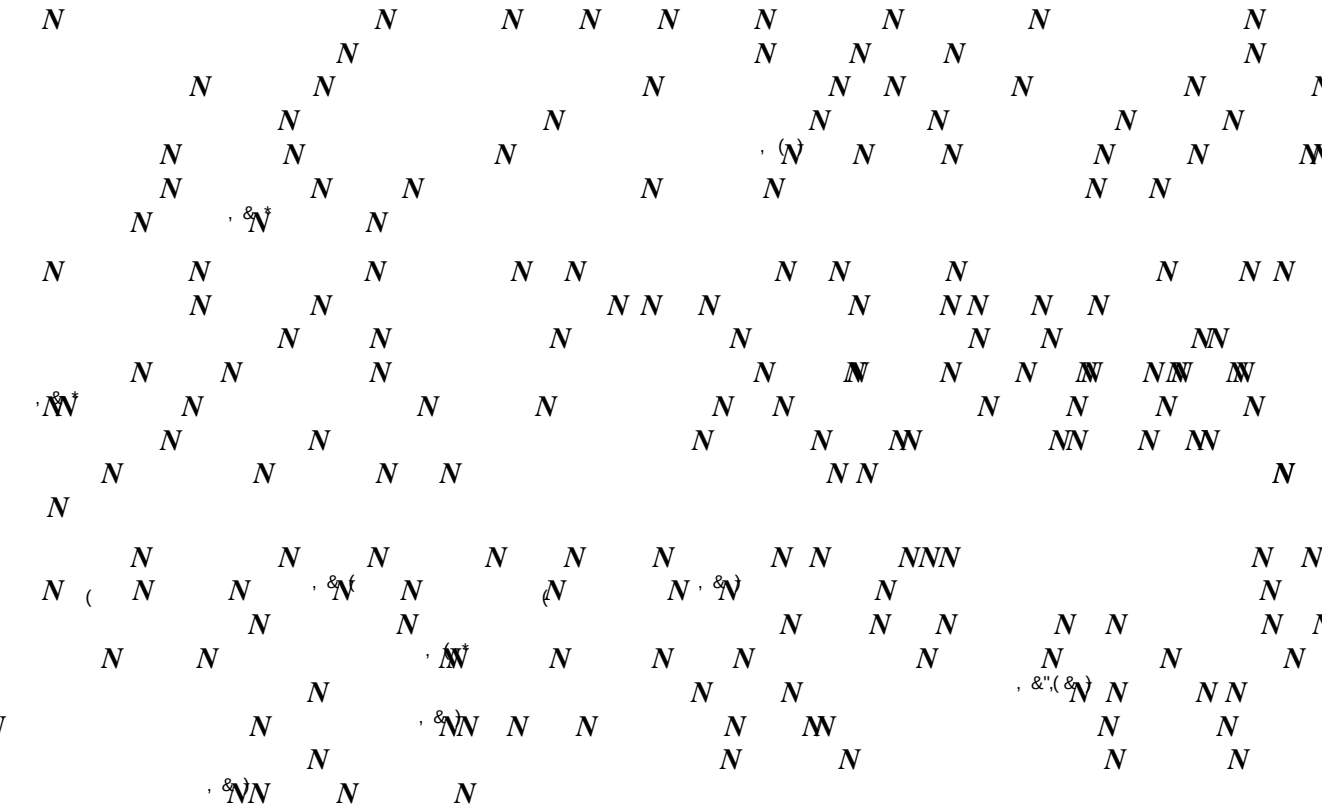


$ # ! % J j j e , G e k J , i 3 D J j k

- B a h M w t h D , e # a S e D i h a n i S s e w 7 h g i g

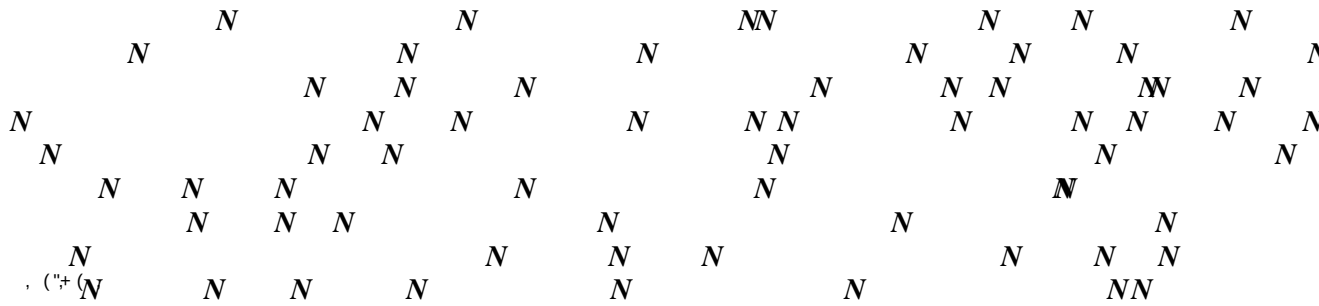


2 a O i S p t h a O a i M i 7 S e O t e t p S S i a O g



$ # & L H l ó n e v H í D , k

5 i a e r e p h e a O p t M i 6 r S e t i D i t O S e a w t g



vector of polaritons can activate circular shift and linear injection type photocurrents in a nonmagnetic and inversion symmetric material.[626] Such photocurrents track higher-order quantum geometry (e.g., shift current dipole[625] or even a momentum-resolved quantum geometry[626]). Indeed, such finite-wave vector quantum geometric optoelectronics are currently being explored even in a single contiguous stack (e.g., twisted spiral multilayer WS_2)[627] and represent a promising new direction for enhanced quantum geometric nonlinearities.

21.4.2 *Stack Engineered Optoelectronics*

Another emerging direction is the use of stack engineering to control optoelectronic response. For example, by twisting adjacent layers of graphene together to form a chiral stack,[102] optical circular dichroism was induced; similar dichroism can be activated even at low frequencies arising from the quantum geometric properties (e.g., an in-plane magnetic moment) of a metallic Fermi surface in such a chiral material. Similarly, bulk photocurrents can be sensitive to AB or BA atomic stacking arrangements in gapped bilayer graphene[600] even as the dispersion relations for AB or BA stacked gapped bilayer graphene are the same; instead AB/BA stacking arrangements are imprinted into the shift vector—a property of electronic wave function. By tailoring stacks rationally engineered in the z direction,[627] artificial materials with pronounced quantum geometric optoelectronic responses can be envisioned.

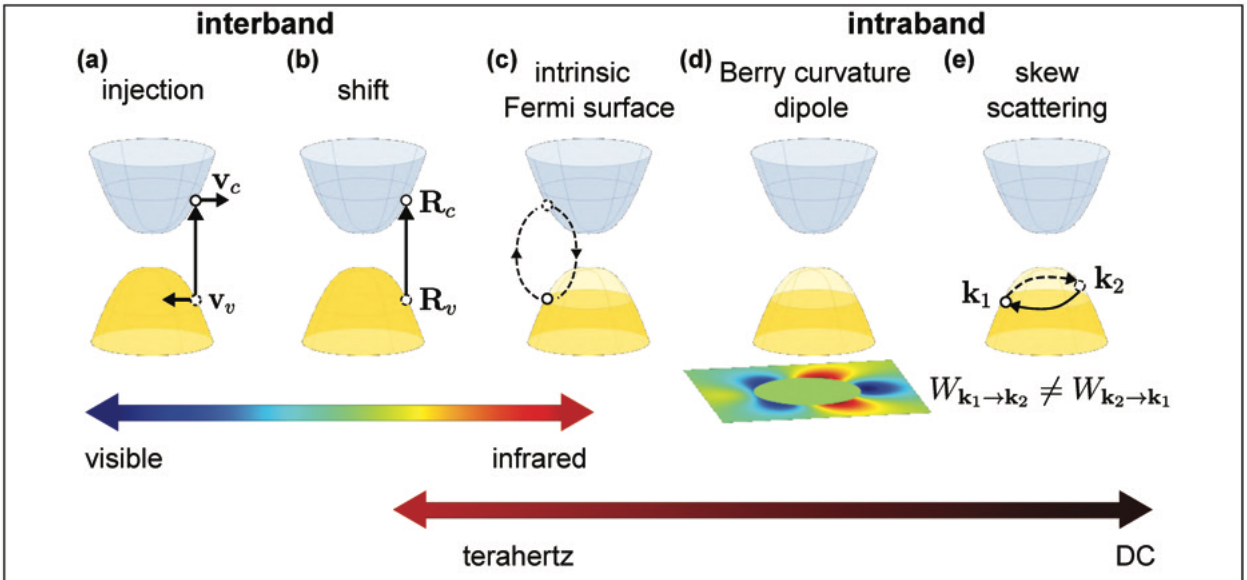


Figure 21. Bulk quantum geometric photocurrents. (a,b) Injection (a) and shift photocurrents (b) arise from the change in electron group velocity ($\mathbf{v}_c$ and $\mathbf{v}_v$ in the conduction and valence bands) and real space displacement ($\mathbf{R}_c$ and $\mathbf{R}_v$ in conduction and valence bands) when electrons are photoexcited from valence to conduction bands in non-centrosymmetric materials. (c-e) In the presence of a Fermi surface, a variety of other mechanisms become activated including (c) an intrinsic Fermi surface effect (arising from virtual interband processes), (d) a Berry curvature dipole (inset; asymmetric distribution of Berry curvature across a Fermi surface), and (e) skew scattering contributions (produced when the transition rates W between Bloch states at momenta $\mathbf{k}_{1,2}$ become imbalanced). These mechanisms provide means for achieving a type of optoelectronics based on bulk non-centrosymmetric metals.

22. SINGULARITIES OF RANDOM WAVES IN 2D MATERIAL PLATFORMS

Tomer Bucher,[1] Alexey Gorlach,[2] Shai Tsesses,[3] and Ido Kaminer[4,*]

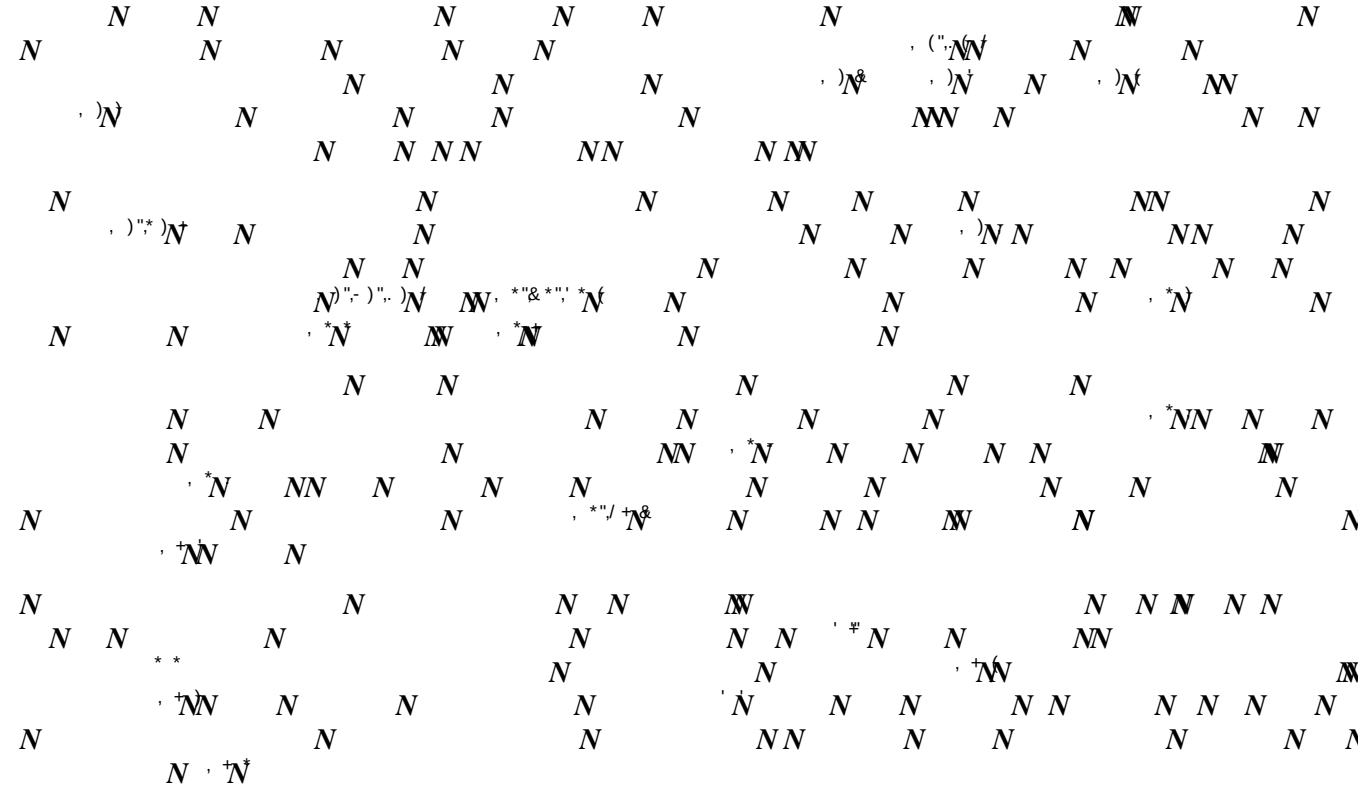
[1]Andrea & Erna Viterbi Department of Electrical and Computer Engineering, Technion–Israel Institute of Technology, 3200003 Haifa, Israel

[2]Department of Physics, MIT, Cambridge, MA, US.

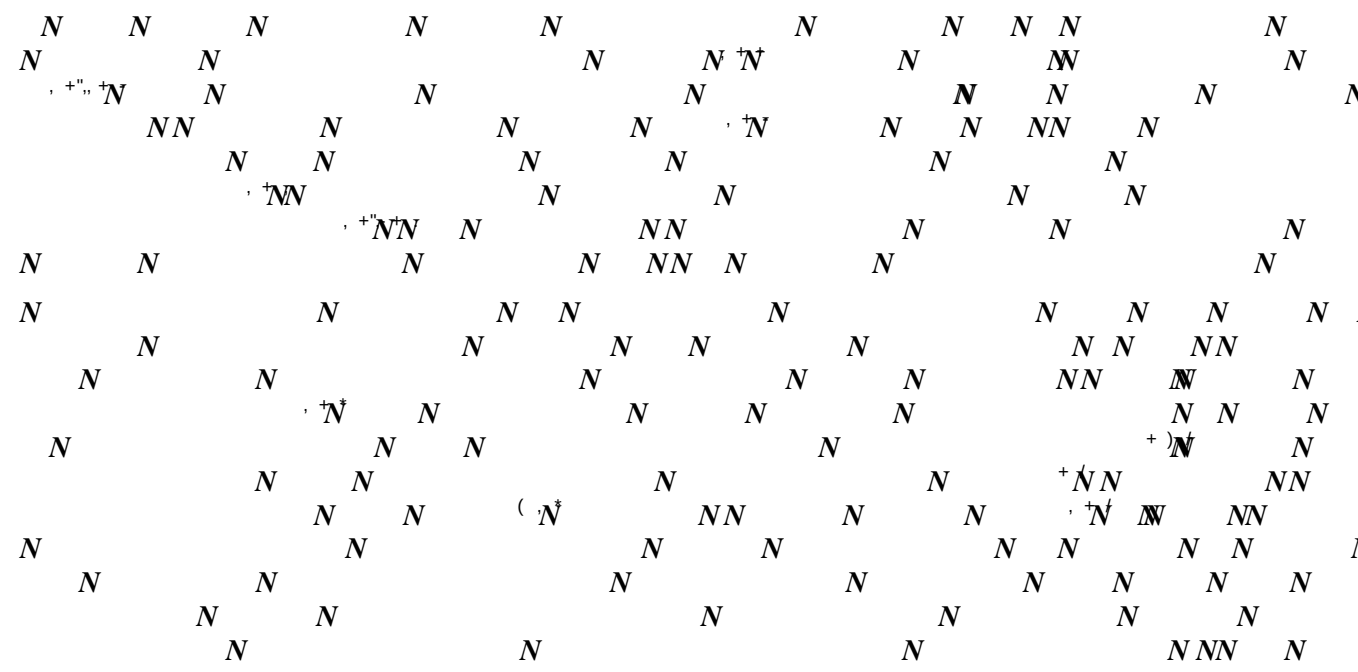
***Corresponding author.** Email: ido.kaminer@gmail.com

22.1 State of the Field

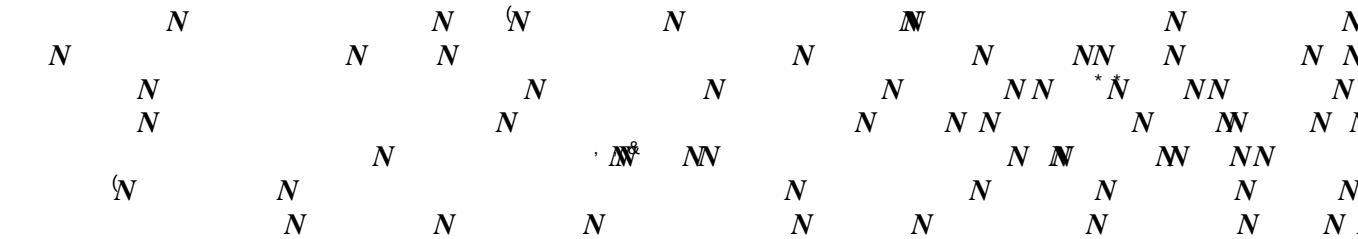
Wave singularities, such as vortices and field dislocations, refer to points or lines in a wave field where intensity vanishes, and the wave phase is undefined. These singularities have been a central topic in all



$ $ I $ J j j e , 3 D e J k j k J , i



$ $ 2 % H L n e 0 í n e v H í D , k J , i / D , v j L k í D , k



complementary approach could be altering the coupling of the electric field to the magnetic field, which will incorporate interesting statistics and correlations among singularities.

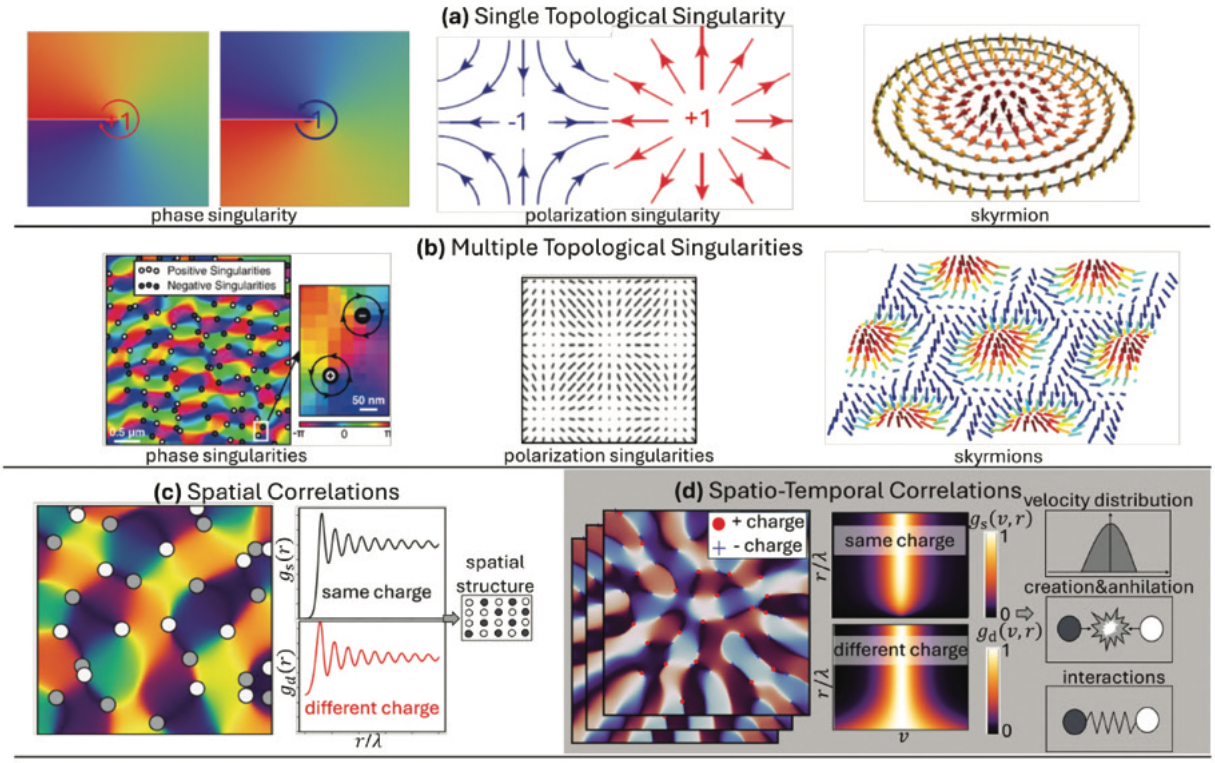


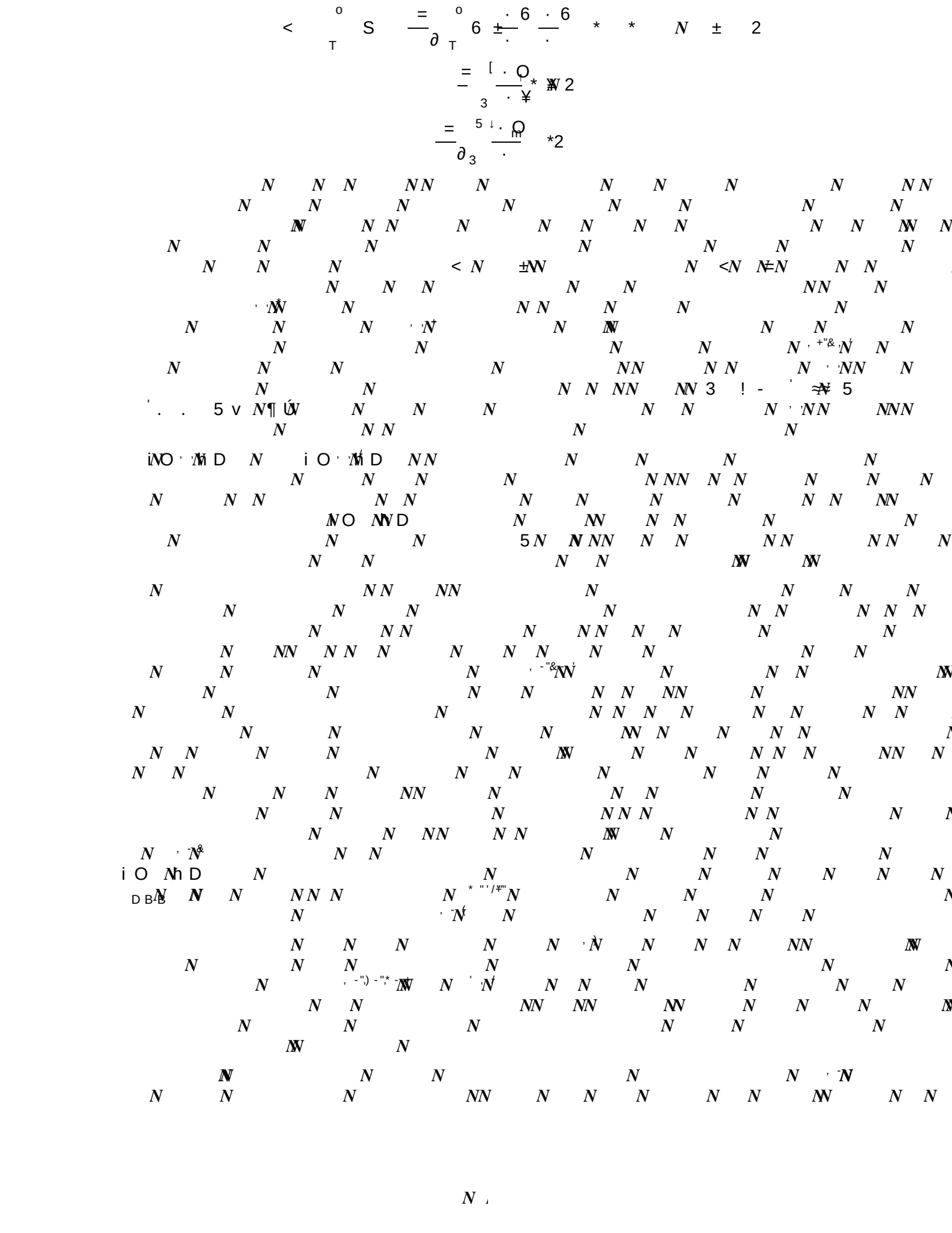
Figure 22. Overview of optical singularities and their correlations. (a) Different types of optical singularities and their experimental demonstrations including phase singularities, polarization singularities, and more complex types of singularities such as knots and skyrmions. (b) A vast range of systems show natural occurrences of multiple singularities, which can interact and annihilate in pairs, conserving their combined topological charge. Adapted with permission from refs 649 and 657 (Copyright 2020 American Association for the Advancement of Science and 2016 American Physical Society). (c) Ensembles of phase singularities emerging from the interference of random waves have spatial correlations as theoretically predicted in ref 656 and experimentally demonstrated in ref 657. Adapted with permission from ref 657 (Copyright 2016 American Physical Society). (d) The interference of random wave packets results in spatiotemporal dynamics of phase singularities, characterized by the creation and annihilation of vortex pairs. The spatiotemporal correlations of these phase singularities remain an underexplored area, warranting further investigation.

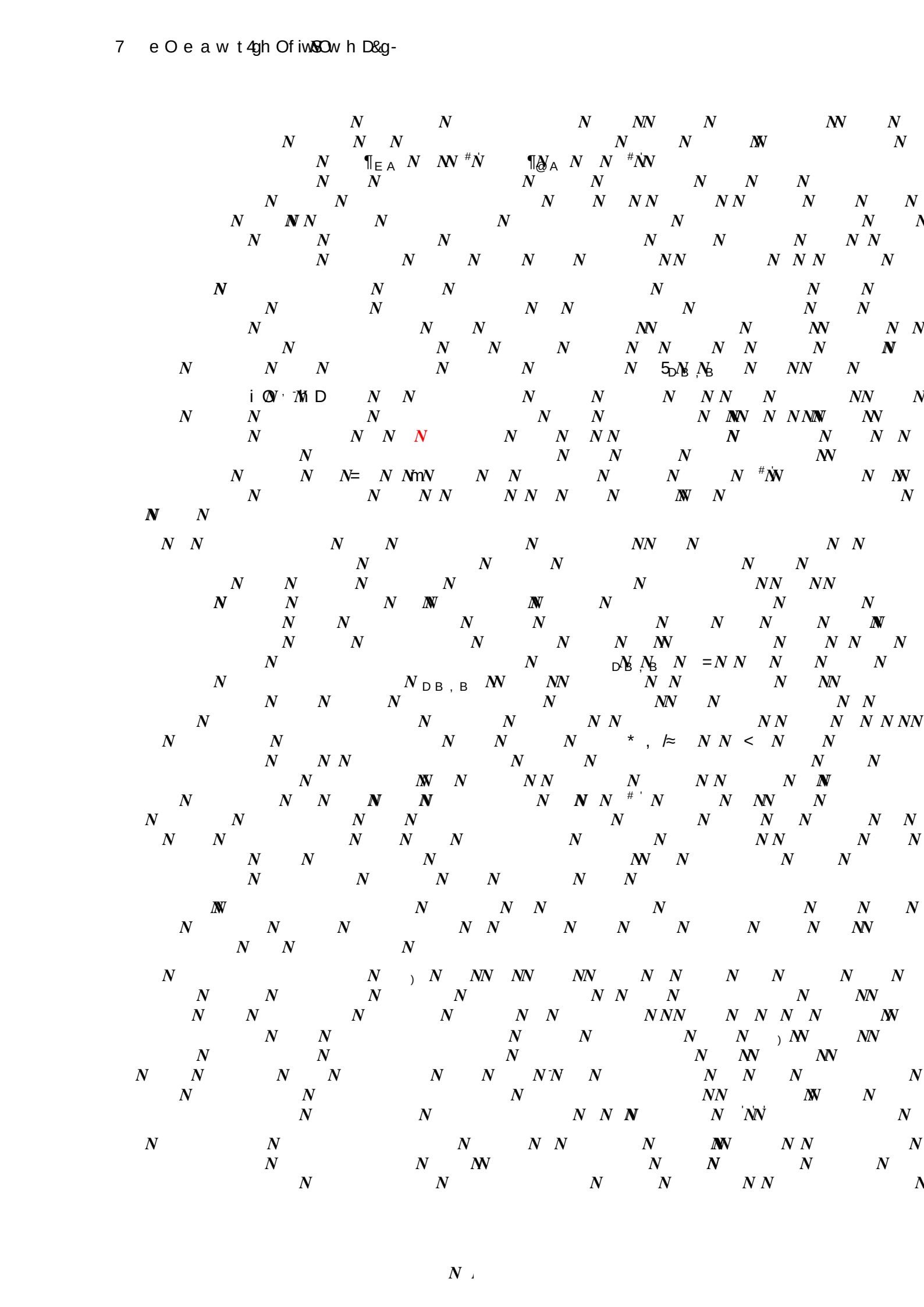
23. 2D TOPOLOGICAL POLARITONICS

Julian Schwab,[1] Florian Mangold,[1] and Harald Giessen[1,*]
[1]4th Physics Institute, Research Center SCoPE, and Integrated Quantum Science and Technology Center, University of Stuttgart; 70569 Stuttgart, Germany
***Corresponding author.** Email: giessen@pi4.uni-stuttgart.de

The advent of topological plasmonics has led to the discovery of plasmonic skyrmions[649] and merons.[661] Methods such as scanning near-field optical microscopy (SNOM) and two-photon photoemission electron microscopy (PEEM) gave the necessary spatial resolution in the sub-10 nm range to explore skyrmions and merons. By combining PEEM with ultrafast laser sources with pulse durations of around 16 fs, it was also possible to reveal the ultrafast dynamics of these excitations.[650,662]

Skyrmions and merons are 3D topological defects on a 2D plane, which can exhibit particle-like properties.[663] They can be characterized by certain vector field properties such as the skyrmion number S, the polarity P, and the vorticity V, which are defined as





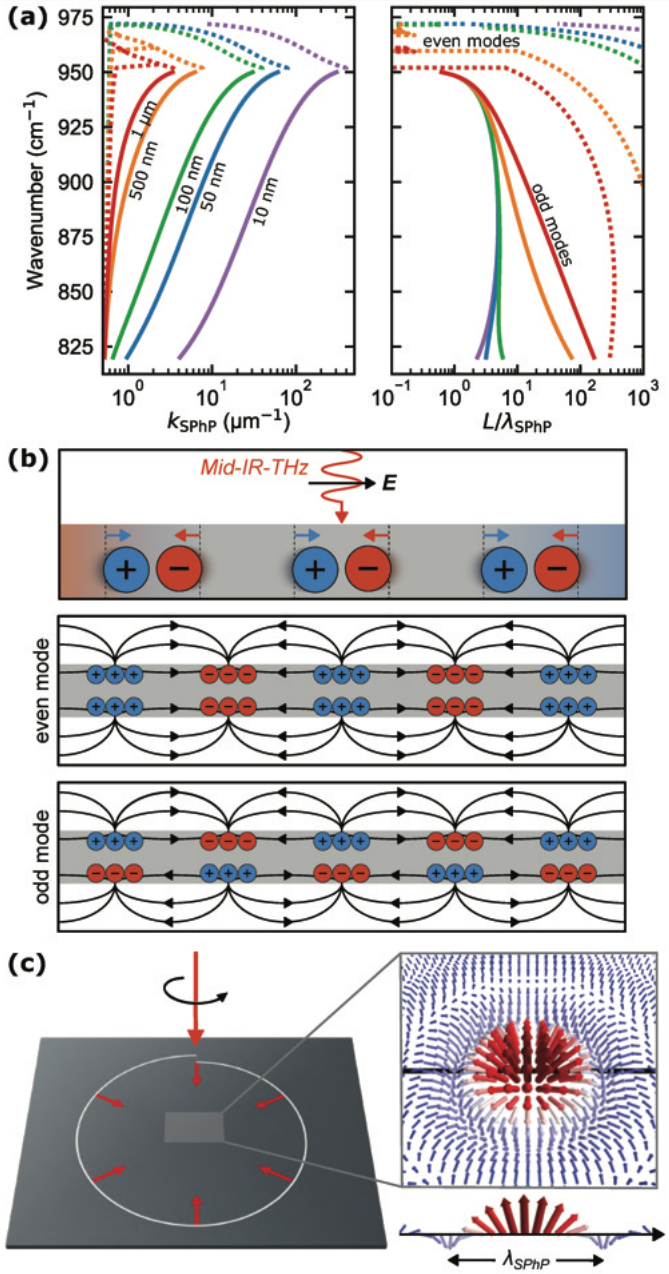
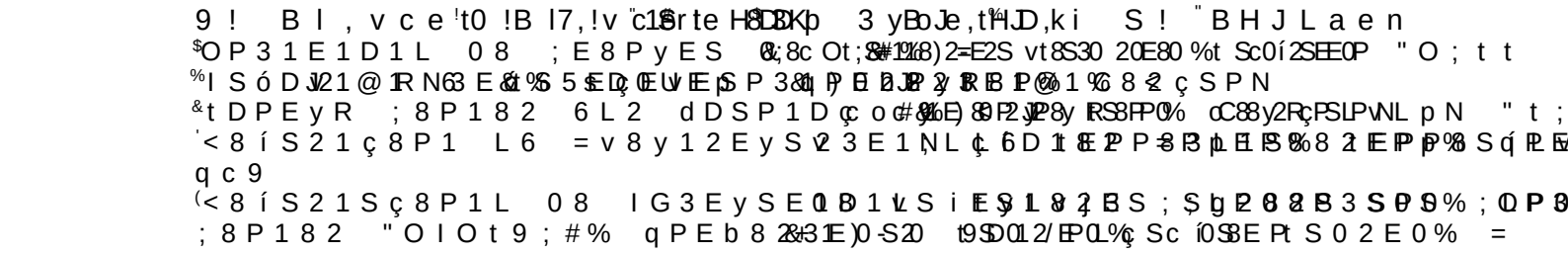
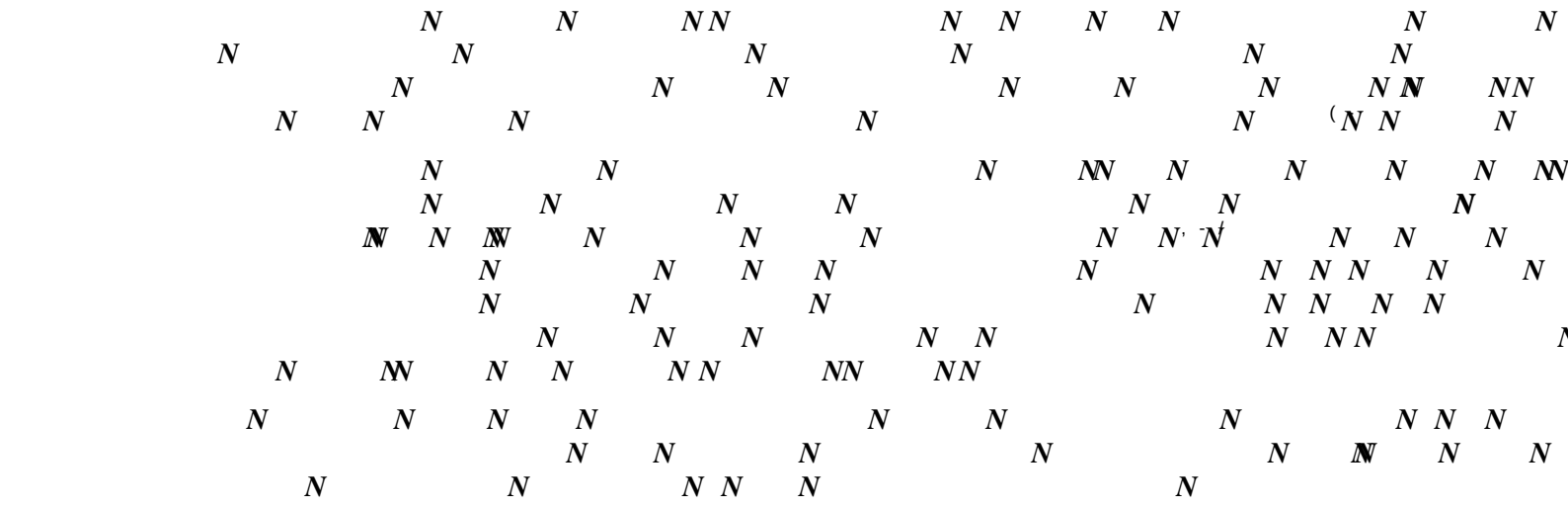


Figure 23. Surface-phonon polaritonic (SPhP) skyrmions and other topological features with varying spatial compression. (a) Theoretical SPhP dispersion for different SiC membrane thicknesses from 10 nm to 1 µm. Displayed are the odd and even modes, calculated using the method outlined in ref 677. On the left, the excitation wavenumber is plotted as a function of SPhP wave vector and on the right the excitation wavenumber is given as a function of the normalized propagation length $L/\lambda_{\mathrm{SPhP}}$. There are two even modes, one of them very close to the light line and the other one with propagation length $L < \lambda_{\mathrm{SPhP}}$. The odd mode features high propagation lengths and strong wavelength compression. Such wavelength compression increases rapidly for thinner membranes. (b) Schematic representation of collective atom displacements in polar dielectrics as the foundations of even (odd) SPhP modes that are illustrated in the center (bottom) image. (c) Exemplary implantation of a skyrmion in the SPhP electric field. SPhPs are launched from a spiral structure with an opening of λ_{SPhP}, which is illuminated by circularly polarized light in the mid-IR. The SPhPs interfere in the center of the structure, creating a skyrmion vector texture in the electric field, as depicted in the vector plot and the 2D cut on the right. The size of the skyrmion is determined by the SPhP wavelength and can be compressed strongly in comparison to the excitation wavelength by using thin SiC membranes.

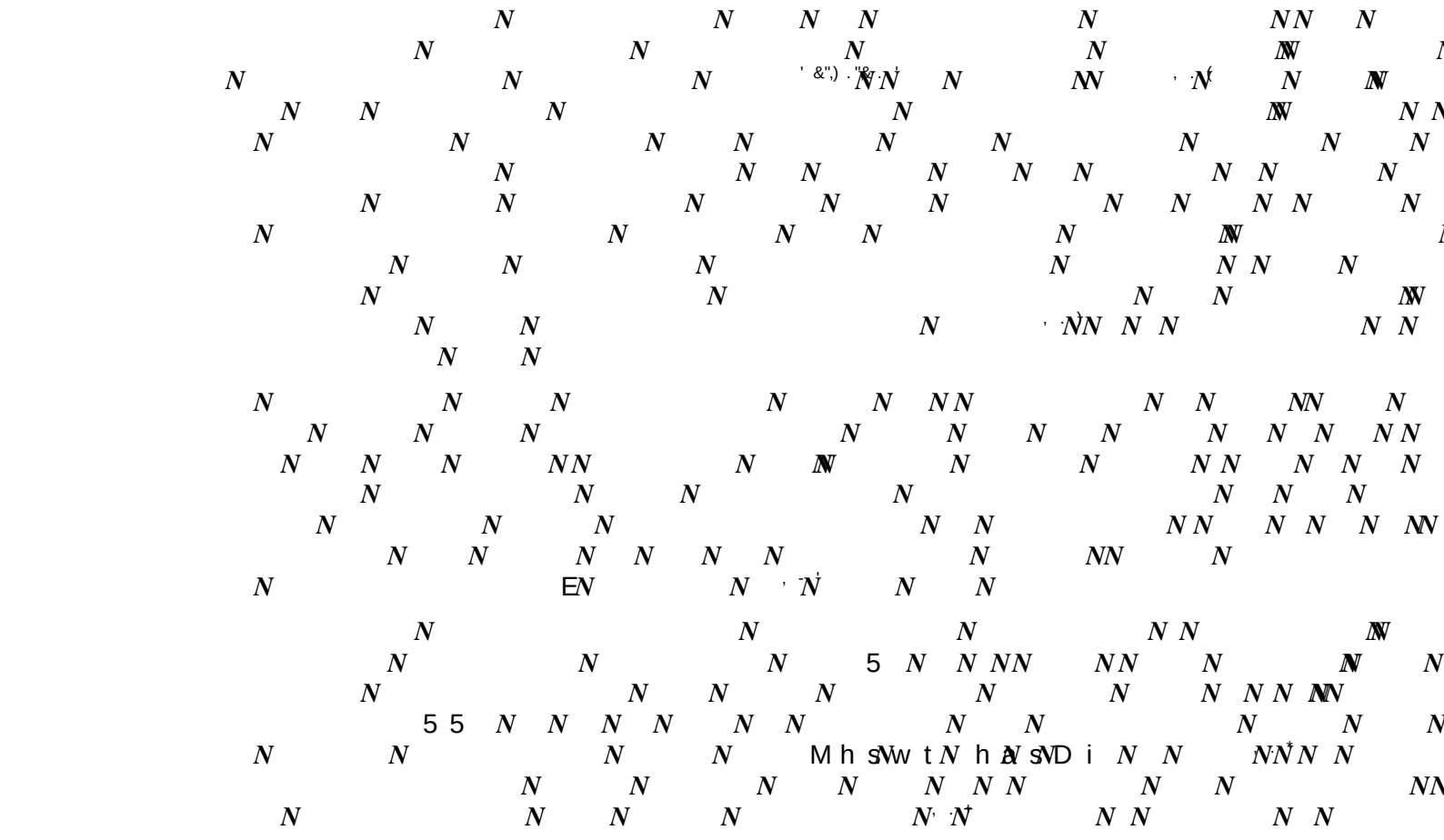
%'0 5 6 1 . 8 6 I D 6 : 9 ; 6 1 U . D . I 2 9 .

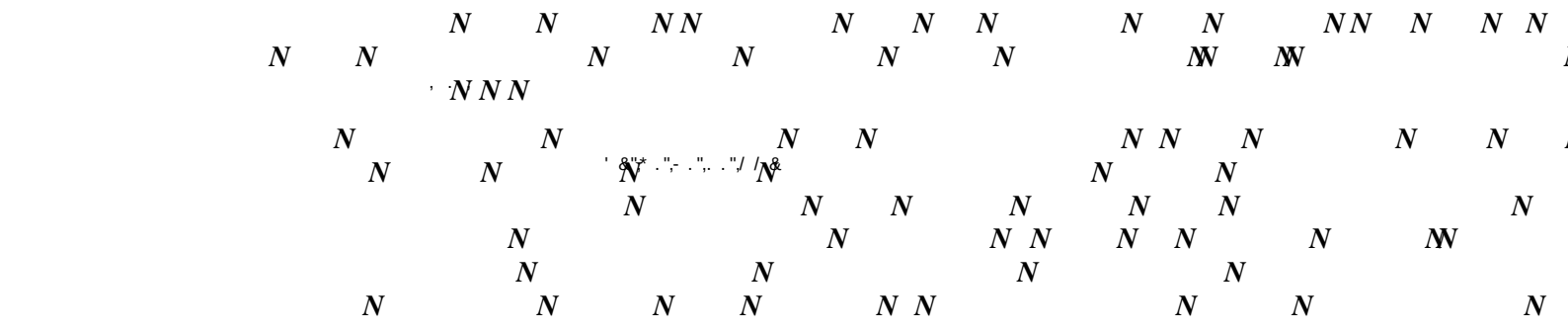


$ & # 5 , H n D i L v H í D ,

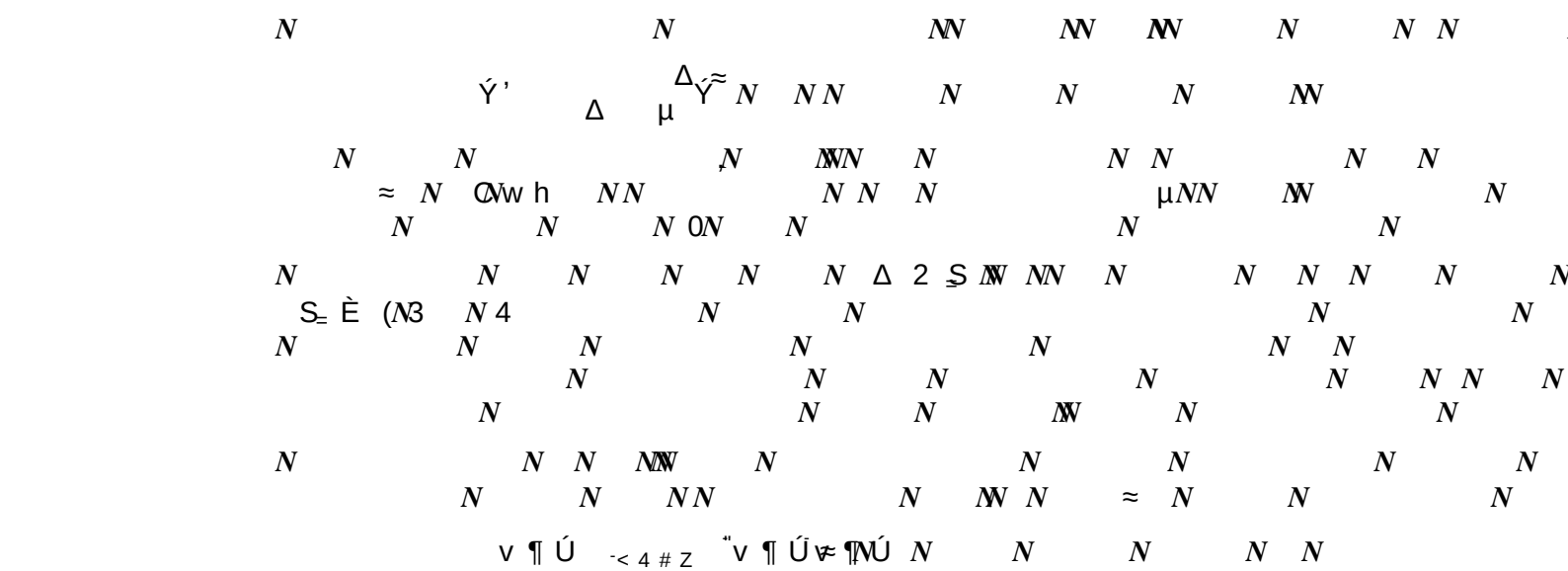


$ & $ / LBHnJeH,eH-DnH Hce

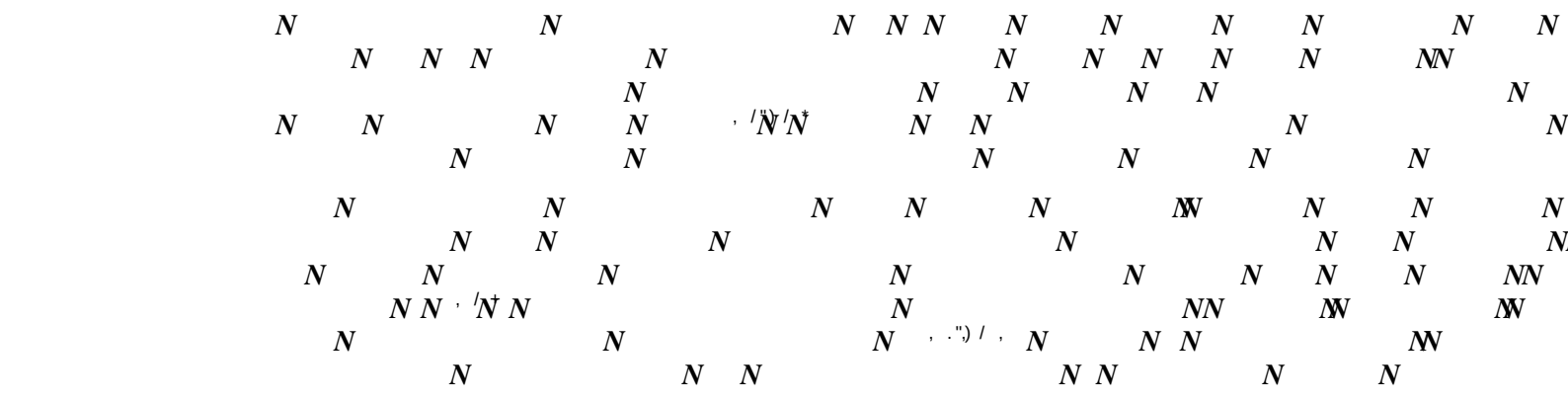




$ & ! % J j j e , G e k



$ & 2 & H 3 D e j k



Finally, chiral molecules are widespread, constituting a significant fraction of pharmaceuticals, flavorants, and biological building blocks. Using light–matter interactions to drive chiral-specific chemistry is appealing for potentially enhanced selectivity and tunability. Chiral graphene platforms can selectively activate bonds in only one enantiomer of a racemic mixture. Achieving enantioselectivity in molecular excitation is challenging because the asymmetry in light absorption between chiral pairs is minimal. However, chiral plasmons in twisted bilayers generate near-field electromagnetic waves with significantly larger asymmetry. These chiral polaritonic platforms would also allow for precise tuning of plasmonic resonances through electrostatic doping and twist-angle control, enabling alignment with the vibrational modes of the target chiral molecules.

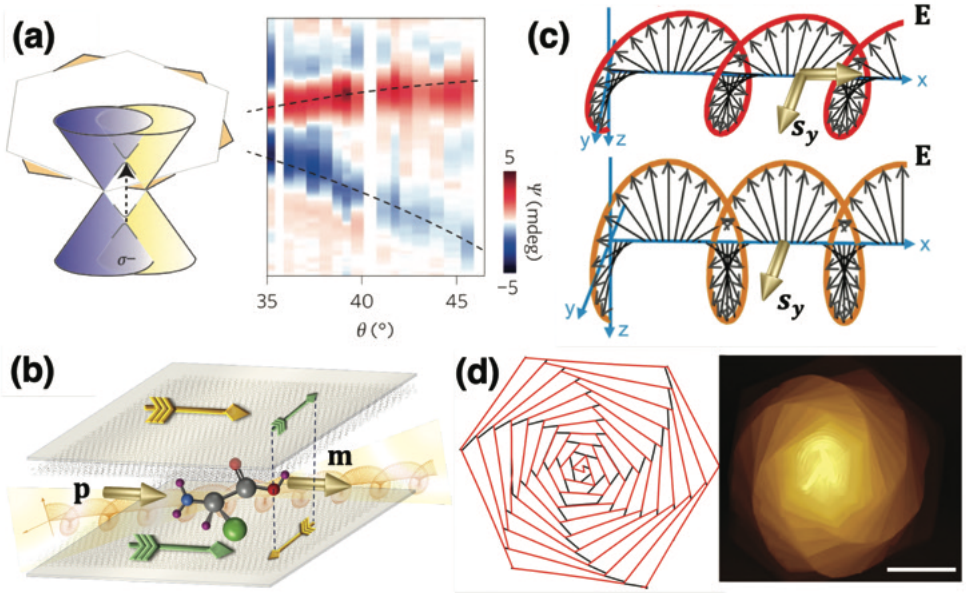
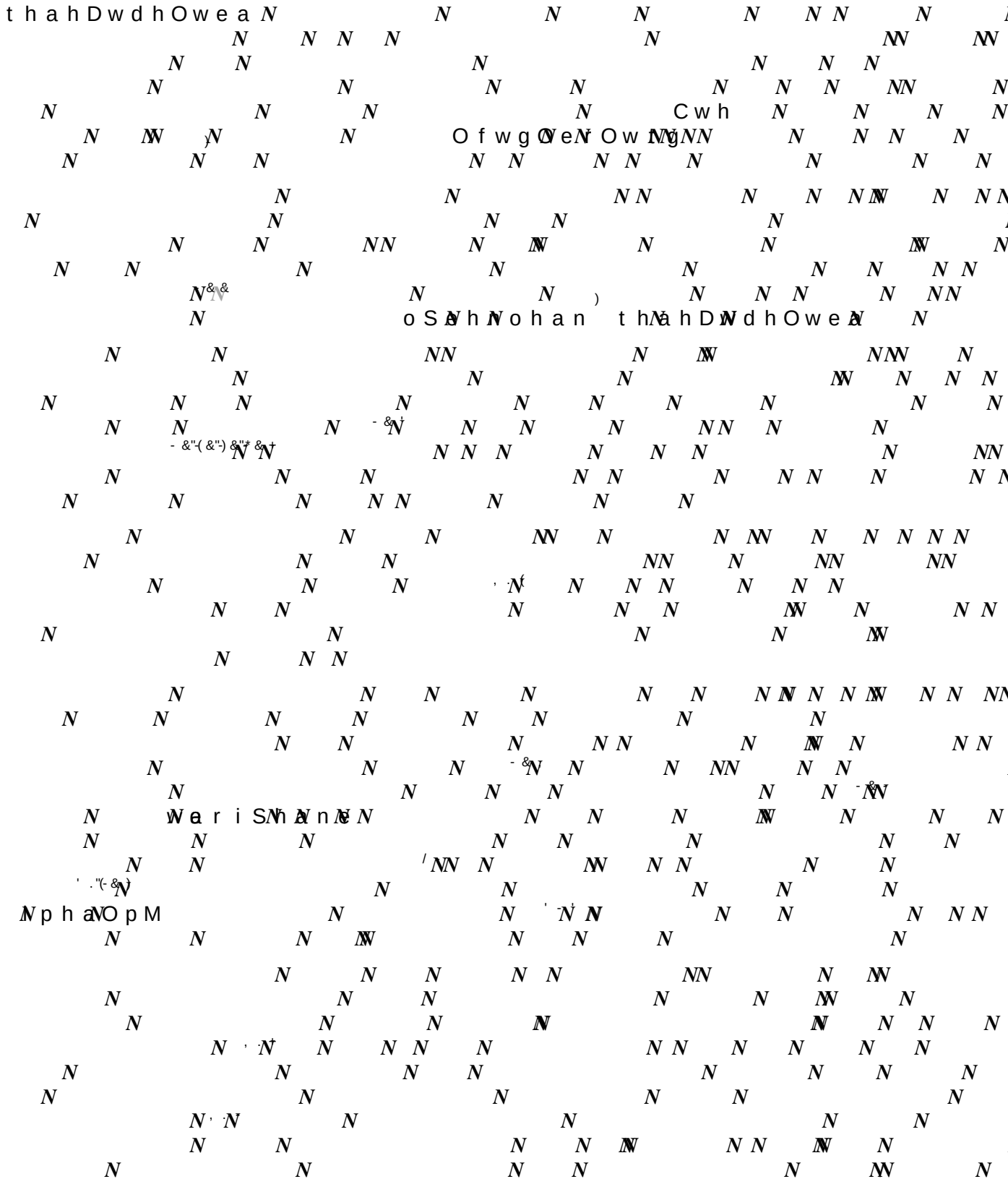
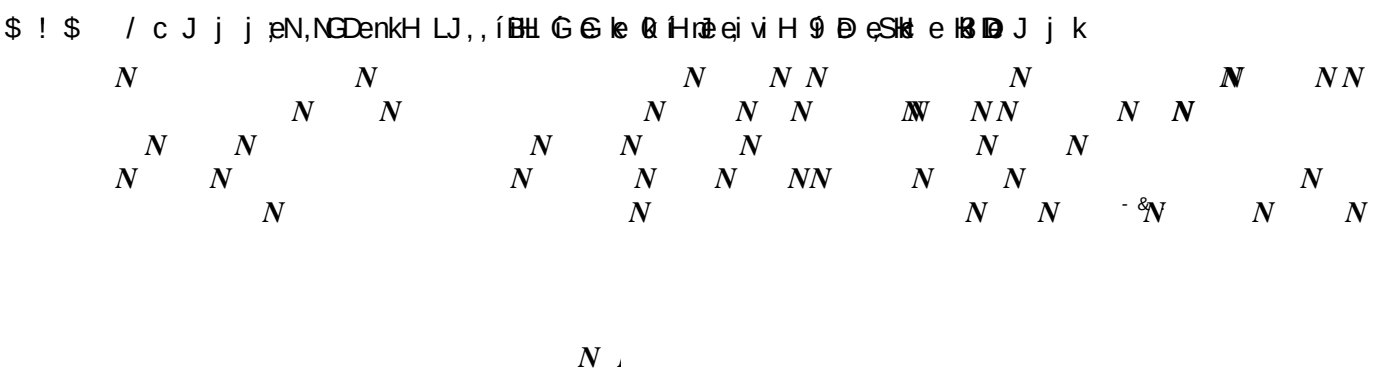
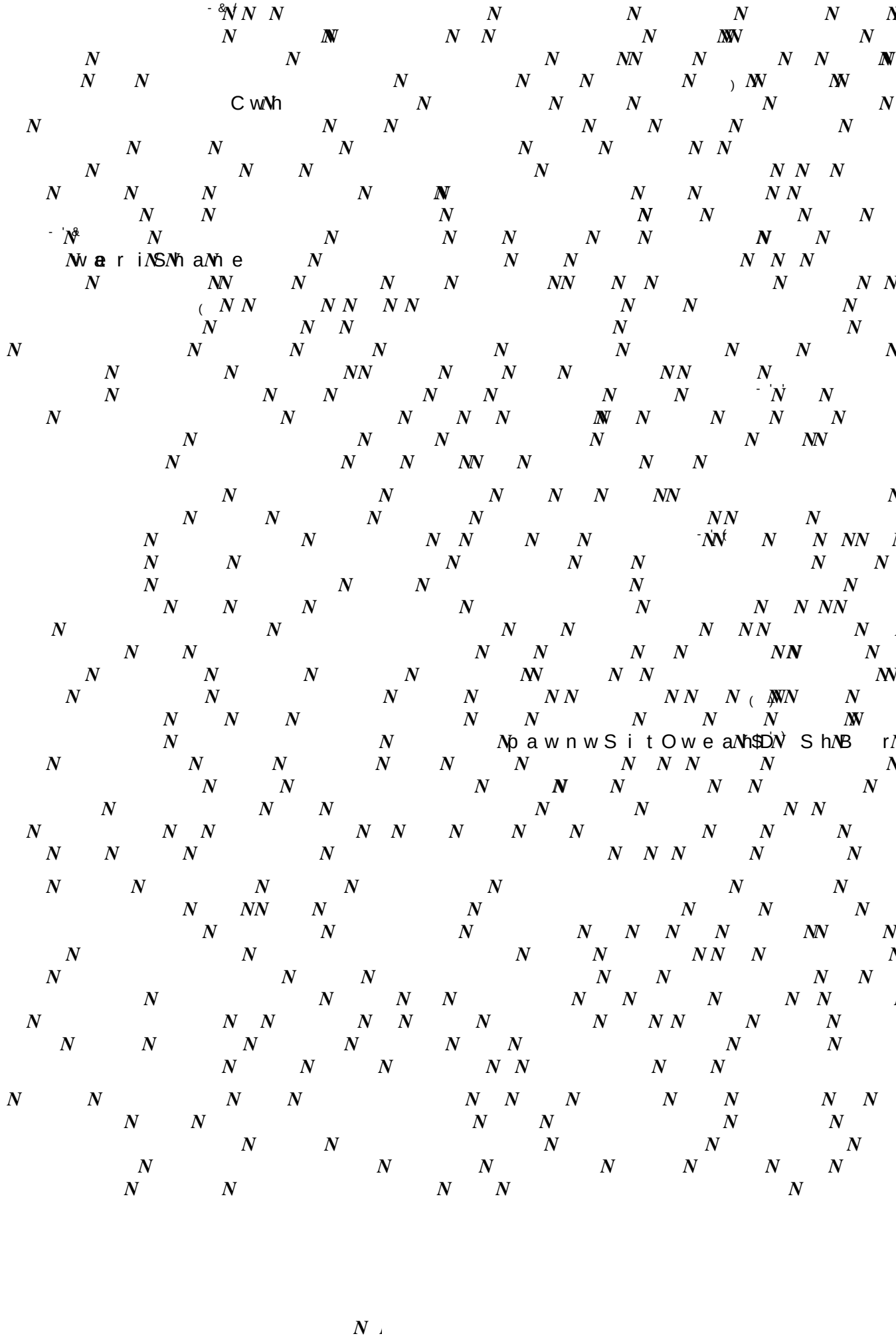


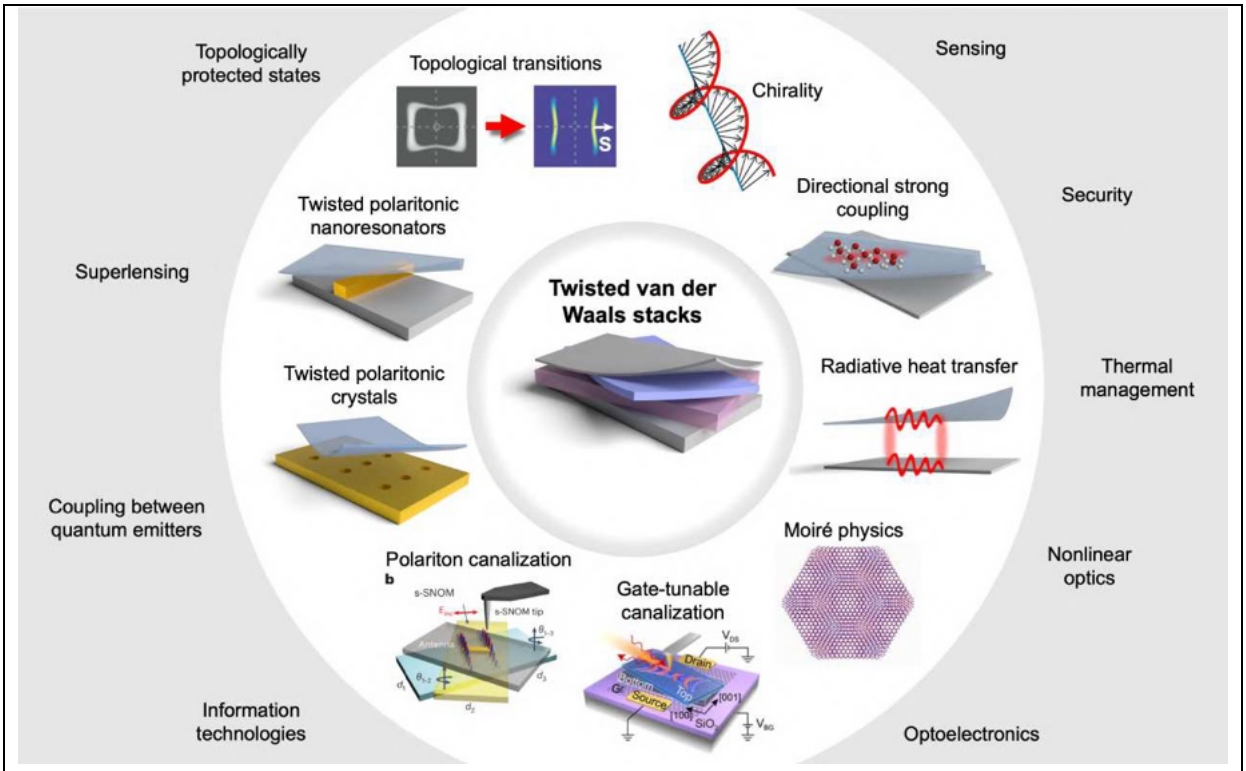
Figure 24. Chiral response in moiré multilayers. (a) Ellipticity or circular dichroism spectra due to the resonant interband transition at the M point as function of the twist angle observed in twisted bilayer graphene. Adapted with permission from ref 102 (Copyright 2016 Springer Nature) (b) Schematic chiral cavity consisting of moiré systems with enhanced chiral near field suitable for sensing. Adapted with permission from ref 687 (Copyright 2020 American Chemical Society). The electric moment **p** due to longitudinal current densities is locked to a magnetic moment **m** due to transverse current densities. (c) The electric field associated with plasmon excitations propagating in the x direction together with its helicity/spin. For ordinary plasmons, the spin points in the y direction, whereas for chiral plasmons there is also a component in the x direction. Adapted with permission from ref 685 (Copyright 2020 American Physical Society). (d) Schematic view of supertwisted multilayers and its AFM image of a representative supertwisted WS_2 sample with continuously twisting layers (scale bar 4 μm). Adapted with permission from ref 694 (Copyright 2024 Springer Nature).



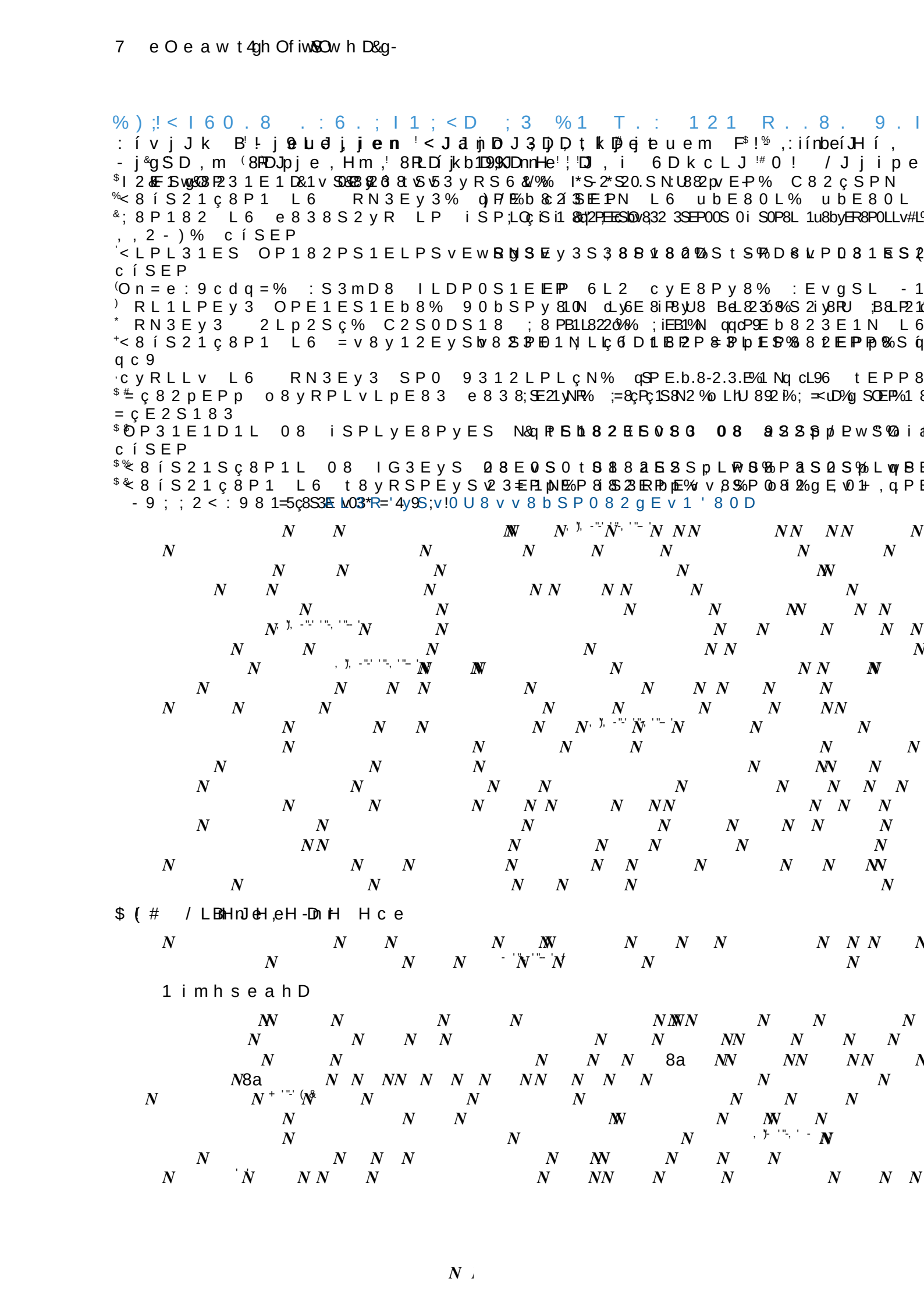








. 5 3 $; ! 2 L S 0 ç S í 6 L 2; D12U2E33P11L íS1PEOy 3í'L 1 8 P 1 E S v" p6 8 D D P 8 Y S 1 g E v L 8 P S í v E v 1 S E 2 8 E
y S P S v É # w ş E E 2 L P % # R 1 N U E E 3 y 1 3 8 % í L v S " # % 2 E 1 L P E p E y 2 S N 3 1 L 8 S S P % y E 1 D E v L P 3 1 2 E p
S 2 2 S N L 6 S í í v E y S 1 E L P 3 E P P S P L í R L 1 L P E y 3 " B 8 P 8 E # P 2 % P E P 6 I
o R 8 Q ; R E 2 S v E 1 N 9 3 ó 8 1 y R ç E 2/3 8 1 6 S ; 0 L S í N 1 2 8 E 0 p R U 1 E 1+R) + í) 8 2 9 ç ç E 8 3 2 3 E E y L S P P 6 2 R
Q C S 1 D 8 P S g v 8 y S P S v E w S 1 E L P 9 í S P 8 0 v) " 2 E ; 3 L í S N 0 2 S E í p 1 R 8 1 0 +U) E+1, R 9 í ç 8 8 2 2 ç E E y
c L y E 8 1 N # '



6 S O e S e M o w t

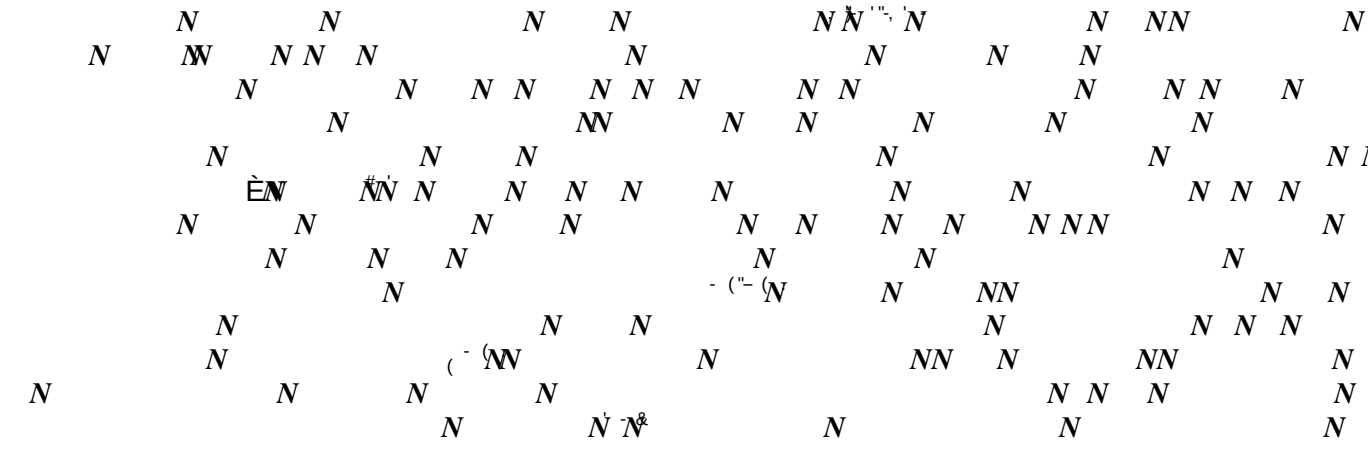
4 e a e t D w a w t " O S w t D w a w t

$ ($ / c J j j 2eL ,HGL0mken eJv,NHí D , k

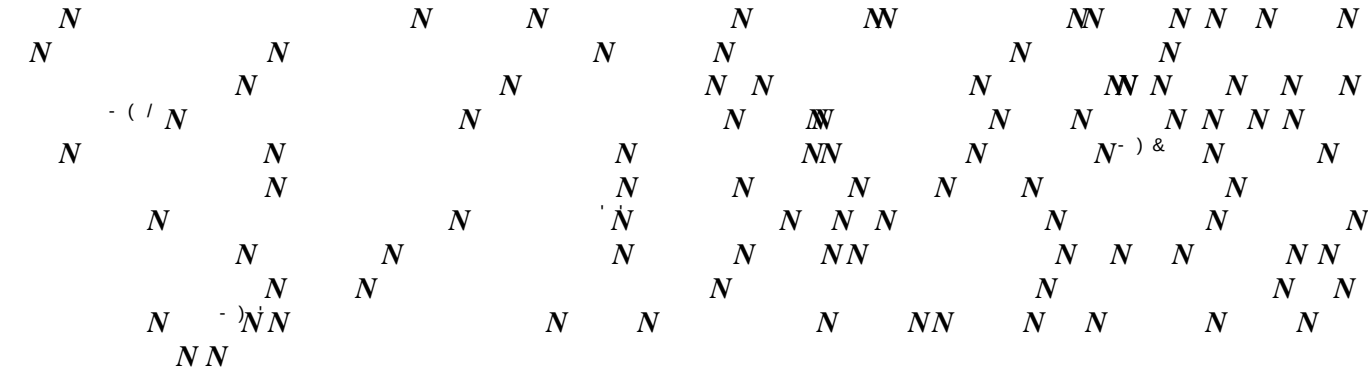
4 h O i S iwhhSDtg

h ow a N O w e

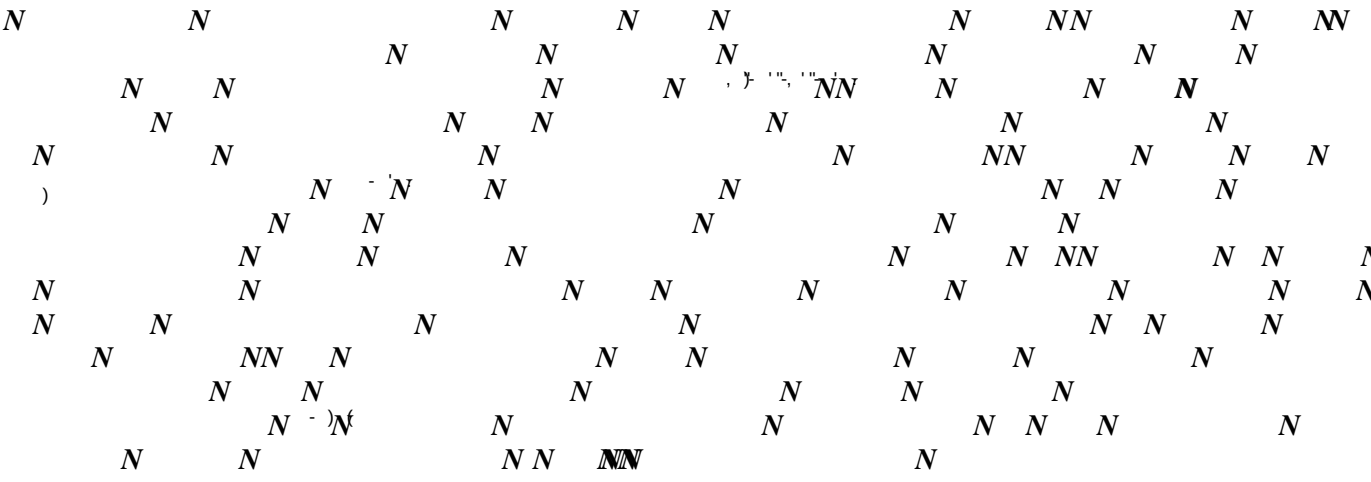
, h S h t O i S w d h O w e a



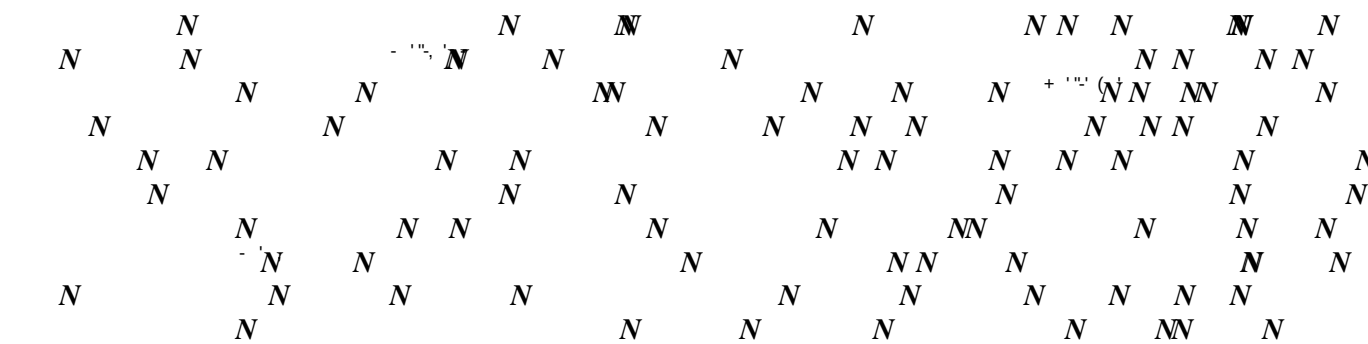
/ h o S w t h O w e a h a n g t h D h o w D w O B



; p a h o w D w O B



/ D h O #h a w r e a e O e a w t n i C w t i g



: i a g w a s

; i SMhD h r r Dw t h Owe a g

/ p a t Owe a h D MhO i Swh D g

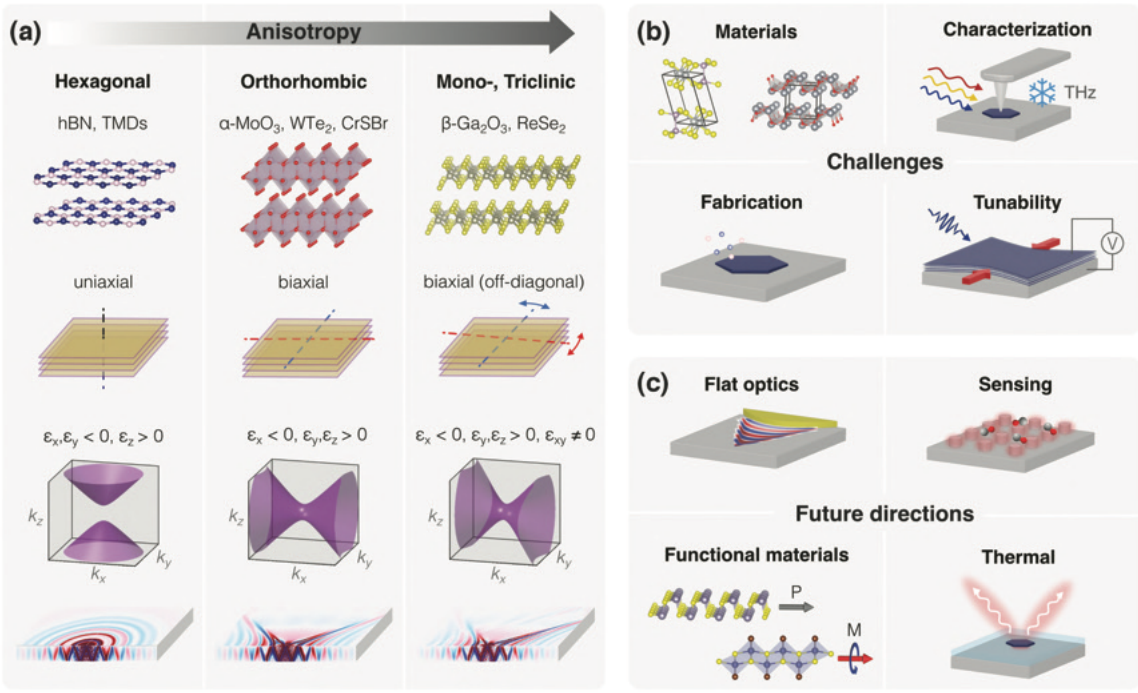


Figure 26. Role of crystalline anisotropy on polaritonic response and function. (a) Role of structural anisotropy in the optical properties of 2D vdW materials, including, from top to bottom, different crystal classes, optical axes leading to birefringence, hyperbolic isofrequency contours, and polariton propagation launched by a point dipole. (b,c) Challenges and future directions.

Metasurfaces and Emerging Materials

27. POLARITONIC METASURFACES / COUPLING 2D MATERIALS WITH PHOTONIC STRUCTURES

Andrea Alù[1,2,*]

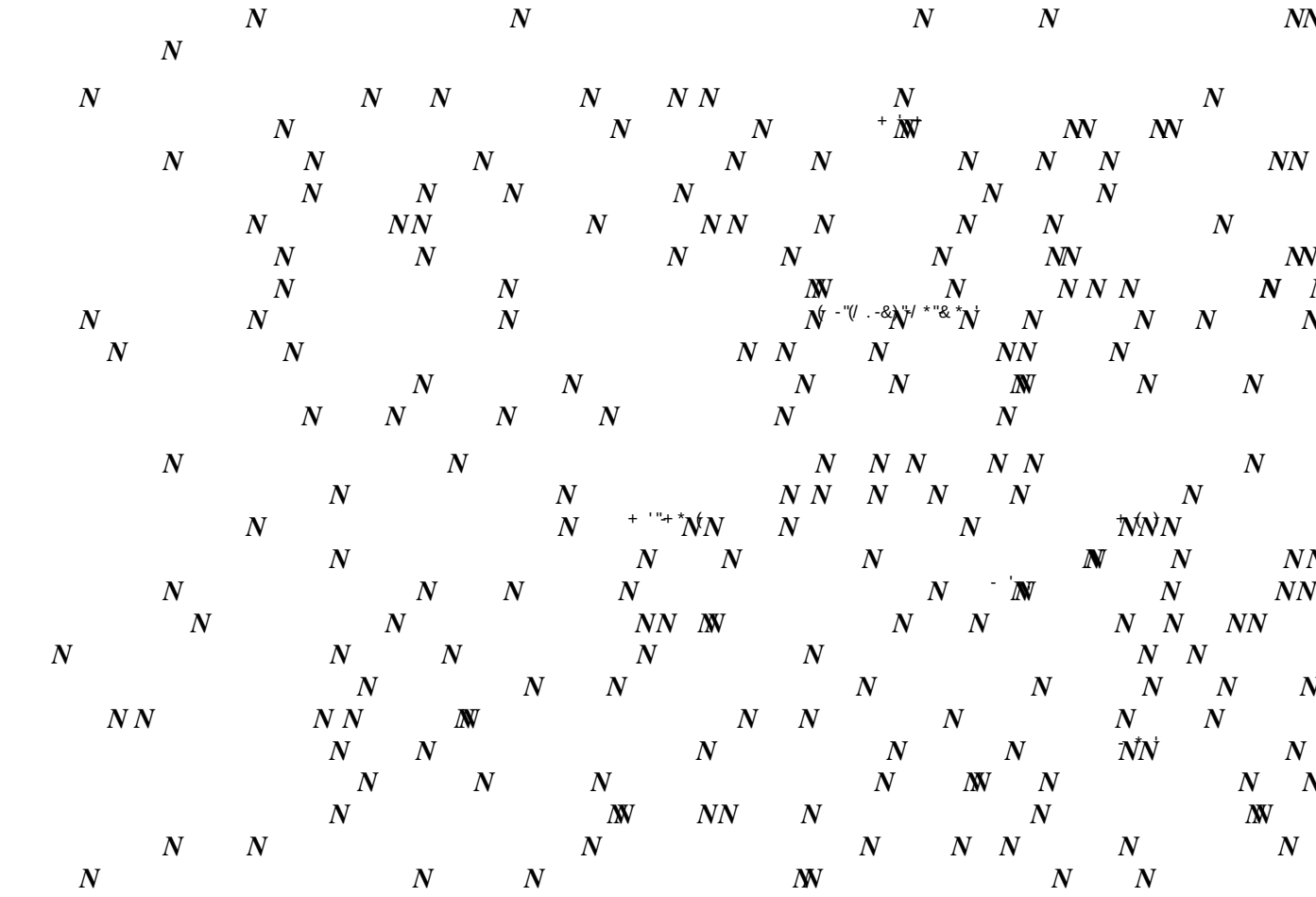
[1]Photonics Initiative, Advanced Science Research Center, City University of New York, New York, NY 10031, USA

[2]Physics Program, Graduate Center, City University of New York, New York, NY 10016, USA

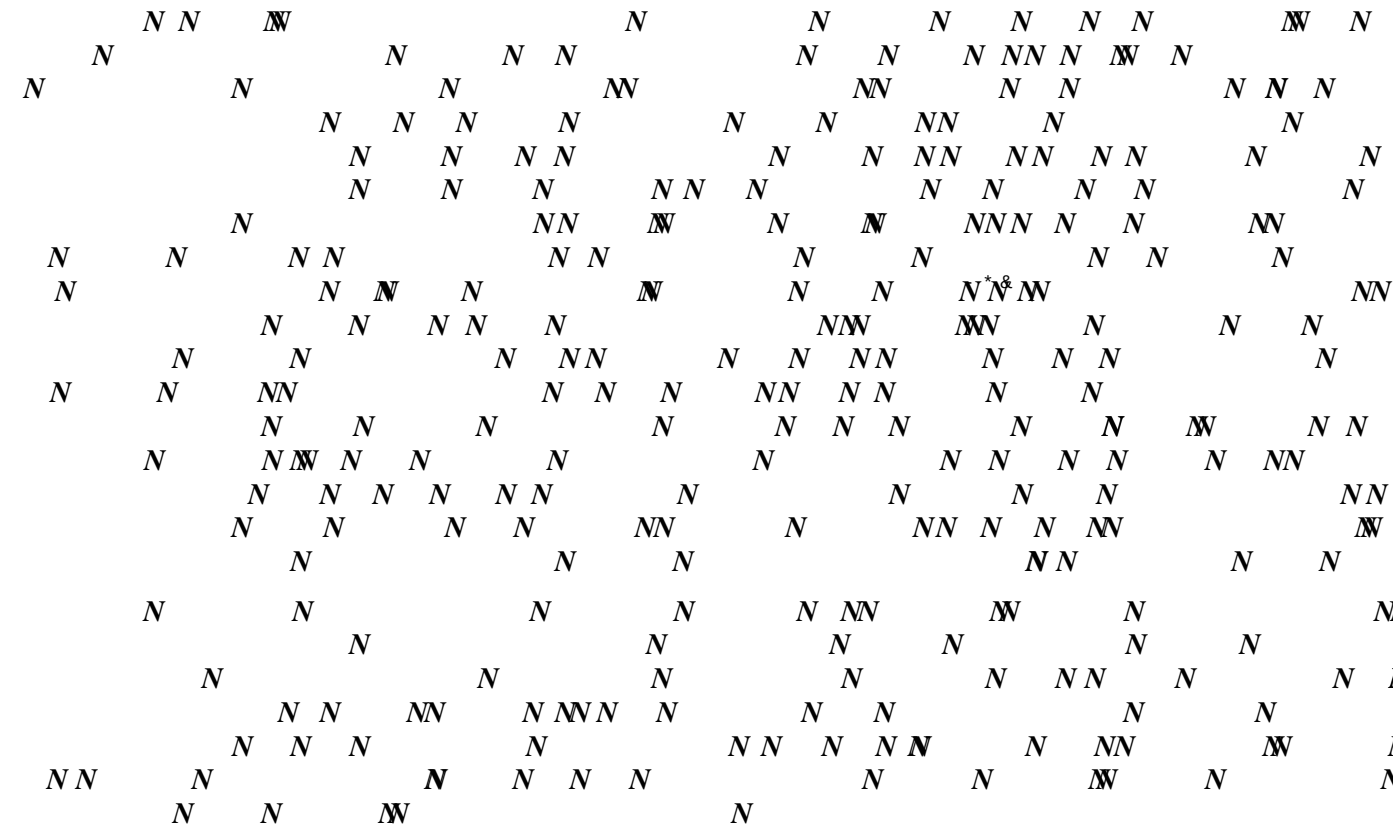
***Corresponding author.** Email: aalu@gc.cuny.edu

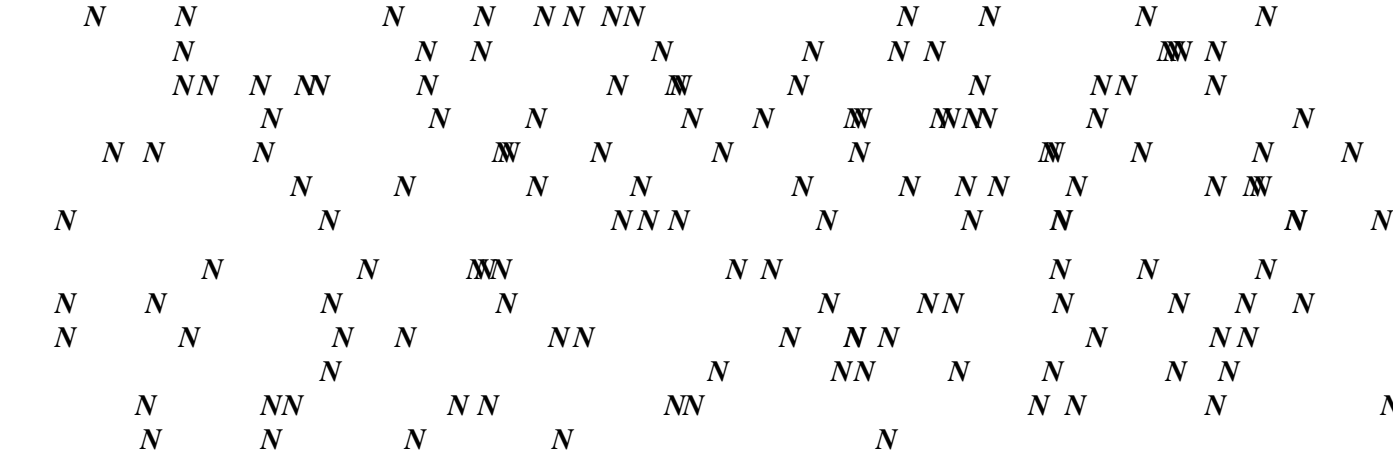
27.1 Current State of the Art

As discussed in other sections of this Roadmap, polaritons are quasiparticles that emerge from the strong coupling between light and material excitations. The ultrathin nature of 2D materials, combined with their strong material resonances, offers a plethora of opportunities in the context of polaritonic phenomena, stemming from excitons, phonons, magnons, plasmons and electronic transitions.[671] While a wide range of novel photonic phenomena have been explored in this context, broadly covered by the other sections of this Roadmap, recently it has been also realized that photonic engineering of polaritonic materials through nanostructuring offers a new playground for fundamental phenomena and applications. In addition, photonic engineering allows tailoring local density of states, field enhancement, quality factor, and modal engineering of the near-field light profiles that engage local material resonances, resulting in tailored polaritonic responses that are not accessible in the unstructured materials. In turn, polaritonic phenomena offer new opportunities to enhance the growing field of metasurfaces – ultrathin devices that exploit nanoscale engineered structures to tailor and control the optical wavefront in all its degrees of freedom. While conventional photonic metasurfaces are fundamentally limited in the way they interact with light due to the limited extent of light–matter interactions at the nanoscale in conventional materials, polaritonics offers a platform to overcome these limitations and realize metasurface responses that go beyond the conventional limits, in terms of field enhancement, nonlinearity, bandwidth, and other constraints dictated by passivity, linearity, and time invariance. Indeed, polaritonic metasurfaces have become in the past decade a blossoming field of

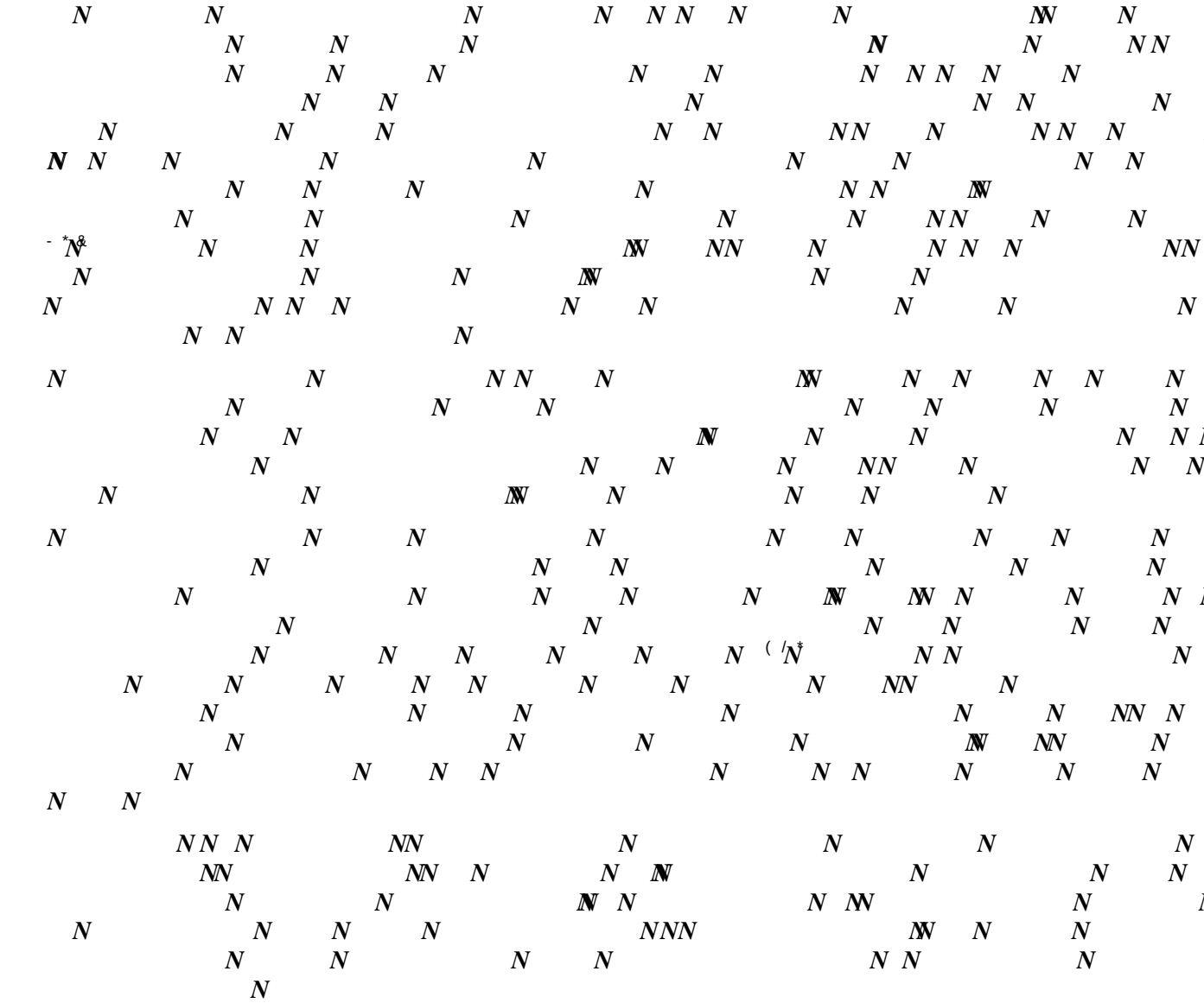


$) $ / c J j j 2eL ,HG1 3 1keJ jJ k, i





$) % B L G0Gíenke-HveHií D , k H D 9 e e H S c e k e 3 D J j k



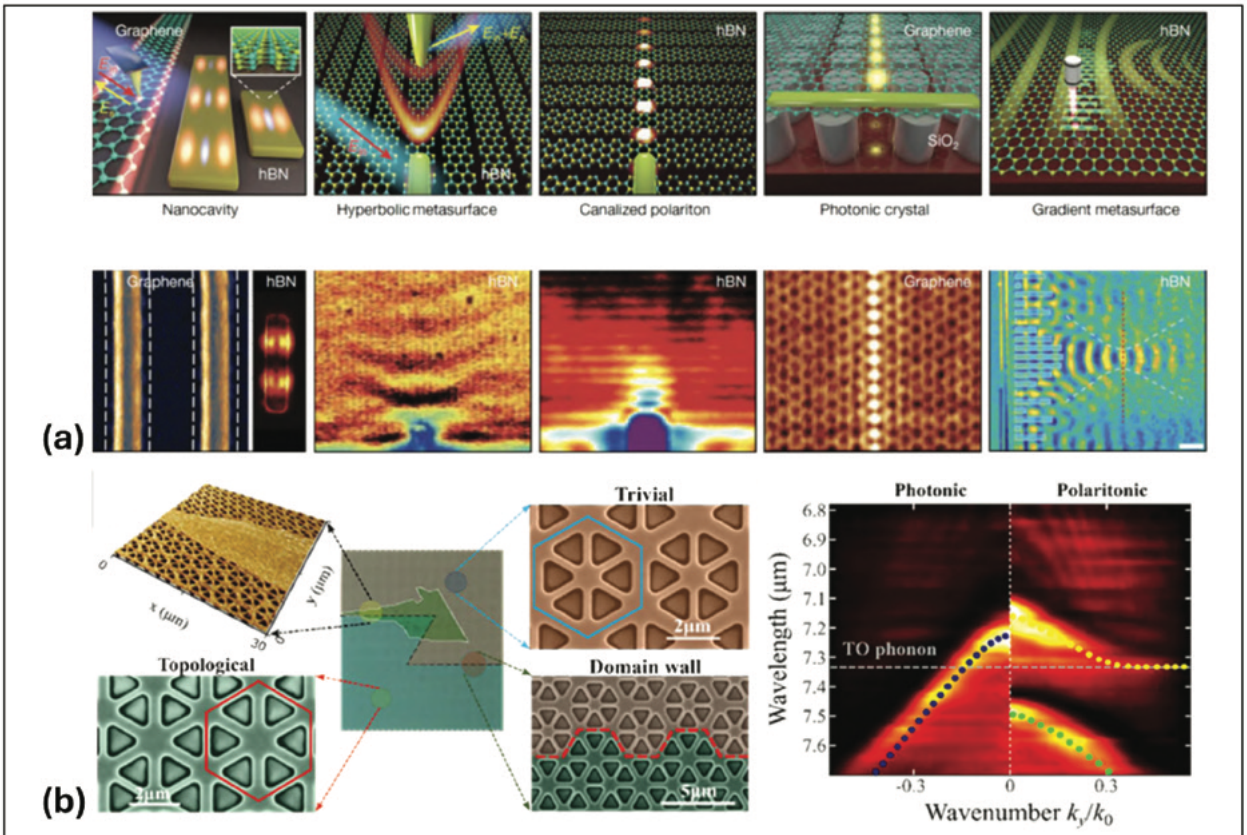


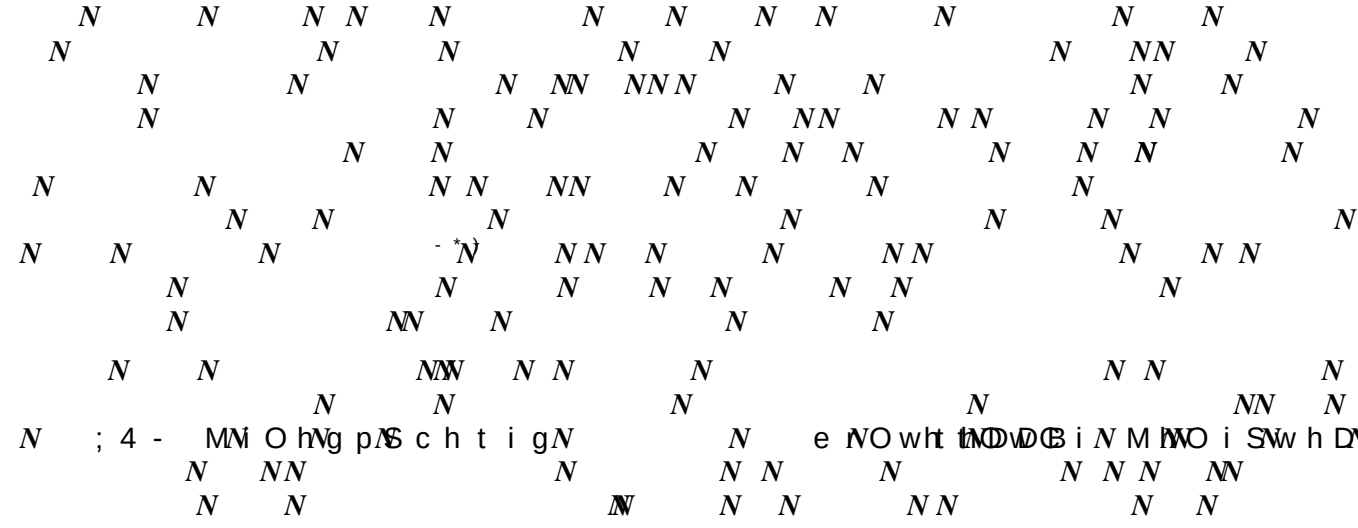
Figure 27. Polaritonic metasurfaces. (a) Polaritonic metasurfaces based on vdW interfaces to demonstrate a range of extreme polaritonic phenomena at the nanoscale. Adapted from ref 741 (Copyright 2021 Springer Nature). (b) Topological polaritonic metasurface obtained by loading a topological photonic crystal with a thin film of boron nitride. The right panel shows the effect of such loading: the topological edge state splits its dispersion within the bandgap of the photonic crystal due to the coupling with the phonon resonance of boron nitride. The topological phase is transferred to the polaritonic response. Adapted from ref 740 (Adapted from ref 6 (Copyright 2021 American Association for the Advancement of Science).

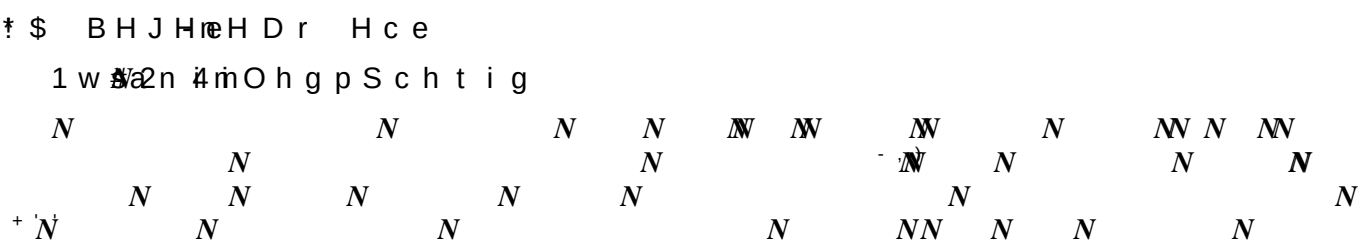
28. TRANSITION METAL DICHALCOGENIDES FOR PASSIVE AND ACTIVE METASURFACES

Deep Jariwala,[1] Timur Shegai,[2] Jorik van de Groep[3,*]
[1]Electrical and Systems Engineering, University of Pennsylvania, Philadelphia, Pennsylvania, USA
[2]Department of Physics, Chalmers University of Technology, Göteborg, Sweden
[3]Van der Waals-Zeeman Institute, Institute of Physics, University of Amsterdam, Amsterdam, The Netherlands
***Corresponding author.** Email: j.vandegroep@uva.nl

28.1 Introduction

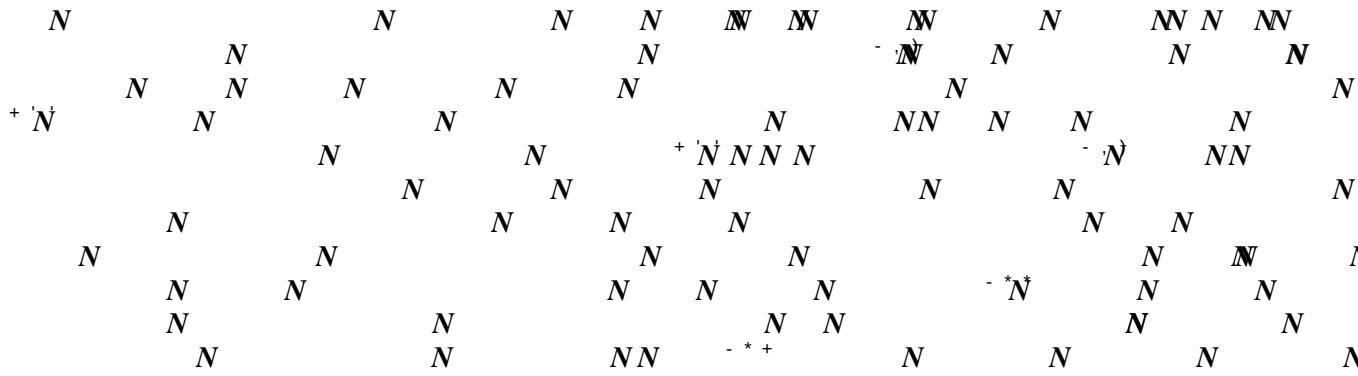
Metasurfaces employ resonant light scattering in compact arrays of nanoscale structures to perform a collective optical function. Accurate control over the local scattering amplitude and phase enables (near-)arbitrary wavefront shaping. While initial metasurfaces employed plasmon resonances in metal nanoparticles, subsequent designs quickly moved to Mie-like resonances in dielectric and semiconductor nanostructures to mitigate the optical losses associated with the metallic light–matter interaction. Leveraging more advanced design concepts including propagation phase and geometric (Pancharatnam–Berry) phase, state-of-the-art metasurfaces now enable high-numerical aperture lensing, multi-color holography, beam steering, and even multifunctional flat optical elements. For dielectric metasurfaces, a high refractive index of the photonic material is of crucial relevance as it controls the scattering cross section and nanoscale confinement of light. As such, titanium dioxide (TiO_2, refractive index $n\sim2.6$) and silicon (Si, $n\sim3.5$) are common photonic materials for metasurfaces.



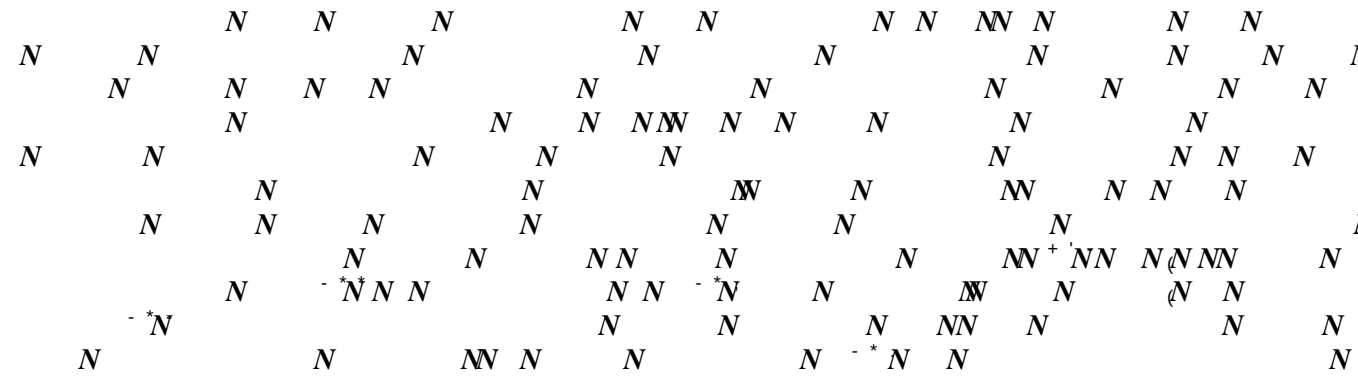


$! $ BHJ-eH D r Hce

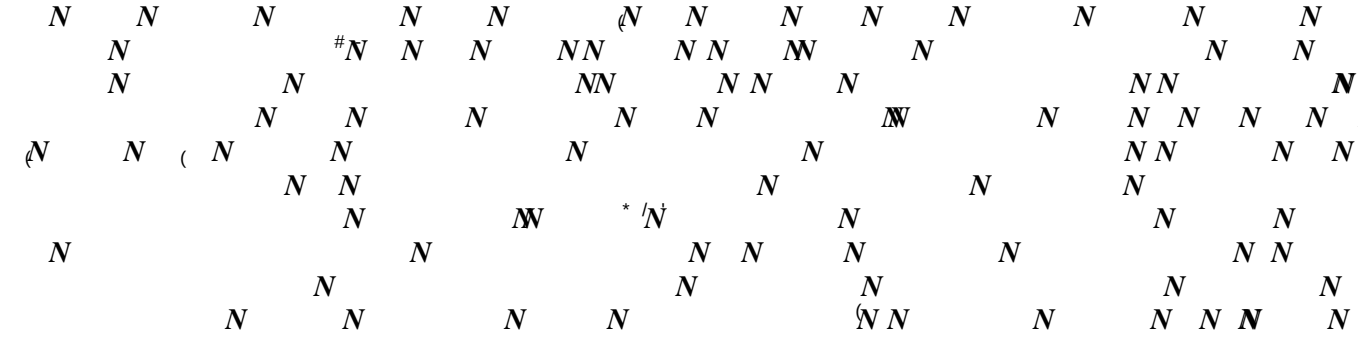
1 w 2n 4mOhgpSchtig

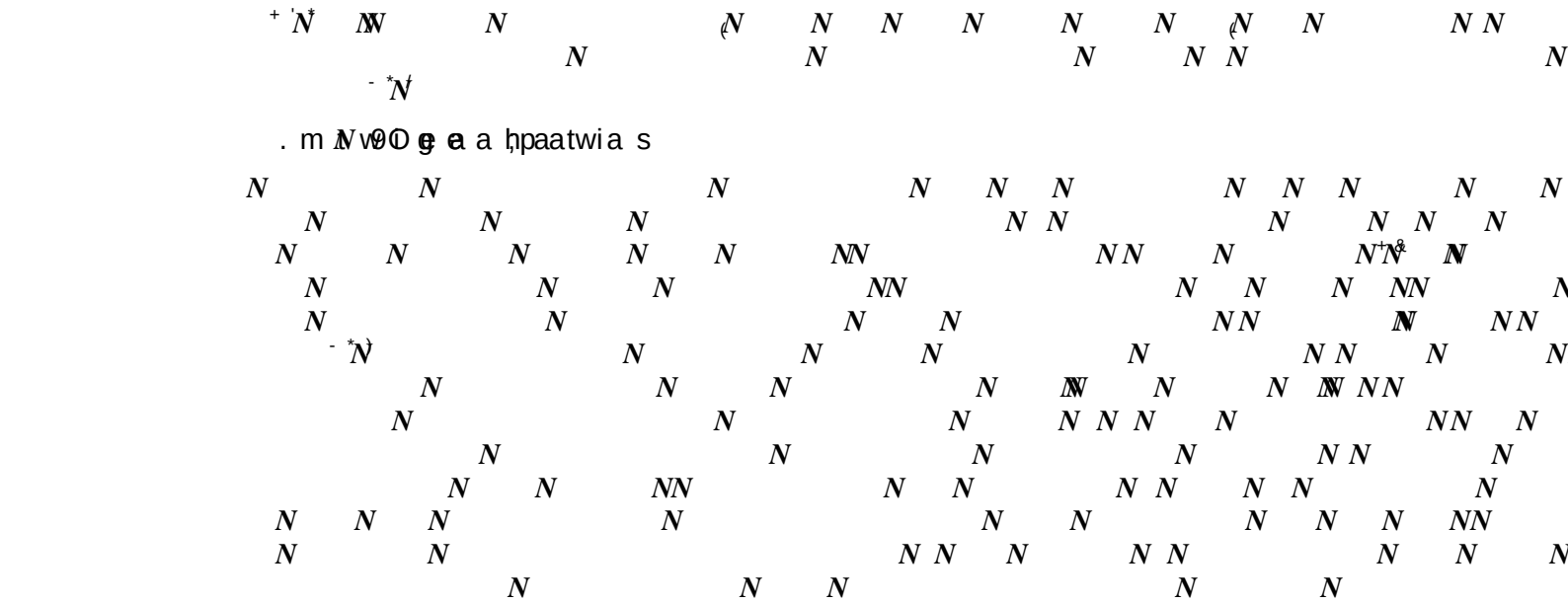


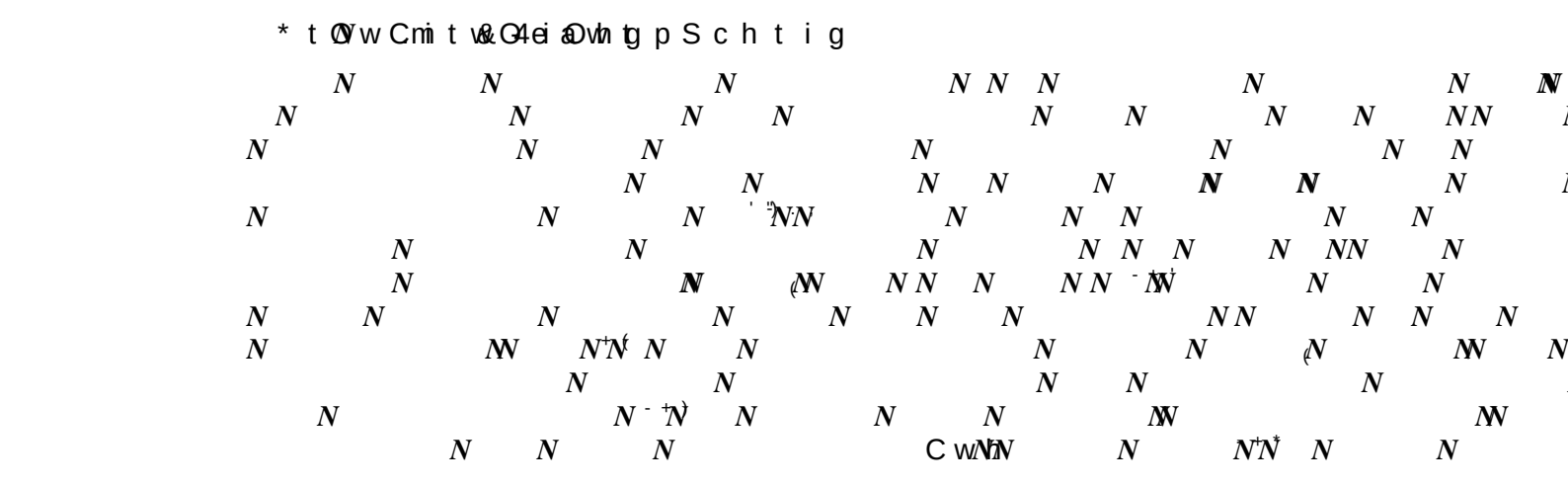
. m wOeZDahwStwOBawStwnwdhOwea

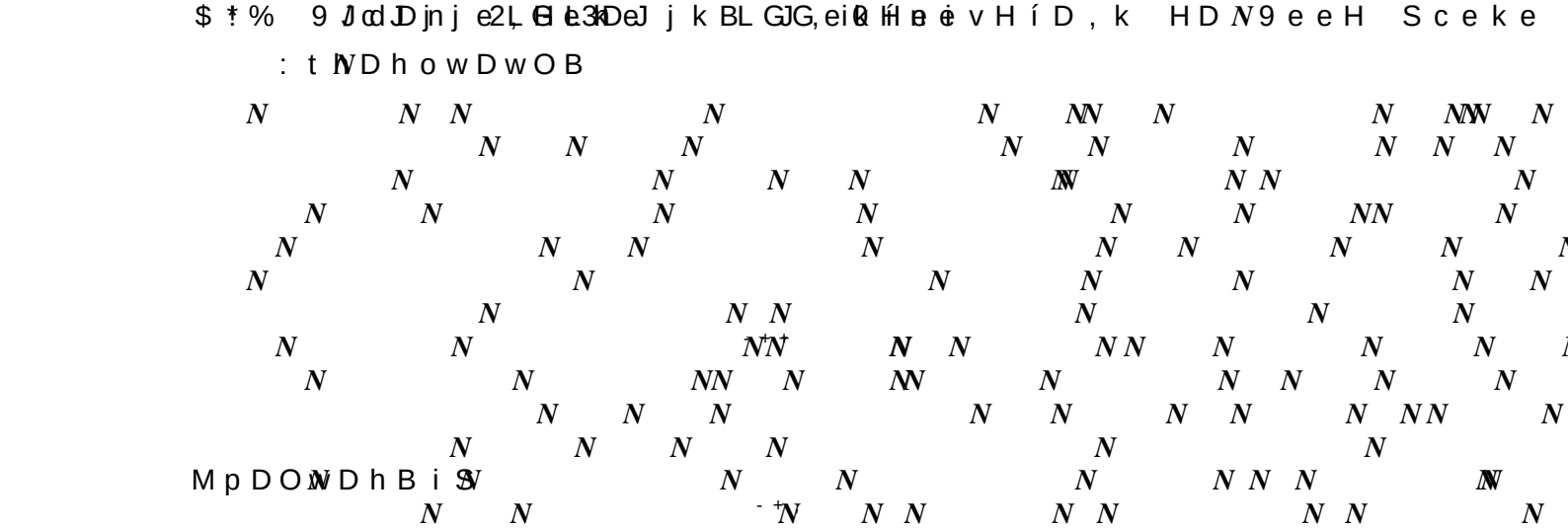


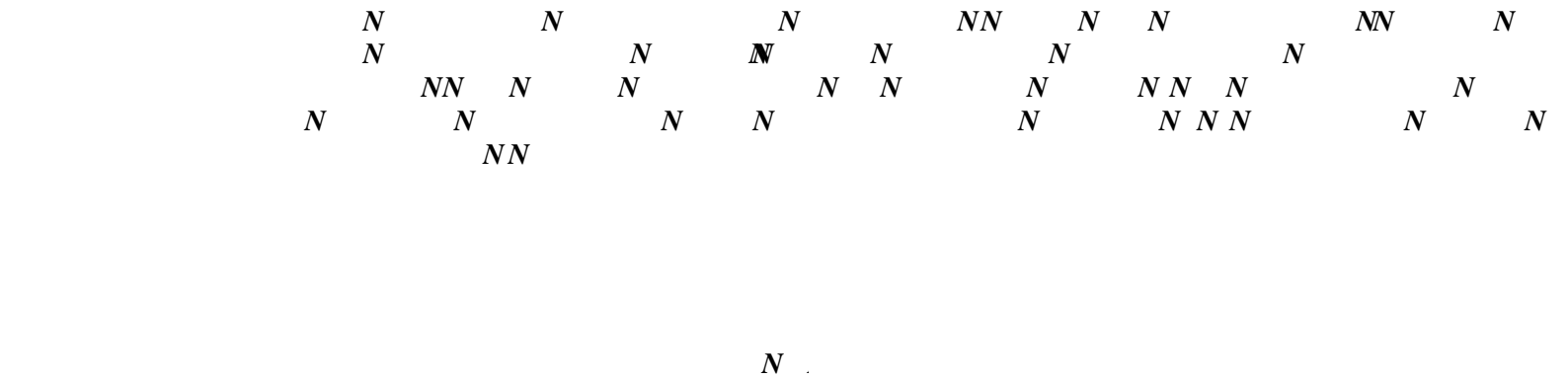
6 r OwVeaDwaihSwOB



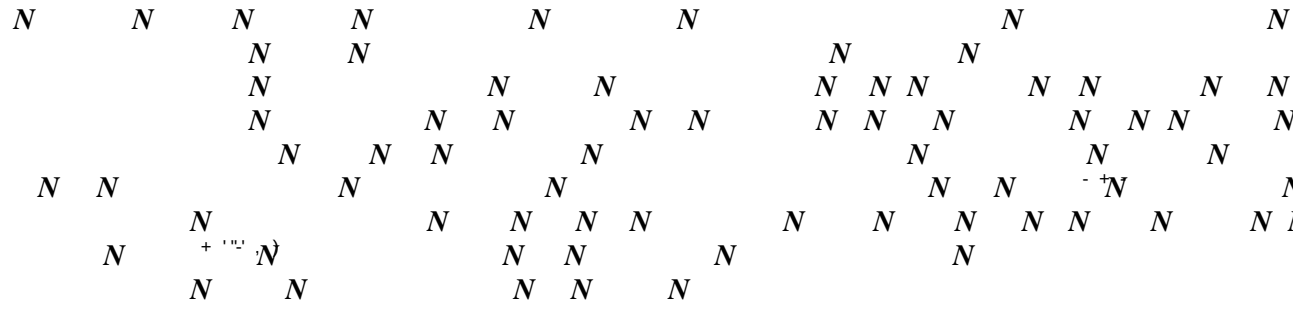




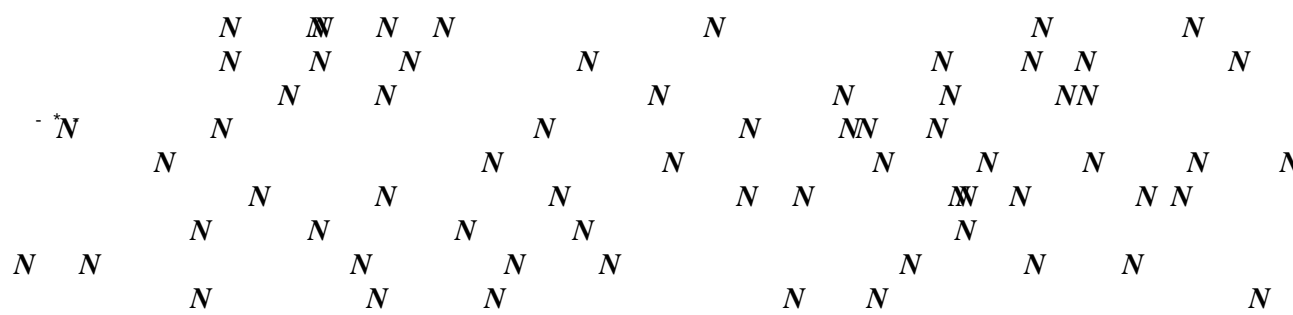




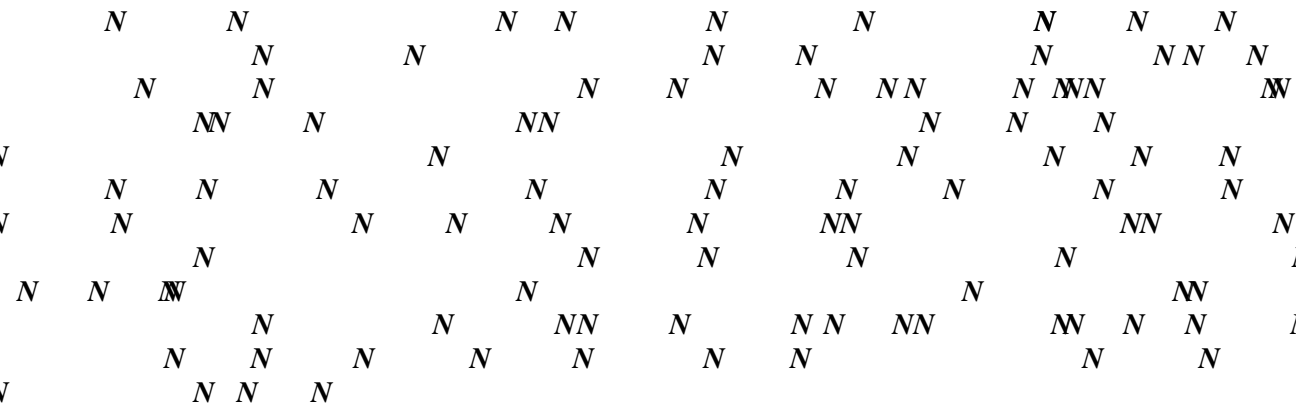
: p#Dh a n s Sh a t e r e O e a w t g



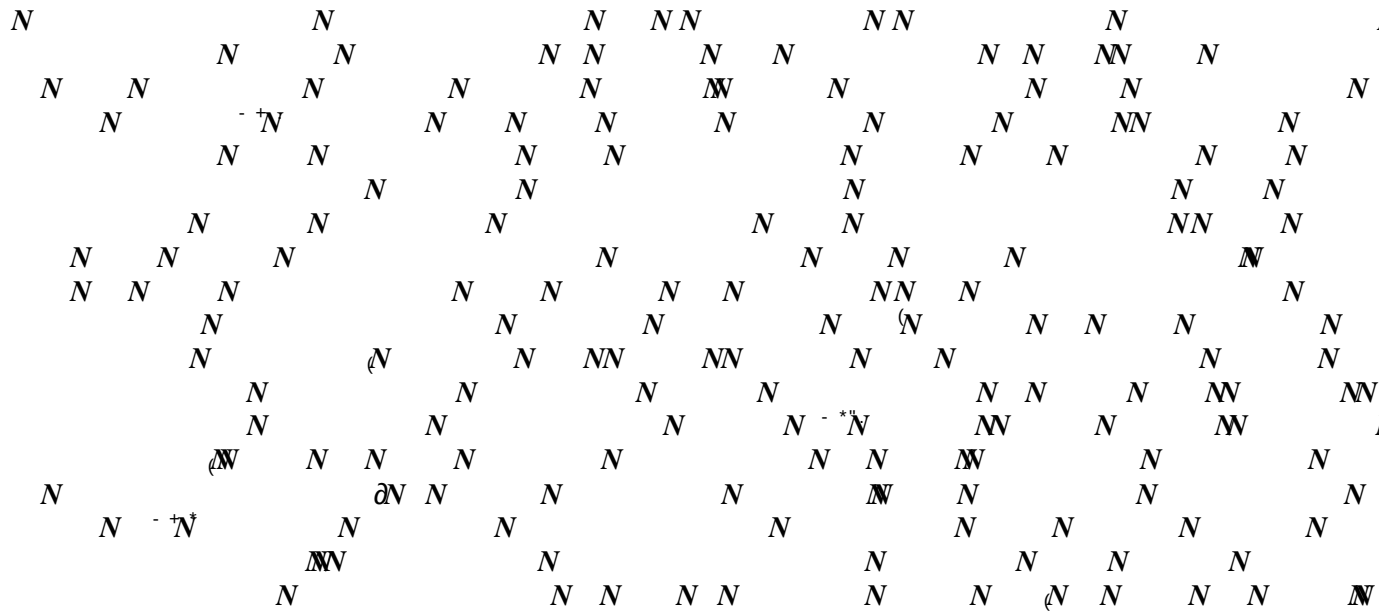
: i DV i .tOOtw Cwi4apsD OwaD h B i *SO e;M4w-tghhDSDeBSSi g

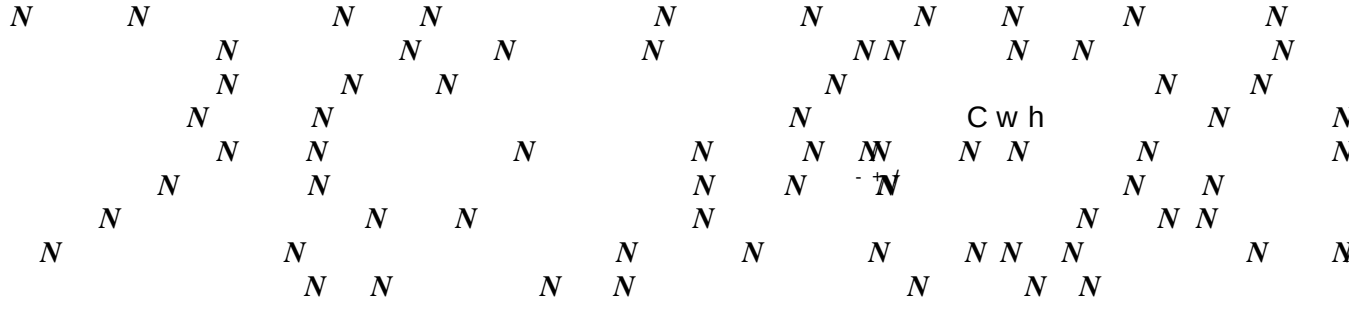


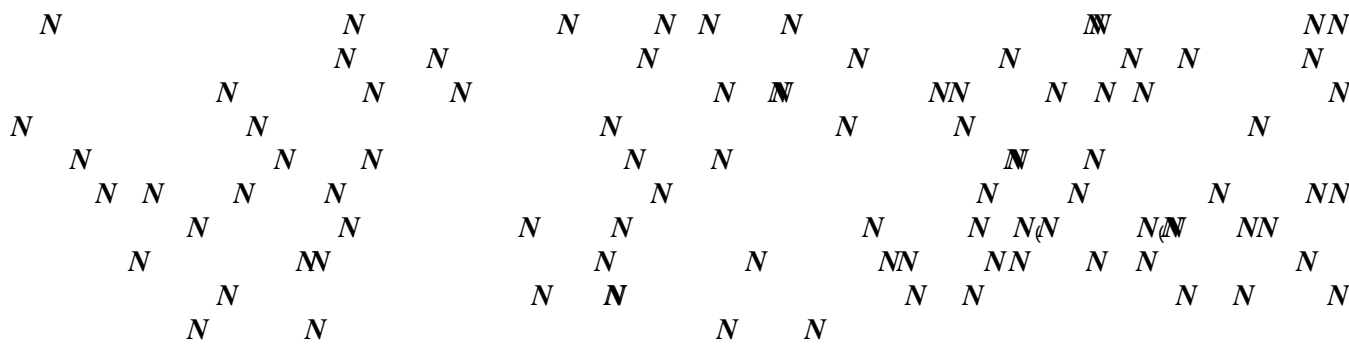
. c aVw t w *i taOtwCi4igO&a-g p S c h t i g

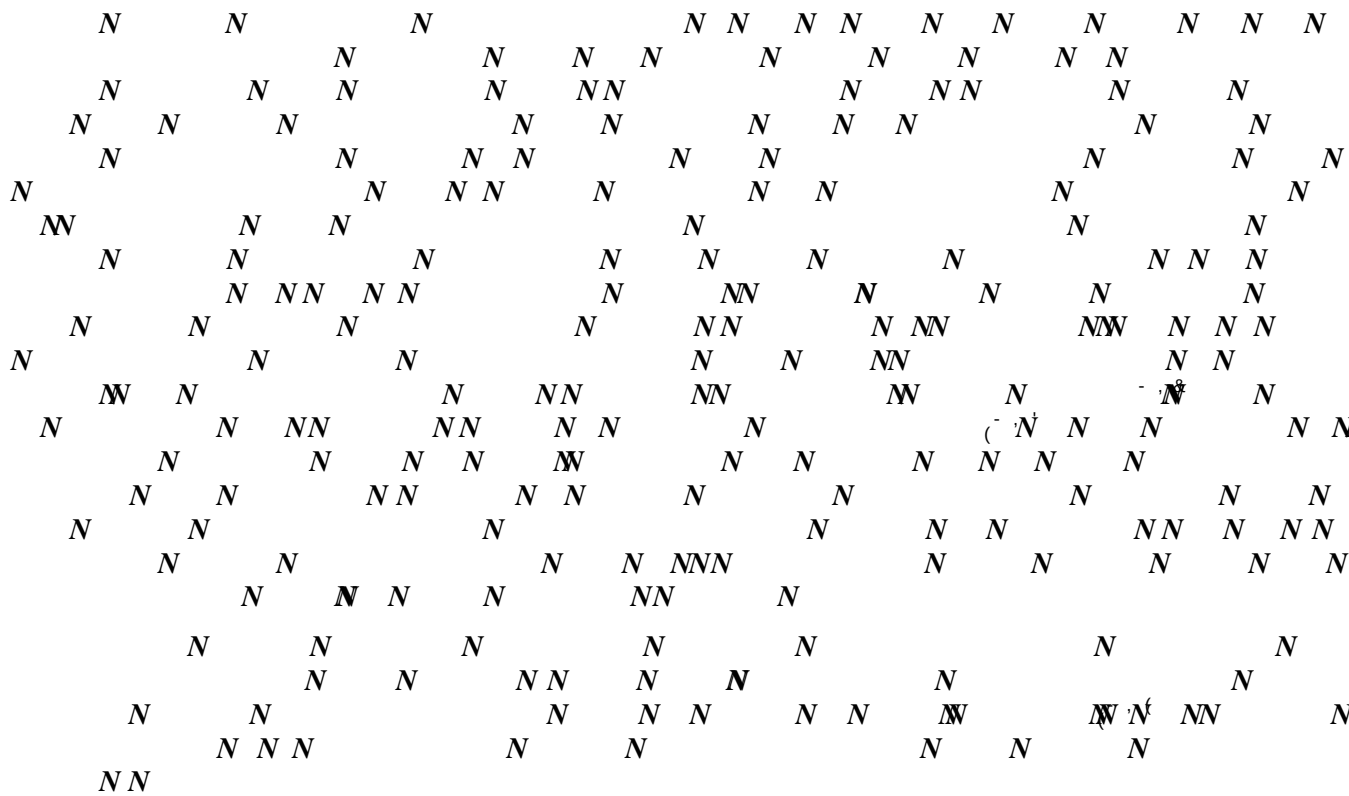


; p aVh o w;Dw0Bh iBSi cSg









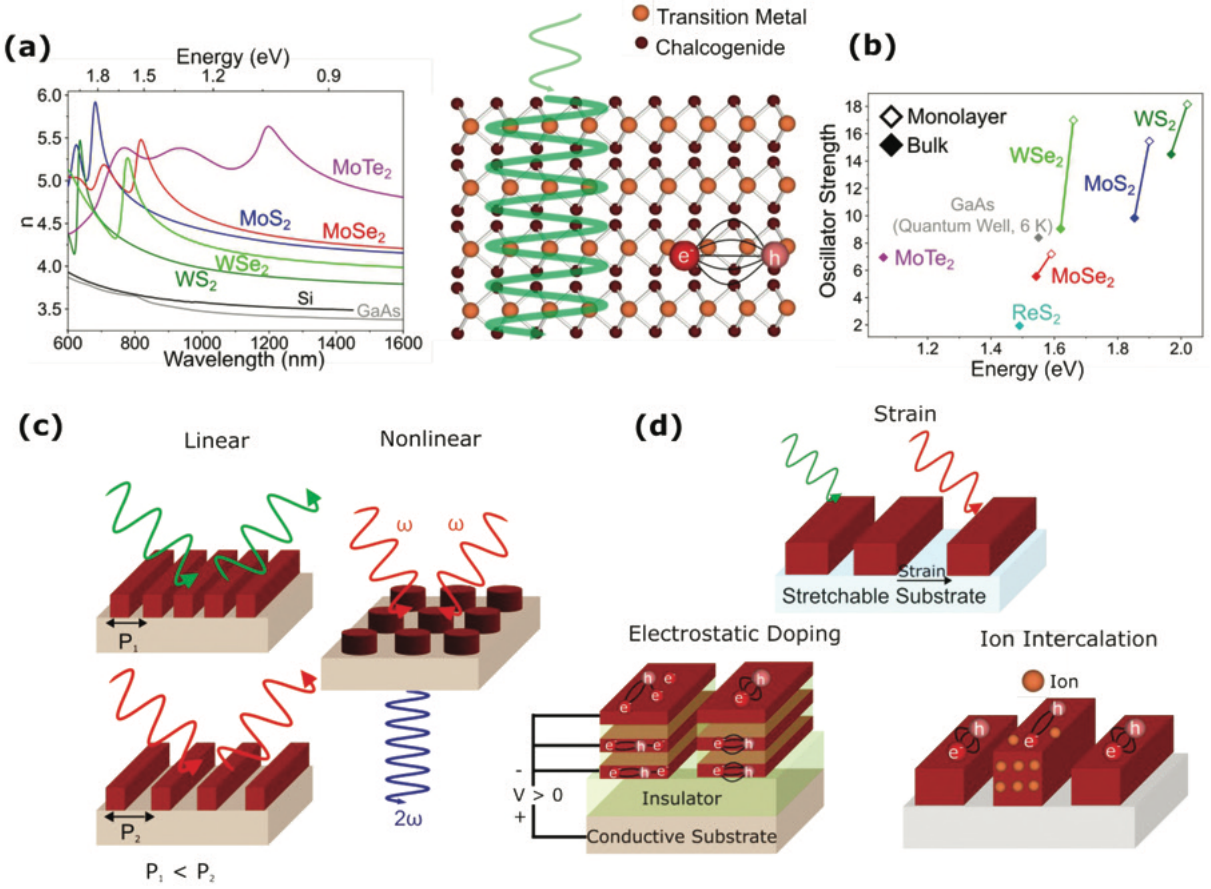


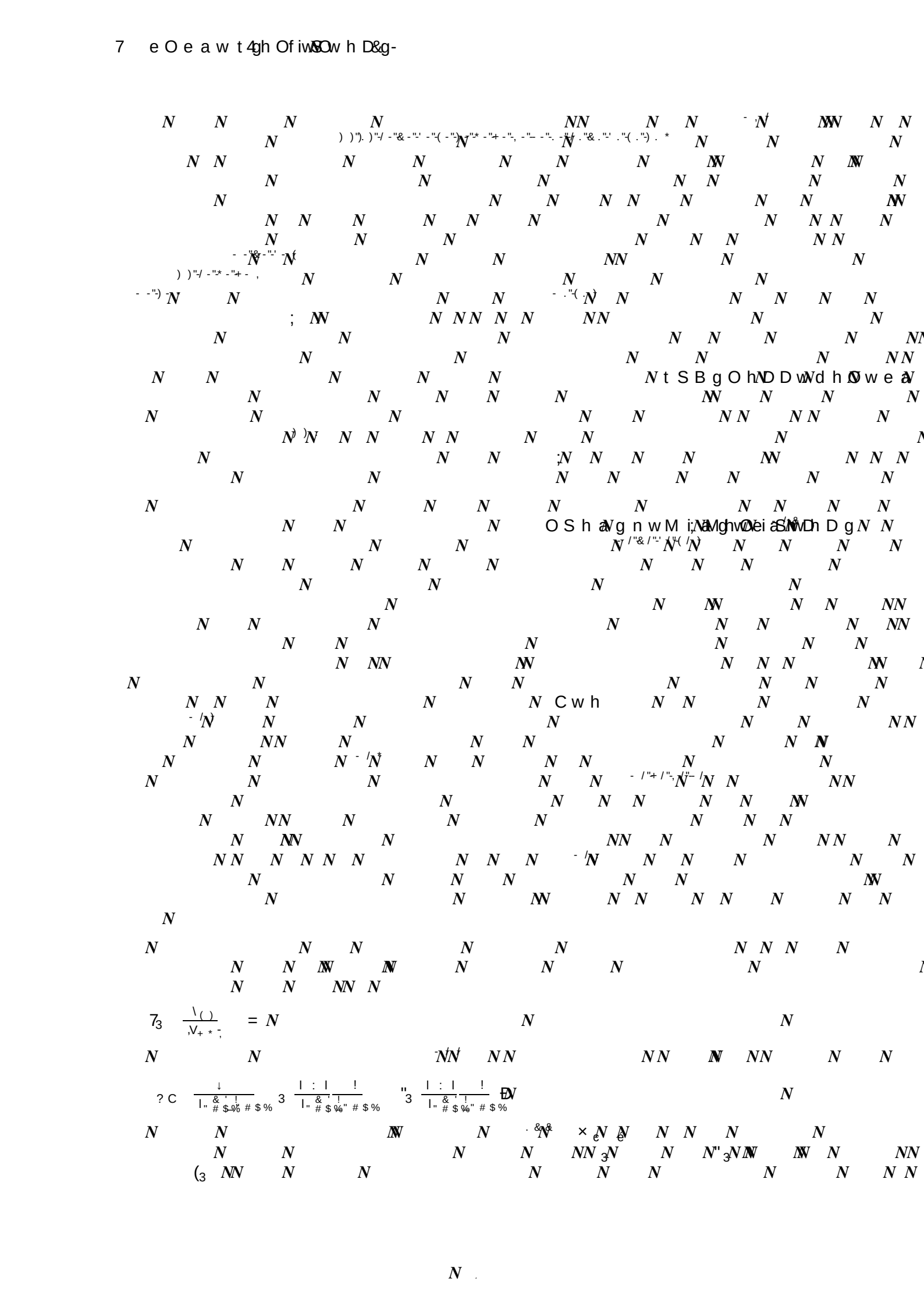
Figure 28. Comparison of TMD optical constants and schematic illustrations of TMD-based metasurfaces. (a) Comparison of the spectrally varying real parts of the refractive indices for the principal semiconducting TMDs in multilayer form together with Si and GaAs.[763,764,765] (b) Comparison of exciton oscillator strengths versus resonance energies of various monolayer and multilayer TMDs as measured at room temperature[517,744,745,766,767] A comparison of GaAs quantum wells at a temperature of 6 K is also provided.[768] (c) Schematic approaches to passive metasurfaces using bulk (multilayer) TMD active layers. Both linear and nonlinear approaches are depicted and discussed. (d) Schematic of approaches to active TMD-based metasurfaces through external parameters.

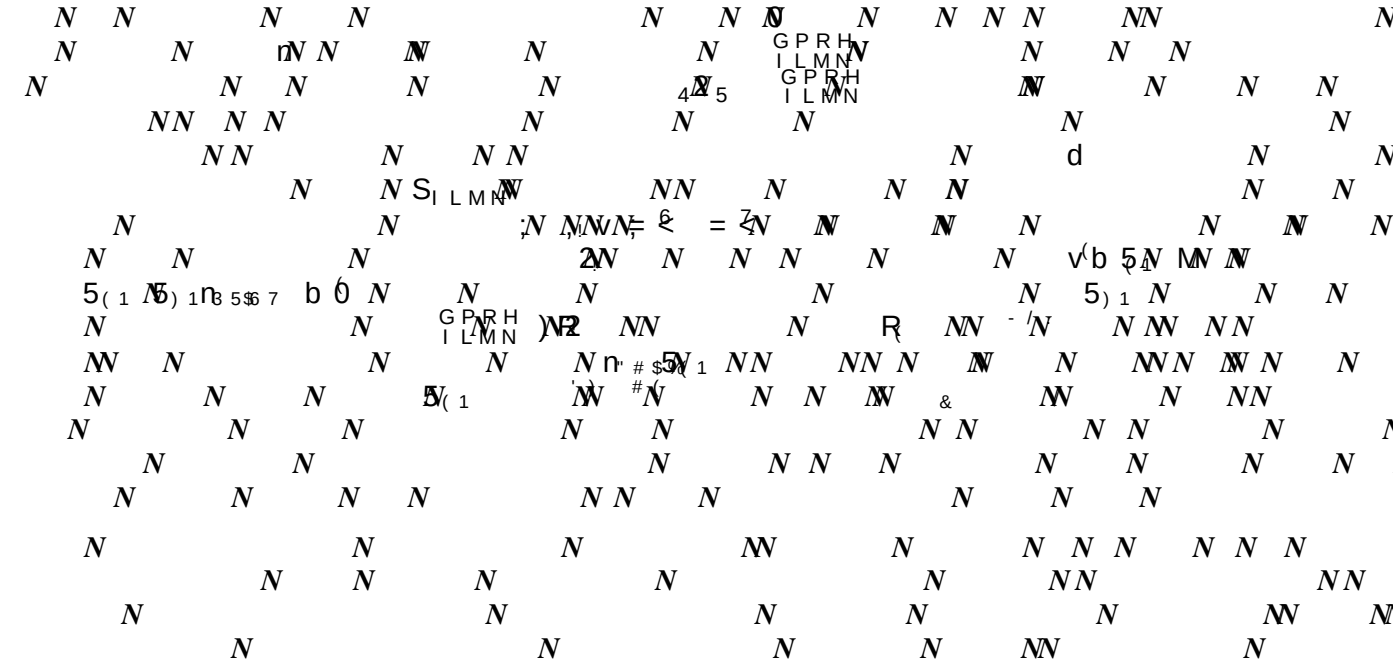
29. TRANSDIMENSIONAL MATERIALS AS A NEW PLATFORM FOR STRONGLY CORRELATED SYSTEMS

Alexandra Boltasseva,[1,2] Igor V. Bondarev,[3] and Vladimir M. Shalaev[1,*]
[1]Elmore Family School of Electrical and Computer Engineering, Purdue Quantum Science and Engineering Institute, and Birck Nanotechnology Center, West Lafayette, IN 47907, USA
[2]School of Materials Engineering, Purdue University, West Lafayette, IN 47907, USA
[3]Department of Mathematics & Physics, North Carolina Central University, Durham, NC 27707, USA
***Corresponding author.** Email: shalaev@purdue.edu

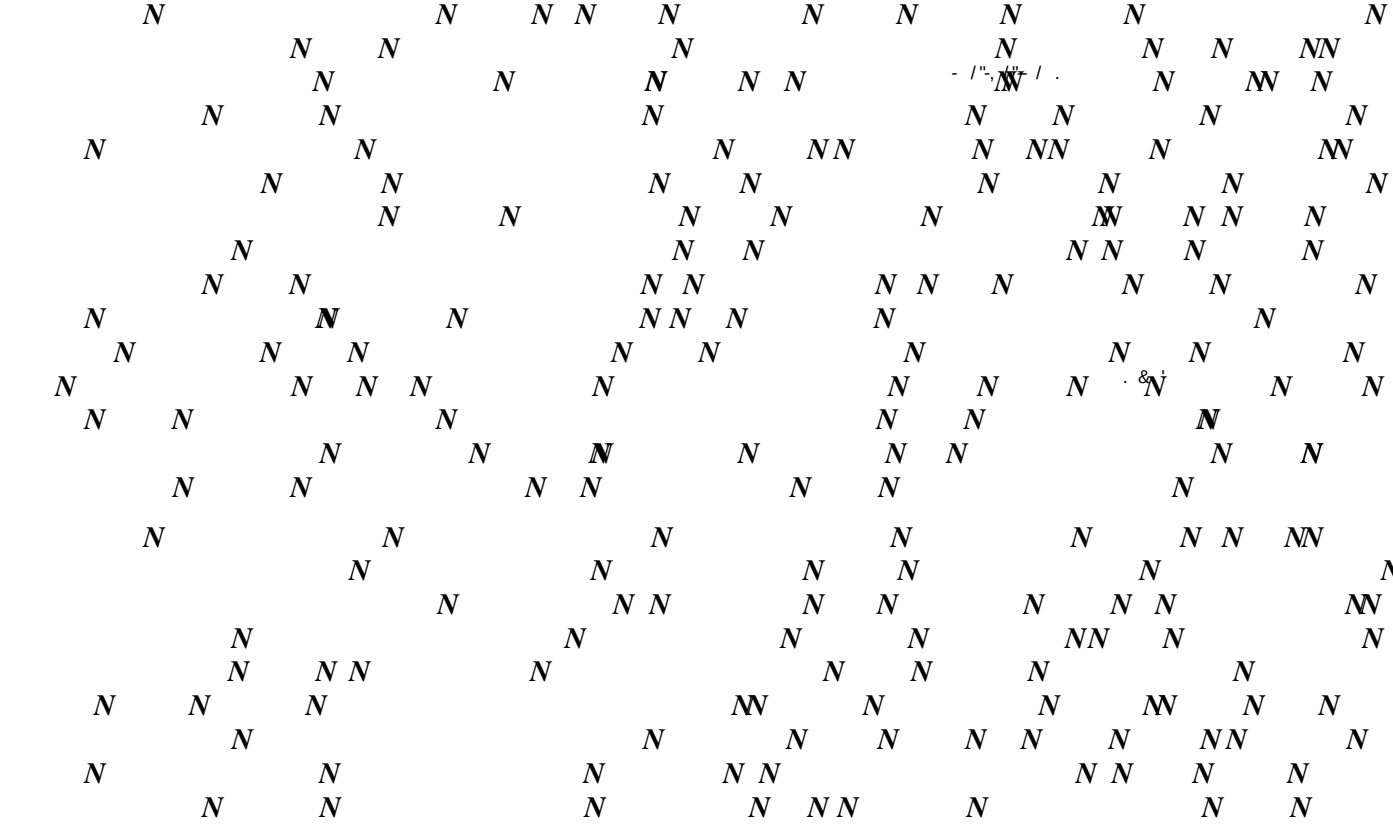
29.1 Status

Systems with strong electron–electron correlations, where the interactions between electrons are strong enough to dramatically influence their behavior, have long been in the focus of extensive studies across solid state physics, materials, and quantum science due to the unique properties that they enable. These include high-temperature superconductivity, unconventional magnetism, and several varieties of metal–insulator–transitions (MITs) related to remarkable physical phenomena, such as quantum- and disorder-related Anderson electron localization, Kondo effect, Wigner crystallization, and beyond.[338,339,769,770,771,772,773,774,775,776,777,778,779,780,781,782,783,784] These effects have been studied in strongly correlated materials, including insulators and metals, for electrons as well as for excitons and their complexes,[785,786,787,788,789] particularly in the low-dimensional regime in systems like semiconductor quantum wells, graphene, and TMDs.

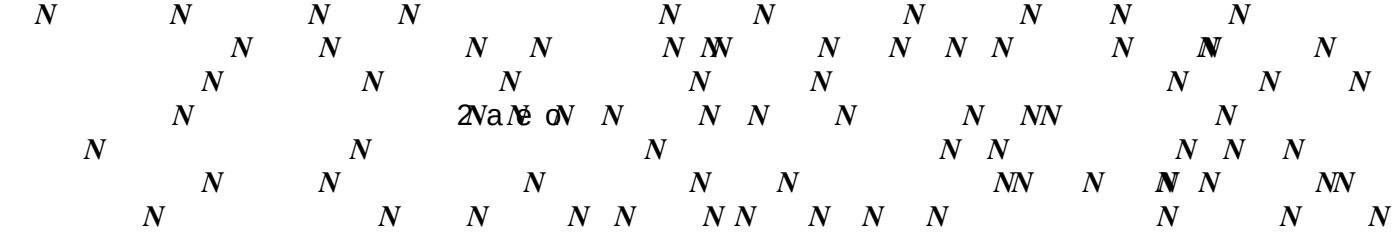




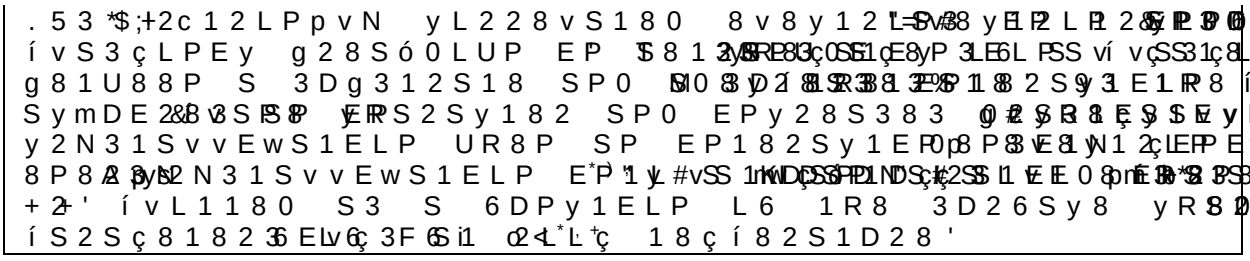
$ + $ / c J j j 2eL ,HG1 3DkeJ jJk, i

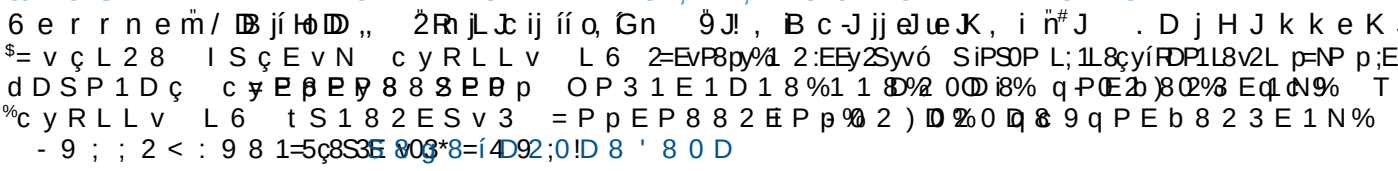


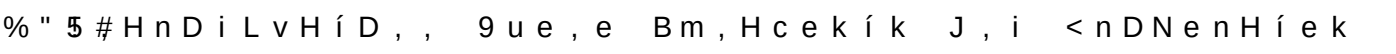
$ + % B L G0Gíenke-HveHi í D , k H D 9 e e H S c e k e 3 D J j k

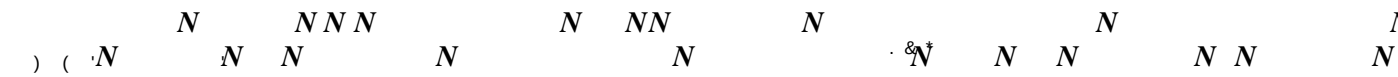



(a)
Superstrate
Film
Substrate
With the film thickness (d) decreasing:
• Interaction between charges increases drastically
• The potential acquires an in-plane character
• Leads to electron confinement
(b)
Strongly correlated electronic systems
(c)
2 nm HfN film room-T exp. data:
PF Ratio = 10.9 >> 1
2.5 nm HfN film room-T exp. data:
PF Ratio = 0.7 < 1
10 nm HfN film room-T exp. data:
PF Ratio = 0.02 << 1

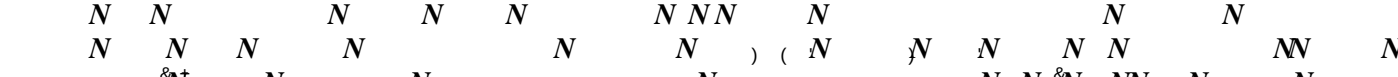


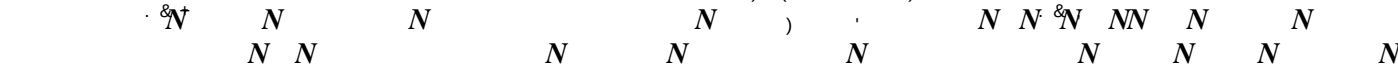




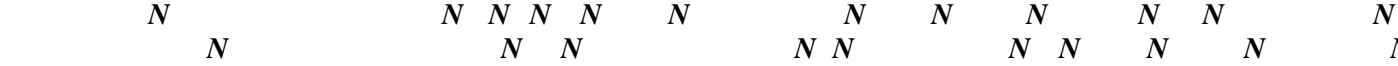


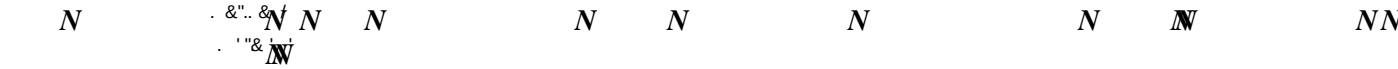


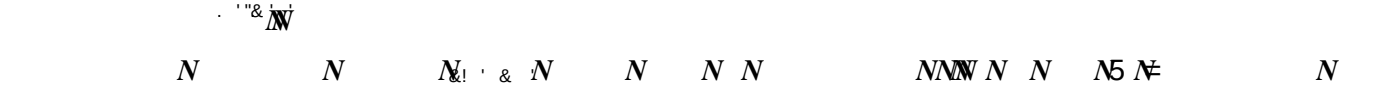


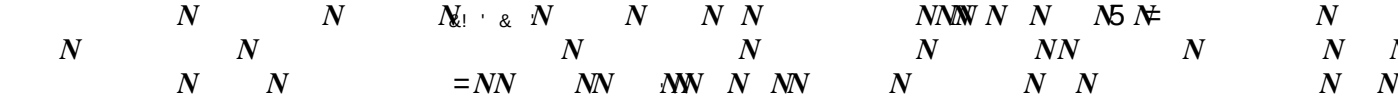


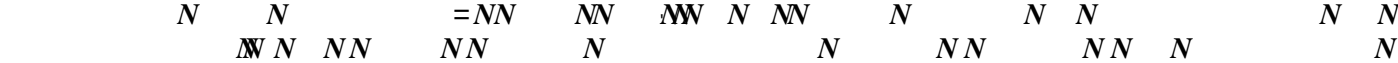


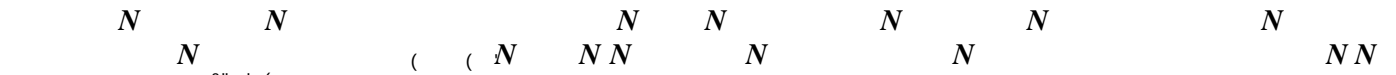


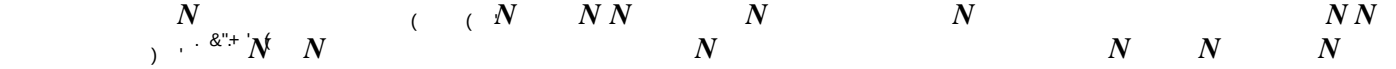




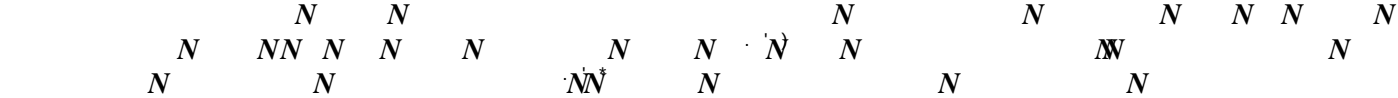


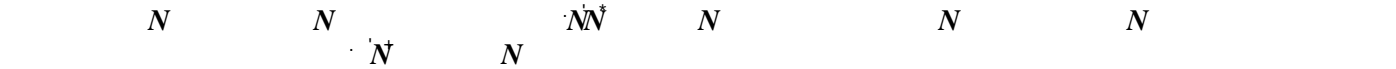




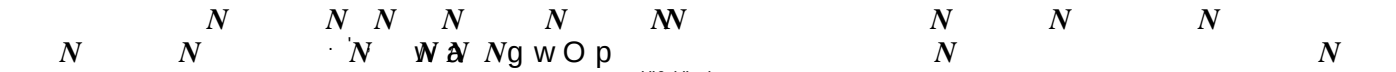






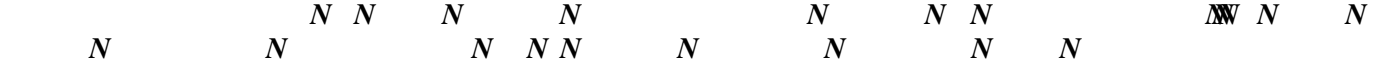


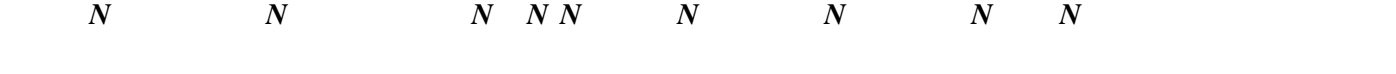










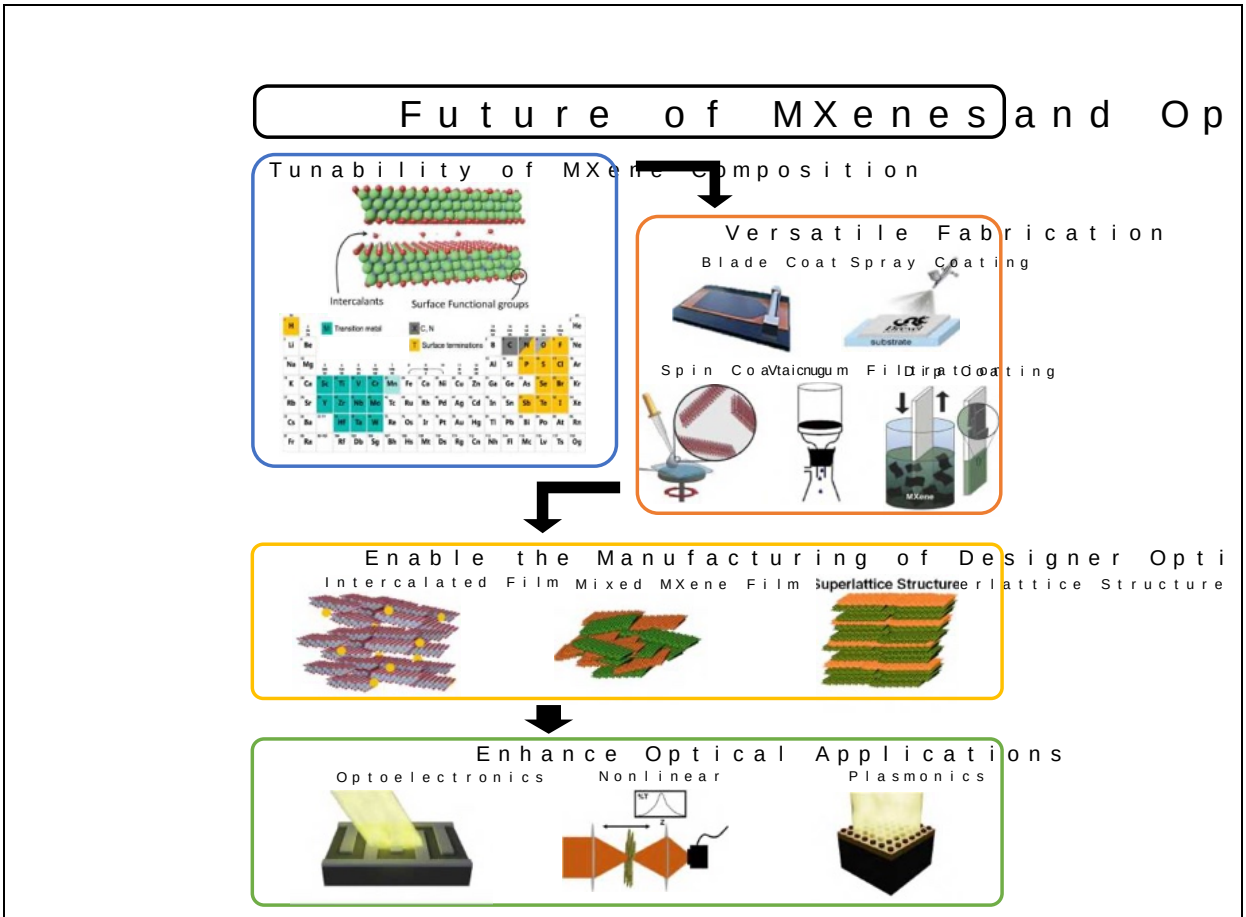




% " I $ J j j e , G e k J , i 3 D J j k

% " ! % N j í v J H í D , k - a D L , i

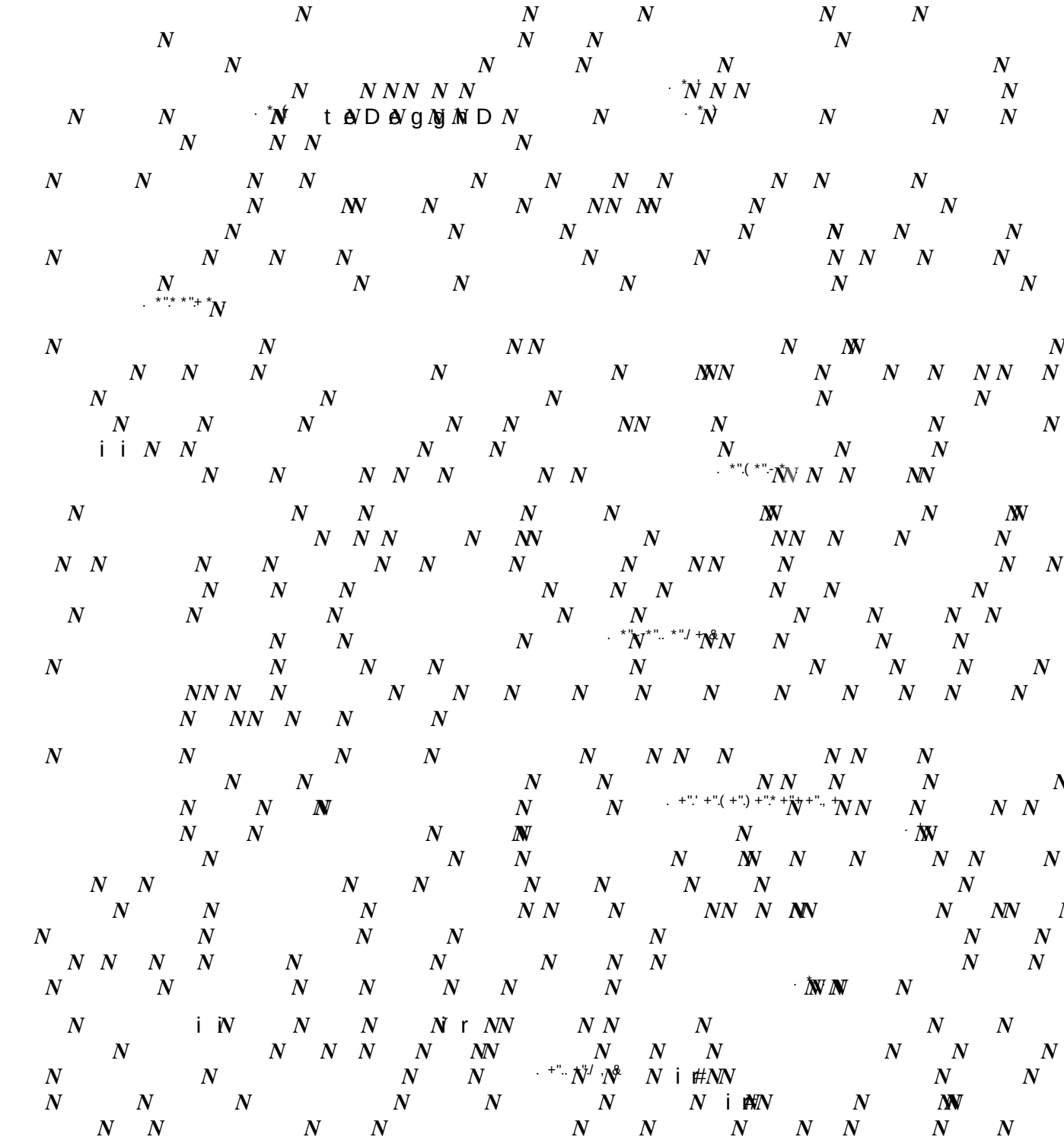
% " ¦ & H j D D b


Future of MXenes and Op
Tunability of MXene Composition
Intercalants
Surface Functional groups
Versatile Fabrication
Blade Coat
Spray Coating
Substrate
Spin Coating
Vacuum Filtration
Dip Coating
MXene
Enable the Manufacturing of Designer Opti
Intercalated Film
Mixed MXene Film
Superlattice Structure
Enhance Optical Applications
Optoelectronics
Nonlinear
Plasmonics

&$5 ; I 2 8 2 0 I 1 ; : 4 2 : 2 1 . I 6 ; : /D 6 : 2 8 . . I 6 0 NT 2O
1 ; 9 6 : . I 2 . 6 : / 8 . 0 7 < 5 ; . < 5 ; 1 N .

3 L J , G t c e 0 í B D e ; D K b d Í ¦ G í S G J , C J J , , i G 4 n K D d e < e H e b
$F 8 6 8 E i S 1 E L P S v e 8 3 8 S 2 y R 1 ; R 8 8 P 1 t 8 E 2 y 2 6 L L 3 2 y S v R 8 N % E B y 8 S y 8 ; d s y 2 E g 8 8 P 2 y 3 8 1 3
q P E b 8 2 3 E 1 N L 6 c y E 8 P y 8 S P P 0 R D 6 E 8 y + R P) L) v + L / % N ; I R 6 E P ; S R E P S % F 8 6 8 E
%; 8 P 1 2 8 6 L 2 9 0 b S P y 8 0 s S 3 E B y 2 3 % o 8 * y) R P) E) m D a 8 S 3 p % 2 8 O g P % 3 1 ; E 2 1 L D S 1 1 8 E S L 6
&< 8 í S 2 1 ç 8 P 1 L 6 R N 3 E y 3 S E P b 0 8 % 9 3 q 1 P 2 E L b P 8 L 2 ç 3 N E 1 S N P 0 L 6 1 R 8 E P 1 6 1 6 3 g O D P 2 E p 1 R E
* . + /) % q c 9
- 9 ; ; 2 < : 9 8 1 = 5 ç 8 S 3 E 8 0 3 * 8 = 6 4 8 9 í ; E ! 1 1 ' 8 0 D

%# # 5 , H n D i L v H í D ,



% # $ A e k L j H k

31.3 Conclusion

The immediate significance of the reported hot electron generation in BP is that it explains its *colossal* photoresponsivity in the UV region.[843] This was attributed by Castro Neto and coworkers to a band nesting in the Γ-Z direction, a common feature in multilayer 2D materials. One would expect that such band nesting results in a high joint density of states for resonant optical transitions.[842,843,849] While this is a reasonable interpretation, our mPP spectra of BP show no evidence of interband transitions between nested bands. Instead, we argue for an alternative mechanism that can increase the density of states and dielectric field strengths of 2D materials. BP, like many other anisotropic 2D materials, has a dielectric function that is hyperbolic in different spectral regions.[870] In a 2D material, the hyperbolicity can be tuned by impurity or photodoping.[852] The ultrafast electronic excitation of BP dynamically performs such photodoping on a few femtosecond timescale. The hyperbolic dielectric functions introduce a large joint density of states for photon absorption and scattering, and can cause giant field enhancements in regions where the real part of the dielectric functions is near zero.[850] The hyperbolic dielectric properties are likely to be intrinsic to all 2D materials because of their anisotropic electronic structures giving them a metallic optical response in one direction with respect to the crystal plane, and semiconducting one in an orthogonal direction. In BP, and related materials with in-plane dielectric anisotropy we even anticipate quasi-1D excitonic, electronic, transport, and optic properties. These features are evident in the electronic[851,852,871,872] and THz[873,728] properties of BP as hyperbolic exciton polaritons and tunable plasmons.

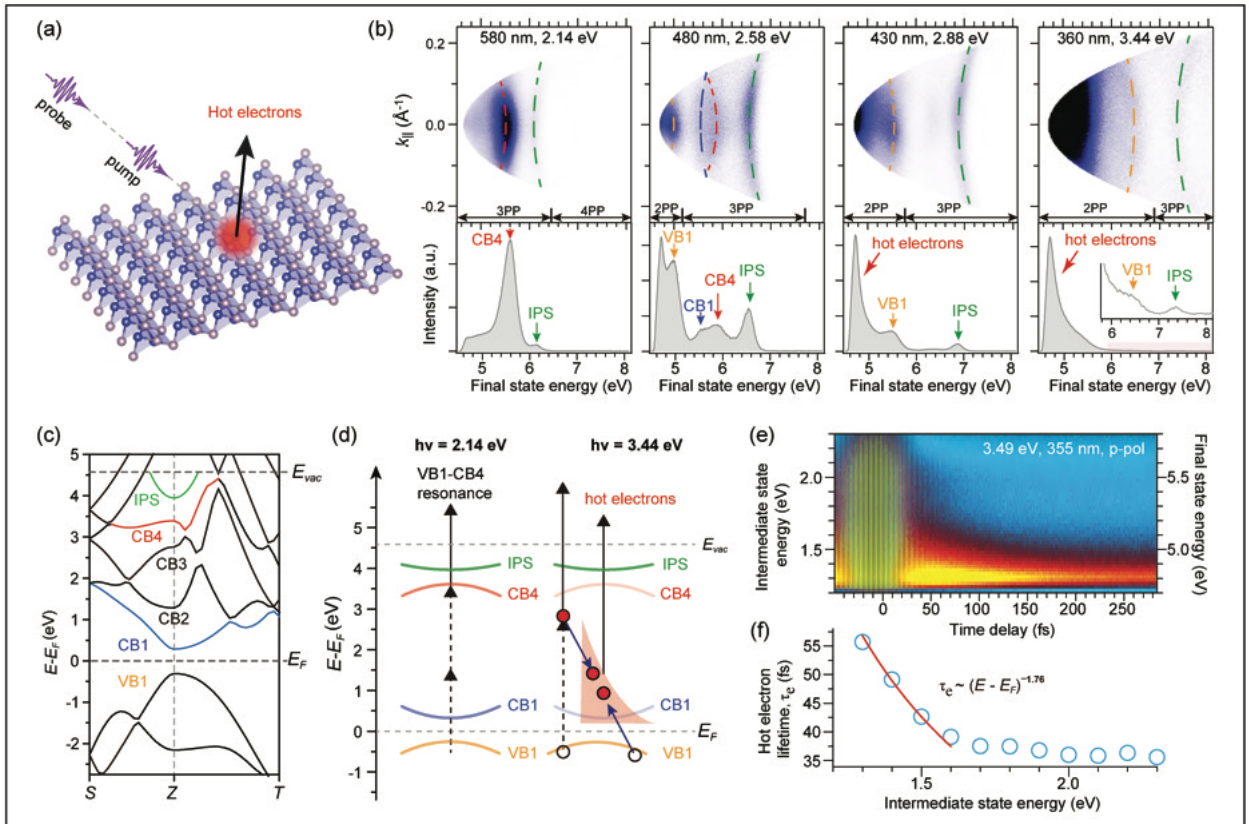
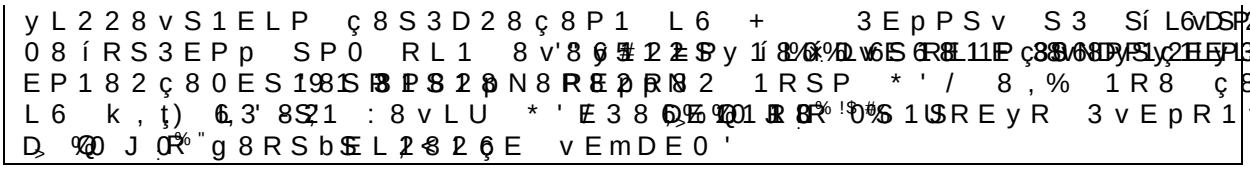


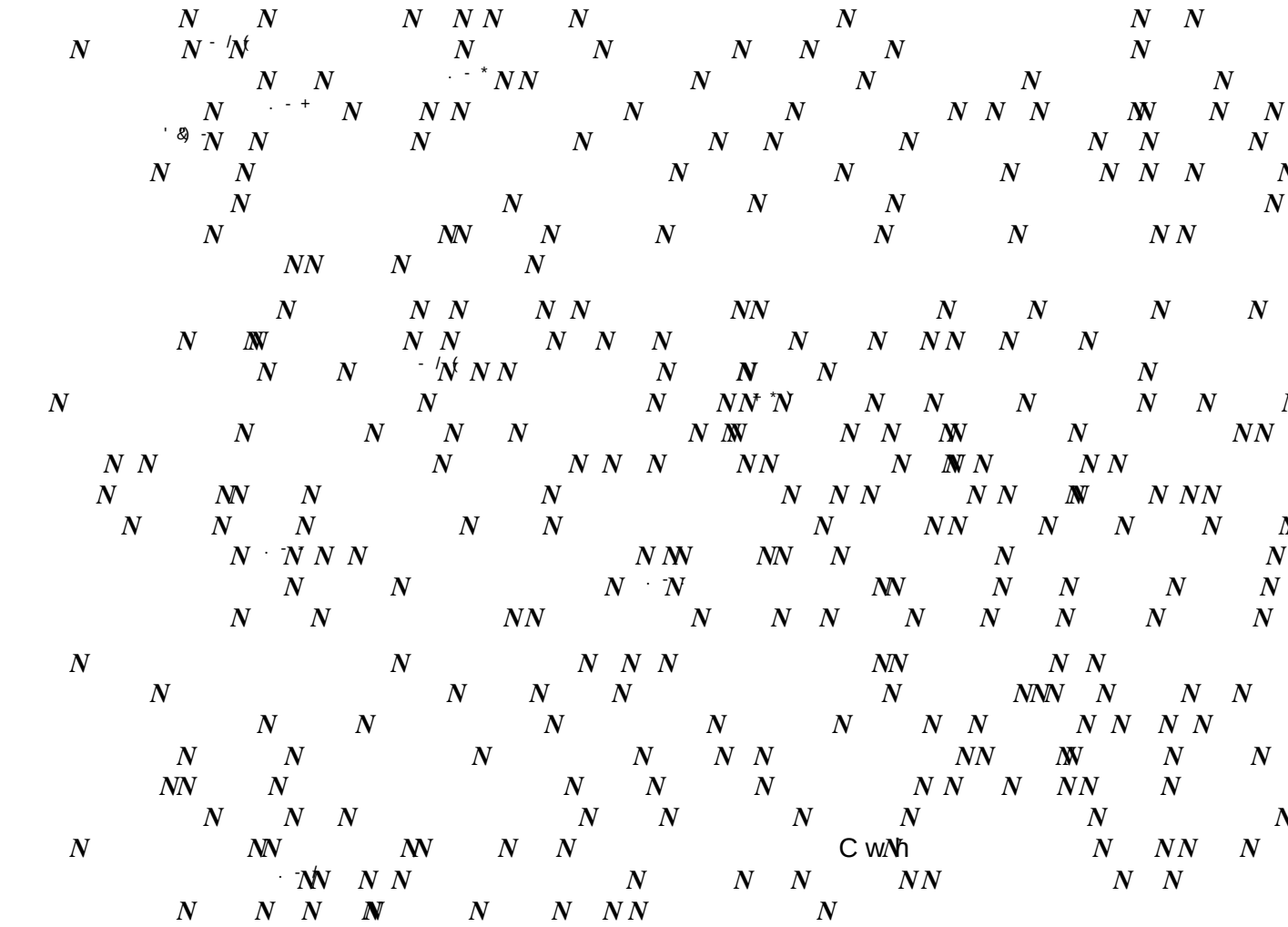
Figure 31. Distinct first-order interband and higher-order inelastic optical responses of BP from the visible to UV excitation regions. (a) Schematic excitation of mPP from BP, a representative 2D material. The frequency tunable pump pulse of ~30 fs duration generates interband and intraband (hot electron) excitations, and the identical delayed probe pulse records their population decay. (b) Representative mPP energy–momentum $E(k_{||})$ maps excited along the zigzag direction of BP with photon energies $\hbar\omega = 2.14$, 2.58, 2.88, and 3.44 eV, respectively. The dashed lines guide the band dispersions. The lower panels are the corresponding line profiles extracted at $k_{||} = 0$ Å^{-1}. The inset for $\hbar\omega = 3.44$ eV expands the mPP signal above 5.8 eV to show the remaining band features. The bottom arrows indicate the spectral regions that are excited by 2PP-4PP processes. (c) Calculated band structure of bulk BP with band dispersions along Z-S (k_{AC}) and Z-T (k_{ZZ}) directions. (d) Illustrative excitation diagram respectively showing band-to-band resonant excitation (left), and inelastic scattering of virtual states promoted from VB1 leading to the production and detection of hot electrons (right). (e) Interferometric two-pulse



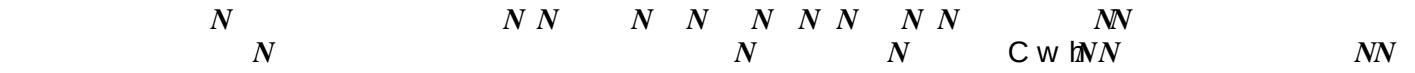
&%<18..9;:60. 6: 32R .I;960 8.D21 92I.8.- ;<I 0;:36:292:I .:1 9;1N8.I6;:

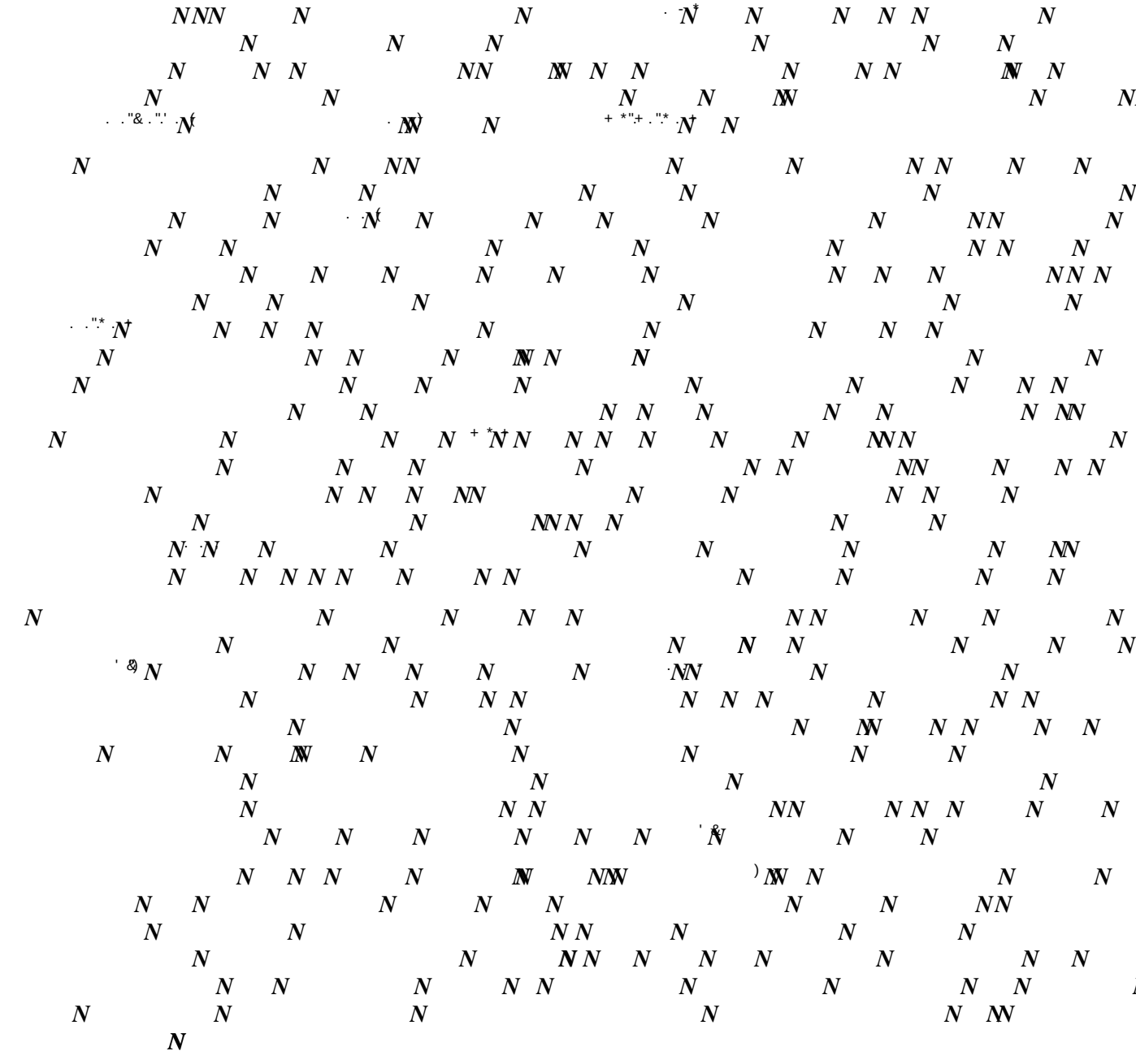
RJcJG, 9b"c fAHeJ,npmeJ;,- JFeLdJ,inD 96J!, d1J,KnJívsJLkeJ,jnHeGJ
26JKíen 3Jnv1(J ie -aJdD
$=vçL28 ISçEvN cyRLLv L6 2=EvP8py%1 2:EEy2Syvó SiPSOP L;1L8çyíRDP1L8v2Lp=NPp;E
dDSP1Dç cyE8Py8 SP0 =PpbE3P2838E21ENP%p TO8P3311 Es1SD61S8N%8 1 1D82%0 DO8i q-P0
%O;kQuP31E1D1 08 ;E8PyE83 IL1LPEmD8 3y%RPuLV8LpN%2y)81 1L/P)S ;GSP3
:S2y8vLPS% cíSEP
&<8íS21ç8P1 L6 =v8y12EyS2N%PpEBP6 2E0p%PE6BPv3EP2N%SgL28B
'OP31E1D1L 08 dDGçEyS IG3EyS :vS3 ;Sg282S "OdI#% ;cO;
(<LPL31ES OP182PS1ELPSvS2R%EvSy3v;8%c1SP2%c*P1%S38E1PSLBP5EDS8v
)<8íS21SçGBEy1S 9%qvPEEybS802S3 EG3S0%3)8)v* 1 ScSjP% c8ígSE3E
O;e&9P31/E,SD9vESPS 08 e8yS123y%S ES3338ED8PE83D9+bS%P)1)) :S2y
-9;;2<:9 81=5ç8S3E yO3*R=E419S;2!8íD20D8'80D

%$# 5,HnDiLvHíD,

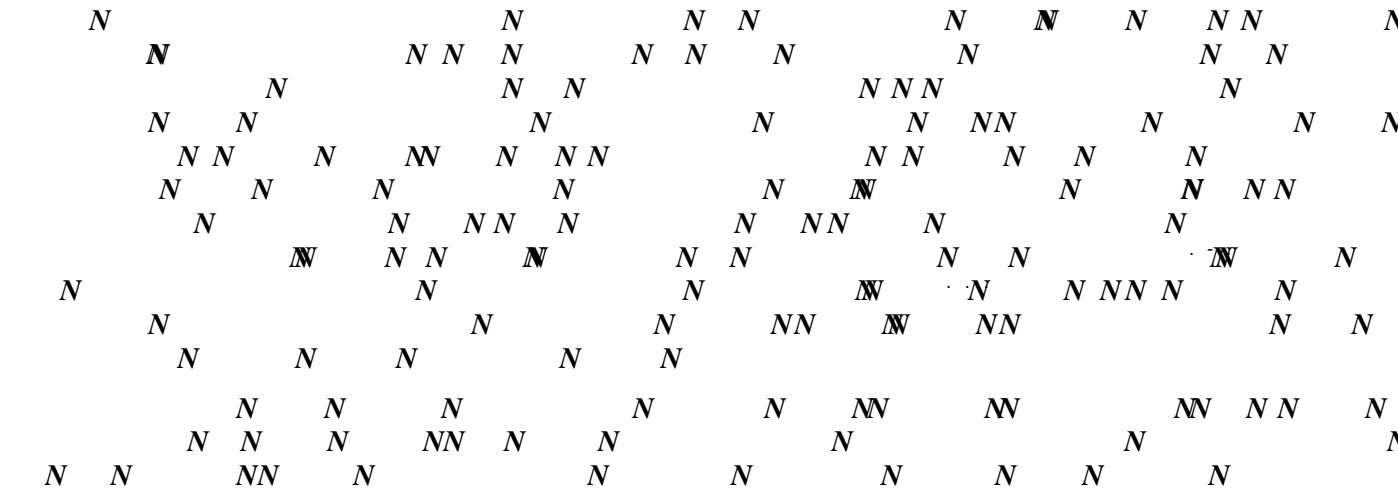


%$$ BHJHe Dr Hce -nH





%$% /cJjje,Gek J,i BLGGekHei 0ínevHíD,k



film into a periodic array of ribbons, as shown in Figure 32d. When examining the reflection spectra of such an array with undoped ($E_F = 0$) or highly doped ($E_F = 1$ eV) graphene, we observe a three-fold effect of doping: (1) the plasmon resonance peak is blue-shifted; (2) the magnitude of the resonance peak increases; and (3) the resonance linewidth becomes narrower for higher doping levels. The figure illustrates a modulation depth ≈ 36% at a photon energy around ≈ 0.9 eV. The doping level of graphene can be controlled through electrical gating at a relatively high speed depending on the design of the electronic circuit. As an alternative that can reach higher speeds, one could exploit ultrafast optical pumping to effectively dope graphene[18,563,889] through its ultrafast photothermal response (see Chapter 17).

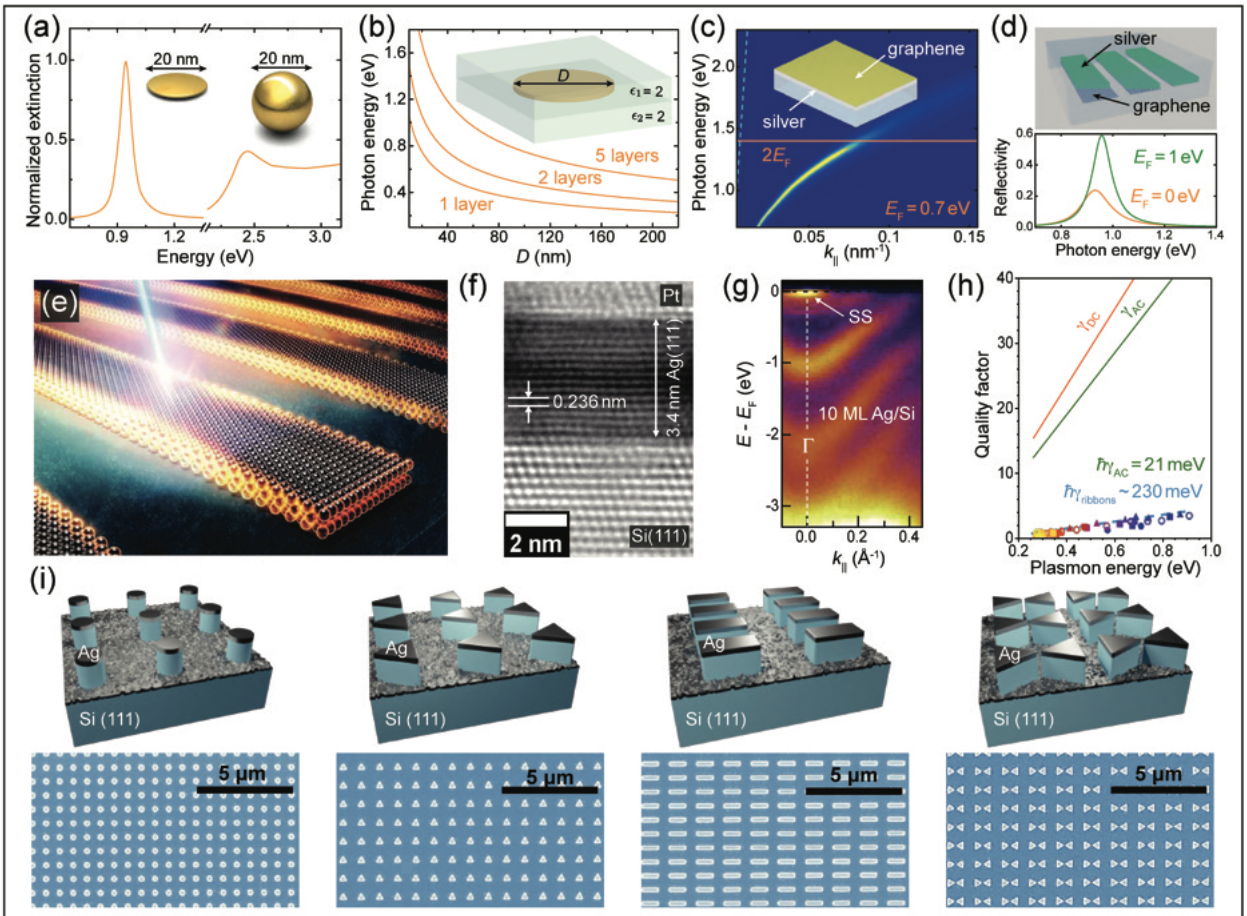
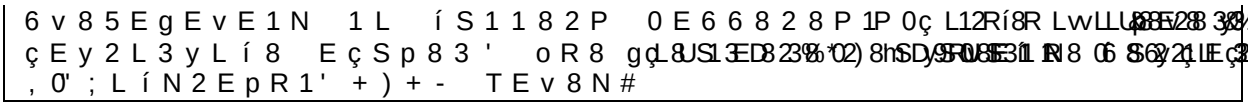


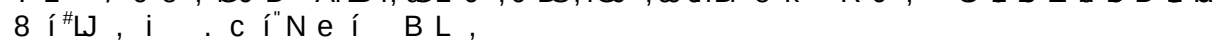
Figure 32. Plasmonics in ultrathin metal films. (a) A single-atomic-layer gold disk with (111) crystallographic orientation exhibits a sharp plasmon redshifted to a technologically appealing spectral region relative to a gold nanosphere with the same diameter. Adapted with permission from ref 792 (Copyright 2014 Springer Nature). (b) The plasmon energy of few-atomic-layer gold or silver disks scales roughly as $\sqrt{t/D}$ with the disk thickness t and diameter D. Adapted with permission from ref 878 (Copyright 2015 Royal Society of Chemistry). (c,d) The plasmon band of an ultrathin silver layer (1 nm) deposited on graphene is quenched at plasmon energies exceeding the graphene optical gap $2E_F$, where E_F is the graphene Fermi energy (c). This effect can be used to modulate the plasmons of a thin silver ribbon array, thus producing a radical change in light reflection depending on E_F (d). Adapted with permission from ref 879 (Copyright 2016 Springer Nature). (e-h) Ultrathin crystalline silver ribbons can be prepared by epitaxial growth on silicon, followed by nanolithography (e). The resulting metal film exhibits high quality and wafer-scale crystallinity (f), reflected in the emergence of sharp electronic quantum-well states observed *via* angle-resolved photoemission spectroscopy (g) (i.e., the electron intensity as a function of parallel wave vector $k_\parallel$ and energy relative to the Fermi level, $E - E_F$). The quality factor (energy-to-width ratio, ω_p/γ) of the obtained ribbon plasmons reaches ~4 (with a measured width $\hbar\gamma_{\text{ribbons}} \approx 230$ meV), which is far from the large values predicted from the bulk Drude-model damping, as measured optically[876] ($\hbar\gamma_{\text{AC}} \approx 21$ meV) or electrically ($\hbar\gamma_{\text{DC}} \approx 24.6$ meV for a bulk conductivity of 6.30×10^7 S/m). This reduction in quality factor can be presumably ascribed to the effect of imperfections introduced during passivation of the film (with a silica coating) and nanolithography (h). Adapted from ref 10 (Copyright 2019 American Chemical Society). (i) Prepatterning of silicon followed by epitaxial deposition of silver crystalline films leads to higher quality structures with great

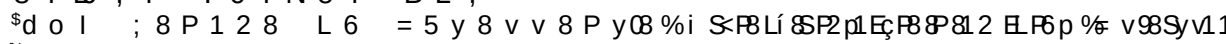


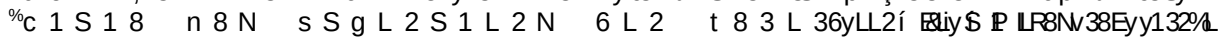


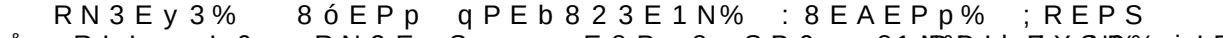


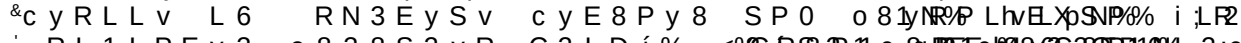










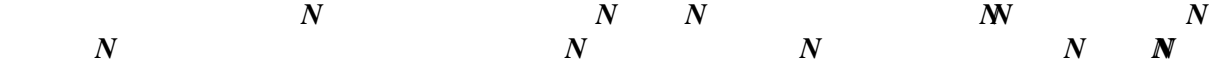


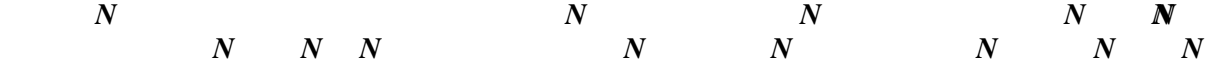




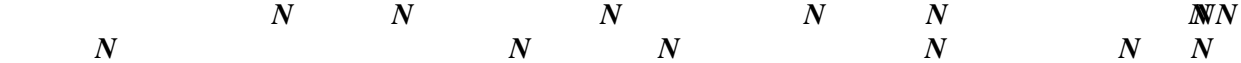






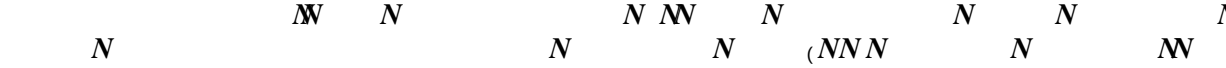


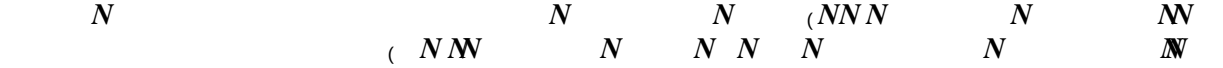


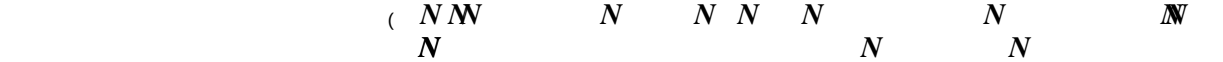
















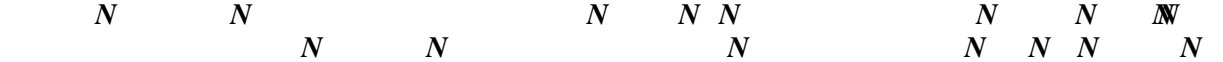














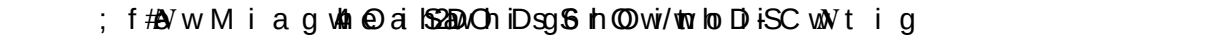






























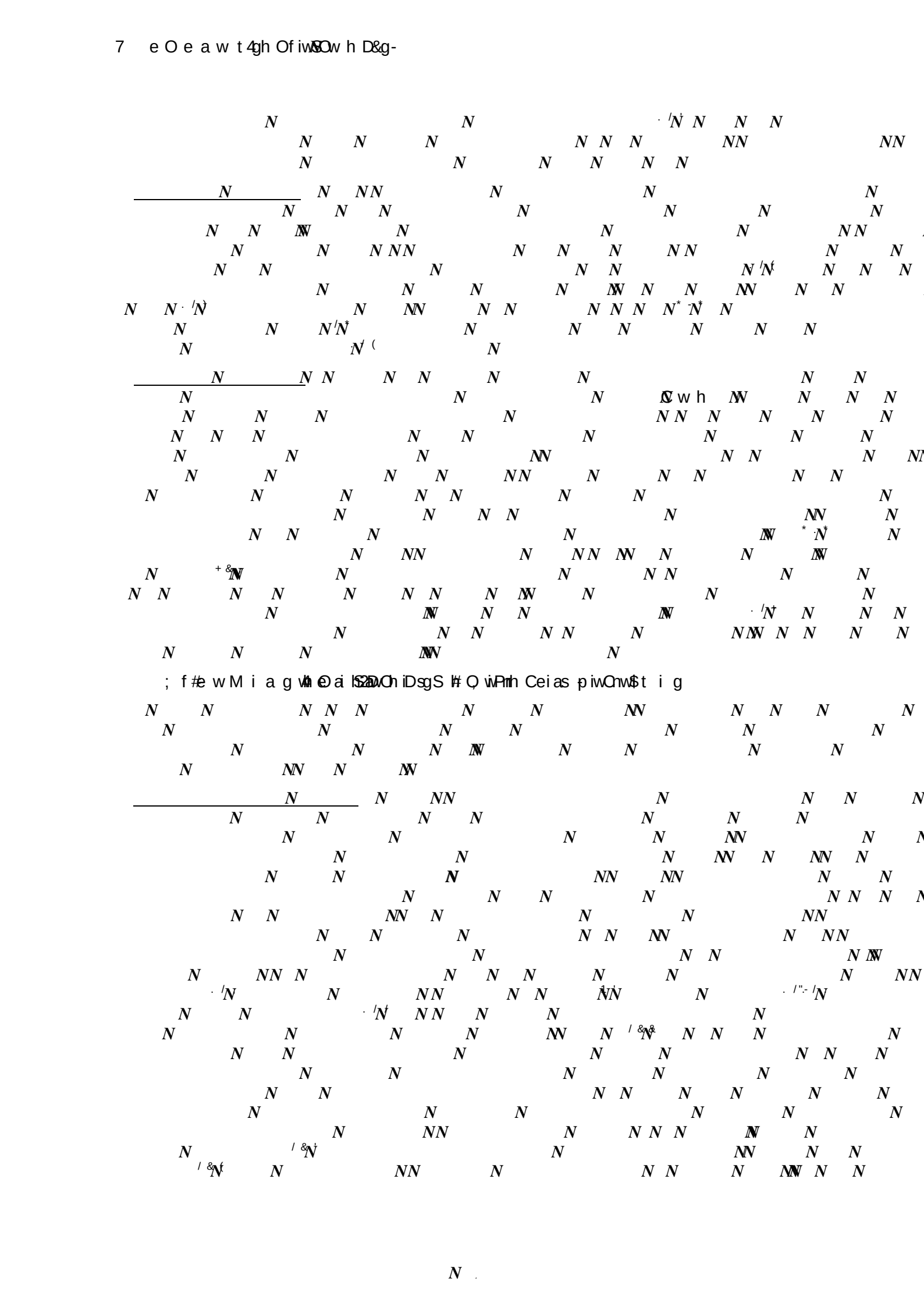


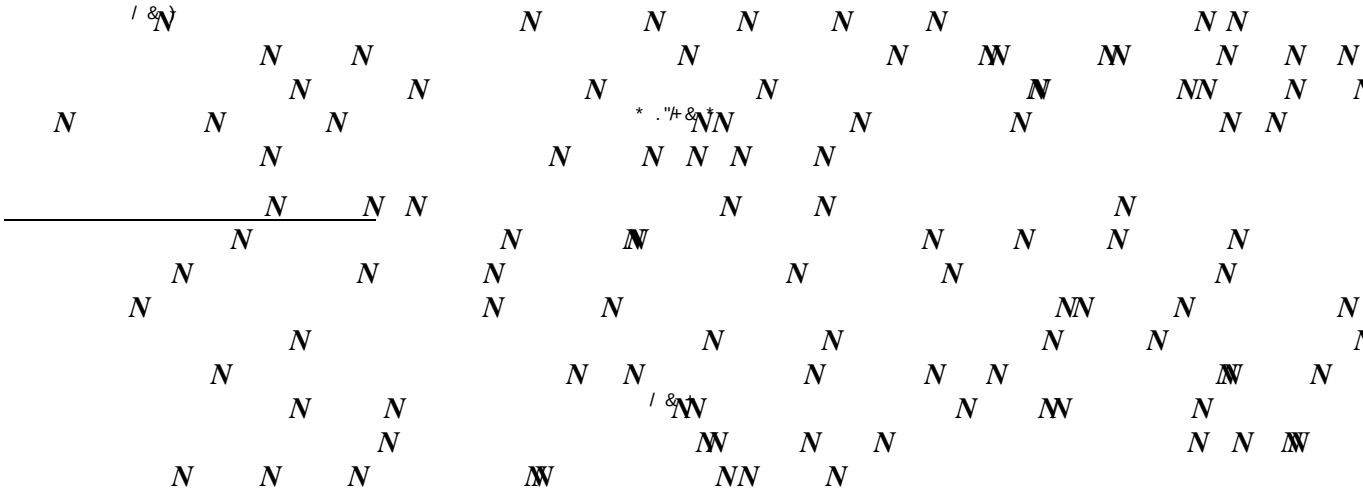


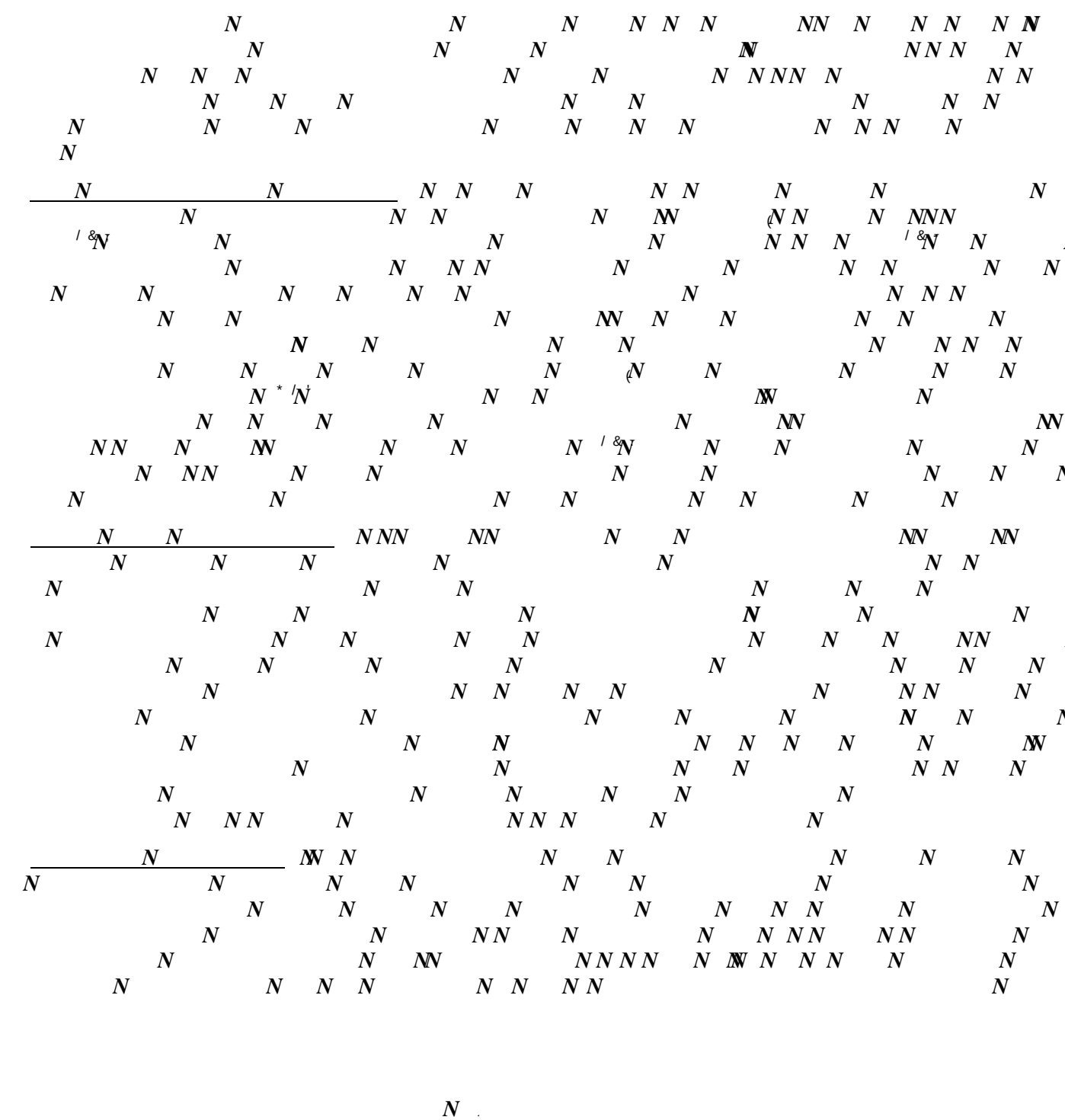


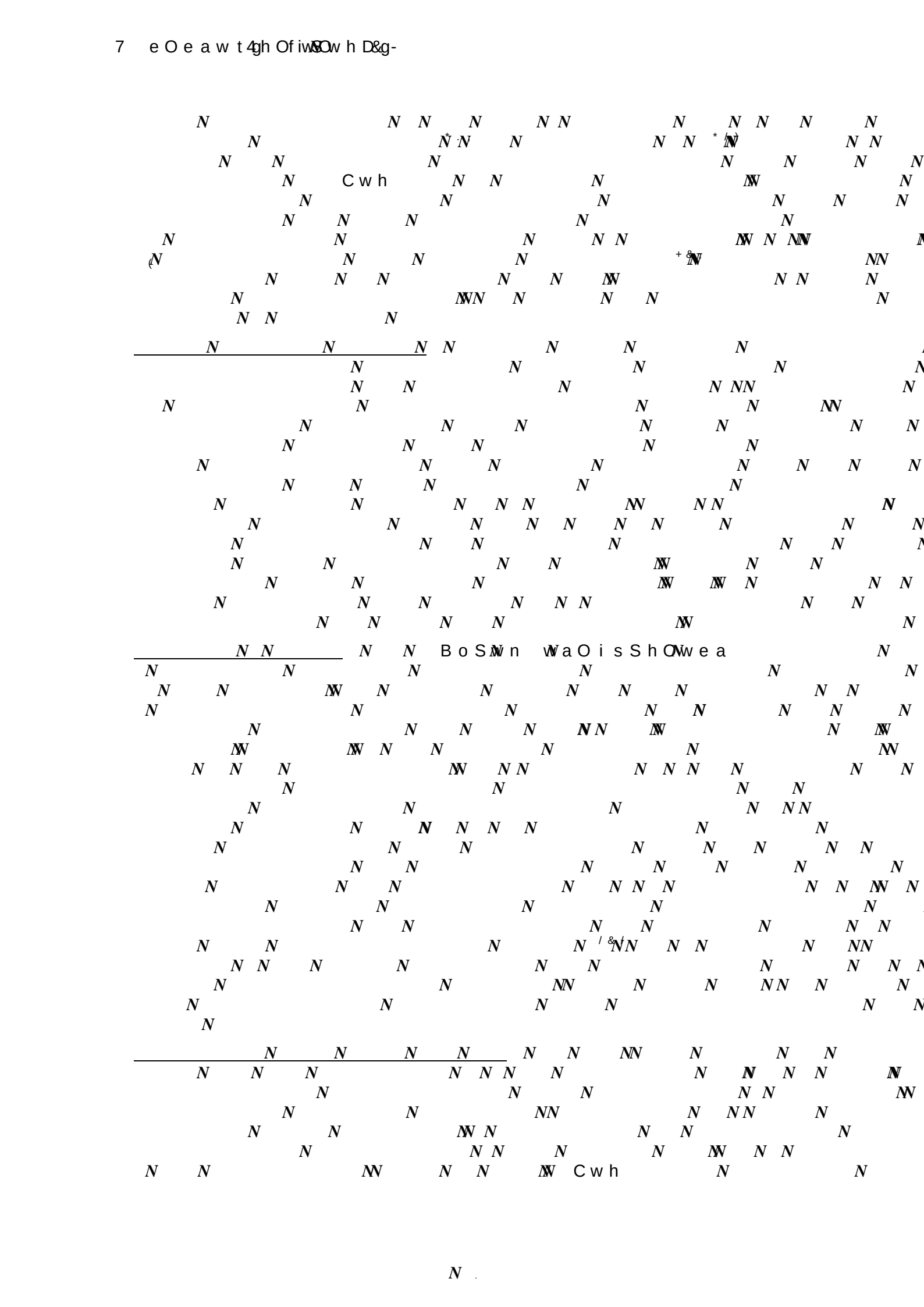


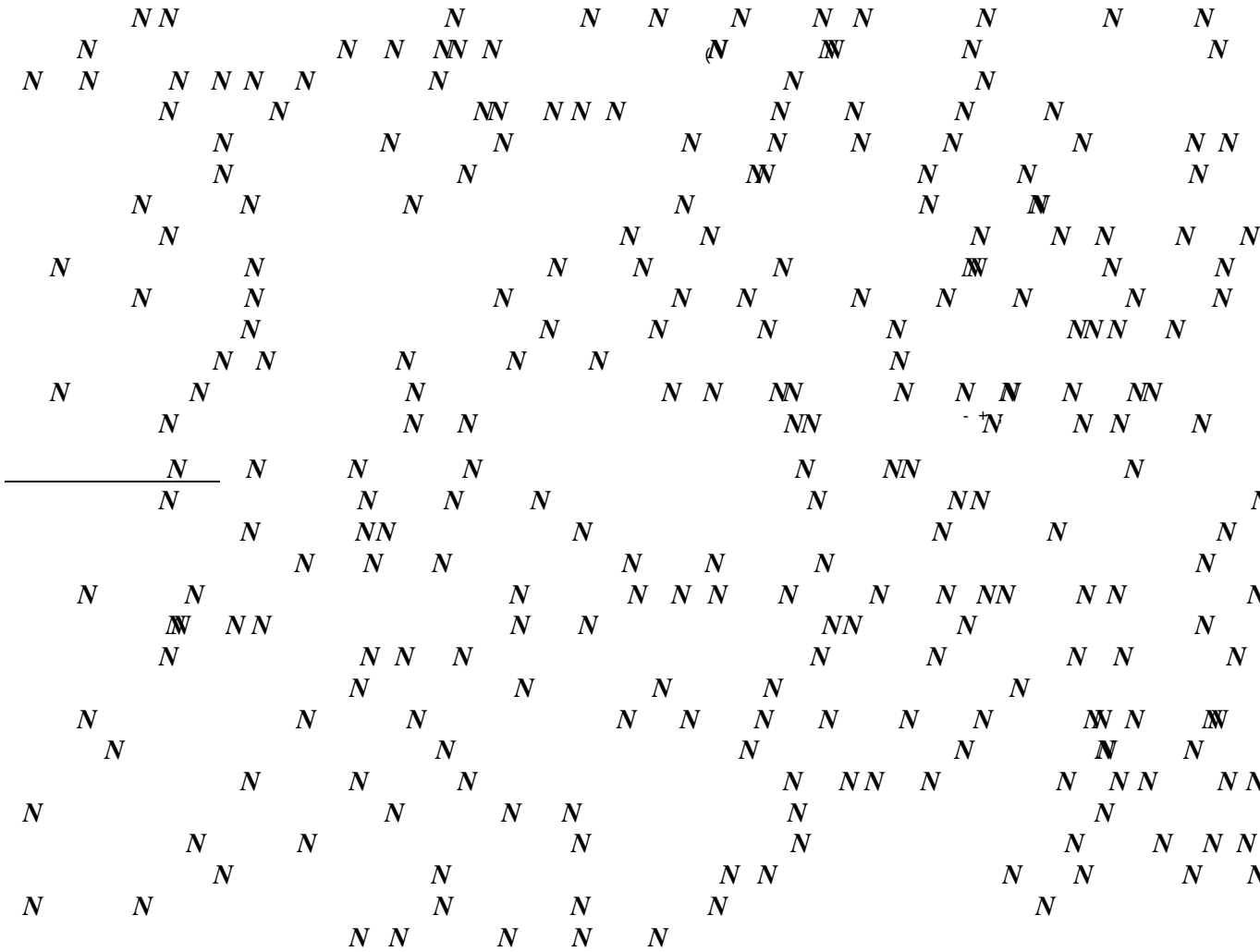


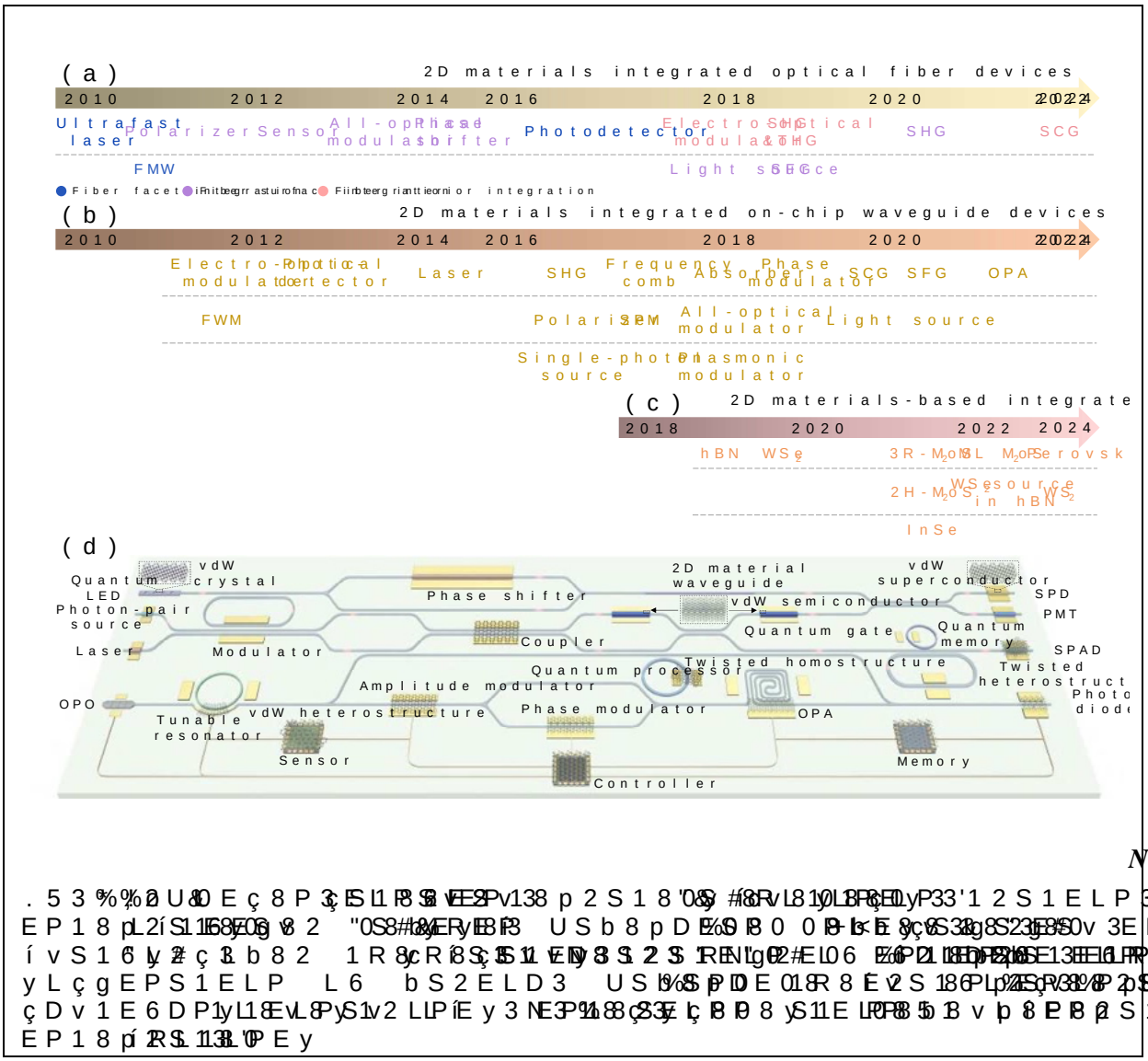




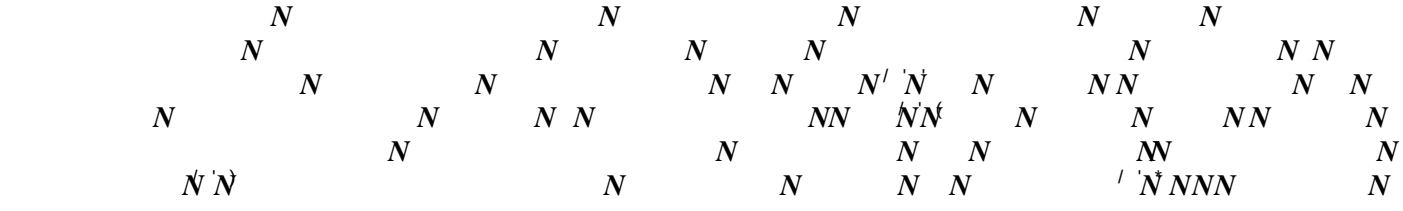




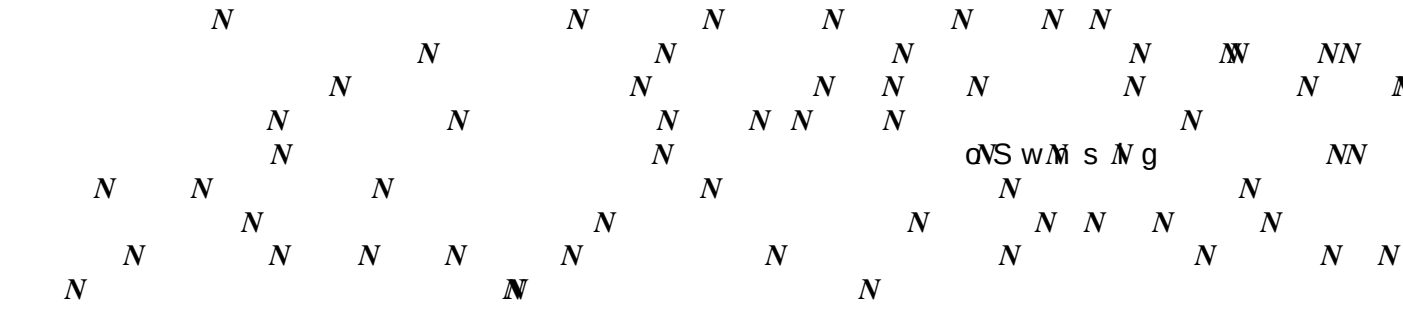




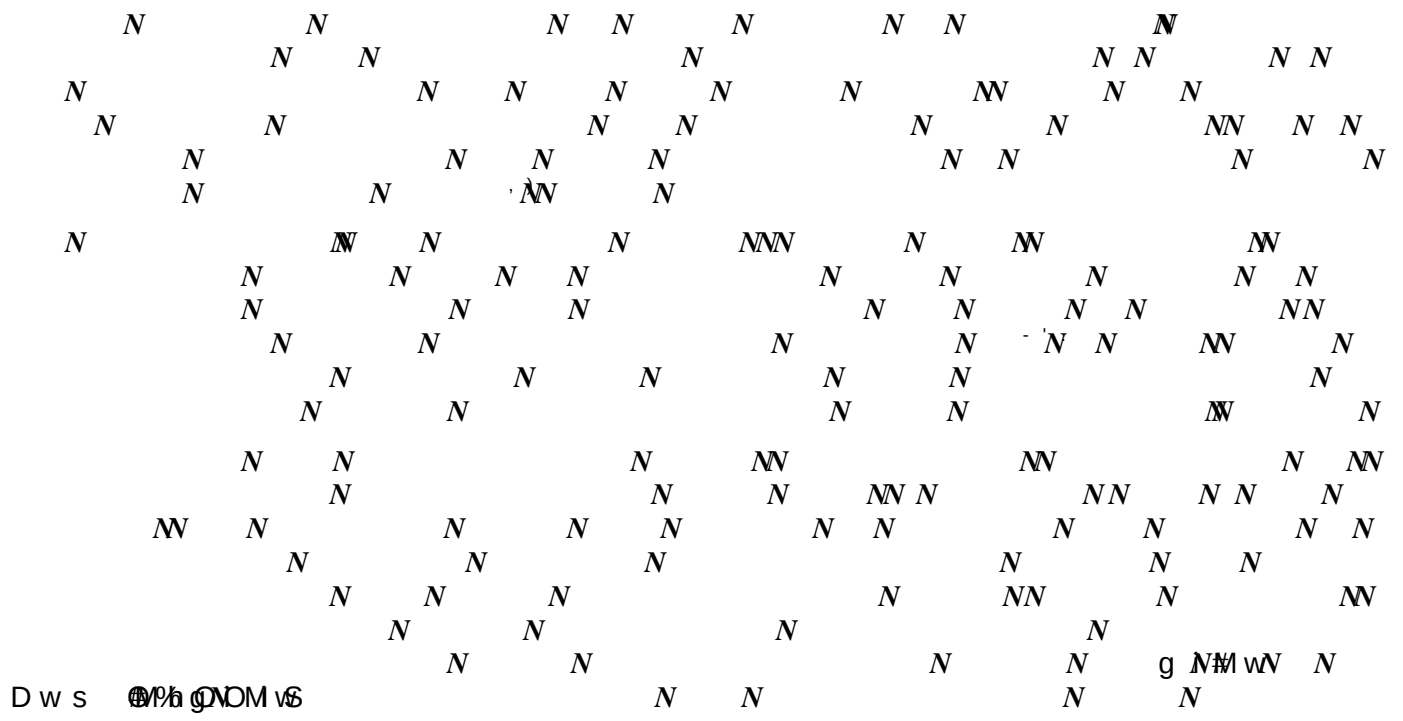
& ' ;! < I ; 2 8 2 0 I 1 ; : 6 0 6 : I 2 1 0 ; : : 2 0 I 6 ; : ; 3 < ; 8 . 1 6 I ;
9 . I 2 1 6 . 8 .

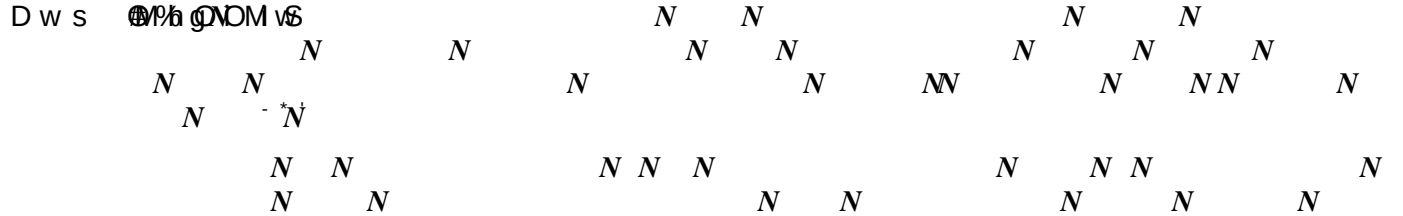


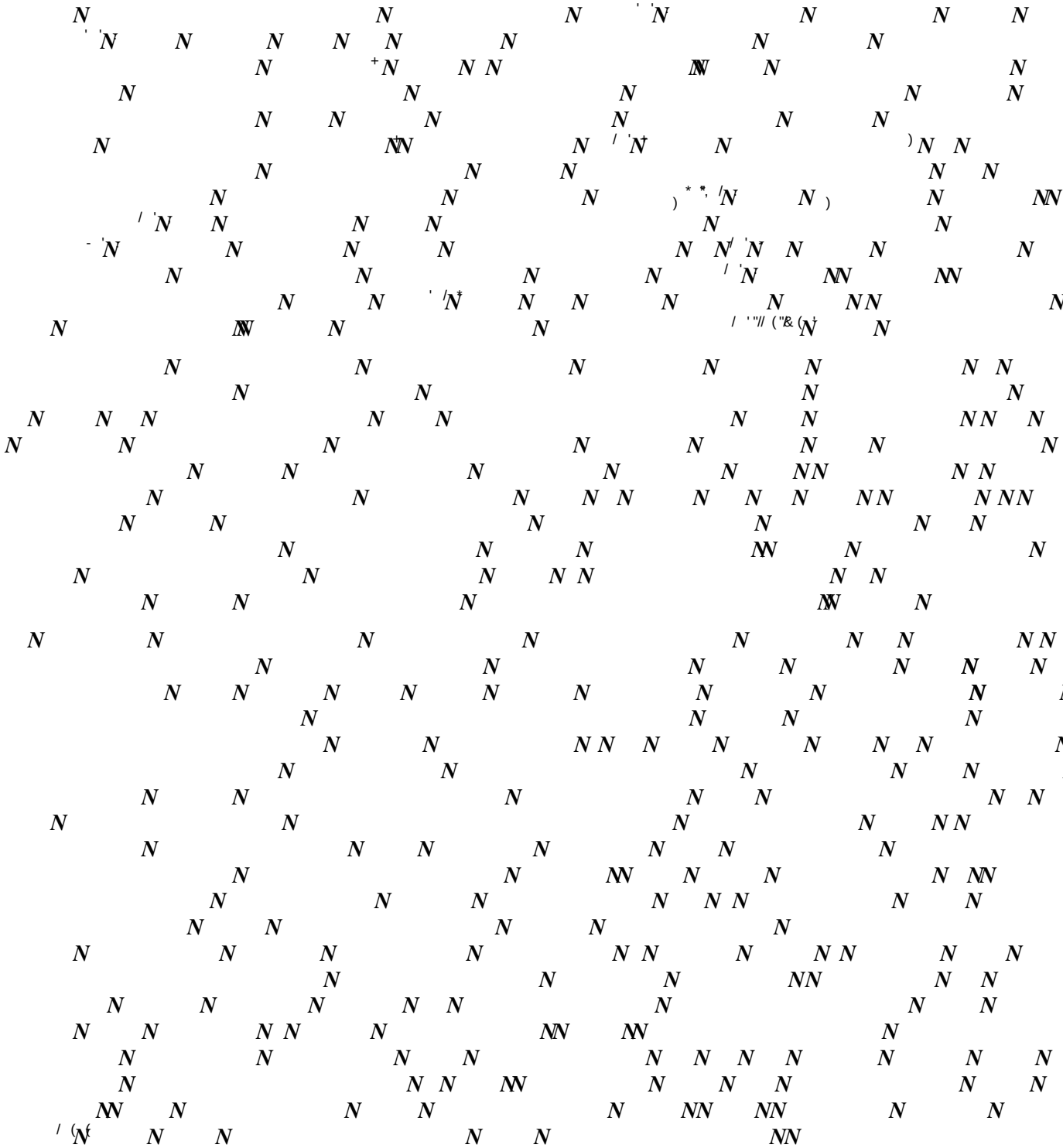
%&$ / c J j j e , G e k J , i 2 L H L n e 3 D J j k



%&% B L G G e k H e i 0 í n e v H D , k H D 9 e e H S c e k e 3 D J j k







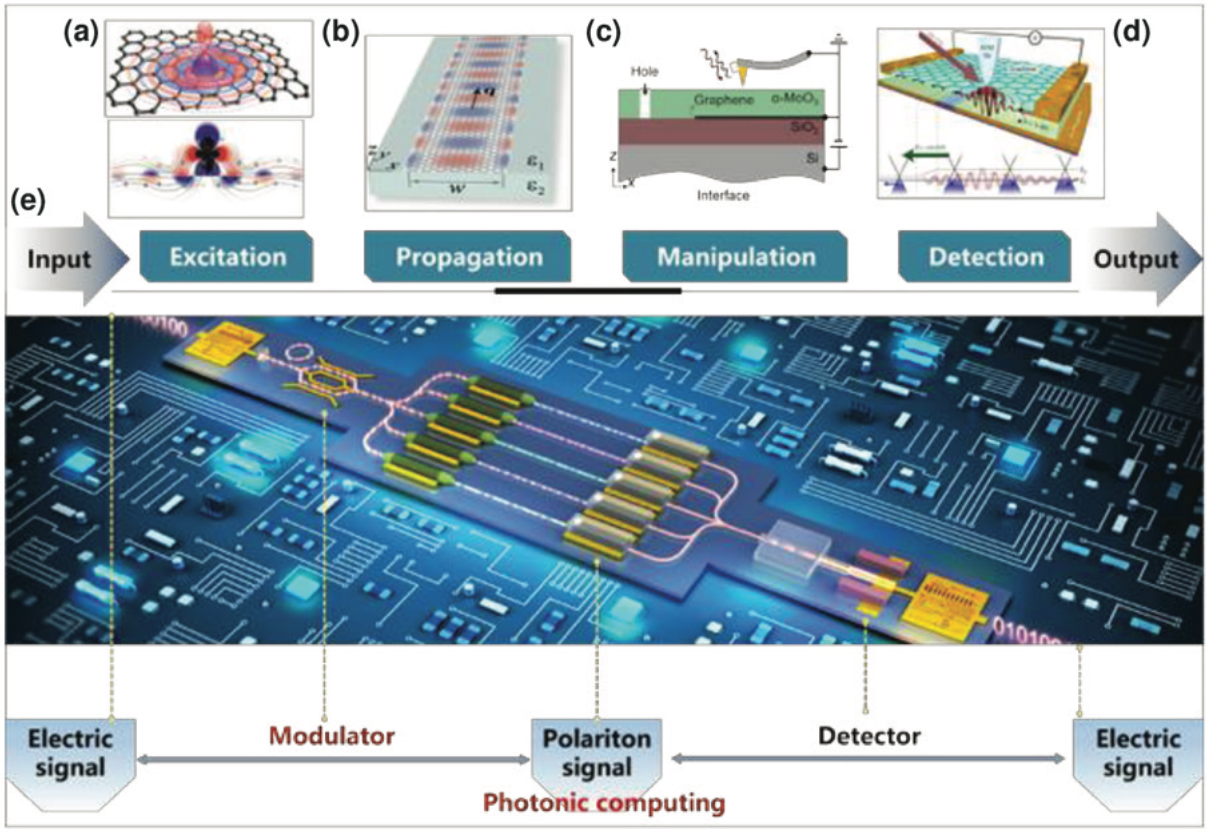
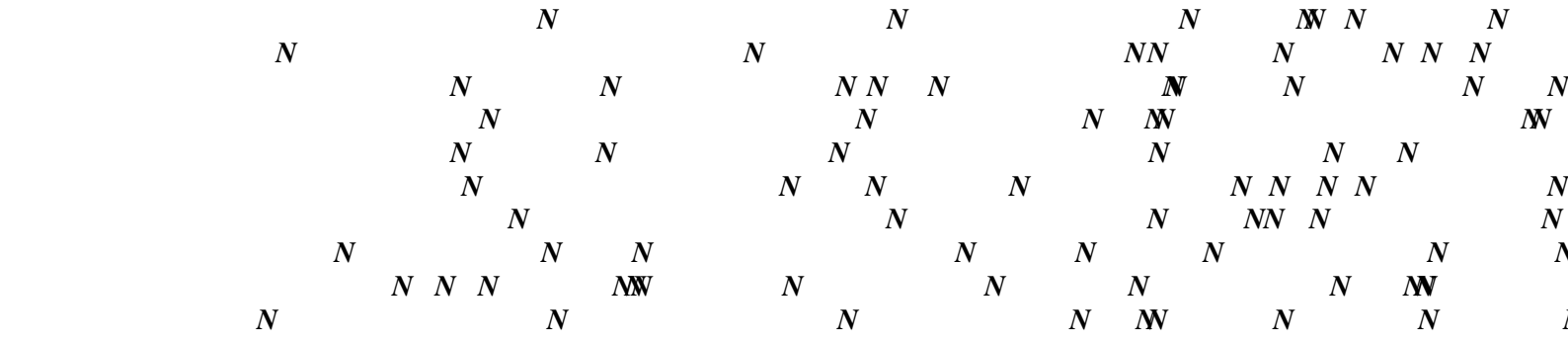


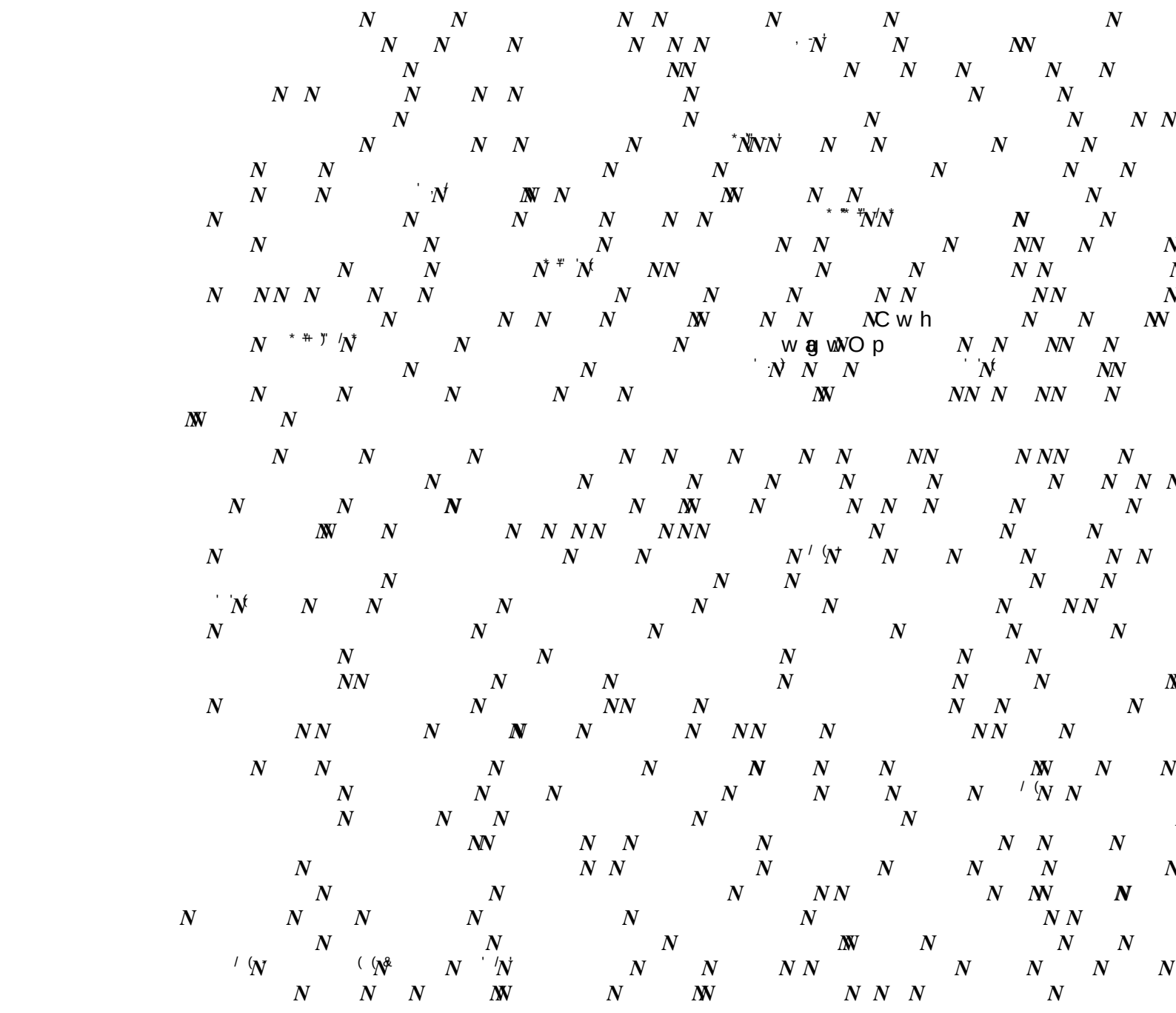
Figure 34. Optoelectronic interconnection of polaritons in 2D materials. (a) Interaction between a dipole emitter and plasmons in doped homogeneous graphene (upper panel) and near-field generated by a perpendicular dipole positioned 10 nm from doped graphene (lower panel). Reprinted from ref 9 (Copyright 2011 American Chemical Society). (b) Edge and waveguide THz surface plasmon modes in graphene microribbons. Reprinted from ref 923 (Copyright 2011 American Physical Society). (c) Gate-tunable topological polaritons in vdW heterostructures with high spatial confinement. Reprinted with permission from ref 194. (Copyright 2023 AAAS). (d) Thermoelectric detection and imaging of propagating graphene plasmons. Continuous-wave laser light is scattered by a movable metalized AFM tip, which excites plasmons in the hBN-graphene-hBN heterostructure. Reprinted with permission from ref 924 (Copyright 2016-Springer Nature). (e) Schematic illustration of the optoelectronic interconnection of polaritons in 2D materials featuring several key components arranged from left to right: the module for converting electrical signals into polariton signals, the polariton waveguide for signal transmission, the polariton signal modulation module, the polariton photonic computing module, and the polariton detection module. Each modulator is individually controlled by an electronic chip to encode the optical signals. Additionally, a silicon waveguide connects the modulators to the photodetector and can be extended and adapted for fiber optics, enabling long-distance signal transmission.

35. EFFECTIVE RESPONSE OF QUANTUM MATERIALS DRIVEN BY OPTICAL NEAR FIELDS

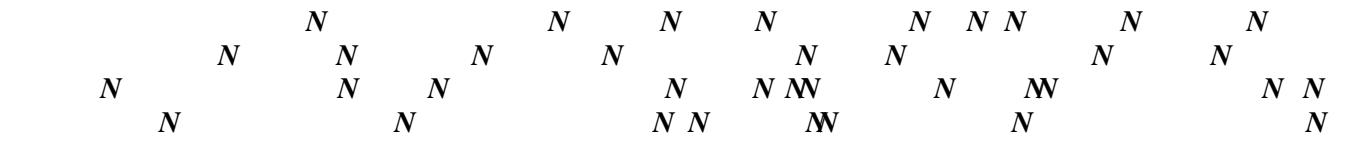
Aaron Sternbach,[1,2,*] You Zhou,[2,3] and Mohammad Hafezi[4]
[1]Department of Physics, University of Maryland, College Park, MD, USA
[2]Maryland Quantum Materials Center, University of Maryland, College Park, MD, USA
[3]Department of Materials Science and Engineering, University of Maryland, College Park, MD 20742, USA
[4]Joint Quantum Institute (JQI), University of Maryland, College Park, MD 20742, USA
***Corresponding author.** Email: ajs01123@umd.edu

The unification of 2D materials, sub-diffraction-limited photonics, and light-induced states is creating opportunities for material design. Emerging possibilities are rooted in the exquisite properties of 2D materials. These compounds often possess exceptionally clean interfaces and sharp lateral boundaries, and they are amenable to experimental control. Moreover, 2D materials can host polaritons—hybrid collective modes that possess characteristics of both light and matter.[112,671] Polaritons often display

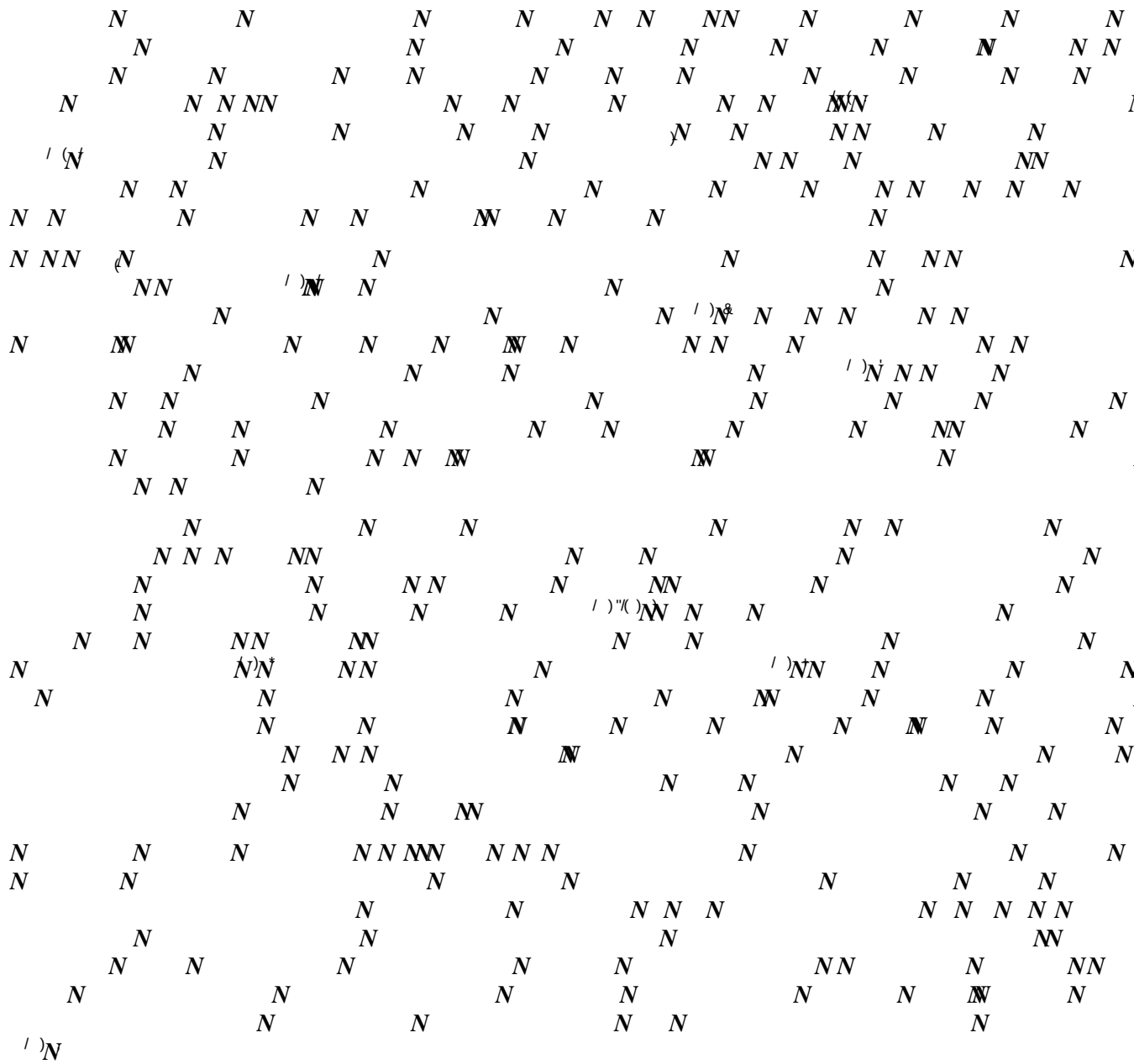




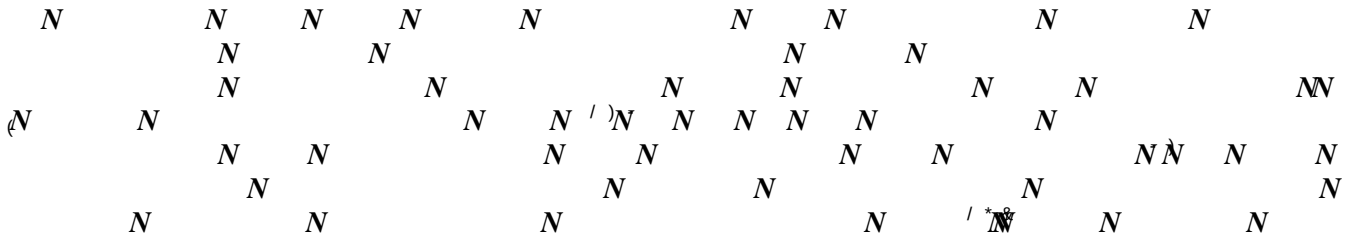
% ! $ J , D& G tJH,. eTk eSD / D , H=LDJj , H9LJoH e N í J j k



8 pVha Op M 4 h O i S w h D g - SwWC i a + B 6 r O w t h D 5 i h S / w i D



4 i n w h8Ow a SQ lMO i7 g g w5a C=Sw i hnC wO w i g



Interest in passive cavities is largely driven by the desire to Floquet-engineer solids. The question of whether the effects that have been witnessed in cavities are unambiguously related to Floquet states generated by vacuum fluctuations remains open. Further work is required to establish general design protocols to produce cavity-mediated states and assess their origins. A third goal is to establish physical observables that can yield unambiguous insight into the physics of cavity-mediated states and rigorously test the agreement between theory and experiment.[78,938]

Even in the absence of a radiation source, passive cavities could change the properties of quantum systems. Unambiguous observables with explicit connections between theory and experiment are desired. The Purcell modification of emission in the polaritonic near field is one example, where the dynamics of optical excitations is not yet fully understood. The collective properties of charge carriers can also be modified by cavities. In a gaped system, the relevant coupling strength is quantified by a strong coupling gap relative to the system's decay rates. The description of strong coupling in a gapless sea of itinerant fermions is subject to subtleties. Recent proposals have suggested that enhancements of the effective mass,[938] or equivalently, changes of the Fermi velocity,[78] could reveal cavity-induced changes of Fermi liquids. Two-dimensional materials are likely to play a central role, as these can be placed precisely within engineered near-field environments.

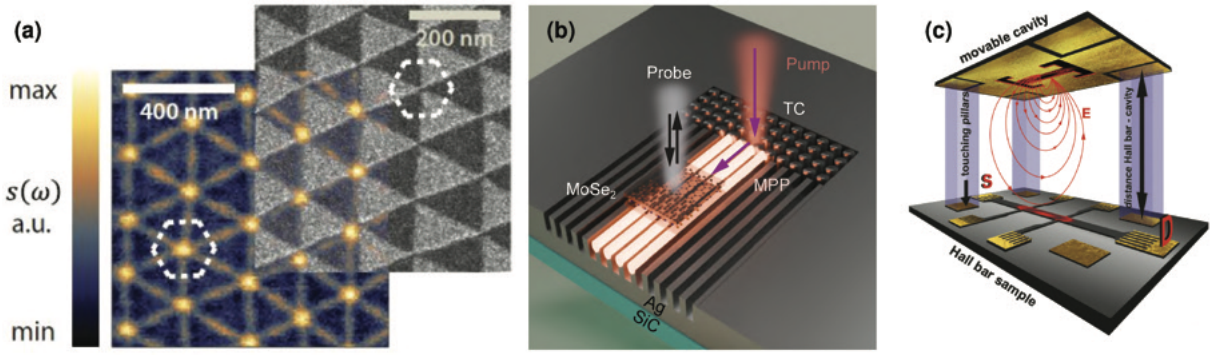


Figure 35. Controlling quantum materials with optical near fields. (a) Producing structured near-field radiation can be accomplished with polaritons, including sub-diffraciton-limited superlattices of IR radiation in moiré-patterned twisted bilayer graphene. Adapted from ref 171 (Copyright 2018 American Association for the Advancement of Science). (b) A 2D material driven by a periodic potential of plasmons with subwavelength periodicity. Adapted from ref 939 (arXiv). (c) Near fields interacting with a Hall bar of GaAs. Adapted from ref 940 (arXiv).

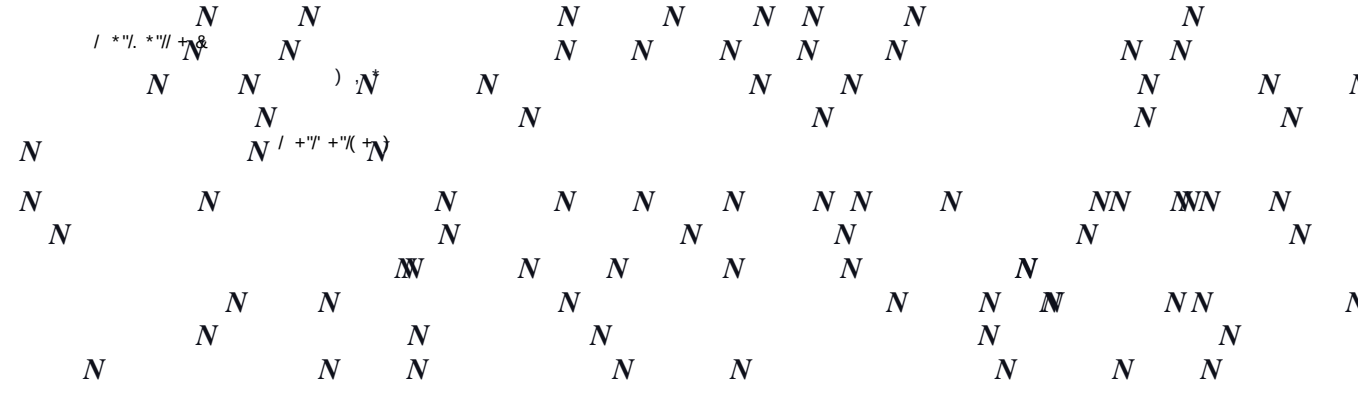
Applications: Light Emission and Detection

36. SINGLE-PHOTON EMITTERS

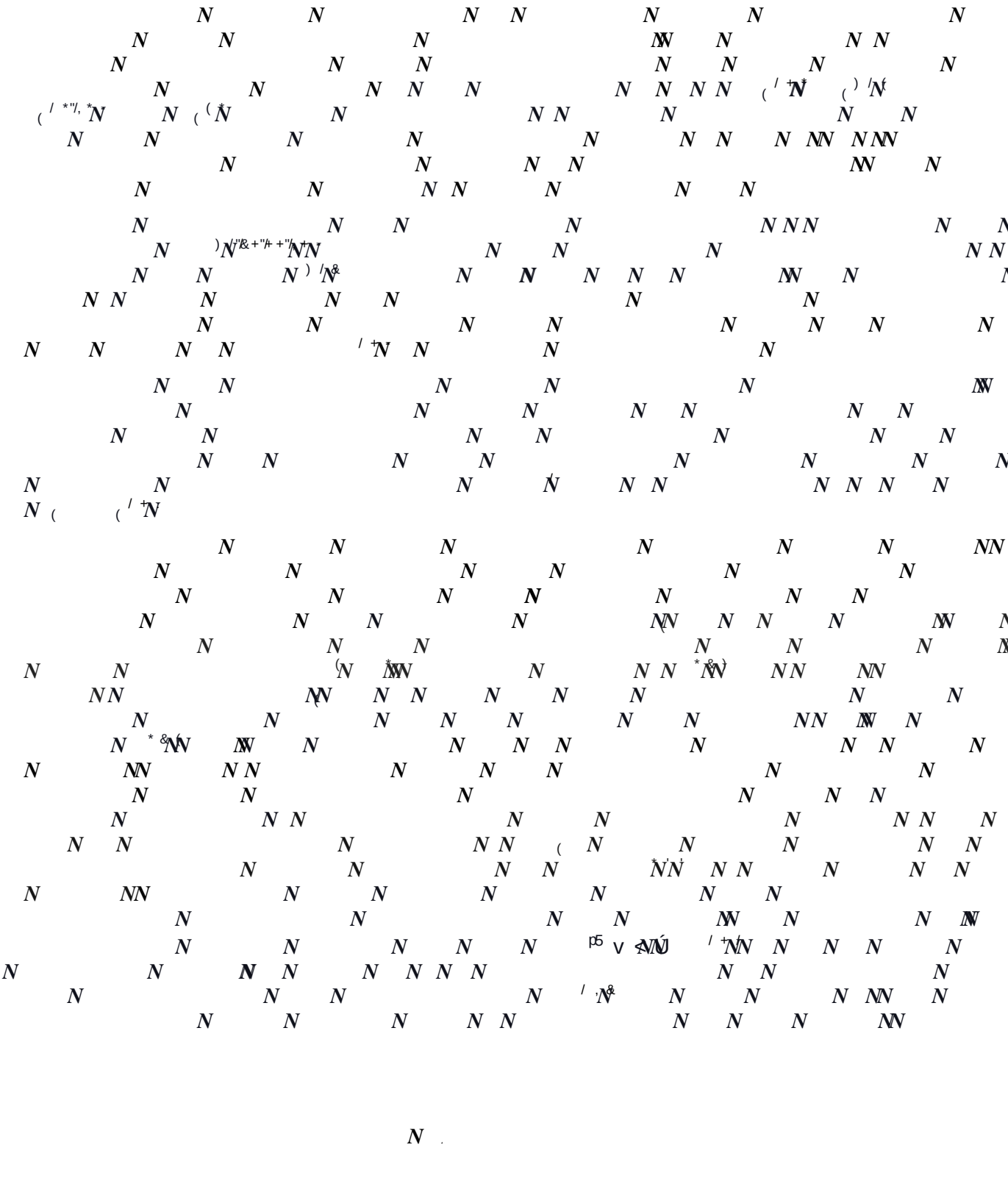
Dmitrii Litvinov,[1,2] Magdalena Grzeszczyk,[2,3] Kostya S. Novoselov,[1,2] Maciej Koperski[1,2,*]
[1]Department of Materials Science and Engineering, National University of Singapore, 117575, Singapore
[2]Institute for Functional Intelligent Materials, National University of Singapore, 117544, Singapore
[3]Center for Quantum Nanoscience, Institute for Basic Science (IBS), Seoul 03760, Republic of Korea
***Corresponding author.** Email: msemaci@nus.edu.sg

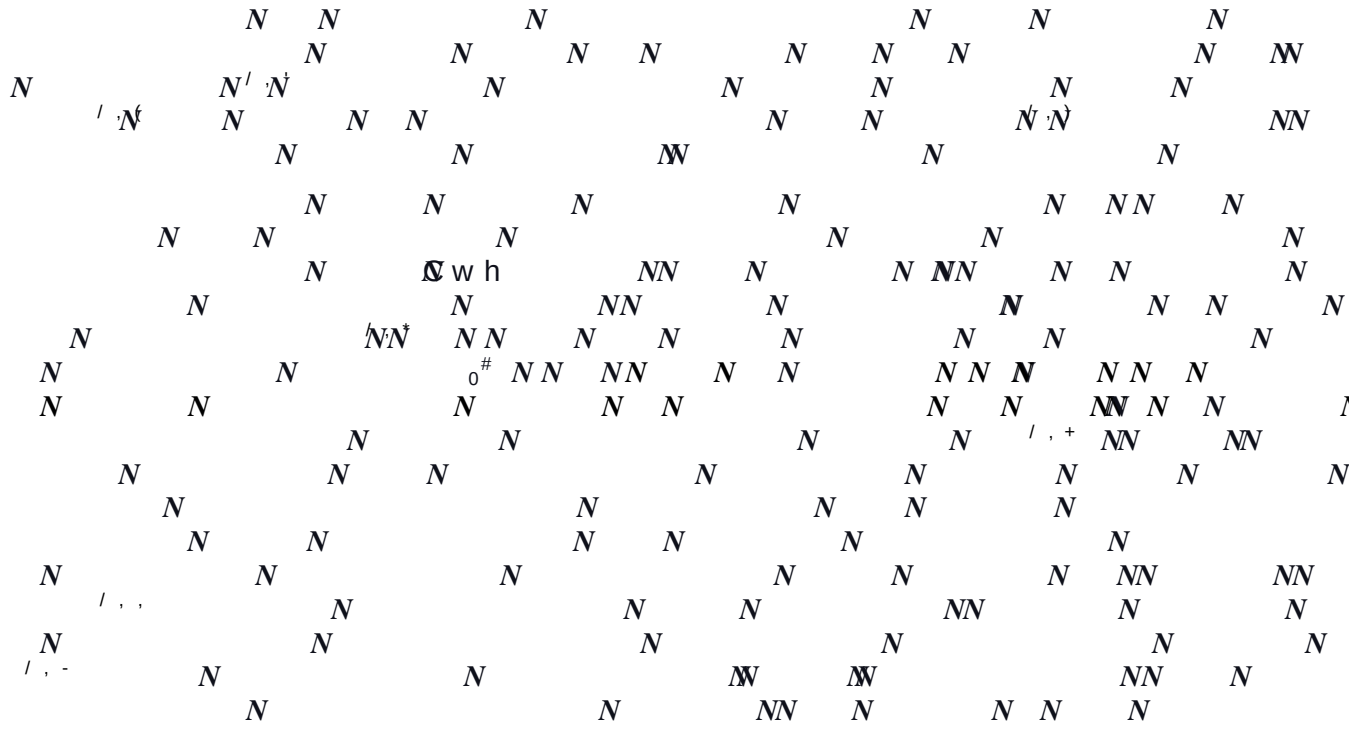
36.1 Introduction

Single-photon emitters (SPEs) in 2D materials originate from quantized energy levels formed by intrinsic imperfections within the crystal structure, as well as through engineering methods such as doping, defect creation, or local strain. These emitters can also be induced by potential traps that confine excitons at the nanoscale. For example, in hBN, point defects like nitrogen or boron vacancies, along with substitutional impurities such as carbon, disrupt lattice symmetry and create mid-gap states that facilitate precise optical transitions across the UV to near-IR spectrum.[256,941] Quantum dots also represent a promising mechanism for the generation of single photons. These nanoscale regions can occur naturally in 2D materials[942,943,944,945] or be engineered *via* fabrication techniques, effectively confining excitons.[946,947] Beyond intrinsic defects and strain-induced traps, functionalization has also been explored to modify optical properties in 2D materials. While single-photon emission has been

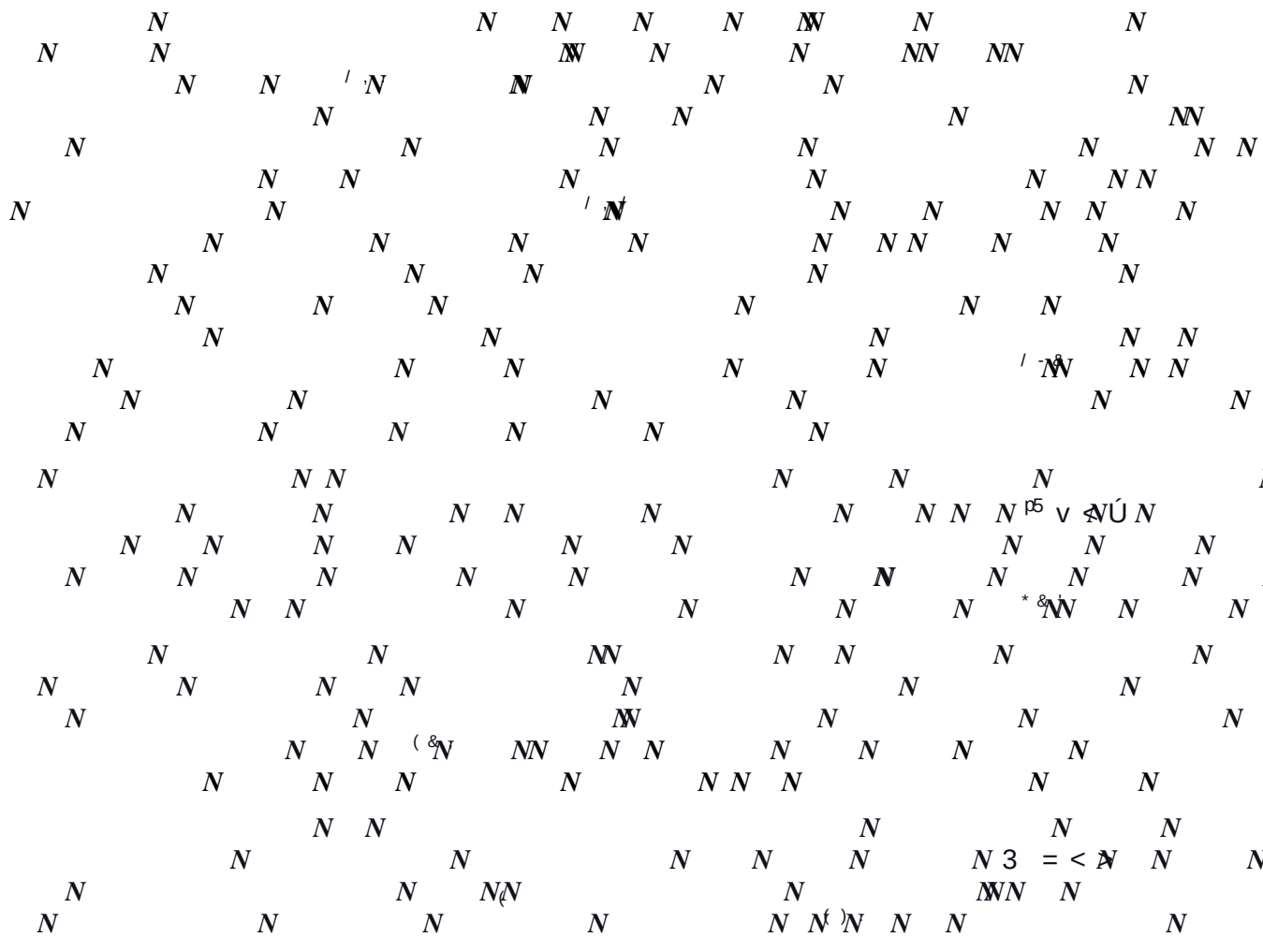


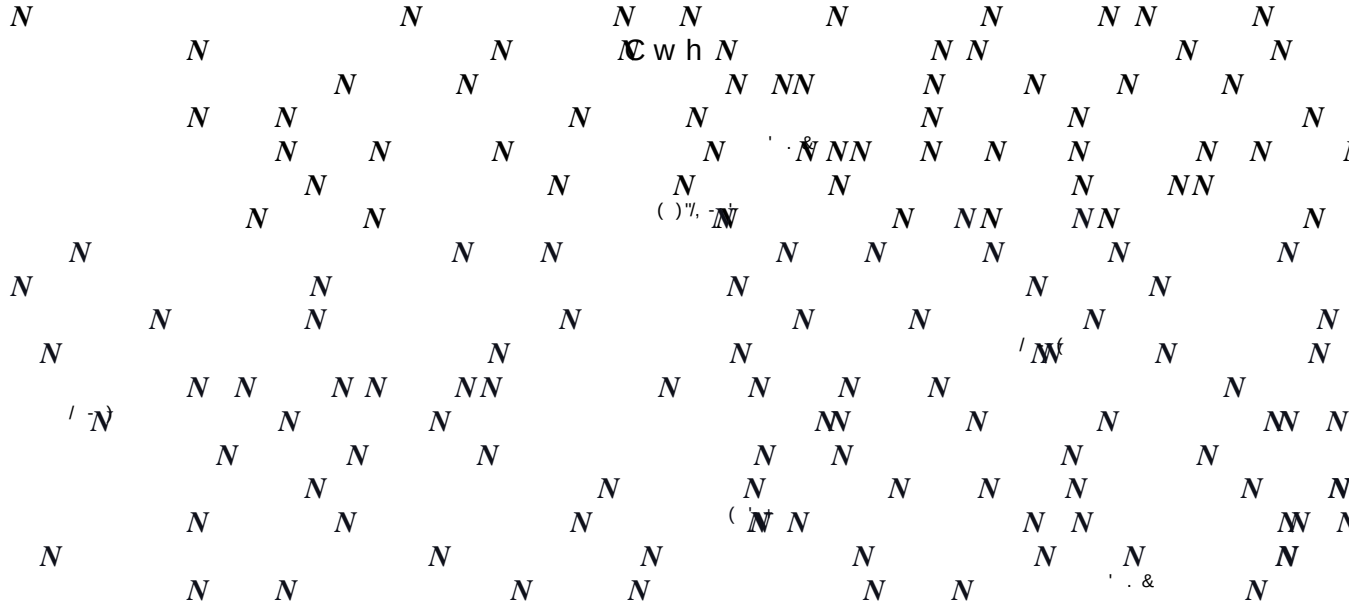
% ($L n/ n B H, J H H e -D n H H c e

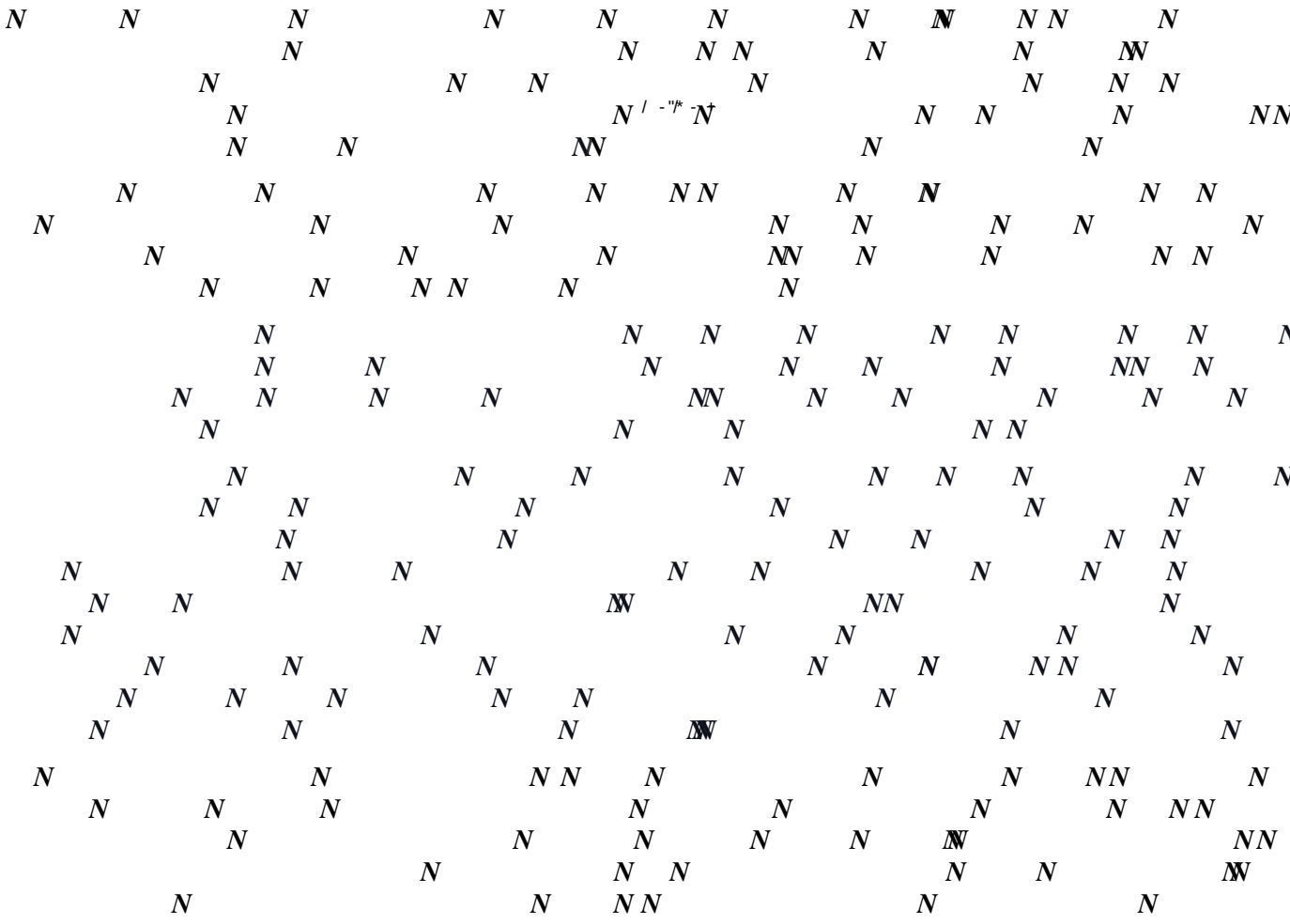


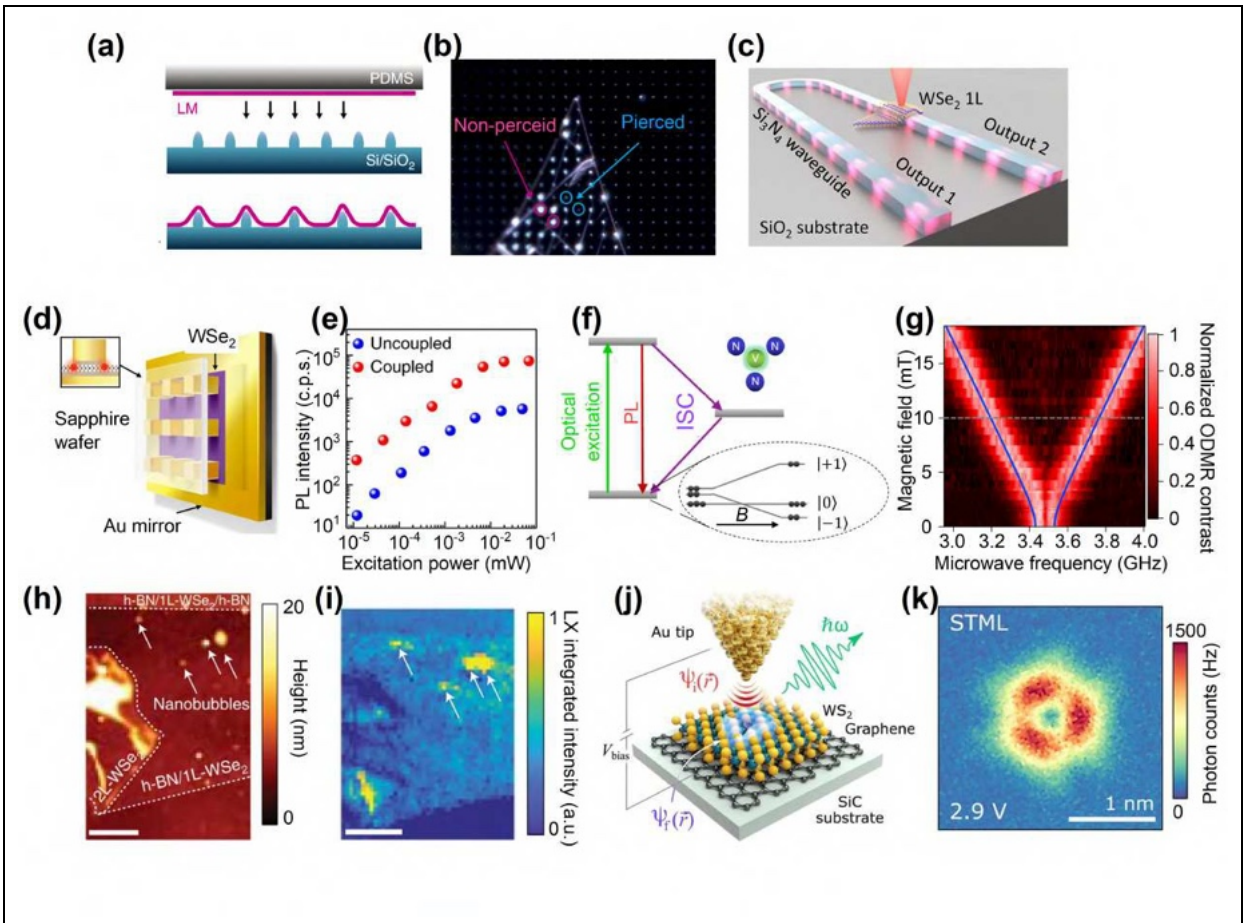


%(%c J j j e , G e k 2 L H L n e 3 D J j k J , i 0 í n e v H í D , k H D 9 e







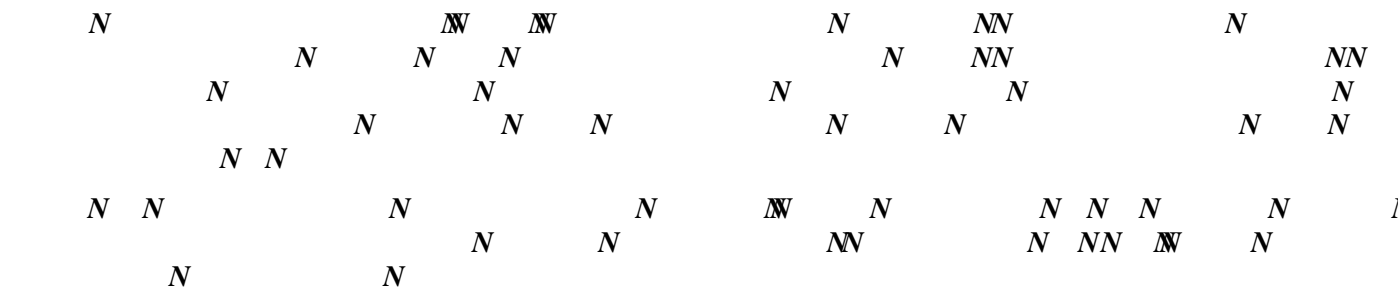


. 5 3 %;(2c E P&ÿpR 8 1 L P 8 ç E 1 1 8 2 '3 Sc#ÿE R 8 ç+S< 1 EçyS 1 EB v 2 vE S 3 v 1 3 2 AS 3 1 E<Ptp& 3 1 2 S E
S 3 3 E 3 1 8 0 1 2 S P 3 6 8 2 L 6 S ç L P L v S N 8 2 o tL<y SLvPE 1wL 8 0 S 0 í 8 2 6 8 L í 2 S ç 1 S 1 1 8 E
6 L 2 ç mD S P 1 D ÿ#ç S 8 6 ÿE E 8 1 v 1 0 8 2 1 3 í '1 E 'y S v ç E y 2 L 3 y L í &N E 8 E 2 ç y S 8 p 0 8 3 8 R 6 1 8 U y E 1 P 3 p
ç S 1 8 2 E S v v S 1 1 E y 8 ' o R 8 N E ç S p p 3 y E ÿ v ç v b D 8 3 2 1 3 2 S S 1 P E L S P 2 8 L S 6 L S 6 ç*L O P) L v î S ç N
U E 1 R S c E Š i ł U S b 8 p D E 0 8 U 6 L 2 D 1 í R D 1 1 L y P R S 2 P L P 8 1 v E 3 P p % o R E E 8 L S P 1 p D 2 2 E 6 P E
8 E 1 R 8 2 1 R 2 L D p R 1 R 8 U S b 8 p 0 D # E 2 0 8 3 3 8 1 y 2 1 E S L P 3 S 1 v S P 3 0 y S R 2 8 0 ç S y 1 L E P y 6 L L y 6 S v S
S p L v 0 ç E 2 2 L 2 S P 0 3 S í í R E 2 8 8 3 # D v g L 3 1 1 2 L S 6 1 8 % s 8 E P H R 1 S 8 P P y 3 E E P 1 p N í b R 8 L 2 1 3
6 L 2 D P y L D í v 8 0 S P 0 y L D í v 8 0 T c 8 E ž 3 3 8 E q L E P 1 1 U 8 R 2 8 3 P % y 0 L 8 D ç í L v P 8 3 0 1 2 1 S L 1 E L
" 6 c # E ç í v E 6 K v 8 8 0 b 8 8 v P 8 0 2 E p S N p 2 S ç 6 L 2 1 R 8 P 8 p S 1 E 1 b 2 8 S v 1 N E P y p R S p 2 2 p L 8 D 0 P 0 g % L 2
S P 0 ç 8 1 S 3 1 p S # g b v L 8 v D 3 1 1 E S L 1 P 8 3 L '6 "1 R 8 u < t e 3 y E p 6 P E S 8 v v 0 U E S 1 R í v S E P 8 0 8 5 í 1 S 8 2
R 8 5 S p L P S v y S 5 E R # 3 9 " I : t Y 1 Y L í y L # p 2 L S 6 í R P N : i L '6 "R : i (T c 8 ž P S P L g D g g
' E % K O R P 1 8 p 2 S 1 8 0 s E P 1 8 P 3 E 1 N b & ç S í K 1 * R 8 V * B c , 8 ž 8 P P 8 S 2 P p N g D 2 g S g P v p 8 3 y ' L E
v L y S v E w 8 0 8 5 y E 1 L P 3 " s h # % y L R # 2 ' 8 v o S R L 8 8 0 3 y U S E v 1 8 R g 1 S R 2 8 E 1 P L 0 í E L y p S 2 1
" A c # y R 8 ç S 1 E y L 6 3 y S P P E P p 8 E 1 P D 0 P D P y 8 8 v 0 E P í p R L ç 1 E L y P 2 L 8 8 g y E L 3 í 3 N E L ' P c o 6 t 2 # L ç
p 2 S í R 8 P 8 S P 0 S c E ; 3 D g 3 1 2 S 1 8 % U R 8 6 2 # 8 í 8 E y P 1 8 2 v S S v 3 v 1 N E y E P 1 1 D 8 P p P 2 8 S v
ç S í L 6 S 3 D v 6 D 2 b S y S P y 1 N S P E 1 P y T D c 2 ž 2 % 8 P S 1 y m L D 6 E 2 0 8 0 5 U + E) 1 R P 2 9 S , S y P L 0 P 3
; L 2 2 8 3 í L P 0 E P p í R L 1 L P S P 3 y 8 L S D % P g 1 # 3 S S 2 2 8 8 2 8 S 6 0 E 8 3 í 1 v 8 S D N 8 6 E 2 p L P ç 2 E P ÿ p) 8 0 2
i S 1 # 0 2 8 S y P 8 v E 3 S 2 8 8 S f " 1 ; 8 0 í N 6 2 E p ç R 1 +) + * 9 ç 8 4 2 E í y S S P P 8 6 v 2 , # R 8 S ç E S y f S 1 v 8 0 c
6 2 L 2 8 ç 6) " + ; L í N 2 E p ÿ R 2 1 E P + p) 8 # 2 í i 3 S P 6 # D v 2 S 8 2 8 S 0 2 8 6 ÿ 1 " 8 ; 0 L í 6 N 2 1 E ç p ÿ R 2 1 E P + p) 8 + 2
i S 1 # 0 2 8 3 S " P K # E v S 2 8 S 0 2 8 6 ÿ 1 " 8 ; 0 L í 6 N 2 1 E ç p ÿ R 2 1 E P + p) 8 # 2 í i 3 S P 6 # D v 2 S 8 2 8 S 0 2 8 6 ÿ 1 8 0 6 2
* 1 ") ; L í N 2 E p ÿ R 2 1 E + y) + P 9 3 3 L y E S 1 E L P 6 # 2 1 R 8 9 0 b S P y 8 ç 8 P 1 L 6

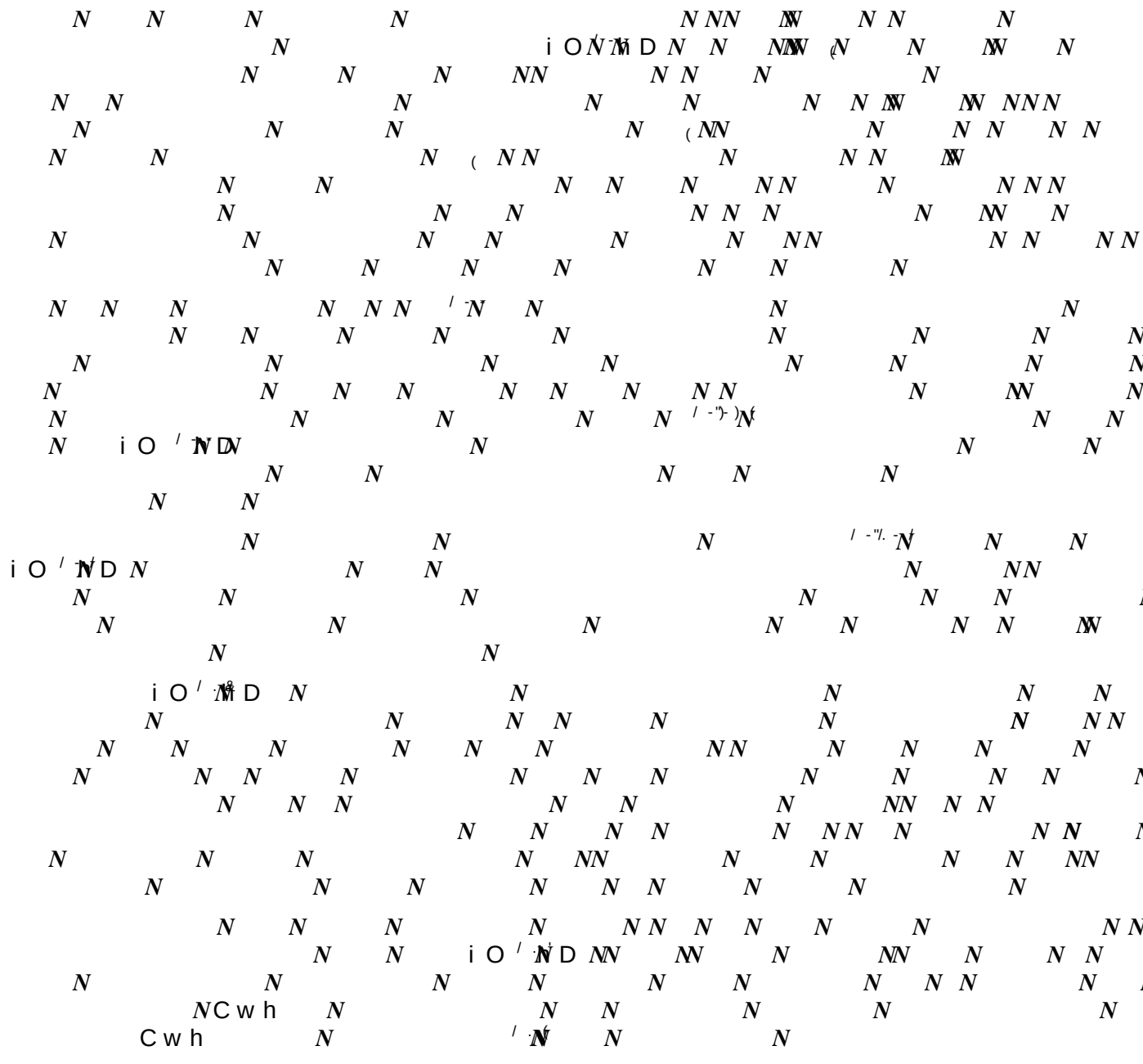
& * /! . : 1 . I 1 N 0 I N 1 2 2 : 4 6 : 2 2 1 6 : 4 3 ; 1 8 6 4 5 I 2 9 6 I I
I N : : 2 8 6 : 4 1 2 T 6 0 2 .

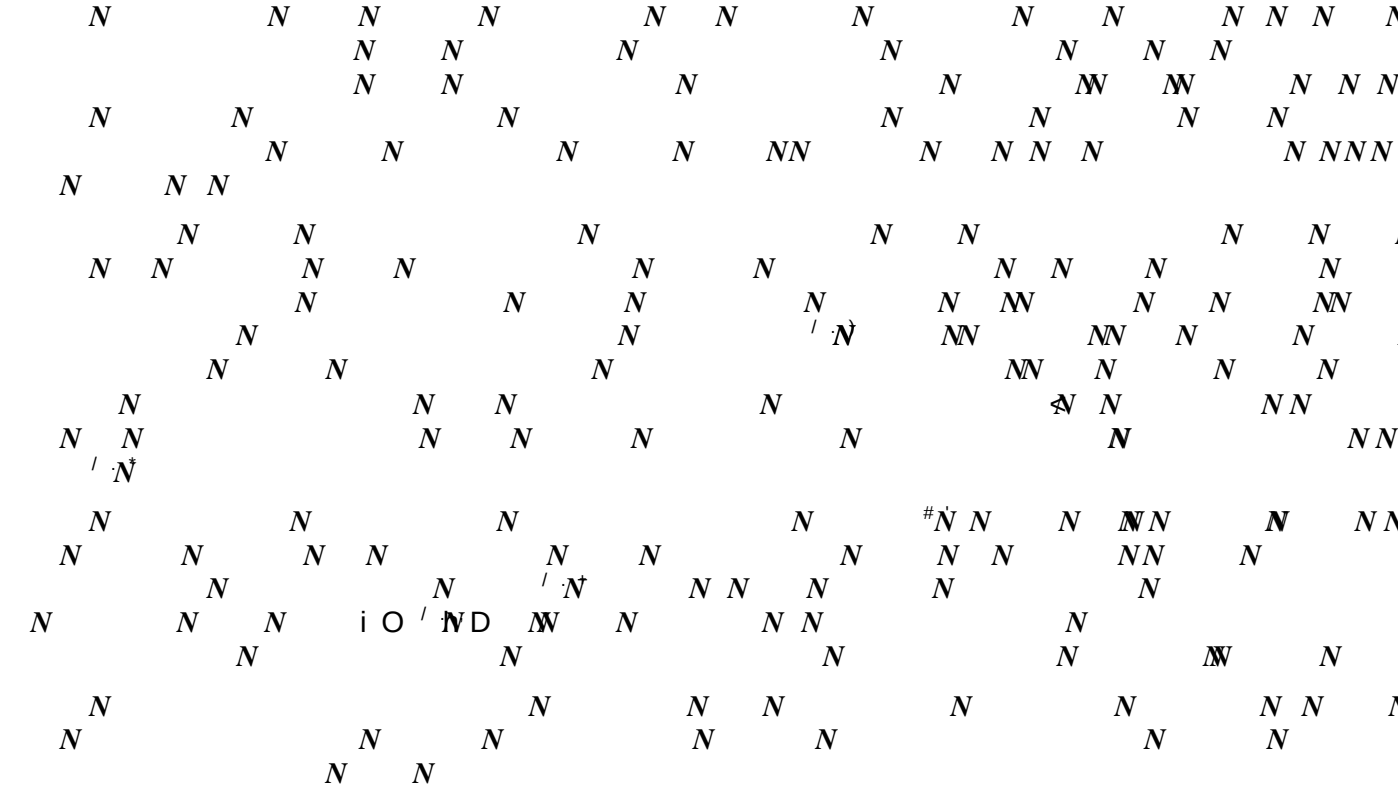
B D H í n í D k <" J N J i D N D U j k D k D K D H , m
$ R L 1 L P E y 3 s S g E L y 2 F S Z k y R D N %) 2 = ρ % a D E 1 w 8 2 v S P 0
- 9 ; ; 2 < : 9 8 1 = 5 ç 8 S 3 E D 0 3 * S = 3 4 ' 9 P ; L ! b L 1 P N 8 8 1 R w ' y R

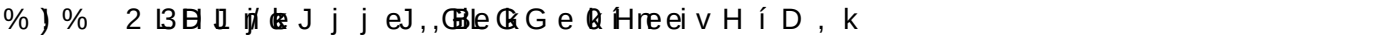
%) F , H n L D v N í D ,

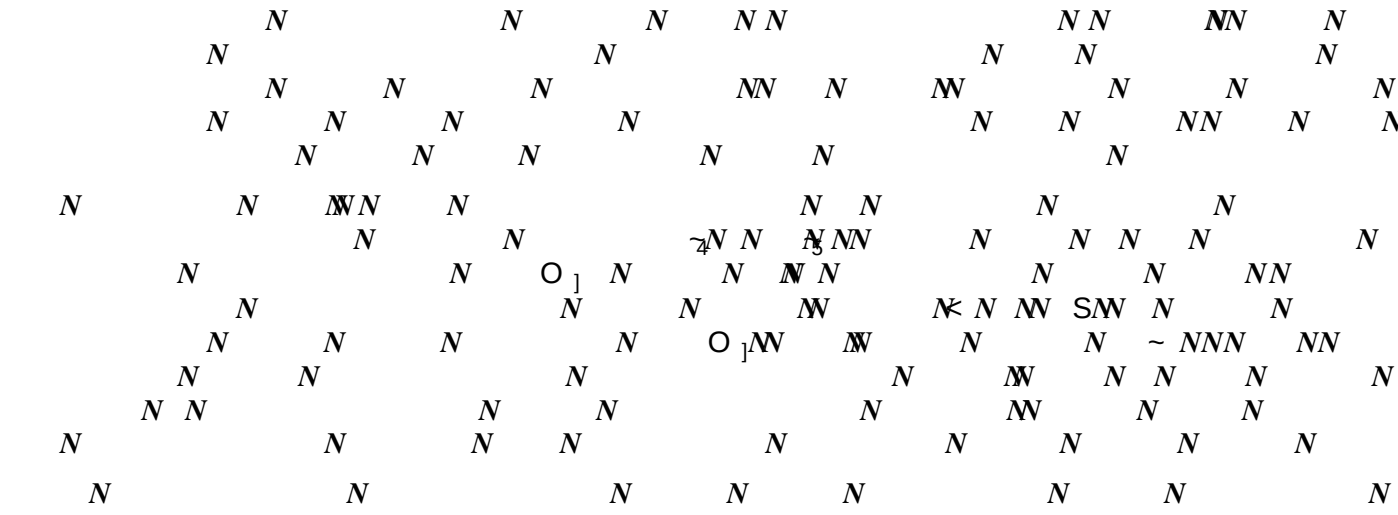


%) $ L n n B H , J H H e - D n H H c e









coupled to the tunnel junction. This is an area of ongoing exploration and it highlights the richness of control parameters involved in the design of simple single-QW structures (Figure 37a).

As pointed out above, the quantum efficiency of a light-emitting tunnel junction depends on the ratio of inelastic to elastic electron tunneling.[988] Elastic tunneling is responsible for a background current that is not coupled to any electromagnetic modes of the system. One way to suppress this background current is to use electrodes with no electronic states of low energy into which electrons can tunnel. Therefore, semiconducting materials like TMDs can be of interest as electrical electrodes. In fact, tunnel junctions with TMD electrodes have been shown to depend on the twist angle,[989] which provides control through momentum engineering as in the case of graphene electrodes. A major challenge, however, is the efficient injection of electrons and holes into TMD electrodes since Schottky barriers are formed at the TMD-metal contact regions. A possible solution is to control charge injection by gating.[92] Gate voltages not only control charge injection but also the Fermi level of a TMD which can strongly enhance or suppress radiative recombination of excitons.[366] All these parameters have to be fine-adjusted to achieve efficient exciton emission.

In conclusion, band-structure engineering of tunnel junctions offers numerous possibilities for device innovation through layer combinations, twist angles, and bandgap selection of 2D semiconductors. However, realizing these designs requires extensive experimentation to address feasibility and to uncover new physical phenomena within these heterostructures.

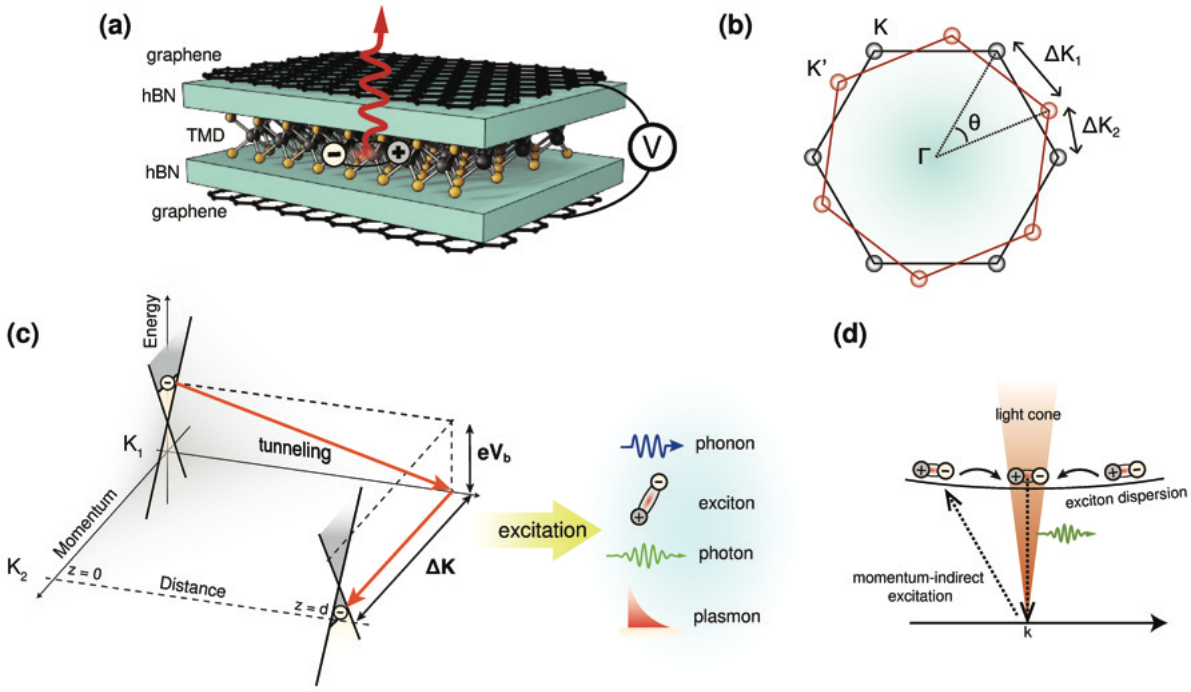
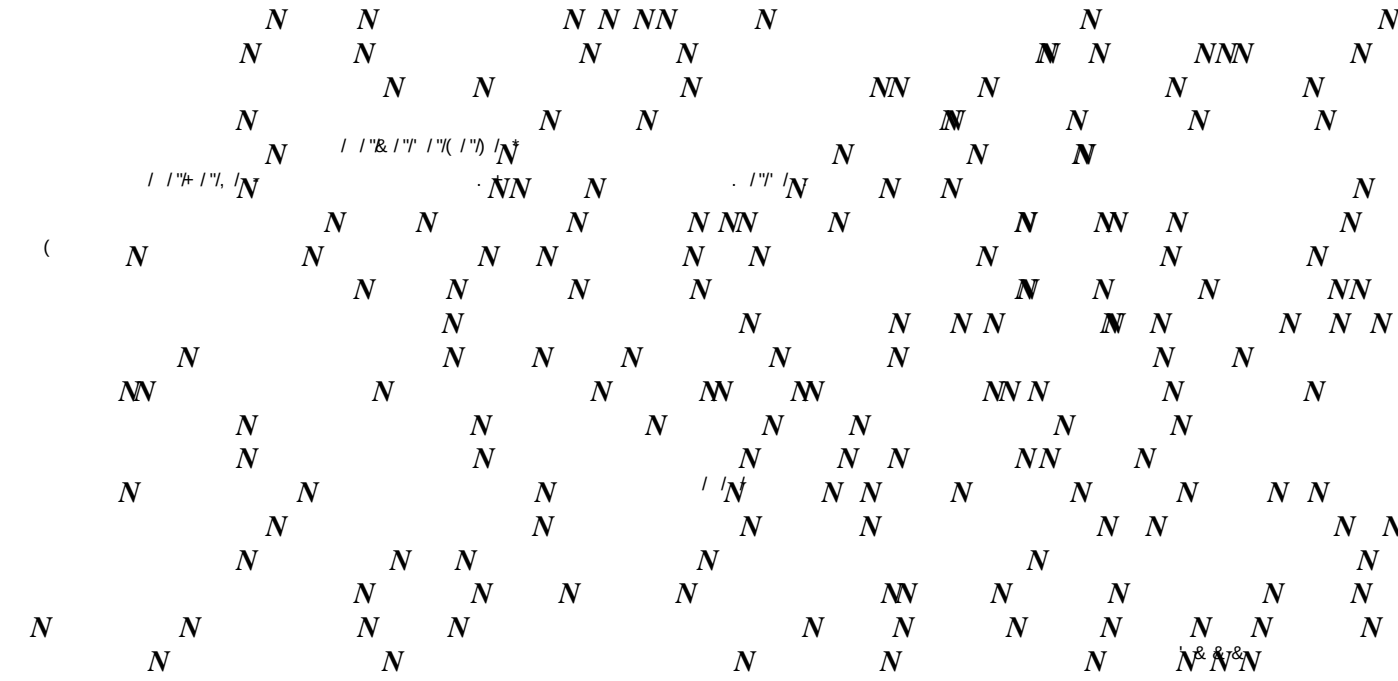


Figure 37. Inelastic electron tunneling between graphene monolayers. (a) Schematic of an all 2D quantum-well type light-emitting device. Charge carriers are injected in the device through the two graphene electrodes. Light emission is facilitated by exciton generation and their subsequent radiative decay. (b) First Brillouin zones (1BZ) of two graphene layers overlapping with a twist angle θ. This leads to a momentum mismatch between the two layers of $\Delta \boldsymbol{K}_1$ and $\Delta \boldsymbol{K}_2$ for neighboring K points. (c) A 3D expansion of a band-diagram to accommodate for both energy and momentum conservation, representing an inelastic tunneling process between two graphene electrodes. The three axes represent energy, momentum, and distance along which tunneling occurs. The initial and final states of the tunneling electron are separated by an energy eV_b and momentum $\boldsymbol{\Delta K}$. The inelastic tunneling process occurs by exciting modes (e.g., phonons, photons, excitons, plasmons) that can fulfill energy and momentum conservation. (d) Momentum-indirect excitation of excitons can lead to direct exciton formation by phononic relaxation at the light cone.

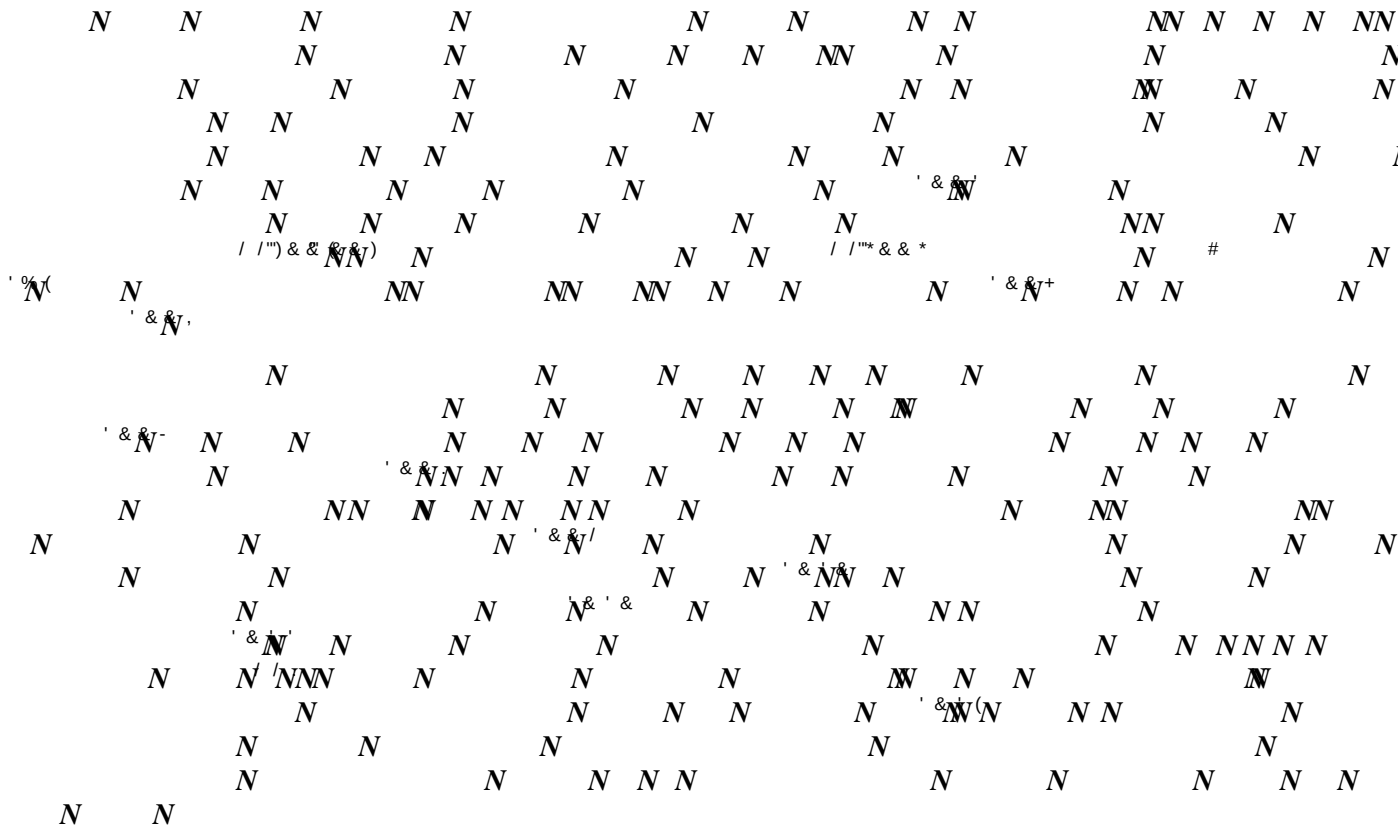
&+<1 ; . < 2 0 I . 6 : 3 . 1 6 : 3 1 . 1 2 1 < 5 ; I ; : 6 0 1 2 T 6 0 2 .
N : 0 ; : T 2 : I 6 ; : . 8 8 6 4 5 I . ; N 1 0 2 .

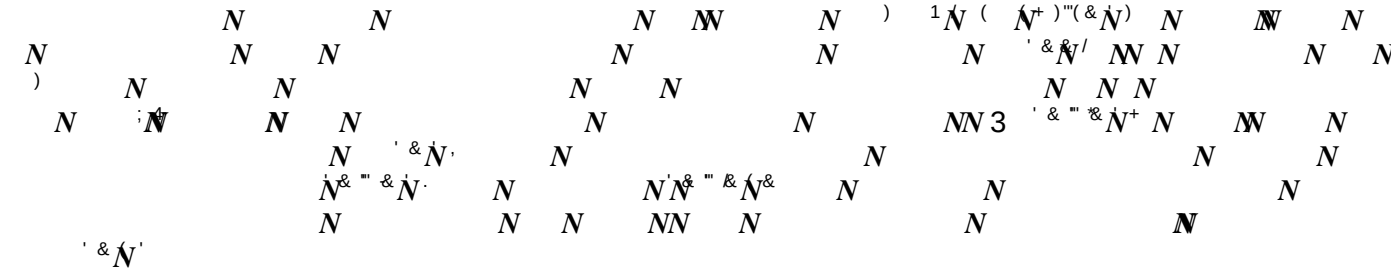
8 e D , J n iJD, 9Rín HíBJeon eR ,í JH Ï e j j D
$i = c o % &O;3 i1eE 1 D 1 L i S P L 3 y E 8 Pw 8 S P 0 c y D L v S* + %L 2 çES3vS8 . c/D* í+8 02%E I
- 9 ; ; 2 < : 9 8 1=5ç8S3E ÇvO3*E=S4ç9' ;b!E 1 E 8 v v L 8 3 P 3 ' E 1

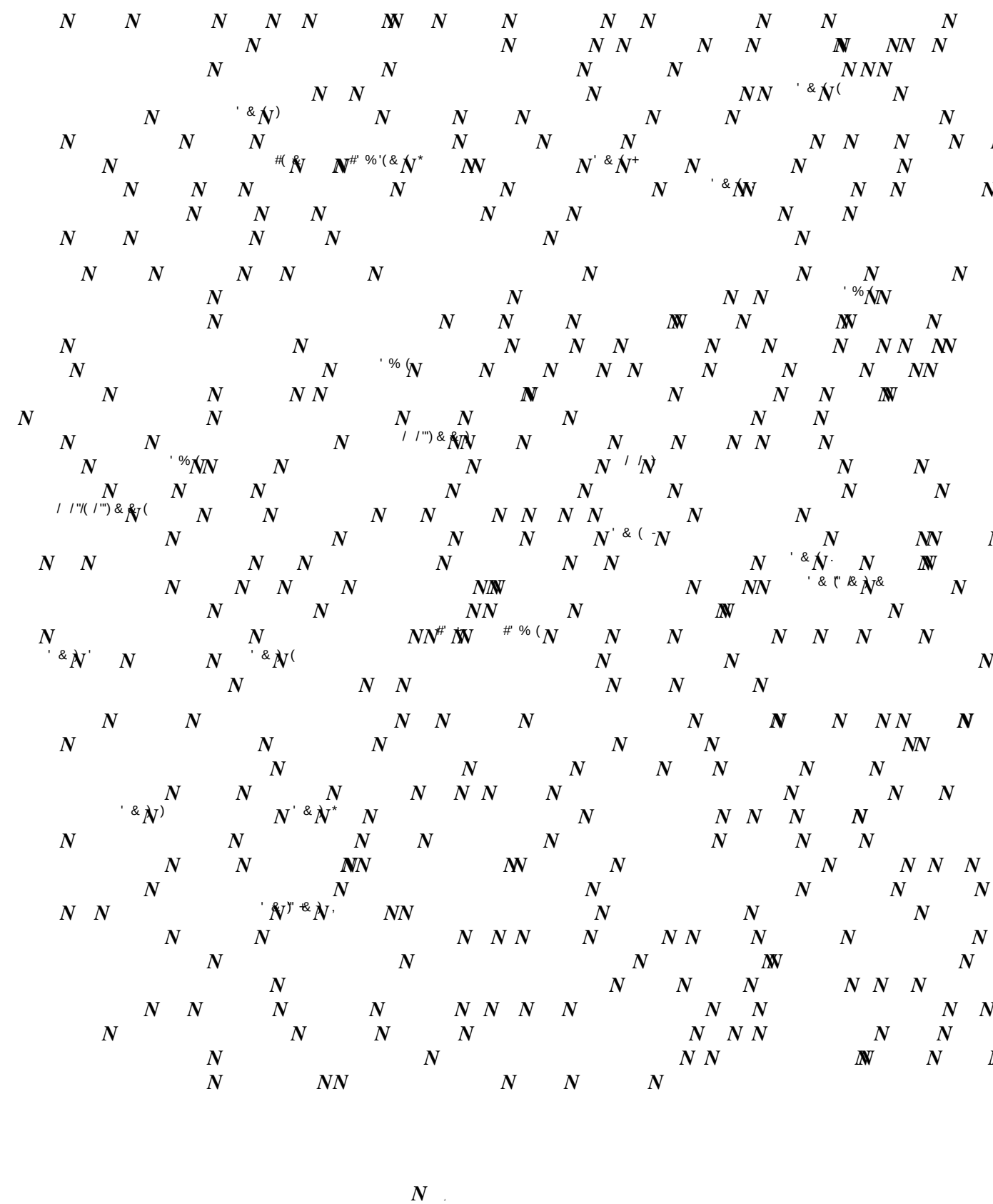
%!# 5 , H n D i L v H í D ,



%!# $ / LBHnJeH,eH-DmH H c e







38.4 Suggested Directions to Meet These Goals

Combining SLG and BLG with hBN (Figure 38b) in a TFET architecture can promise a rectifying capability of the junction (Figure 38c), orders of magnitude larger than that achieved in a standard FET, which translates in significantly higher sensitivities. The concept is frequency scalable (from 0.1 THz to 10 THz) across the entire sub-THz and THz ranges. TFETs can hence offer concrete perspectives for detecting nonclassical states of THz light that could be for instance generated by miniaturized quantum sources such as THz QCL frequency combs. This can open exciting opportunities for developing THz quantum platforms all based on miniaturized solid-state devices, which can also be integrated on-chip.

Graphene can also potentially allow one to develop a miniaturized solid-state platform for the generation of nonclassical squeezed states of THz frequency light. High-order $n > 5$ harmonic frequency combs with quantum-correlated sideband modes and a custom-tailored output spectrum can be for instance sculptured by embedding on-chip integrated local graphene frequency filters (Figure 38d) that suppress non-harmonic modes, preserving defined high-order harmonic modes.

The recent demonstration of third-harmonic frequency upconversion in graphene at high THz frequency (9.63 THz)[1021] anticipates major advances in the field of innovative nonlinear light sources. As an example, novel integrated solutions for light generation in the *Reststrahlen* band of conventional III–V semiconductors (6-12 THz), where optical photon absorption hinders band-structure engineering for light emission, can be conceived. A spectrally narrowband technology to entirely access this range does not exist. Available technologies (thermal sources commonly adopted in Fourier-transform IR (FTIR) spectroscopy, spintronic emitters, or time-domain spectroscopy (TDS) systems, which rely on III–V photoconductive switches) suffer from poor performance or are cumbersome and lack stability (as, for example, difference-frequency generation in gas lasers (e.g., NH_3)). Distributed feedback Bragg grating cavities in double-metal QCLs are particularly suited for graphene intracavity integration, stemming from the possibility of lithographically engineering gratings of shape, pitches, and depth designed from scratch and tunable on purpose. Although technologically challenging, engineering graphene plasmons in a specific fashion in a ribbon grating superimposed to a distributed-feedback-laser pattern on a QCL resonator can provide the field enhancement needed for harmonic generation (HG) and can offer a valuable solution to engineer a monolithic, electrically pumped solid-state source in the 6.5–12.0 THz range. The patterned ribbons can allow optimizing the nonlinearity, since the HG efficiency depends on the carrier concentration, which can be locally tuned, for example, by gating. Importantly, unlike in other spectral domains, only moderate THz fields (< 40 kV/cm) are required to induce HG in graphene,[1014] comparable to those available from THz QCLs when electromagnetic radiation is confined, for instance, *via* plasmonic effects. This represents a long-dreamed frontier in THz photonics.

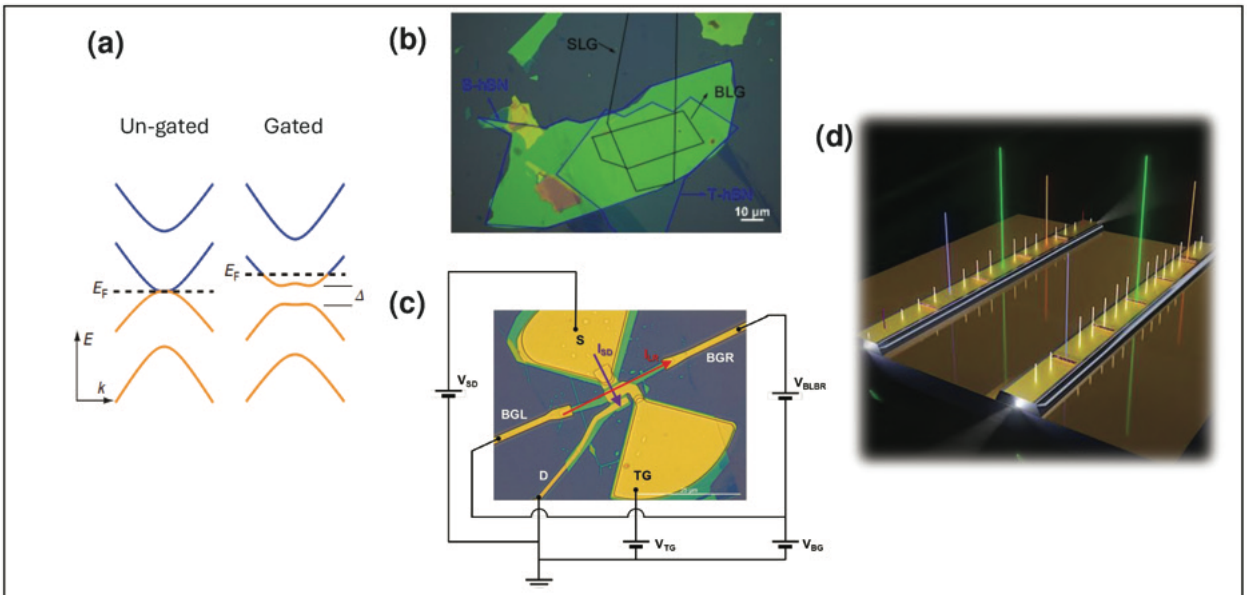
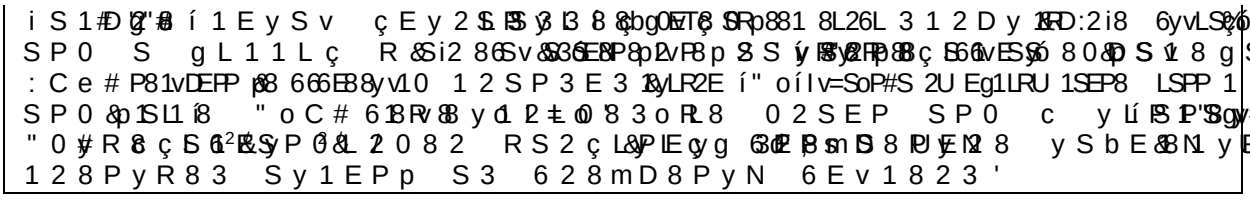
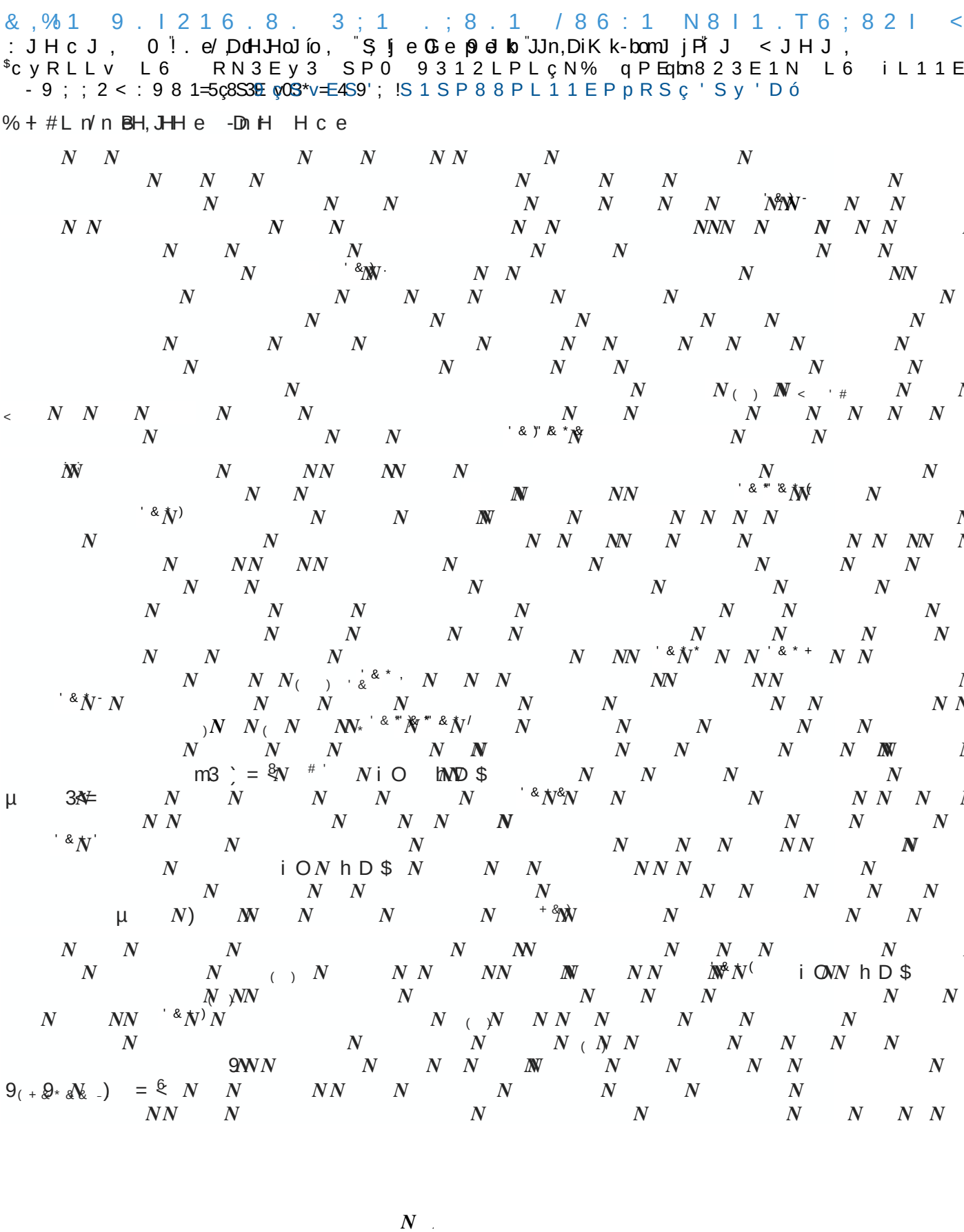
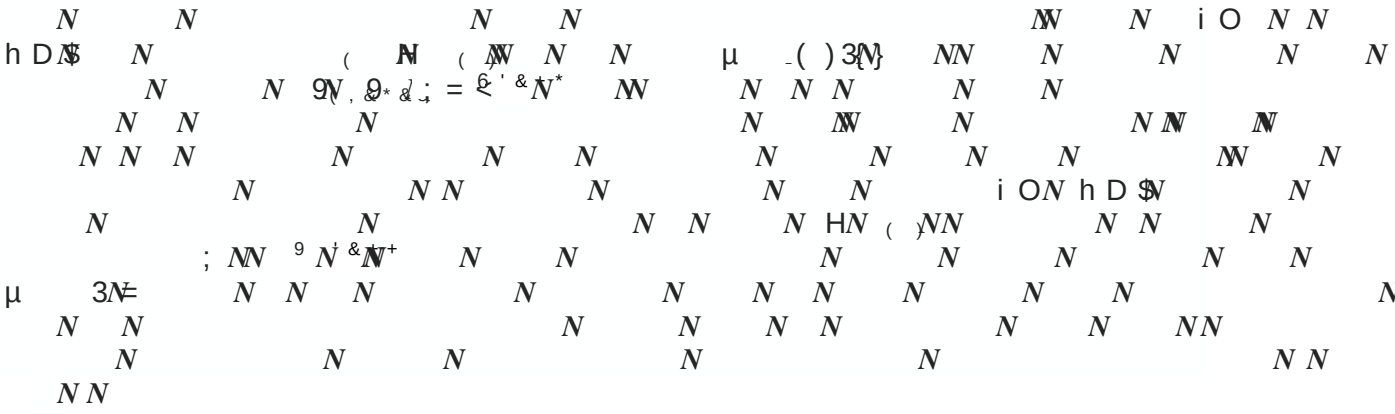


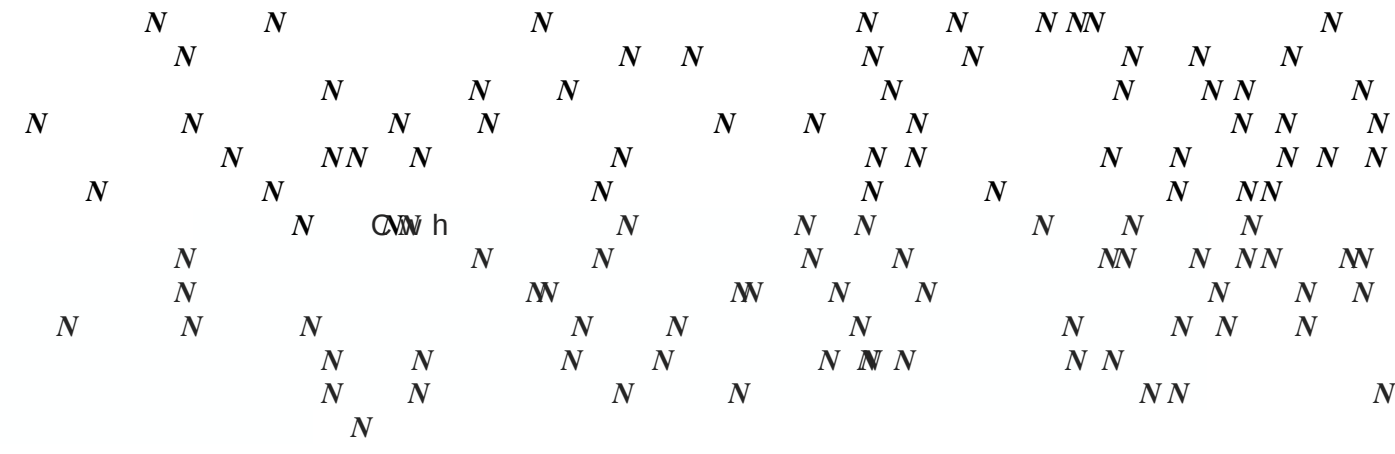
Figure 38. Graphene-integrated THz frequency devices (a) Schematic representation of a bandgap opening in bilayer graphene (BLG) induced by an out-of-plane electric field. Adapted from ref 1030 (Copyright 2009 Springer

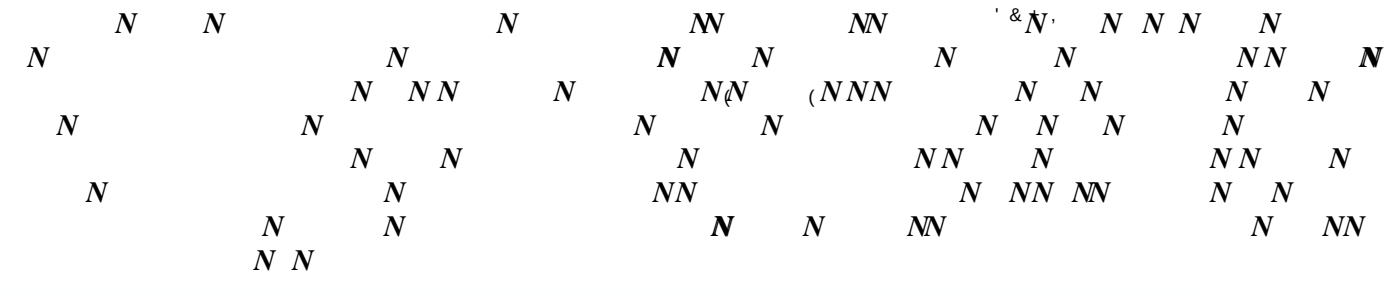




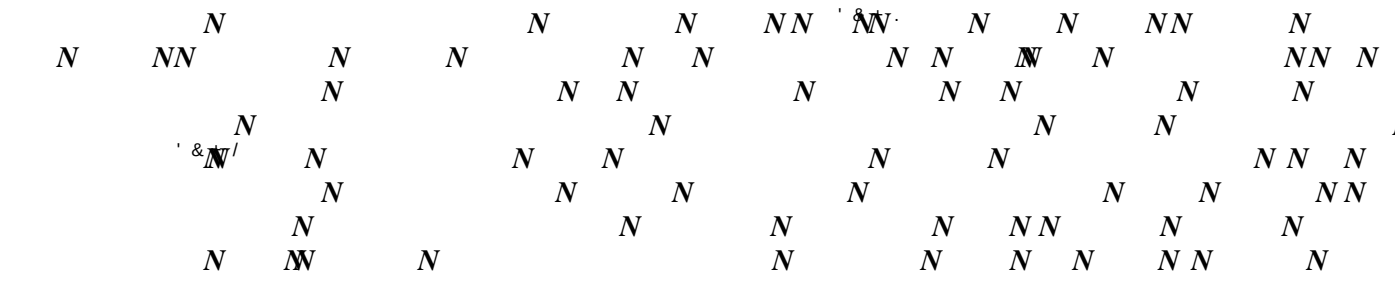


%+$cJjje,2LeHkL3nDeJjk





%+%L GBGe0HHeevHíD,k HD 9eeH Sceke 3DJjk



less common due to the high entry-level costs of the necessary infrastructure and/or the specialized requirements for operational expertise. The fabrication of single and arrays of photodetectors for UV imaging also presents significant challenges. Bespoke fabrication strategies are needed to minimize process-induced material damage and flexibility in the integration of ultrathin and flexible single-crystalline 2D membranes on different platforms, such as with silicon-on-insulator (SOI) waveguides for photonics and Si-CMOS-based read-out circuits.[1060] In particular, new approaches are required to optimize light–matter interaction in the deep UV. Localized surface plasmons can be used to enhance the photon absorbance of 2D materials, but current approaches work mostly in the near-UV and visible ranges.[1061] Finally, as the growth and fabrication of 2D materials advance, new regimes of photodetection can be expected. The reduction in thickness of 2D materials to a few layers or the combination of 2D materials to form new 2D–2D layer structures, such as moiré superlattices,[1062] can dramatically impact electronic properties, leading to new forms of charge, magnetic, and superconducting order, driven by weakly screened electron correlations. These phenomena could enable new concepts for fast and sensitive photon sensors *via* the manipulation of carrier correlations. Other device technologies are phototransistors based on 2D ferroelectrics for self-powered applications and polarization-sensitive detection.[1063] In summary, we can expect a myriad of further developments in this field by advances in the science and technologies of 2D materials.

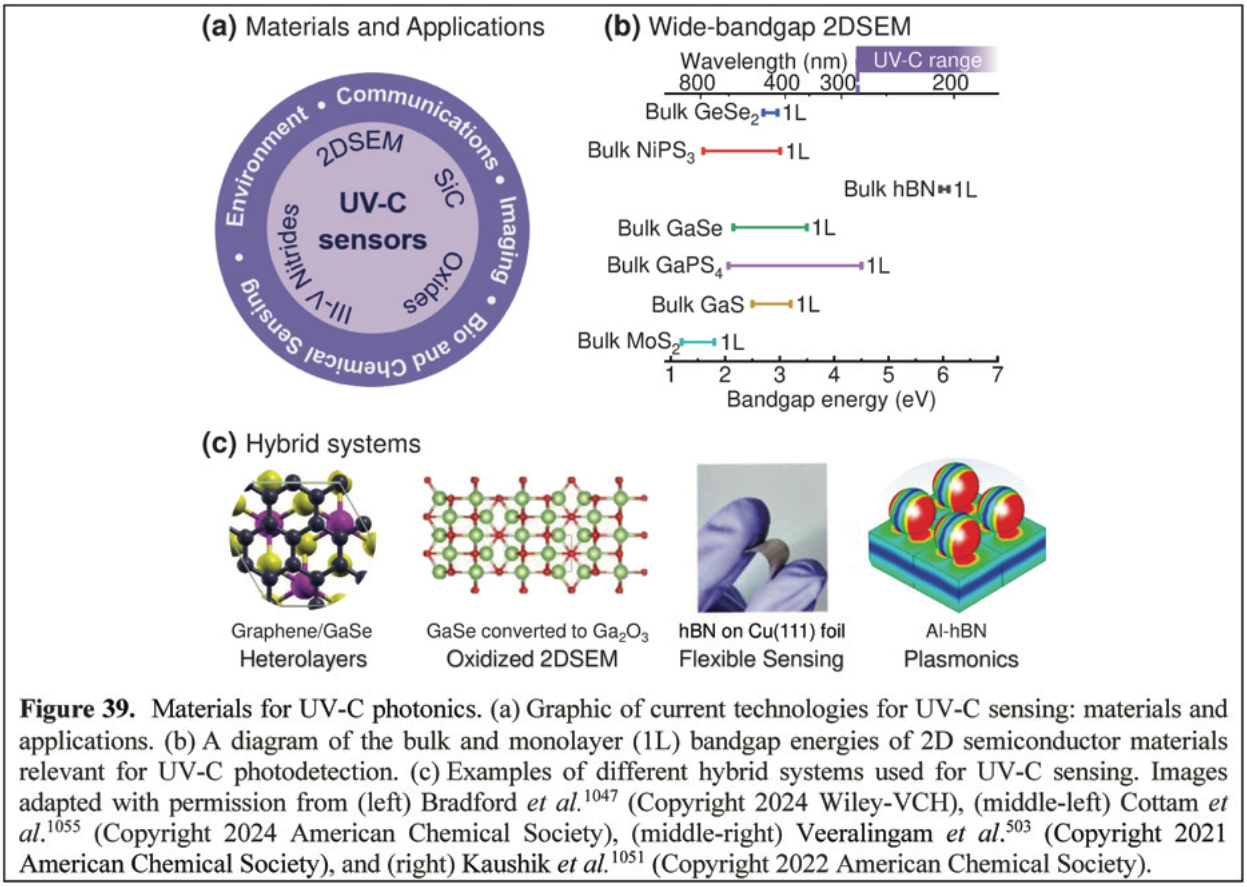


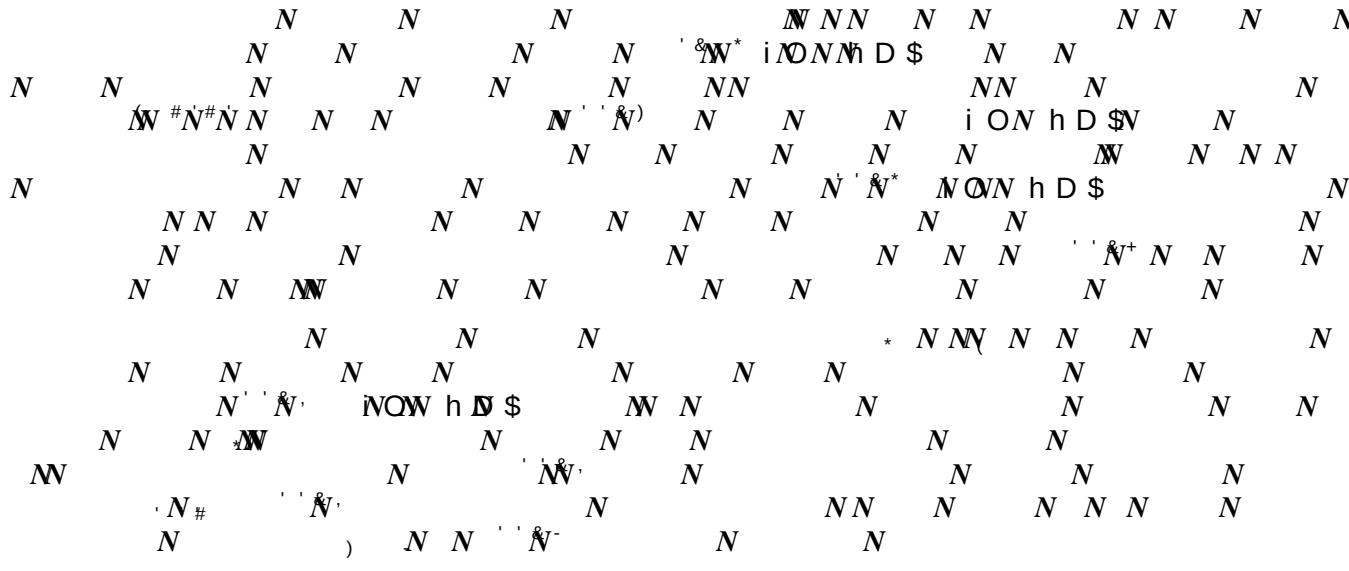
Figure 39. Materials for UV-C photonics. (a) Graphic of current technologies for UV-C sensing: materials and applications. (b) A diagram of the bulk and monolayer (1L) bandgap energies of 2D semiconductor materials relevant for UV-C photodetection. (c) Examples of different hybrid systems used for UV-C sensing. Images adapted with permission from (left) Bradford *et al.*[1047] (Copyright 2024 Wiley-VCH), (middle-left) Cottam *et al.*[1055] (Copyright 2024 American Chemical Society), (middle-right) Veeralingam *et al.*[503] (Copyright 2021 American Chemical Society), and (right) Kaushik *et al.*[1051] (Copyright 2022 American Chemical Society).

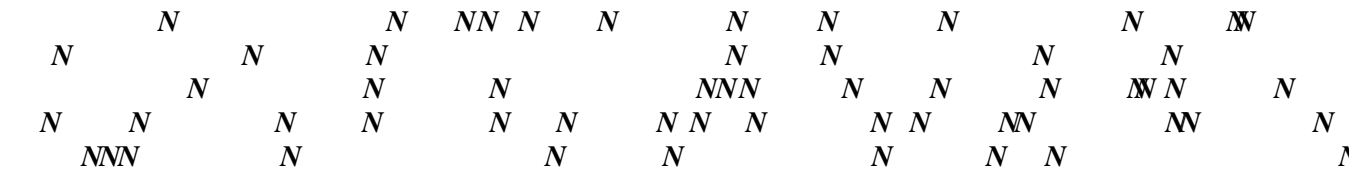
9 iVg i h S t 7 S e s S i g g N e a * S g i a w t 7 e g r e S p g

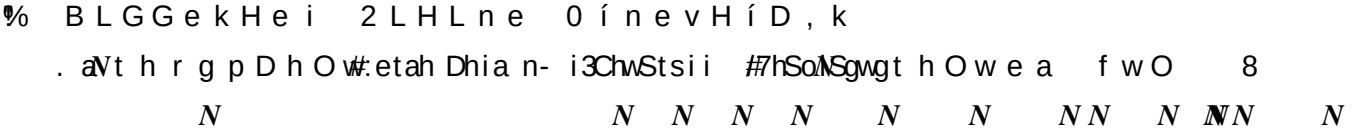
& 9 J H e n í J j / c J j j e , G e k J , i A e v e , H < n D G n e k k

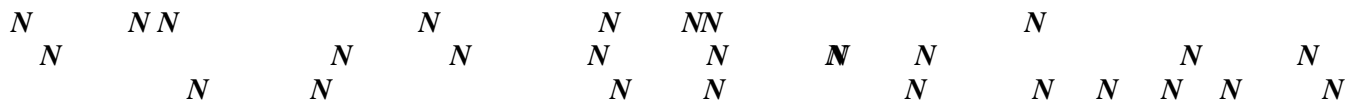
: OVh dVw D w O B

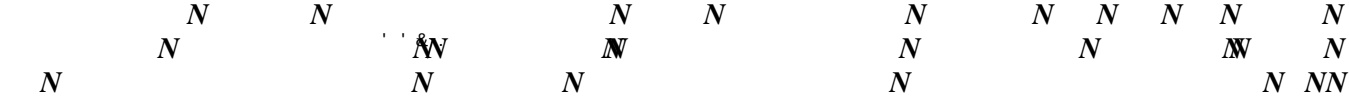
3 hVS s i : t h DVi 7 S e n p t O w e a

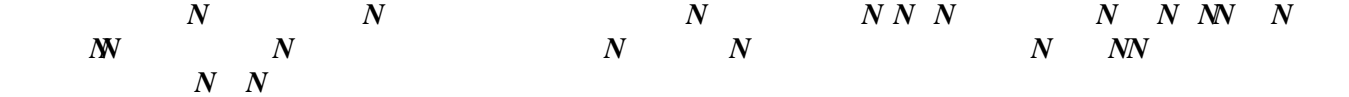


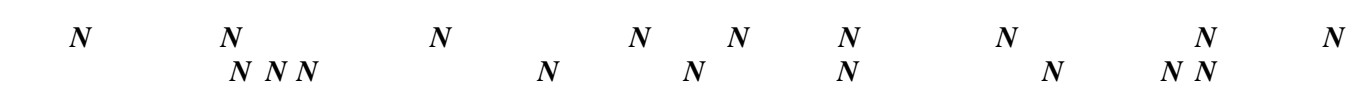


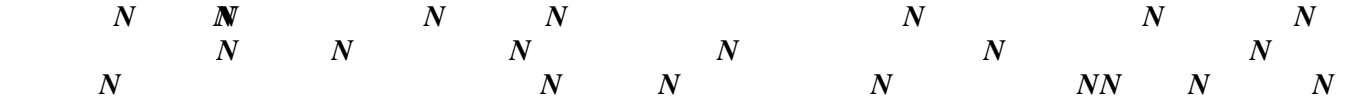


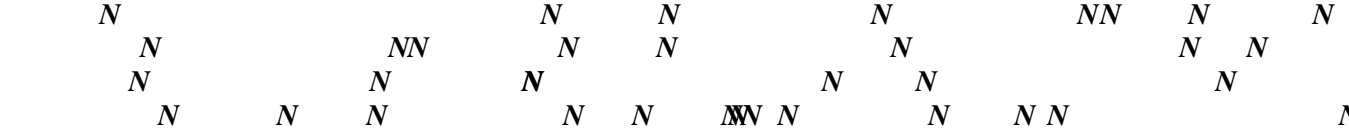


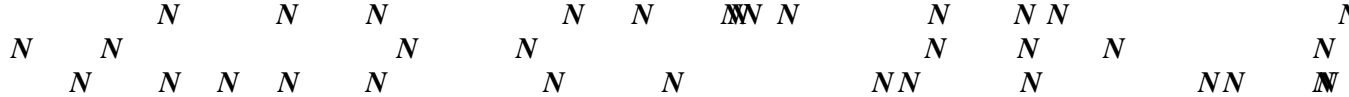




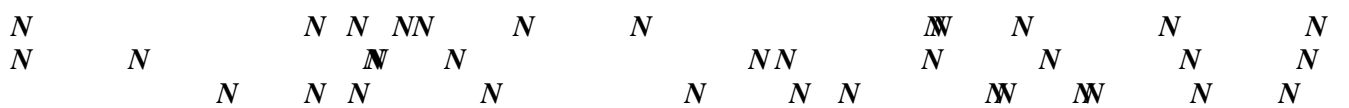


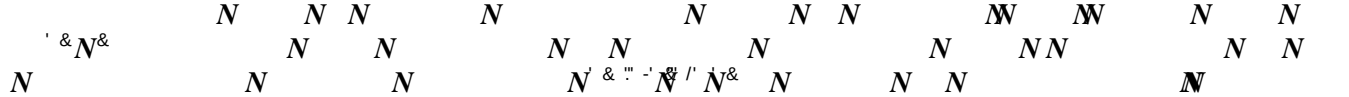


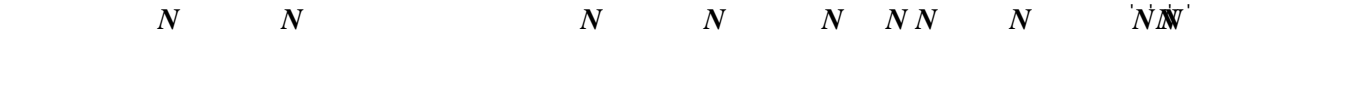




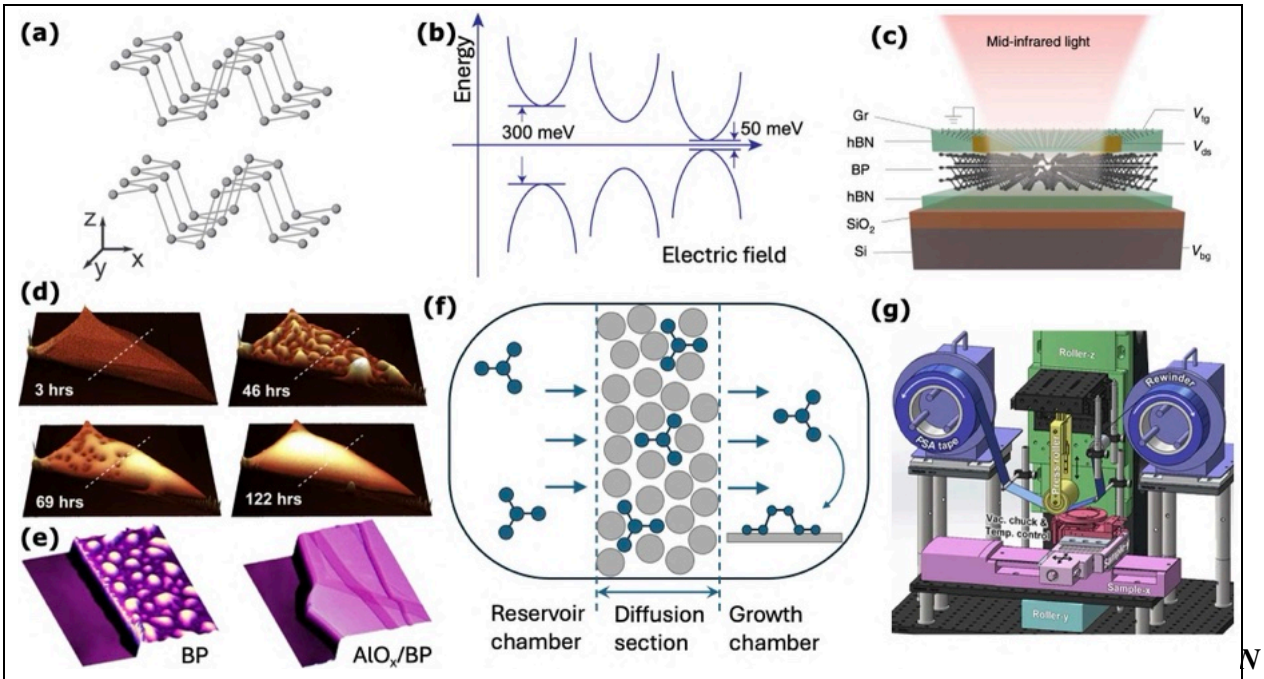












- N N j í v, J H 0 L í N D H , k K e 0 í n e v H í D , k

' $ % 1 9 . I 2 1 6 . 8 . 3 ; 1 < 5 ; I ; : 6 0 = N . : I N 9 6 : 3 ; 1 9 . I

8 e e - ! "A<Dctéjo íJNN "76!Dk6íéN", b.e]dDJoí," J.,niJL<,cíjíN# $CJjHce

$ I S y D v 1 N L 6 R N 3 E y 3 % , E 8 P P S ; 8 P 1 8 2 q 6 P L E 2 b 8 d 2 D 3 S E P 1 1 N D ç L 6 c y, E E 8 P P y F

: L v 1 w ç S P P p S 3 3 8 . % *) 2) , E 8 P P S % 9 D 3 1 2 E S

% I S y D v 1 N L 6 R N 3 E y 3 , E 8 P P S < L y 1 % L 2 : S L v v 1 o w y ç P S L P L P v p S E 3 P 3 8 R . N % 3 E

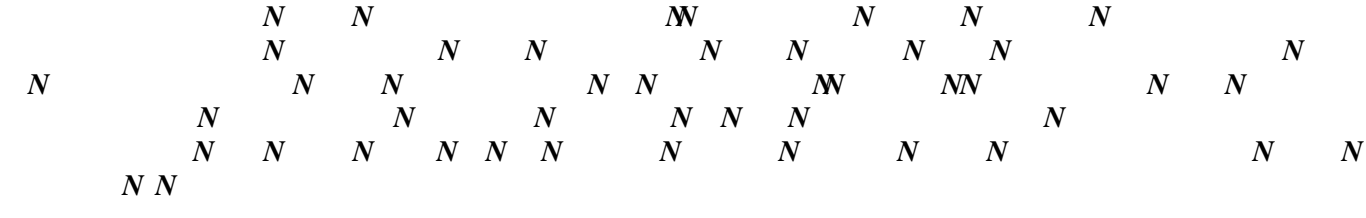
, E 8 P P S % 9 D 3 1 2 E S

& e 8 3 8 S 2 y R i 8 1 U L 2 ó d D S P 1 D ç 9 3 í 3 8 1 y E 1 S 3 P L < 6 L í c í í v S 8 y 2 8 s o S E g ç L 8 2 S ' 1 o L q 2 e N D

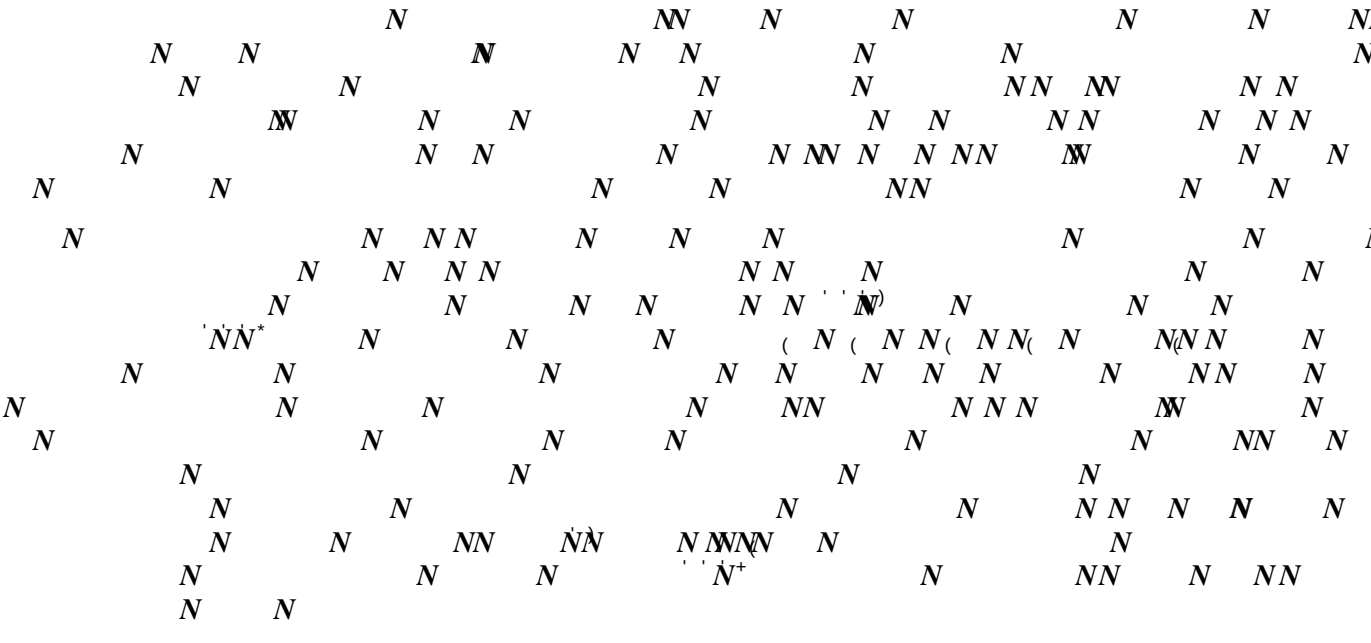
d D S P 1 D ç ; L ç í D 1 8 2 % q P E b 8 2 3 % E 1 * N) 2 L) 6 , , E E 8 8 P P P S S % % 9 : D L 3 v 1 1 2 w E ç S S P P p S 3

- 9 ; ; 2 < : 9 8 1 = 5 ç 8 S 3 E 8 0 3 * ' = 2 4 L 9 w ; 8 ! ç S 8 D P E b E 8 ' S y ' S 1

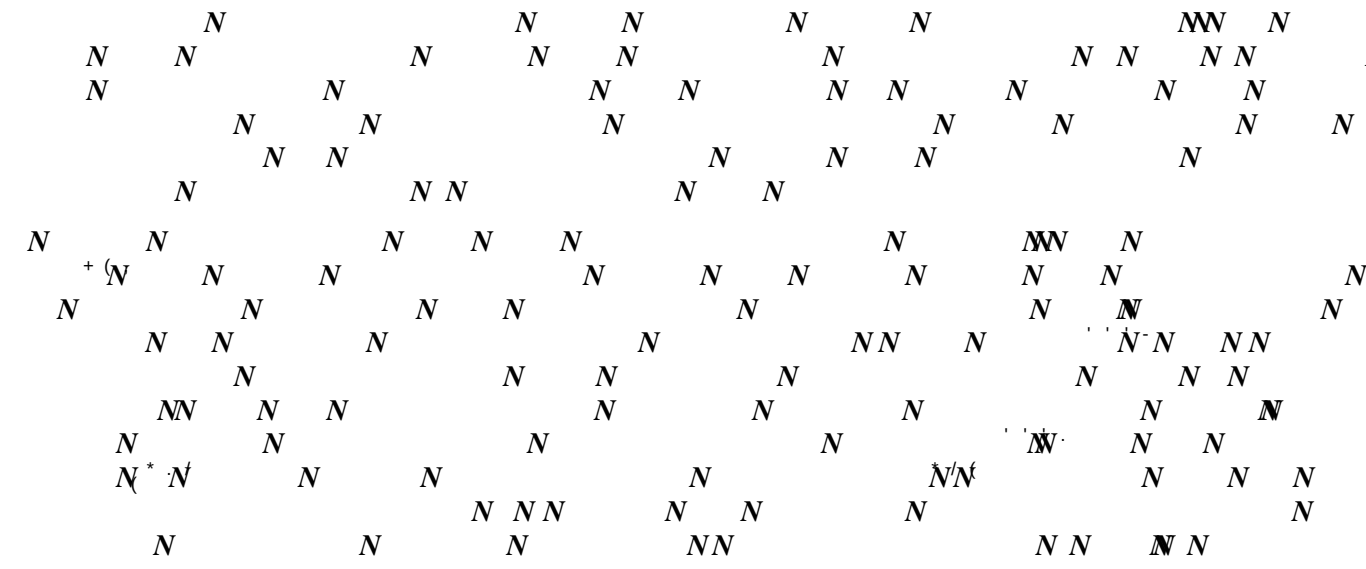
& # # / L n n e , H B H J H e D r H c e - n H



: w a s D i . M w O O i S g



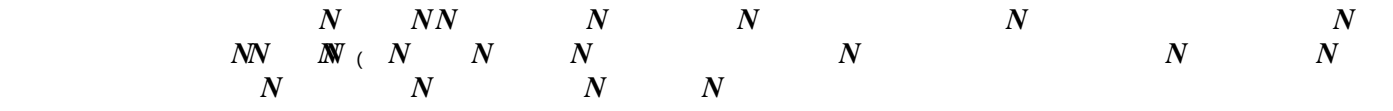
: r a O h a i e p g 7#h S a M i S S w a - e f a



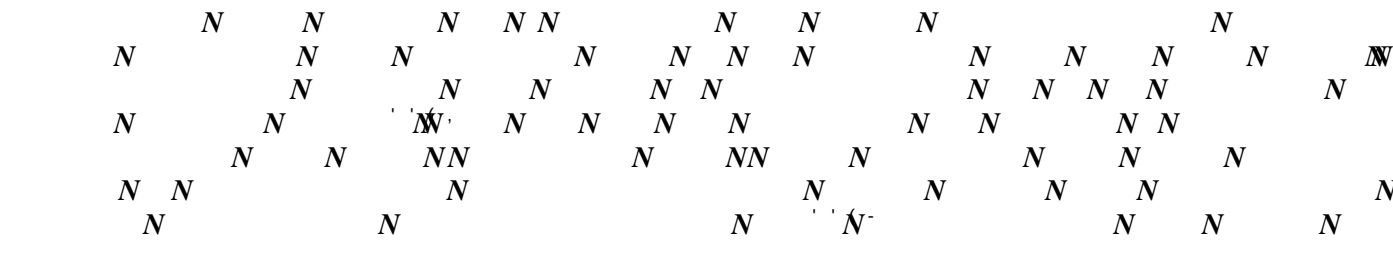
7 D hVg MVe a w t g

& # $ / c J j 2eL, HGLemke 3 D J j k

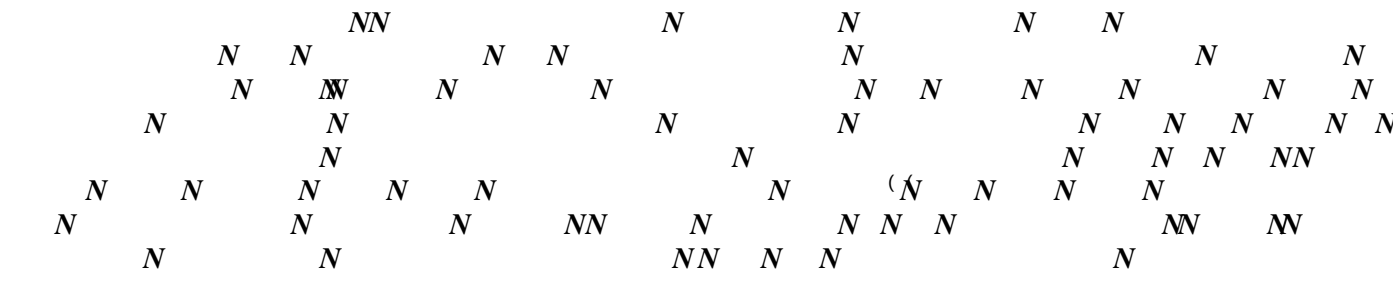
: w aVs D i N . MwOO i S g



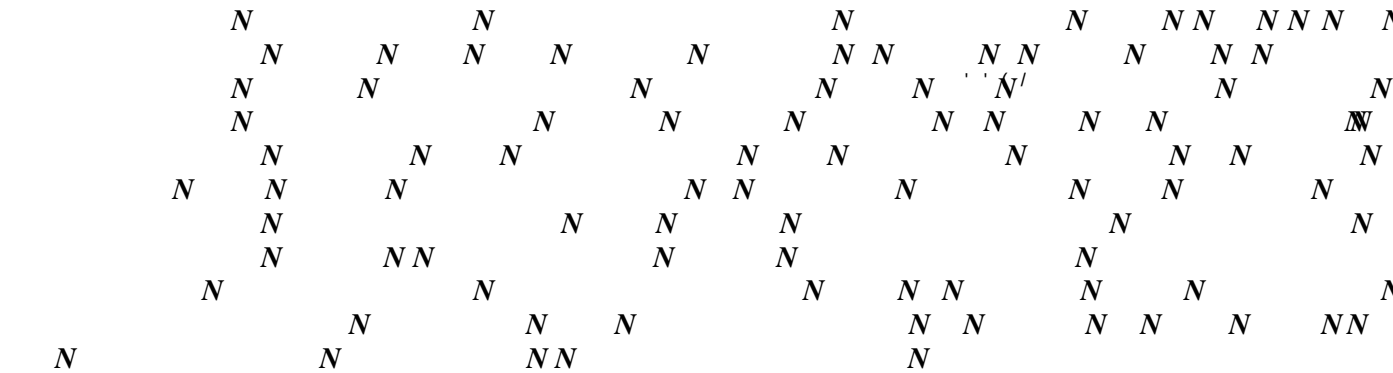
: r aVa Oh a i e p g 7#,eSaMiVSSwe a - e f a

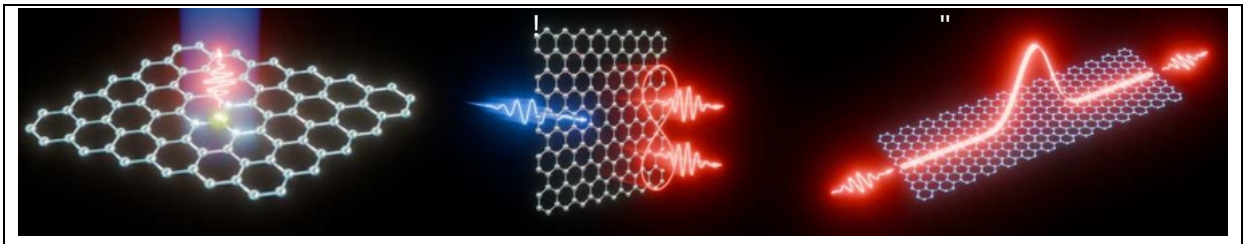


7 D Vg MVe a w t g



&#% B L G0Gíenke-HveHi í D , k H D 9 e e H S c e k e 3 D J j k

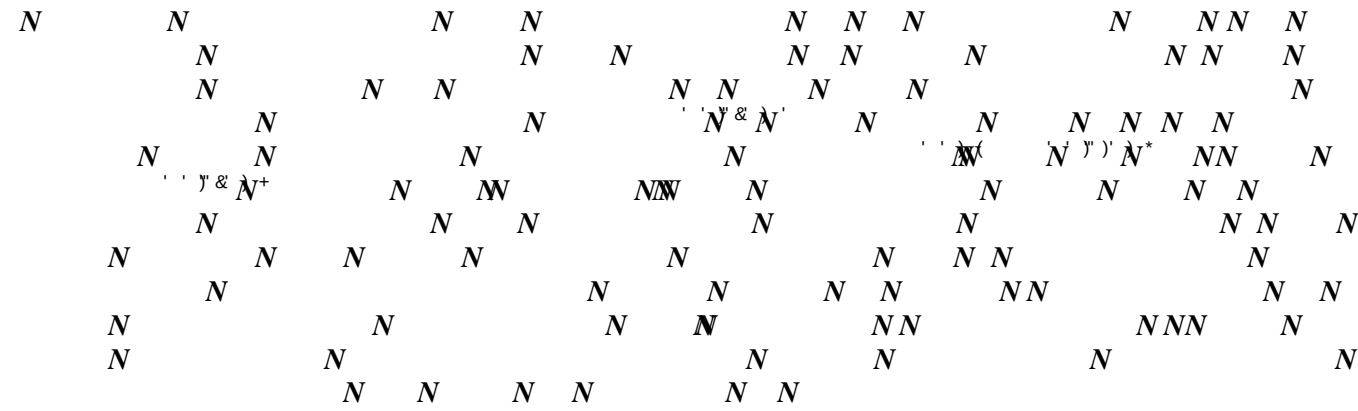




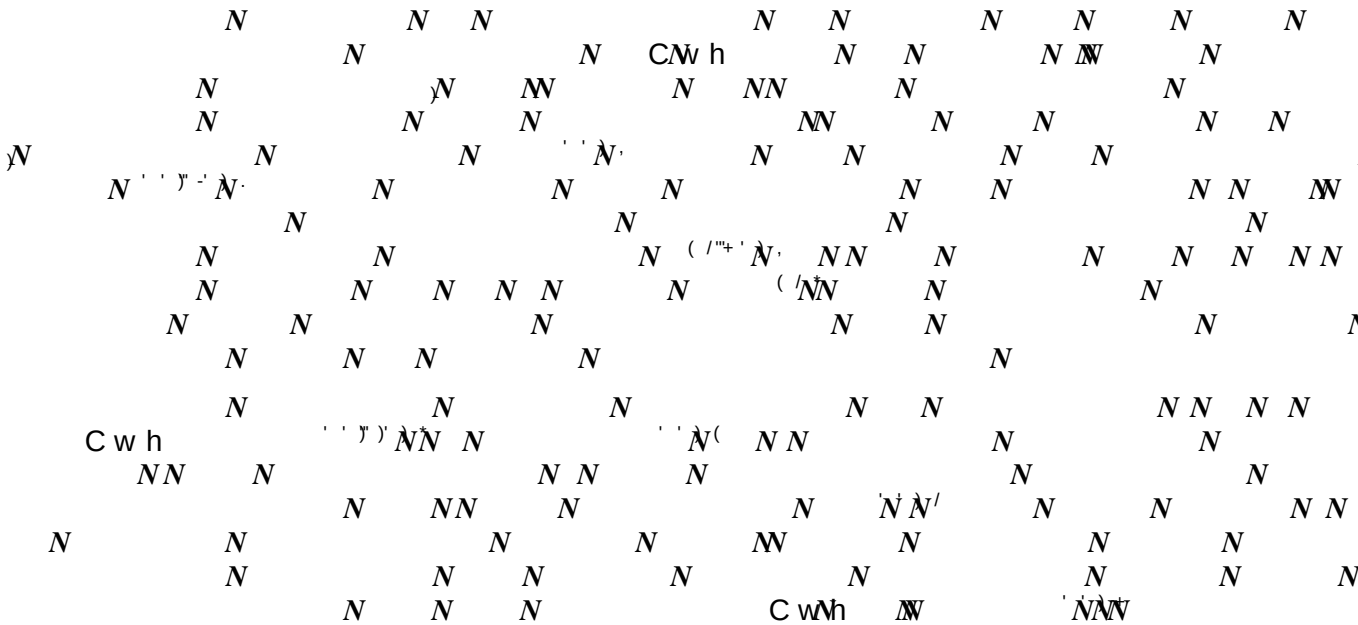
. 5 3 &#2< çS182ESv3 RSb8 1R8 íL18P1ESv 1L 28bLvD1ELPEv
çSóEPp 3EpPE6EySP1 EP23LESRQpSRvL8E1PL P1R8çE01 1 8 2 v 3 1 % í ç' 8 g P # 1 & 3 L í 6 L P ' 1 S #
yLPb8 2 3 E L P % SP0 " y # PLPvEP8SE2mDíSvPS13Dçç L PvELyp3E%y UpES1R8 3 í ' L 1 8 P

'%%%1 9.4:2I60 <5;I;:60.

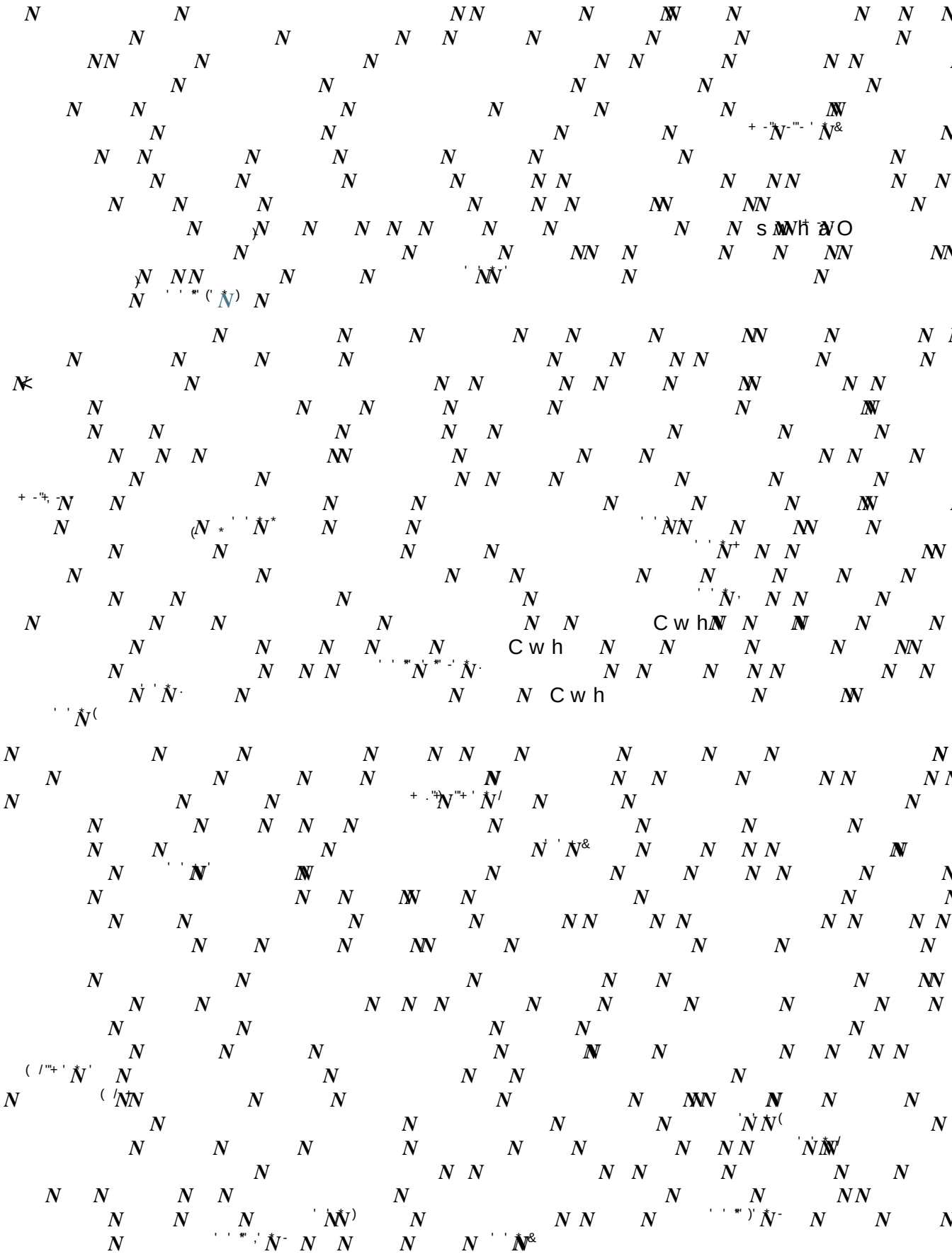
7e,,eHc !B8íLmJjy¨eR.íc,JDDi 9!# $9íeJ,DDi,D%,&G :L
$<8íS21ç8P1 L6 RN3Ey3% :L6t19P ;Lvv8p8% ;R831PD1 FEvv
%<8íS21ç8RN3Ey6% qPEb8 2 3 E 1 N L 6 tEyREpSP% 9PP 92gL2% tO
&<8íS21ç8P1 L6 RN3Ey3% ;E1N qt.9v8p8 L6 i8U BL2ó% i8U
'<8íS21ç8P1 L6 RN3Ey3% oER18N CL26S0iD8SU18BL;28óP%1 8i28%U ;BEL12Nó%qPiE
(<8íS21ç8P1 L6 RN3Ey3%1qR8Zb8 2 3 E 1 N 2 L % tS39REPp1LP% c8S
)<8íS21ç8P1 L6 tS1 8 2 E Sv 38 2c3yEE18NP yL86 STPS03 R=EPPppE1PL8P8%2 EcP8pS%1 1qvP8E
- 9 ; ; 2 < : 9 8 1=5ç8S3&gDv03*y=R4ó98;8!g y ' 8 0 D

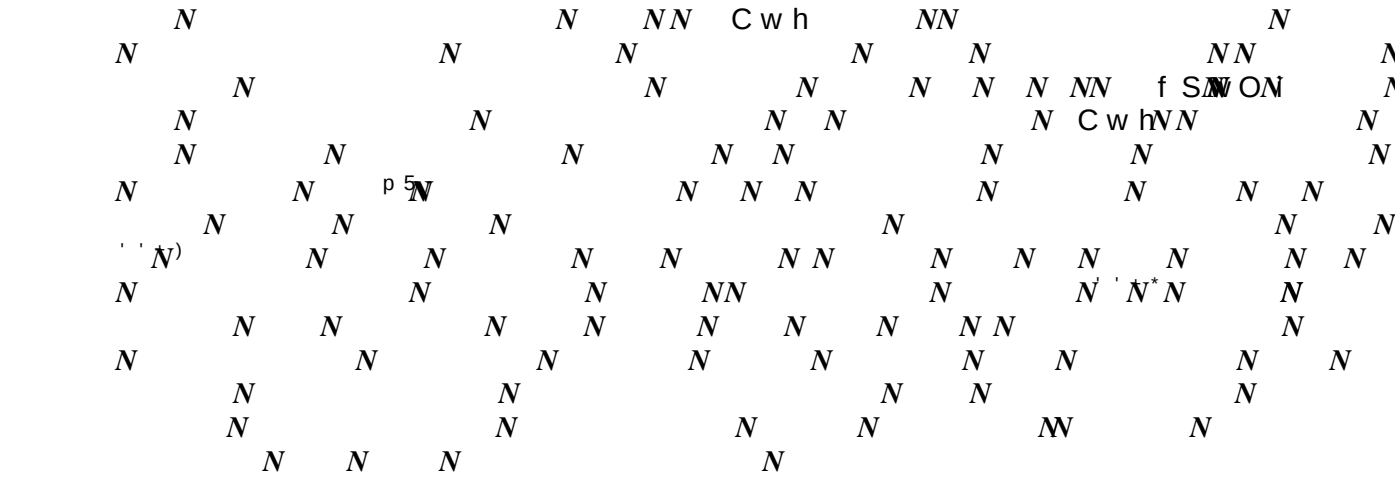


&$!# 2LHLne 0eKívek

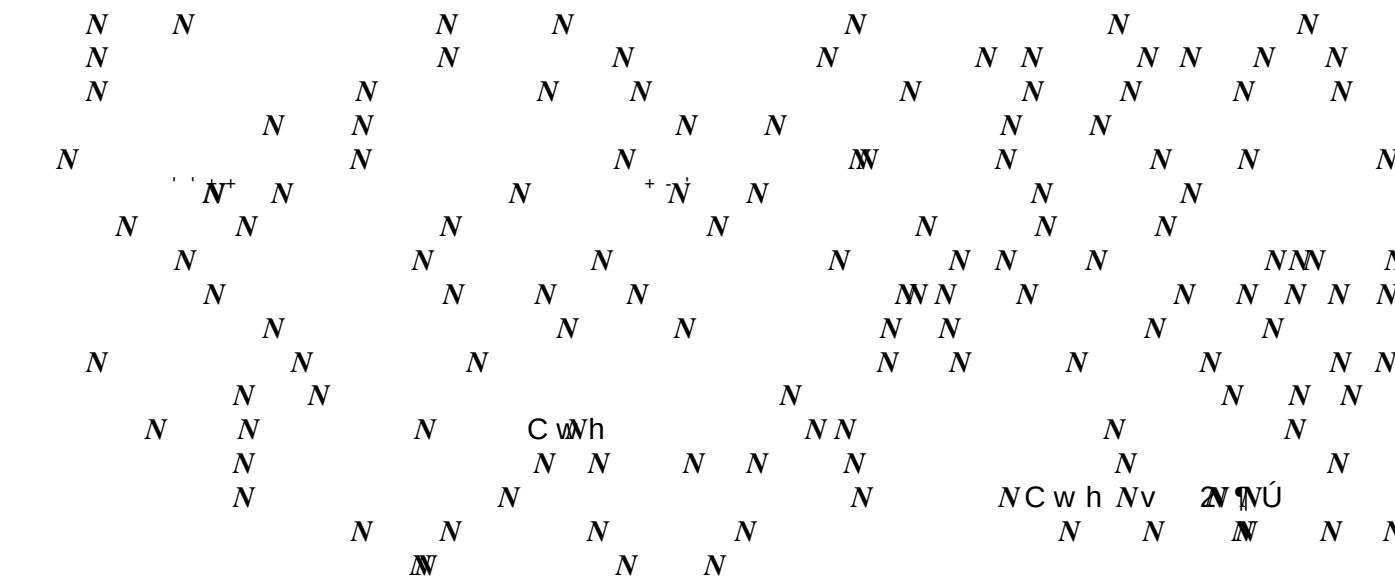


& $! e p < n D a e k





& $‰< c D H D , í v / D , H n D j D r 9 J G , e H í k o



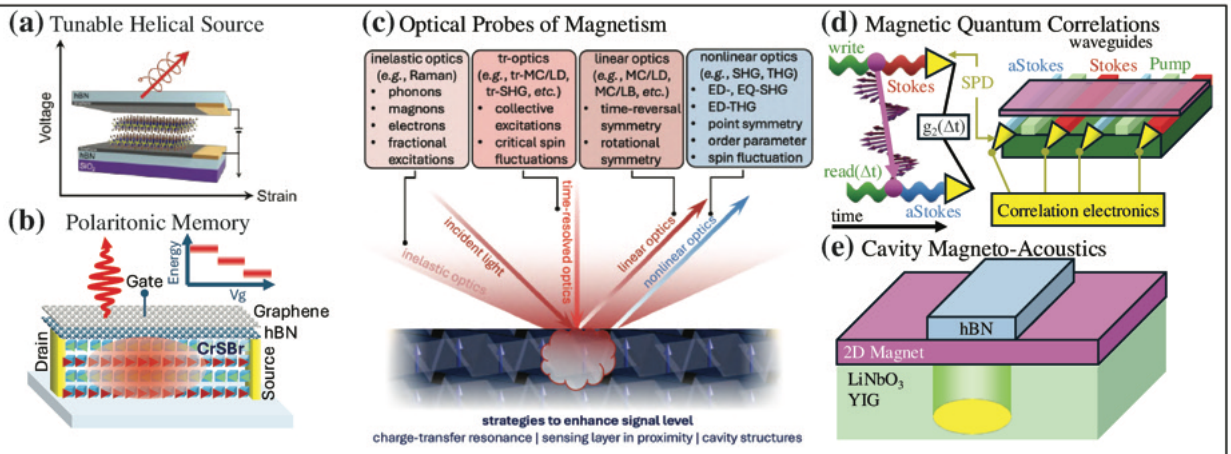


Figure 42. Photonics meets magnetism in 2D. (a) Exploiting the electrical and strain control of 2D magnets for on-chip sources of helical light needed for protected quantum communications. (b) Self-hybridized polaritons optically read out the multilevel magnetization.[1151] (c) Various means by which optics is employed to probe the magnetic properties of 2D atomic crystals. (d) Stokes/anti-Stokes scattering, allowing for the detection of single magnetic excitations and their quantum correlations. Incorporation into photonic structures provides nonlocal corrections. (e) Combining optical, acoustic, and magnonic cavities to enable fine-tuned control of 2D magnets toward novel ground states.

Conclusion

43. CONCLUSION

F. Javier García de Abajo,[1,2,*] D. N. Basov,[3] and Frank H. L. Koppens[1,2]

[1]ICFO-Institut de Ciencies Fotoniques, The Barcelona Institute of Science and Technology, 08860 Castelldefels, Barcelona, Spain

[2]ICREA-Institució Catalana de Recerca i Estudis Avançats, Passeig Lluís Companys 23, 08010 Barcelona, Spain

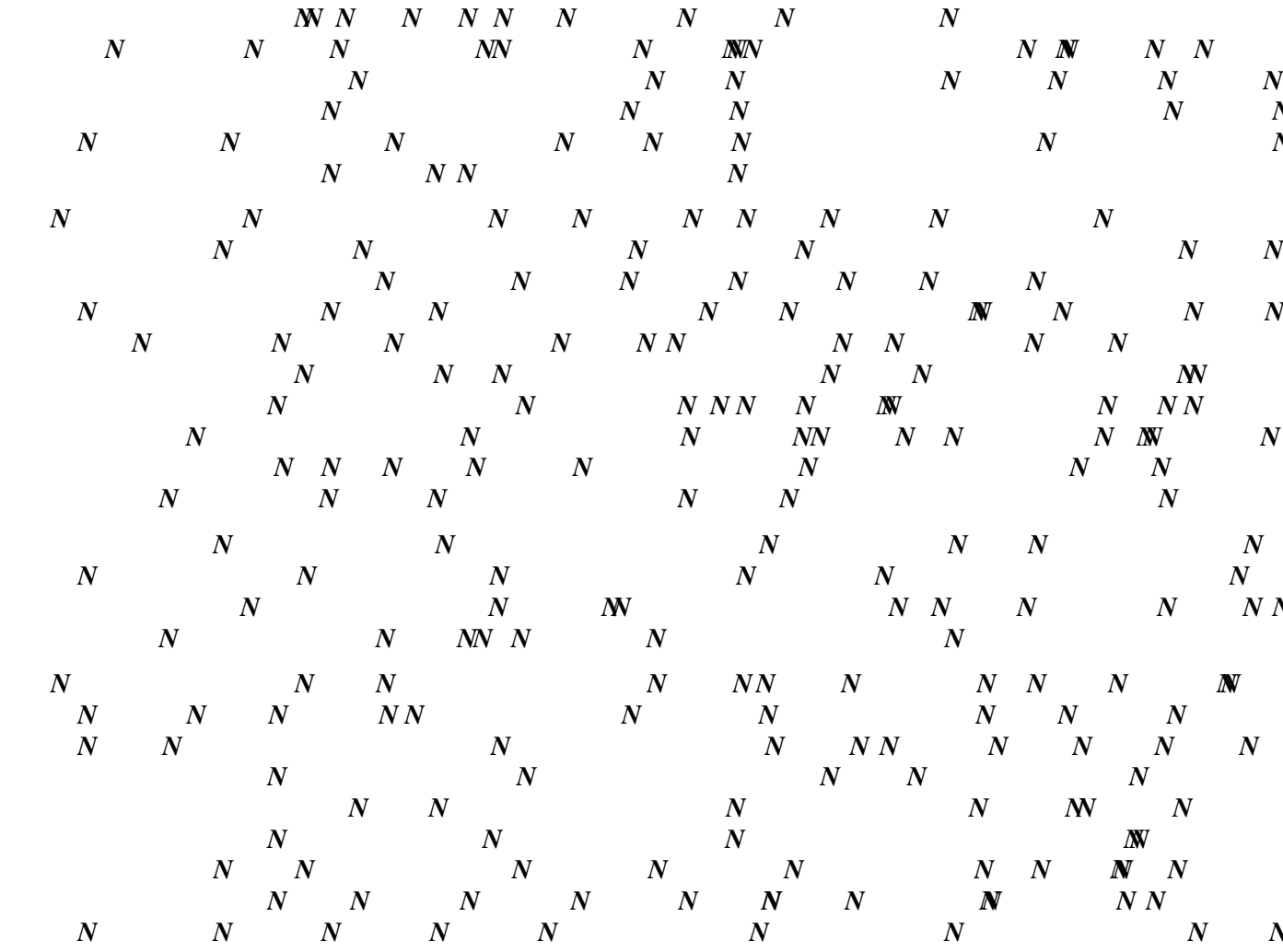
[3]Department of Physics, Columbia University, 1150 Amsterdam Avenue, New York, New York 10027, United States

***Corresponding author.** Email: javier.garciadeabajo@nanophotonics.es

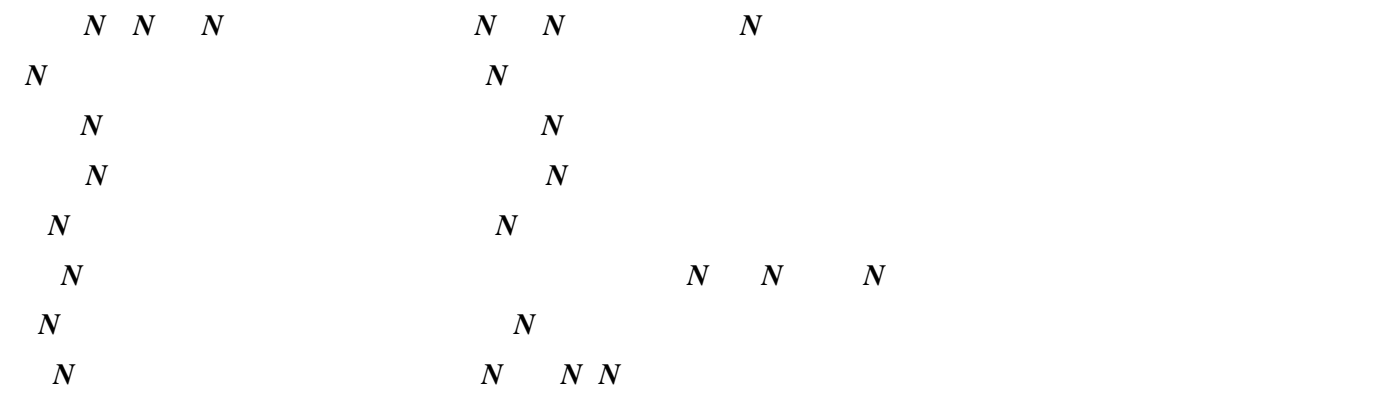
From the standpoint of the complexity inhering in biological systems and their astounding degree of dynamical evolution, interrelations, and functionalities, materials science is still in its early infancy. Moving from bulk to surfaces (famously described by Pauli as a devil's invention) has kept chemists and physicists engaged for decades. Once the domain of surface science, the combination of exfoliation, stacking, and twisting has now emerged as a powerful alternative for creating atomically controlled structures. In-plane complexity in 2D materials represents a natural extension of this evolution, enabling the integration of increasingly complex structures, dynamics, and functionalities in atomically thin structures—a small step in the complexity ladder. This evolution is already unfolding in the field of photonics.

We are witnessing a shift in our understanding of material response functions and light–matter interactions, driven by concepts from topology and quantum geometry. Quantum properties of light and materials are now being combined in an effort to identify intrinsically joint quantum states. Additionally, hyperbolic media are broadening our understanding of nanoscale photonics, previously focused on field confinement, and now extending this concept to include propagating rays, opening new possibilities for light manipulation at the nanoscale.

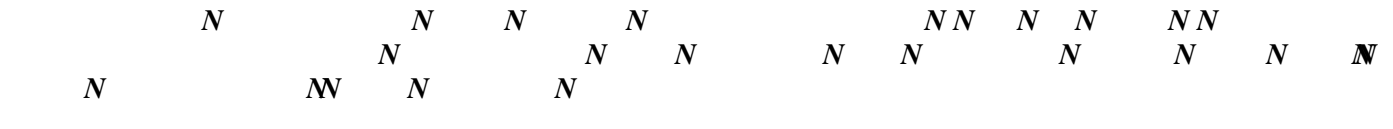
The wide range of topics covered in this Roadmap underscores the transformative impact of 2D materials on photonics. These materials not only provide better opportunities for exploring and practically exploiting several previously known effects, but also facilitate the discovery of new phenomena and the development of innovative applications. These include 2D polaritonics (Section 2–6), excitons with exceptional properties (Sections 10–13), substantial advances in nonlinear (Sections 14–20) and magnetic (Section 42) nanophotonics, insights into chirality and moiré systems (Sections 21–26), new uses of metasurfaces and emerging materials (Section 27–32), and applications in integrated photonics (Sections 33–35) and light emission/detection (Section 36–41). Tip-based



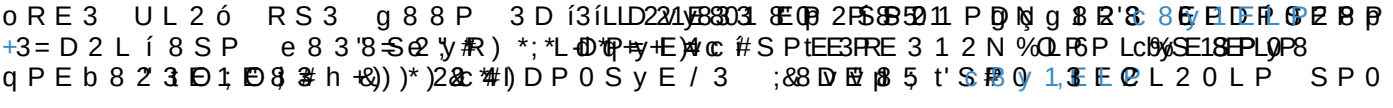
8 6 . I ; 3 . 2 8 2 0 I 2 1 . 0 1 ; : D 9 .



. N I 5 ; 1 0 ; : I 1 6 / N I 6 ; : .



. 0 7 : ; R 8 2 1 4 9 2 : I .





c ;)) +#-%c-l. ; 9 e'<= t=e& 0 - # 0 ' t '3<tu =<"=&c ;)) +#.l4, ')'h<3 u = &c<=)) *#% * 0 *
9 l uctequ eO"9 2 &*.&) *) &, #s ' ; ' S1PR9SP ó < ' : S&F38L2b2%8 2 L'% -IS'2 EnvLvíLí 8 P 3 %
6 L 2 çSPN D 3 8 6 Dv ' e0 E 3 yD S3 y 3 6 E P. E P U3 v 8 0 p 8 3 1 R 8 2R0 LR38 í ES1DS1vREL12N3 LL
c 8 y 1+E1LRPSP ó dEPpRDE BSP ' 6 L 2 6 2 DE 1 6 Dv 0 E 3 yD 3 3 E L P 3

: D H e

, E 8 U 3 % 6 E P 0 E P p 3 % y L P y v D 2 3 8 E 3 L 3 P 8 3 0 % ESPP 0 1 R 2 E B 3 y L e ç L ç S 8 0 P ç 0 S S 0 1 E S 1 2 P 8 1 B F 5
P L 1 P 8 y 8 3 3 S 2 E v N 62D8P60vE8Pyp1 S1pR88P ybEE883U'3 L 6 1 R 8

1 2 3 2 1 2 : 0 2 .

* i L b L 3 8 v L b % n ' c ' 4 C 8 E ç % a9R'S Pnp'%4 Bt 'L42 L<wDLgbL%P Lc3'% ,c' '4 ,-'E4S PQ
l E 2 3 L b % 9 ' 9 ' = v 8 y 1 2 E y l E 8 ç 9n'T=36 K9 8 T%)K8%, E R/// 9 2 1 L ç E y S v v N
+ i L b L 3 8 v L b % n ' c ' 4 t E 3 R y R 8 P 0 L % 9 ' 4 + <, S 2 P 5 S 0 8 2 E % T 9 S v 8 3 P F '
F 8 1 8 2 L 3 1 2 D y K 9 D % 2 (% 3 'S S y 2 - , 2
, < D % s ' 4 t L v S 3 % t ' e ' 4 F E D S P % p L % E 2 a L '14 L PaERýS3PLp8%v P 8 C y '14 2 LTP S E P y p 3 %' l
$ " %)%-%/ 8 S 0 'p)) * -
- T L 8 3 3 P 8 2 % 9 ' 4 s D P 0 8 g 8 2 'p4% 9 K C 'L P:3 'L4 v 8 C v S % L % 'B4' 4 ; S 222E8PpySE%í Et%' 4
o S P E p D y R E % o ' 4 , E p P S v 8 8 % P g C 2 'S4 P 0 % L v e E 'P 34 E P % E m p t R ' L v 4 P 8 6 H E 3 E P % 8 8 0 1 %' -F' '4
sL U & ls 3 3 S 3 ç LCP2 3 S í E R X 8 L P 2 8 1 E P 1 2 F E 0 1 8 2 L 3 1 r 2 s D C y $ 1 D $ 2 s 8 C 3 l '1 # K * + $.
. i E % C ' h ' 4 t y s 8 L 0 % 9 ' c 'L4 3 1 c % D P % ' Ta ''44 cTDSPPópD % % s c ' '4 dh 'E4L P - p E % S
< 8 S P % ; ' e ' 4 I L p v 8 2 % t 'sE ç E 1 C 2 S ís R 3 8 L 8 8 % ç L < P s E C y $ 3 1 '# l * D P 0 S ç 8 P
+ + . ';K) , ',
/ 9 v 6 & S P 2 w S w % l ' - ' 4 e & C D P 2 W E p v L % w % ' C 4 4 , 9 v 8 W % L c '%4 s<'L v=S'04L % C
t S 2 & 1 C P 2 8 P L % s ' 4 F E v v 8 P g 2 S P 0 g % S e 8 4 v 8 P P E p 1 E V 1 S E 2 R E % 1 P L 9 P E y B '; 2 <N 8 3
t S 0 8 b L S 6 P S 0 8 2 S T 8 8 E V S v ' 4 N 7 % 'n % 9 $ - +
0 9 D 1 L 2 8 % t ' 4 < X 9 í D w w L % l 'ç 4 S A < % E uC 'S 4 3 íeSL2N 8 % % 9 '' 4 4 :C 2 E S v P E v g 8 ó 2 % 1 E
C S C & S y 0 8 9 g S A L % l ' K - R 'L 4 P L s P D íOEP % 1 8 c 2 'S y 1 v E S L 3 P ç 3 L P E P '0 M Á 6 v L p E y S
M C $ $ s % 6 % 1 $ K * + 0 ,
1 F D % l ' 4 % & 3 D 4 S P % t y = L '14 1 % - B 'S 4 P t % & - P C 0 '24 D h 3 H D 4 % a l ' 8 E O ç = S p y E & 1 L p v P S 2 o P 2 S 1 P 2 P í L 2 1 E P
t L c % 8 T S b 8 p D r E s D C 8 c 3 N 'C N $ 9 ' 3 % T) 4 * K % / ') . /
2 n L í í 8 P 3 % l ' F ' s S S ' 4 0 8 ; R 9 S g P S p A % L % < ' I '= ' -4 ' C C S 2 2 S y í R 8 P 8 v S 3 ç L P E y
s E p R 1 µ t S 1 1 8 2 s 0 D N P 1 $ < 3 ' D & S % y 1 E K L P 0 3 0 '
*) 9 g 0 & l = S v 1 1 S R % a ' t ' 4 t ó R E 1 S 2 N S P '%4 ,C 'D 4 L % : 2 d 8 '0 4 8 % C R - L '3 4 R % l 8 9 2 'P 4 j P
= y R S 2 2 E % 9 ' 4 i S b 8 R % <S ' 4 0 8 h E 9 S g % S A I L % 4 l u '2 1 - 8 'p S % v S - 3 'ç L = P 'E 4 y 3 C
; 2 N 3 1 S v v E P 8 4 0 E v $ b " 9 % 2 + % l E K 0 ç 8 2
* *; S v 0 U 8 v v % - ' < ' 4 9 R S 2 L P L F b E 4 y R C % E v O % 4 : '; 4 S 3 3 S S 3 g L L E % 8 % < C ' i 4 ' = 0
: L 2 L P i E 1 C 2 E 0 8 8 A $ # + . s . K G - l / ' 1 0 $
* + t S % T ' 4 & C L 9 R v w L J P v 8 L w % ' 4 s E % c ' 4 & c i j E P ý E R 3 E v P % & C - D 9 1 4 E f 6 2 S 4 g 8 L W 5 % 0 S P % 4
9 ç 8 P S g S 2 % O ' 4 s E % ' 4 R S P p % w % ' 4 ' 4 2 & E S % 6 ç & R P % % ' 8 4 ' 4 4 4 S + 8 S E % %
F E v v 8 P g 2 S P 0 & % v e S P 4 8 2 9 1 S ' E % y L & s P L & % D R q 3 v 3 1 2 S L v S 2 E 1 b L S P P 3 0 E B P 2 S T S i S S v 1 3 D
; 2 N 3 r 1 s S C v $ ' 1 # * + . , . K 0 " / ' +
* , S 2 1 L % n ' 4 9 w w S ç % c ' O ' 4 2 S E 8 2 A + 8 9 % P 8 8 4 E P % p + P 6 N 9 % 8 C P L + 8
c E & 1 8 P 1 2 L v & 8 R 0 L 1 c L E P P p = v ç 1 8 E 3 . 3) E r L n P C $ D í 4 N 7 $ # 9 $ 1 .
* - o R L p 2 S % 1 C S S P 2 S y 3 G E S 2 % 0 8 l u ' 9 g - E B Y & S + v P 0 R S P y 8 ç 3 2 P 1 P 9 g 3 N C P L 1 P 8 2 S y 1 E L P E P
C 2 S í R i S P 8 3 1 2 ' D y h 1 4 D $ 2 8 a $ l ' % # $ ' " & 1 C C $ *
* .; R 8 P % - ' 4 : S & C E P w E % 8 w % 4 9 4 L 0 R L P p 2 S 1 - 1 'S 4 P S c 3 íES 2 3 E 8 % P L c b ' E 4 Č % F D t 1
; 8 P 1 8 P L % 9 ' 4 8 3 m D 8 2 S % 9 '94' 4C L ; C S E ç p S P 2 C S P % % 9 % g ' S 4 A 'LC a S D 2 2 y 4 D G 1 S D w S
F E v v 8 P g 2 S P 0 % e ' 4 n L íX C ç 8 S P p 3 E % P p k o ' D 1 F S ' G C v S 8 1 ' 8 C u 2 íS 1 íE R y 8 S P v 8 1 i l S v P S L 3 ç L
$ " # $ *0.K1 *
* / l 8 E % a ' 4 e L 0 E P % 9 ' c ' 4 9 P 0 T 2 S 8 p 8 P b 8 % 2 % C 't 'u 4 ' 4 a R : S S P L p % % T s ''4 t t 'y 4 s
o R E 8 ç 8 P 3 % t ' 4 < L ç E P p D 8 w % L % ' 4 ' I E p 4 v 8 2 2 % D % ' ; 't ' 4 ' 4 , S 8 3 1 2 v
i ' & o S D 1 P 8 E P p L 6 C 2 S í R 8 P 8 v S 3 K C L ç P S 3 p E e P 8 p b 8 3 1 S # v $ 8 * 1 D . K 1 g . ' N O P 6 2 S 2
* 0 = í 3 1 8 E P % O ' 4 o 8 4 2 D 2 3 (S 3 % & 3 1 ' E 4 % e R R 9 8 8 % % < 9 ' 9 - 4 I 2 S P ó % : ' 4 a
T S 1 S P S g 8 % n ' 4 o S P E p D y R 4 E % F L c P ' 8 4 % C - E ' 8 3 ; 3 ' 8 4 P % 8 F 2 ' 8 4 3 % o L i P ' p S t N ' %
i 8 & q 2 P E 1 N s E p R 1 9 g 3 L 2 í % b S P P 0 E P 2 8 S 8 8 L 3 L 2 D N 8 2 D 2 8 < c l ; C S C b $ E 1 N '
$ " %('% , . - ' µ , . . +











* 1 < L P%p ' 4 %sE' L4P p %&E P #%aN' D4P%e- ' E4P pt %9 s'c8 ' L40 %cR' S4P%ps' E4D%e S' 1 4S% C S L
F ' 4 %a L' P4%e ' S4P %- 0F p S4 2 &F S8 2 2E%8 v2 4L s%8 b E 4 L%0 E- v' v4E 3%t L' tp ' v4 8 2
: S P 0%& 29E' P4 %<S' i3 ' L b I E 2v S8 pC 2 E S F R 8 S 8 ç L rP sE C y$ 3 1 '%+ #/%* K. **, / '
* 1 a/ R%L' 4 %cR S4E ' s4E %cS' P4 p %C S P4 p %t 1' S :ç ' S4 S P%P ' 4 %B E 4S P%p E 4S 1%B ' L 1 4
T S 1 S P%S' g4 8 o S%E p 4 D%R 4E 1%N S' P p= 6 6 E y<E 2 8 S Pp 1 6 I 2 E=wç 8 S y<D E 2 I S P y 3 E P
t L P L v C S 2 N S 8 í 2 R r 8 s P C 3 8 $ 1 '%+ #/%* K. *+0* '
* 1 F 0 8 %i í '; F ' 4 %0 L' 2 4 2 8 &E S D 2 %& v L P 4 3 F 8 2 w %F p ' 4c RT 8 S%P S 6 4 D S 5 g 8 %E p 4 D y%R E 3 R P S
n D ç%e 2 ' 4 n %í F í ' 8 P 3 i &S 0 S p E R P p 1 L 2 8 3 í t L P E 2 P %E ; 8 E v P vt E S L P 6 E ç o S V E 3 N 1 8 0
: E v S C N 2 8 S 2 í R r 8 s P C 3 8 $ N ' 7 7 $ 8 9 '%+ #/% * / -) '
* 1 T 1 S p P%t 8 ' 2 4 %a l' 8 4E t %9 s' c 8 ' L 4 0 %9 L c 0 ' E 4 P%T : ' S 4 L O%+ E C P ' 3 4 ó%a R 8 4 L C 1%t v ' 0 4 6%v s S E ç D
t ' 4 < L ç%E P 4 p D 8 R%E 8 4 ç 8 P%6 ' p t v ' 8 4 2 ; S 3%9 1 2 F L ' 4 %; 8 ' S ' 6 D 4 9%ç S 2 4 E 8 8%E v ç S P P
I ' 4 : S i 3 ' L b q v <1 ' 2 i S 6 P S L 3 3 1 y v S S 3 R ç 0 L R P 8 E P y L ç 8 = P 6 S L E C E 2 S S 1 í 8 R 0 8 P 8 S v 8 0 g N
O P 6 2 S D 2 ç 8 %0 2 L g S 8 P L 3 y r L s í N ' $ $ <" %C 8 %6 + '
* 1 t 2 2 8 %t 8 ' P 4 B S%6 p 4 2 1 s %9 b ' S 4 P L c P D%F R ' L U b 3 2 ó S 4 P y 3 E X 8 L E V P 5 2 < N 1 P 5 P ç E y 3 %g N P T c 8
q v 1 2 S 8 6 S 8 2 8 1 Q ç S p E n P t 2 3 M $ 8 " %%% + '
* 2 h) D%c ' 4% $ 8 E 4 %e, P 1 4 %t L E 4 P p c 1%8 2 P g 4 S%a R 4 P p D%P p R 4 %ç 8 4 v L 2%y O b 4 8 2
B S P ó L%U E 4 1 w d %e 8 ' E 4 2 1 %N E - v ' v 4 E 3%t L ' t p ' v 4 8 2 %; 8 e S ' P 4 S%9 D í ' S 4 1 %F N L ' P 4 %8 s E D
t ' 4 %< S ' 8 L b = v 8 O y 1 8 2 2 5 P y E 1 y E L L v P D 3 E , E E 3 P D S < v E E 2 S 5 8 & L 0 8 2 g S R c 8 3 2 1 y %8 1 E ç 8
O P 1 8 2 6 8 = 2 v 8 8 P y & L 8 2 L L 1 P K D P S 3 E í S n 2 T 8 2 3 E M $ & v " 8 %3 %% - , '
* 2 c* E 0 S N%% o ' 4 F S N 8 3 %% - ' 4 c y R E 8 p v %4 I a E 4 w v c S 1 P 8 0 2 P 8 2 2 %% I t ' 4 4 t 8 8
s E P p v %% c ' 4 e 8 í í %% - ' 4 T E E ç 8 R 8 1 v %% B - ' 4 9 & u ' 4 D E g P 8 9 %% 2 %% D g 9 N 9 v 8
t E y 2 L 3 y L í N L P 9 1 r L s ç C E $ y 1 '%& 8 %% p K 1 + R 2 - c y S v 8 3 '
* 2 e+ E w%v L ' 4 c%R S 4 y S%P 8 c 3 ' 3 4 8 P%a R ' S 4 P pt %9 s c 8 ' L 4 0 & e D 9 %E p 4 %e S ' 1 4S ; %% 1 R 2 E P 8
t ' 4 B S P %< C ' 4 S P%S p 2 D 4 8 2 %9 D ' g 4 E %F L ' P 4 %< 8 e S P 4 S%9 D í ' S 4 1 R%N S 3 L b
< ' i ' i S P 8 c y 8 1 8 2 k P S 1 - 8 D 2 P S y v 1 E í L P 3 8 e D E P F v 8 C 1 2 8 S 2 í L R 3 8 1 P 2 8 9 (N / $ $ P " 2 8 8 $ $ C '
(% *K 2 2 / , '
* 2 n, E%ç c B ' 4 c 1%8 2 P g 4 S%y, R K ' L 4 %a c ' D 4 P%e S ' 1 4 S %& c R 4 S L t %9 s ' 8 c L ' 0 4 %s h ' E 4 L %k p L P p
B ' 4 %o R D P 4 p e S%A 8 #%c 2 ' E 4 P 1%E ' í 4 S P%8 R S 8 4 a%B P ' p 4 %h S ' g 4 S 0%E E - v ' v 4 E 3
c y R %y - ó ' 4 %< e S P 4 %F L ' P 4 %< S ' i 3 ' L b 9 ç g E R í S L 2 v 8 8 S 2 P C 2 6 S 8 í 2 R 8 S 8 ç L P E y
; S b E 1 E $ 8 3 C ' $ 1 %(% % K 1 + - 1 , '
* 2 F- D%F ' 4 %i R 4 P%6 8 4 %e B D 4 %t h ' D 4 8 %n R 4 P%B E 4%B d D 4%< F D 4 %; R 4 %a c D 4 P ' s 4 E
C S 2 y G S %0 ' 8 4 ' 9 %g S E A K & 6 P 8 i g 8 v p 8 S 1 e E 6 2 8 S y 1 E & P F 6 2 S K 2 v 8 S 0 2 E 1 8 P 9 T
$ " %)%-%/ K. ./1* '
* 2 -%a ' 4 %F ' S 4 2 ó%t S ' 2 - g 4%2, F D 4 T S%1 S P S g 8%B E p 4 D%y F R ' E 4 & h ' D 4 %c R a 8 ' P & s L y S v
2 L g 8 D v L 6 = C S p P 8 1 S 1 8 2 S E y P 1 E S L P 8 S 3 v D v, S R 8 1 2 8 P 1 '%, &)%+ K. 0 1 1, '
* 2 h/ E L%B p 4 B ' s 4 E F S%v ' g 4 8 2 c 1 %& ç / ç 4 L %a c ' D 4 P%c s ' E 4 D %- F p S 4 2%c s L 4 U %L ' p v 4 8 2%< 8 S P
; e ' 4 %E - 9 v ' v 4 E 3%L ' b < ' L v S 2 E 1 L P E y & O P L 1 2 8 1 p E B y 2 8 3 , R N S E 2 < 1 p R C %& F S v 6
2 + K 2 / + / * '
* 2 h 0 E%8 ' 4 %B R ' S 4 P p%S ' P 4 w 8 %P ' F p S 4%2 h ' D ' 9 1 & L L ç & y B y 2 L 8 S y 1 6 E N ç & 8 L ç S E P
o U L & E ç 8 P 3 D E 6 2 P S S 2 R 8 L 0 3 í 8 y 1 2 $ C 3 9 N C N $ T " c %8 %% 5 *K*) 1 . '
* 2 B L S P%t S ' E 4 F%t S ' v 4 v 8 %D E 4 ç N C%9 2 v 4 S y%R E ' b 4 8 2%S S i 3 ' L 4 b n %O ç ' E P u 8 í 2 í L 2 1 D P E 1 E 8 3
i S P L 3 y 2 S 1 v g 8 E P S p 3 & 8 L 2 6 b R 8 S P 8 2 8 S P 3 E r 1 $ C L c R $ 4 " '%(& % *K; 1 1 1 '
* 2 2 R %; P ' 4 %; ' R 4 D :%L ' g ; E 3 4 y %t E s < v ' v 4 %T F L , E 8 U E P p 1 R 8 O P 1 8 2 E L 2 L 6 S c
, E g 2 L P E y S v v N e 8 3 L v b 8 0 e R 8 L 3 1 L L v P D 1 C %& 4 S P p ' E 8 C 0 %' S %1 + c D g ç) L + 8 y D
+) ;) R %h P ' 4%c h ' D 4 c%R S 4 S%R E 4%L I 4 %E - 9 v 4 E 3%t L ' t p ' v 4 8 2 S%3 D í ' S 4 1 %R s N E 4 D
: S 3%L ' b < ' t S y R E P 8 s 8 S 2 P E P p 6 L 2 í u N 1 ' M $ E x y S $ 1 '%) %S P P 2 E P p * ' 2 L g
+) I* %t ' 4 %c h ' D 4 %a c R ' S 4 P%e S ' 1 4 S %- S 4 y ó%e S 9 N ' 8 4 2 %h R 4 P %L S L ' 2 4 8 %< E - w ' v 4 L %8 3 3 8 P
: c ' 4 ; %t 1 ' P 4 2 E P%8 P ' O 2 4 9 3 T S%1 S P S g 8%B E p 4 D%y R E P 4 S%9 D í ' S 4 1 R N
: E 3 %, p ' P 4 E c%y R D 4 ó%9 E - v ' v 4 %t 3 E 4 D %S ' 8 L b 9 y y 8 v 8 & 2 í S 1 1 E 8 y 0 S v i 1 S R P 2 L S D p E R P p
c í S 2 3 8 c r S ç 9 N $ $ E ' P %p & 8 % +K* * 2 / '
+) e+ E w%v L ' 4 t %9 s c 8 ' L 4 0 ; %; 2 ' P 4 S R c %& P v 6 4 2 6 E 8 ç D 4 8 3 %e 3 9 y ' L 4 P 3 %B L ' P 4 p
i D y ó%t ; v 4 3%< 8 e S P 4 S%9 D 9 í S 4 1 R N 4 N %h E 4 S L %< S ' i 3 ' L b , E 3 D S v E w E P p 9 1 L ç E
s S N 8 2 8 0 t S p P 8 2 1 M E A 3 s ç C $ $ E 1 P %) $ %; 2 + c + : 2 *))) '
+) c, D P%ó D %4 F %< v ' g 4 8 2 c%t S S v 4 g%6 P 4 P t %9 s c 8 ' e L 4 E D ó%R 0 1 ' 8 4 2 : 8%3 ô = L ' U 4 E ; 1 s w L '
: ' 4 C L 8 P y w 8 S b%8 8 3 w L ' 4 %F L ' P 4 %< 8 e S P 4 %t L ' p v 4 8 2 %< S ' 8 L b F N í 8 2 g L v E y
= P R S P y 8 ç R 8 L P 1 1 L y L D 6 2 1 2 1 8 8 P 2 1 E P 3 E ç o 6 V E v 3 N 1 E 8 v 0 S C N 2 8 S 2 í R r 8 s P C 3 8 $ N ' 7 7 $ m 9 +' * %%
* / : *
+) – E%P e p 4 %6 R 4 %a l' 8 4 E, s L ' 4 , %e 1 9 S ' v 4 L %e 8 D 1 4 S c %- S ' D 4 P 1 6 L R P 8 ; P ' p 4 t %y v 8 L 0
9 ' c ' 4 %a c ' D 4 P %- E : S ' 4 P p B %h R ' 8 4 P %t L ' p v 4 8 2 %9 E - v v 4 E %3 s 4 D ; %< g F 0 ' 8 4 P %h h ' D 4































12 Sun, Z.; Hasan, T.; Torrisi, F.; Popa, D.; Privitera, G.; Wang, F.; Bonaccorso, F.; Basko, D. M. Ferrari, A. C. Graphene Mode-Locked Ultrafast Laser. *ACS Nano* **2010**, *4*, 803–810 '





2 2Xia, F.; Mueller T.; Lin Y. M.; Valdes-Garcia A.; Avouris, P. Ultrafast Graphene Photodetector. *Nat. Nanotechnol.* **2009**, *4*, 839–843.

2 2Vicarelli, L.; Vitiello, M. S.; Coquillat, D.; Lombardo, A. A.; Ferrari, C.; Knap, W.; Polini, M.; Pellegrini, V.; Tredicucci, A. Graphene Field Effect Transistors as Room-Temperature Terahertz Detectors. *Nat. Mater.* **2012**, *11*, 865–871.

2 2Koppens, F. H. L.; Mueller, T.; Avouris, P.; Ferrari, A. C.; Vitiello, M. S.; Polini, M. Photodetectors Based on Graphene, Other Two-Dimensional Materials and Hybrid Systems. *Nat. Nanotechnol.* **2014**, *9*, 780–793.

2 2Viti, L.; Purdie, D. G.; Lombardo, A.; Ferrari, A. C.; Vitiello, M.S. HBN-Encapsulated, Graphene-based, Room-temperature Terahertz Receivers, with High Speed and Low Noise. *Nano Lett.* **2020**, *20*, 3169.

2 2Asgari, M.; Riccardi, E.; Balci, O.; De Fazio, D.; Shinde, S. M.; Zhang, J.; Mignuzzi, S.; Koppens, F. H. L.; Ferrari, A. C.; Viti, L.; Vitiello, M. S. Chip-Scalable, Room-Temperature, Zero-Bias, Graphene-Based Terahertz Detectors with Nanosecond Response Time. *ACS Nano* **2021**, *15*, 17966–17976.

2 2Liu, M.; Yin, X.; Ulin-Avila, E.; Geng, B.; Zentgraf, T.; Ju, L.; Wang, F.; Zhang, X. A. Graphene-Based Broadband Optical Modulator. *Nature* **2011**, *474*, 64–67.
2 2Di Gaspare, A.; Pogna, E. A. A.; Salemi, L.; Balci, O.; Cadore, A. R.; Shinde, S. M.; Li, L. Di Franco, C.; Davies, A. G.; Linfield, E. H.; Ferrari, A. C.; Scamarcio, G.; Vitiello, M. S. Tunable, Grating-Gated, Graphene-On-Polyimide Terahertz Modulators. *Adv. Funct. Mater.* **2021**, *31*, 2008039.
2 2D0 Gaspare, A.; Pogna, E. A. A.; Riccardi, E.; Sarfraz, S. M. A.; Scamarcio, G.; Vitiello, M. S. All in One-Chip, Electrolyte-Gated Graphene Amplitude Modulator, Saturable Absorber Mirror and Metrological Frequency-Tuner in the 2–5 THz Range. *Adv. Optical Mater.* **2022**, *10*, 2200819.
2 2R1ccardi, E.; Pistore, V.; Kang, S.; Seitner, L.; De Vetter, A.; Jirauschek, C.; Mangeney, J.; Li, L.; Davies, A. G.; Linfield, E. H.; Ferrari, A. C.; Dhillon, S. S.; Vitiello, M. S. Short Pulse Generation from a Graphene-Coupled Passively Mode-Locked Terahertz Laser. *Nat. Photon.* **2023**, *17*, 607–614.
2 2B2ida, D.; Tomadin, A.; Manzoni, C.; Kim, Y. J.; Lombardo, A.; Milana, S.; Nair, R. R.; Novoselov, K. S.; Ferrari, A.C.; Cerullo, G.; Polini, M. Ultrafast Collinear Scattering and Carrier Multiplication in Graphene. *Nat. Commun.* **2013**, *4*, 1987.
*) Yakil, A.; Engheta, N. Transformation Optics Using Graphene. *Science* **2011**%))%(+ E**+.2 -
*) Miseikis, V.; Marconi, S.; Giambra, M. A.; Montanaro, A.; Martini, L.; Fabbri, F.; Pezzini, S.; Piccinini, G.; Forti, S.; Terrés, B.; Goykhman, I.; Hamidouche, L.; Legagneux, P.; Sorianello, V.; Ferrari, A. C.; Koppens, F. H. L.; Romagnoli, M.; Coletti, C. Ultrafast, Zero-Bias, Graphene Photodetectors with Polymeric Gate Dielectric on Passive Photonic Waveguides. *ACS Nano* **2020,** *14*, 11190–11204.
*) Castilla, S.; Terrés, B.; Autore, M.; Viti, L.; Li, J.; Nikitin, A. Y.; Vangelidis, I.; Watanabe, K.; Taniguchi, T.; Lidorikis, E.; Vitiello, M. S.; Hillenbrand, R.; Tielrooij, K.-J.; Koppens, F. H. L. Fast and Sensitive Terahertz Detection Using an Antenna-Integrated Graphene pn Junction. *Nano Lett.* **2019**, *19*, 2765.
*) Viti, L.; Cadore, A. R.; Yang, X.; Vorobiev, A.; Muench, J. E.; Watanabe, K.; Taniguchi, T.; Stake, J.; Ferrari, A. C.; Vitiello, M. S. Thermoelectric Graphene Photodetectors with Sub-Nanosecond Response Times at Terahertz Frequencies. *Nanophotonics* **2021**, *10*, 89.
*) Asgari, M.; Viti, L.; Balci, O.; Shinde, S. M.; Zhang, J.; Ramezani, H.; Sharma, S.; Meersha, A.; Menichetti, G.; McAleese, C.; Conran, B.; Wang, X.; Tomadin, A.; Ferrari, A. C.; Vitiello, M. S. Terahertz Photodetection in Scalable Single-Layer-Graphene and Hexagonal Boron Nitride Heterostructures. *Appl. Phys. Lett.* **2022**, *121*, 031103.
*) Viti, L.; Hu, J.; Coquillat, D.; Knap, W.; Tredicucci, A.; Politano, A.; Vitiello, M.S. Black Phosphorus Terahertz Photodetectors. *Adv. Mater.* **2015**, *27*, 5567–5572.
*)), E 1 4E % ; Is m D 4E v vlS v1E 1 S<P Ln '94' 49 vmEL 6bP % Sag: S'P4v No%8 2t8'3=R y 4R 8 nPF 6 S L %% u '
T 4 ; R D v,ó'L4b %, E=1cE'8vvSvX LS%b 8t 'o 8 2 S R 8 2 1 w < 8 1 8 y 1 E L P t 8 0 E S 1 8
O P 3 D v S 1 L 2 3 'rcsD 2 N 6 S<'%8C(%cK1 S) 1' 8 3
*) Viti, L.; Riccardi, E.; Beere, H. E.; Ritchie, D. A.; Vitiello, M. S. Real-Time Measure of the Lattice Temperature of a Semiconductor Heterostructure Laser via an On-Chip Integrated Graphene Thermometer. *ACS Nano* **2023**, *17*, 6103–6112.
*) Vitiello, M.S.; Tredicucci, A. Physics and Technology of Terahertz Quantum Cascade Lasers. *Adv. Phys. X* **2021**, *6*, 1893809.
*) Riccardi, E.; Pistore, V.; Consolino, L.; Sorgi, A.; Cappelli, F.; Eramo, R.; De Natale, P.; Li, L.; Davies, A. G.; Linfield, E. H.; Vitiello, M. S. Terahertz Sources Based on Metrological-Grade Frequency Combs. *Laser Photonics Rev.* **2023**, *17*, 2200412.
*) *- D 3 1 L C D S 8 2 4 2 8 9 2 4 L E o 6 L 4 2 ' g S %c 1 s c 8 ' v vF L S % d D t S ' P E S y $ S S 0 3 8 8 8 2 2 S R 8 2 1 w
I 2 8 m D 8 L P ç y g N B S g v 8 D v g 1 K O 2 S S N 8 R 8 B 8 8 b E c y 1 S N 1 ' 1 8 2 8 M c N $ C ' N % 9 % 8 T * K 1 , .
* 1 ' *
*) *: ' E S P y R E % ' 4 , ' 4 E 4 1 ; E S % 2 E 8 % N % s E 6 P 6 E 8 v 0 % = ' F ' 9 4 ' 4 < S B b 4 E L 8 P 3 % % < 9 ' C ' 4
n S 2 S p E S P P s E L 0 ç E g 3 S % 2 4 0 E 6 % L ç S 4 y R E L % I ' 4 I 8 2 2 S 2 E % o 8 2 S R 8 4 2 1 w L 2
c S 1 D 2 9 S g 8 v L 2 g 8 s E 3 m D 8 E 2 B 1 3 5 6 L v E S C 2 1 S L R E s C 8 $ 4 N 7 # % 9 $ ' 0 / ,
*) *< E C S 3 í S 2 8 % 9 ' 4 E 3 1 L 2 8 4 % :, 8 ' 8 4 2 8 e % y F y S 2 = 0 E 4 % e = E 4 1 y R E L 8 % R S % '
C ' 4 s E P 6 E 8 v 0 % = ' F ' 4 6 K 8 P 2 0 2 D S y 2 8 E 8 % L t 9 6 ' E 8 P , p ' 4 E P, E = 1 v E 8 y & 1 v 2 L E % y S t v ' v
O P 6 2 S 2 8 0 e ' S 2 M 0 A $ ç ' h $ T % & 3 8 + 2 + 3) / 1 + -
*) *F S 6 8 w % 4 n L F b ' S v 9 8 ' b % c & - 4 ' 4 o E : 8 4 v P 2 P L % L P E 3 A y % R % 2 n 2 ' y R E c P 8 L 2 b S E R y 8 R 2 % 1 w < i L P v E P
u í 1 E y 3 L 6 C 2 S í R 8 P 8 3 1 I E 2 E L ç E S 2 ç S 1 P D E 2 y S 3 g v 9 8 8 A P 8 g 2 3 S M 1 2 E 3 L T E 5 P = s C l
$ " % . % * 2)) 0 0 *
*) Hafez, F ' 4 n 9 L ' b S v 9 e n t, J. C.; Mics, Z.; Green, B.; Awari, N.; Chen, M.; Germanskiy, S.; Lehnert, U.; Teichert, J.; Wang, Z.; Tielrooij, K.-J.; Liu, Z.; Chen, Z.; Narita, A.; Müllen, K.; Bonn, M.; Gensch, M.; Turchinovich, D. Extremely Efficient Terahertz High-Harmonic Generation in Graphene by Hot Dirac Fermions. *Nature* **2018**, *561*, 507–511.
*) Kovalev, S.; Hafez, H. A.; Tielrooij, K.-J.; Deinert, J.-C.; Ilyakov, I.; Awari, N.; Alcaraz, D.; Soundarapandian, K.; Saleta, D.; Germanskiy, S.; Chen, M.; Bawatna, M.; Green, B.; Koppens, F. H. L.;

Mittendorff, M.; Bonn, M.; Gensch, D.; Turchinovich, D. Electrical Tunability of Terahertz Nonlinearity in Graphene. *Sci. Adv.* **2021**, *7*, eabf9809.

*) Deinert, J.-C.; Alcaraz Iranzo, D.; Pérez, R.; Jia, X.; Hafez, H. A.; Ilyakov, I.; Awari, N.; Chen, M.; Bawatna, M.; Ponomaryov, A. N.; Germanskiy, S.; Bonn, M.; Koppens, F. H.L.; Turchinovich, D.; Gensch, M.; Kovalev, S.; Tielrooij, K.-J. Grating-Graphene Metamaterial as a Platform for Terahertz Nonlinear Photonics. *ACS Nano* **2021**, *15*, 1145–1154.

*) Giorgianni, F.; Chiadroni, E.; Rovere, A.; Cestelli-Guidi, M.; Perucchi, A.; Bellaveglia, M.; Castellano, M.; Di Giovenale, D.; Di Pirro, G.; Ferrario, M.; Pompili, R.; Vaccarezza, C.; Villa, F.; Cianchi, A.; Mostacci, A.; Petrarca, M.; Brahlek, M.; Koirala, N.; Oh, S.; Lupi, S. Strong Nonlinear Terahertz Response Induced by Dirac Surface States in Bi_2Se_3 Topological Insulator. *Nat. Commun.* **2016**, *7*, 11421.

*) Tielrooij, K.-J.; Principi, A.; Reig, D. S.; Block, A.; Varghese, S.; Schreyeck, S.; Brunner, K.; Karczewski, G.; Ilyakov, I.; Ponomaryov, O.; de Oliveira, T. V. A. G.; Chen, M.; Deinert, J.-C.; Carbonell, C. G.; Valenzuela, S. O.; Molenkamp, L. W.; Kiessling, T.; Astakhov, G. V.; Kovalev, S. Milliwatt Terahertz Harmonic Generation from Topological Insulator Metamaterials. *Light Sci. Appl.* **2022**, *11*, 315.

*) Cheng, B.; Kanda, N.; Ikeda, T. K.; Matsuda, T.; Xia, P.; Schumann, T.; Stemmer, S.; Itatani, J.; Armitage, N. P.; Matsunaga, R. Efficient Terahertz Harmonic Generation with Coherent Acceleration of Electrons in the Dirac Semimetal. *Phys. Rev. Lett.* **2020**, *124*, 117402.

*) Kovalev, S.; Dantas, R. M. A.; Germanskiy, S.; Deinert, J.-C.; Green, B.; Ilyakov, I.; Awari, N.; Chen, M.; Bawatna, M.; Ling, J.; Xiu, F.; van Loosdrecht, P. H. M.; Surówka, P.; Oka, T.; Wang, Z. Non-Perturbative Terahertz High-Harmonic Generation in the Three-Dimensional Dirac Semimetal Cd_3As_2. *Nat. Commun.* **2020**, *11*, 2451.

*) +< *E C S 3 '4 S 2 B P % p % ; ' 4 '4 c y E P % 6 S 1 1 8 4 2 B P % E % 3 % 9 ' C ' 4 '4 s E P 6 E 8 v 0
: S v y '4 E % l 8 u 2 2 S 2 E % '4 9 ' , E ; 1 ' E 4 c 8 ' v < v R (L E % ç 4 t S P % 6 S 2 1 ç v L C P 8 E P y 8 2 S 1 E L P E P 1 R 8
e 8 3 1 3 1 2 S q 1 R E v P C P 2 g S S P R & ç g 8 0 0 8 8 1 D S o í w E E y P e p 8 3 L P 9 S 2 1 2 L S 2 N C $ 4 ' N 7 7 m 9
$ " % ' & % + ' , * +

*) +H Ð ó D 0 4 S % n E < ó D c y E P P E p % v l 8 d & S P 1 0 < 1 8 P 1 8 y q 1 3 E E D P í 8 2 y L P o 2 1 S P y 3 1 = E D P p E B L P
c 8 P 3 ' L v 2 1 8 N S M B S " $, & % * , K * 0 ' .

*) +: ¸ S 3 8 v % ç S P 3 ' 9 ' 4 4 l S S 3 y y D R S E v P % s S l p D 8 P P 3 1 % L 8 P % < ' 4 ' s 4 v l t P ç 2 1 S P 2 1 8 % S
i 4 0 8 , E 3 3 & 8 2 P % 3 E 1 ' E t E 8 y 2 d q f M M 2 8 8 1 E D y y 1 < 8 P 8 y 1 l D 2 1 3 c 2 6 8 l y 2 8
o 8 v 8 3 y 2 L 4 í C 8 1 3 N 4 9 C S m ' T % , $, % + 9 * 0

*) +e L p S % v 3 6 N c 8 ç E 8 y 1 8 P y 0 1 D l y L 2 y 3 S 2 A S P P 2 8 2 S N l 3 S & P 6 0 L 2 2 S ç 2 S 8 p 0 E P M p C ' N y 6 5 l T C 1 N 9 $
a l 8 A $ % (0 % K -) + / / '

*) +n S 2 S 3 E ó % : ' c ' 4 u v S N S % R 8 < P 4 L P F % 8 E % ' = " 4 n 8 l 2 8 8 ç D 3 2 2 8 v % 8 b % ' c F
c 8 2 p 8 8 b % 9 s L U , ' i = F e L 8 1 + y M E 8 2 y 0 0 t P E 2 1 L S P P i 5 E P ç g L v L : ç 6 8 6 1 6 8 2 o 3 $ ' 2 M M 5 $ n m M l
$ " % ') % K + 2 2 ' , 0

*) += / y R 1 8 % 2 P S ' y R t ' 4 8 í í 8 2 % : ' - ' 4 R L e 1 8 < 8 y F 0 % y 1 0 E 4 P e S 2 0 6 E 0 S 6 1 L E 2 L 0 P % F w
U E 1 R D 1 S P 8 1 ; S D ç S y E < 3 8 S 1 8 w r 8 s % 2 4 C S $ N 9 % (% K 2 0

*) +t 0 S 3 3 E y L 1 1 8 % t ' 4 c L S b E & % ' C ; F S 4 2 1 2 E 2 8 2 E 2 8 3 ý E K 8 P E P % 0 S 9 ç ' 8 4 P 1 o S E v 8 3 v 2 S L P L 0 E A
9 í í v E y 6 S 1 9 E N L 4 P 8 T ' 9 % 5 # % 1 K 1 0 7 * *

*) +F 1 D P 1 % : 8 B S ç S P p y E P 3 8 R v E % - ' < ' 4 B L D P p % 4 9 ' T S I 1 ' S 4 P S B g S 8 P % ó L n U ' E 4 1 w o % S
o ' 4 t L L P % ' 4 & F 8 2 2 R E P 2 L % t ' 4 9 S P 2 E W 8 2 2 E ç % E L e P ' 3 ; S ' P 0 t S F 3 L 3 6 E 3 b 1 8 S
: D 1 1 8 2 6 v N E P 8 S 1 8 b 2 S L P 3 1 0 2 8 3 2 y $ 1 T B 6 2 8 8 % ' 3 * K * + 0) '

*) +u 2 R 1 S % o ' 4 : L 3 1 U E y ó % 9 ' 4 = ç 8 N L v P 8 2 = % 8 y E 4 l p 2 P D E y 8 1 B E % 8 S n ' 8 4 2 e L 1
C 2 S í R n 8 T P 3 8 I $ 9 ' T %) l (' %) K 2 . . * -

*) ¸ a) R S P p % B & o 4 ' 4 o S C P E p 2 % E 1 0 % ' ; ' 4 F S L % a ' 4 % t t S ' 2 1 I E ' P 4 % c t R ' 8 P ¸ % ' 4 B ' a 8 e 1
< E 2 u 8 g y 3 1 8 2 b S 1 T E D 1 8 D V N 6 g S & P 8 0 p S E i v S D 2 8 S 2 i R 8 s P C 3 $ N 1 % ' + + % / K 1 + +) ,

*) Ç * S N 0 D y R 8 P ó L % O ' 4 h D % c ' 8 C 1 ' N 4 S ó 9 L v b N % ç L C b % 4 C o ' S 4 P E t p L D 3 y ó R L E 1 % E P o % '
C L v 1 3 ç S P % C ' 4 C 8 E ç % 9 ' n ' 2 4 E P I % 8 0 < L ' 2 9 E ' 8 & % e 0 6 C 8 2 y 4 S 3 P v 3 1 E E 3 F 1 1 3 2 L 3 b %
6 L c 8 2 P 3 E o 8 1 2 1 8 R < 8 8 2 1 8 w y r 1 s E C 1 $ P ' 4 N 7 % ' # % (9 $ ' . - ,

*) ¸ t + N v P E ó L b % < ' 9 ' 4 o E 1 L b 6 S 1 % P l = ¸ b ' % 4 O O a ' 4 R D m ó S L 3 b R % y R c 8 ' P ó c L ' % 4 t c ' 8 ç 9 ó ' E 4
i L b L 3 8 v L b % n ' c ' 4 : S P 0 D 2 1 E v P % R < L ' 1 9 y ' 4 P 0 c D y E 1 P E L 3 8 E 1 b N % E < P 9 E
C 2 S í R 8 P 8 o 2 S P 3 E 3 1 L 2 3 3 = & D P E 0 D 8 y P 8 y 0 8 r - 6 & 1 9 2 N y 1 6 E D N & P & $ ' v + E + P) p u + S + 1 / C S

*) ¸ p L 0 L 2 ' 4 L b % P 0 8 2 8 U 3 % 9 4 ' ; t L ' v 4 L ç 4 g S 8 p w P v 8 E E 3 % % e O 2 9 4 S 3 P 3 0 8 2 0 % E ' 0 C 1 2 1 2 E P % ;
s E p & t R S 1 1 8 2 ; L D í v E P p E & P E & D 8 g y S 1 2 8 B y 8 P P ç y 1 2 R L y 8 8 1 S ' y E 8 3 4 $ S 1 o 8
a l A $ $ < % ' G & % ($ * 1 ' / -) +

*) ¸ s - 8 8 4 % ' B L ' 4 L % 9 b < L 4 0 2 E 8 ' 4 4 0 % u R o % C ' 2 c S ' í P 9 y 8 P D 3 v 1 S E 3 y ç 8 1 P L P S 1 q v L 2 2 S 6 1 8 2 P 3 E 1 E b 8
O P 6 2 S í 2 8 8 y 0 1 2 L r 3 s y C L $ í N ' s 9 $ N " C % l + % c & , N * 5 2 $

*) ¸ s E S P p % C ' 4 F D S P 4 p % R E ; P ' 4 4 h ' t - 4 E P % ¸ S P 2 1 N 4 % 2 % R 2 8 4 3 1 E R S % 3 L P % t ' 4 B D
e L g D = 6 6 % y E 8 y P 2 1 % ç y 8 S 1 v 2 8 8 3 1 8 0 D v S 1 E L 3 2 E 3 g S v 6 8 8 v 8 ' P ¸ p C 1 $ R 3 v ¸ $ N C % N % 3 T 4
2) K 2 * ' ,





